

**Faculty of Science and Engineering
School of Earth and Planetary Science**

**Using Underwater Acoustic Data To Predict the Distribution of Demersal Fish
in Western Australia**

Marcela Montserrat Landero Figueroa

This thesis is presented for the Degree of

Doctor of Philosophy

of

Curtin University

December 2018

Declaration of authorship

I, Marcela Montserrat Landero Figueroa, declare that to the best of my knowledge and belief this thesis contains no material previously published by any other person except where due acknowledgment has been made.

This thesis contains no material which has been accepted for the award of any other degree or diploma in any university.

The research presented and reported in this thesis was conducted in compliance with the National Health and Medical Research Council Australia code for the care and use of animals for scientific purposes 8th edition (2013). The proposed research study received animal ethics approval from the Curtin University Animal Ethics Committee, Sonar monitoring of marine animals from a vessel: AEC2013_26 and Baited Remote Underwater stereo-video: AEC_2014_09.

31/12/2018

“How inappropriate to call this planet Earth when it is quite clearly ocean”

Arthur C Clarke

“No man ever steps in the same river twice, for it’s not the same river and he’s not the same man”

Heraclitus

Abstract

Coral reefs are diverse ecosystems, providers of a series of environmental services and offer habitat for a variety of ecological and economically important species of fish. Coral reefs and the communities dependent on them are at risk of degradation from local and global stressors. Conservation efforts are currently focused mainly on Marine Protected Areas which are expected to protect a significant portion of the fish populations. However, a successful management of the MPAs will partially depend on effective monitoring of the fish population's changes over time. The collection of biological information in coral reef areas is logistically complex and expensive, and the observational methods currently available present some limitations and bias. The use of species distribution models based on benthic habitats surrogates can help to extrapolate point biological measurements to full coverage maps which can assist in conservation and management decisions. This study focuses on two main objectives aimed at helping in the assessment of demersal reef fish distribution in the coast of Western Australia: i) The development of models of potential distribution of demersal fish species, using biological data from Baited Remote Underwater Stereo-Videos (stereo-BRUVS) and benthic surrogates based on acoustic data; and ii) the possibility of combining optic and acoustic methods to produce a comprehensive evaluation of demersal fish distribution. These aims were explored mainly in the Ningaloo Marine Park (NMP) in the Northwest part of the coast of Western Australia considered as a hotspot of biodiversity.

Three interpolation methods were used to produce a full-coverage bathymetry using single-beam echosounder data (SBES). The best interpolated bathymetry was selected based on the minimum root mean squared error. A Random Forest (RF) classification analysis was used to produce species distribution models for six demersal species of fish using records from stereo-BRUVS, and depth derivatives based on SBES, and multibeam echo-sounder (MBES) data. The accuracy and spatial distribution of the residuals from the SBES were compared to the MBES models.

The performance of species distribution models for seven species was tested in three areas of the NMP before and after the addition of MBES seafloor backscatter. A RF classification analysis was used to produce the models, and changes in the accuracy of the models were assessed.

The possible value of adding historical data of water column backscatter from an SBES into models of the distribution of abundance and relative biomass from stereo-BRUVS data collected years apart was tested. A correlation analysis between the acoustic and stereo-BRUVS data was used as an exploratory analysis. A RF regression analysis was used to produce models of the distribution of abundance and relative

biomass before and after the addition of the water column backscatter data. For a broad-scale analysis, a Kruskal-Wallis rank sum test was used to evaluate the difference in biomass distribution recorded by the echo-sounder and stereo-BRUVS grouped by seafloor backscatter classes.

Two experiments were conducted to test the possibility of combining optic and acoustic methods in the assessment of spatial distribution of fish abundance and biomass. Cockburn Sound (CS) was one of the areas, and NMP was the other one. Correlation analyses were conducted between the acoustic variables and the relative abundance and biomass from the stereo-BRUVS. The differences in the biomass observed by the two methods in two benthic habitats were tested using a Wilcoxon rank sum test.

Kriging was found to be the best method to interpolate the SBES data, showing less error in the interpolated surface and similar accuracies in the RF model, compared to the MBES models. The inclusion of the MBES seafloor backscatter in the models of species distribution did not always improve the performance of the models, which was species and location dependent. However, the seafloor backscatter showed to be valuable for species with roaming behaviour and an affinity for rocky bottoms. The historical SBES water column data did not increase the variance explained by the RF model for the relative biomass or abundance in the NMP. The temporal variation between the two data sets is possible the main reason for the lack of relationship between them. A broad-scale analysis showed a possible relationship between the biomass distribution recorded by the two methods and the seafloor backscatter. The experiments conducted in CS and NMP showed significant correlations between the acoustics and stereo-BRUVS data.

In summary, this study shows the value of using underwater acoustic surrogates to help in the modelling of fish species distribution, to produce spatially explicit information to be used in conservation and management. The possibility of using SBES data which is easier and cheaper to collect and process, could reduce the cost of producing reliable information of species distribution, particularly, for roaming species with a wide niche. The addition of seafloor backscatter data can improve models of species with an affinity for rocky bottoms and roaming behaviour. Historical data from water column backscatter proved not be useful to detect fine-scale patterns of distribution of biomass or abundance detected by stereo-BRUVS when there is a significant temporal difference. However, it provides some insight of broad-scale drivers of the biomass distribution. Although further studies are needed, the results suggest acoustic and stereo-BRUVS data can be combined to comprehend the spatial distribution of fish biomass in reef areas. However, the simultaneous collection of both datasets is advised.

Acknowledgments

A big thank you to my supervisors without whom I would not have been able to walk this path. Special thanks to Iain Parnum for giving me the opportunity of joining the CMST family and the support during the PhD process. Also, a big thank you to Miles Parsons for always be willing to help and for helping me see things when I was not able to do so. Thanks to Ben Saunders and Chandra Salgado-Kent for their time and constructive comments which contributed to improving the manuscripts.

My gratefulness goes to the whole CMST family for making me feel as part of it, and for making going to work a happy experience. Thanks to my colleges and friends from the dungeon, without you, the PhD experience would not have been the same. Special thanks to all the great people I have the privilege to share my beloved room with, the old and the new ones including Tristan Lippert, Sven Gastauer for all the laughter, the coding help and for making me feel part of the group. Infinite thanks to Arti Verma and Bec Wellard, for the coffee, the doughnuts, the walks, the food, and the happiness that you brought into my life, I cannot imagine a happier place to work, thanks for all the technical and emotional support.

To all my friends in the office: Asma, Angela Recalde Salas, Sylvia Parsons, Arnaud Griffond and Mariana, for the coffees, lunches and long chats and for being there for me when needed.

A big thanks to Malcolm Perry, Ben Saunders, Sylvia Parsons, Ashleigh Roddick, and Iain Parnum, for your amazing collaboration and infinite patience during the fieldwork in Cockburn Sound and Ningaloo, I would not have been able to do it without you. To Lauren Hawkins for your help with fish identification and measurements, without you, the hours looking at the screens would have been longer. To the people at the Fish Ecology Lab, for your help with fish identification, and calibration of the cameras, I would not have been able to finish without your help.

To my sponsor in Mexico (Conacyt), and the financial support from CMST. This work would not have been possible without both of your support. And to the Australian Acoustical Society for the Education Grant which allowed me to conduct fieldwork in Ningaloo Marine Park.

To my friends in Mexico, because time and distance were not enough to prevent you from making me feel loved. Infinite thanks to Sagy Martinez, Daniel Mendez, Saul Pensamiento, and Johnny Valdez, for the calls, the text messages and skype meetings which gave me strength in difficult times.

To my friends in Perth, the old and new ones, thanks for making me feel at home. Special thanks to Siao Hui, Ruth, Libby, and Julieta. Thanks for the walks, the coffees, the drinks, and the long chats, thanks for being there for me sharing not only the happy but the difficult times during this process.

Last but not least, thanks to my family. For the unconditional love and moral support in this and all the other journeys of my life. Special thanks to my brother Julio Landero for always believing in me even when I could not do so, for the long phone calls and humour which was sometimes desperately needed.

Statement of candidate contributions

This thesis is presented as a series of four manuscripts to be submitted as scientific journal papers linked together by a general introduction and an overall discussion.

The design of the methodology was conducted in collaboration with my supervisors, and the data collection was conducted with the support of the CMST colleagues.

I carried out the analysis and write-up for each of the chapters with support and edits from my supervisors and collaborators.

Dr Iain Parnum assisted in the training for data collection and analysis. Dr Ben Saunders proved support and advice during field work. Dr Miles Parsons provided analytical advice for the acoustic data.

This thesis was written by me, with edits from Dr Iain Parnum, Miles Parsons, Ben Saunders and Chandra Salgado-Kent.

Marcela Montserrat Landero Figueroa

(Student)

Dr Iain Parnum

(Primary supervisor)

Contents

Declaration of authorship.....	i
Abstract	v
Acknowledgments.....	vii
Statement of candidate contributions	ix
List of Tables	xv
List of Figures	xvii
Chapter 1	1
1. General introduction.....	1
1.1. Random Forest.....	3
1.2. Collecting species biological data	4
1.2.1. Baited Remote Underwater Stereo-Videos: stereo-BRUVS.....	4
1.3. Collecting environmental data to predict the presence of species where biological data is not available.....	5
1.3.1. Using acoustics to characterise the seafloor	5
1.3.2. Water column acoustic data	7
1.4. Key knowledge gaps.....	7
1.5. Aims and objectives	8
1.6. Research significance	9
1.7. Study site	9
1.8. Thesis structural overview.....	12
Chapter 2	13
2. Can single-beam echo-sounder depth data be used to produce models of demersal fish distribution that are comparable to models produced using multibeam echo-sounder depth data in Ningaloo Marine Park, Western Australia?	13
2.1. ABSTRACT	14
2.2. INTRODUCTION.....	15
2.3. METHODS	16
2.3.1. Study area and data collection.....	16
2.3.2. SBES data processing	18
2.3.3. Spatial interpolation methods	18
2.3.4. Selection and comparison of best interpolation approaches	19
2.3.5. Digital Elevation Models	20

2.3.6.	Seafloor depth and its derivatives.....	20
2.3.7.	Demersal fish species distribution models	21
2.4.	RESULTS.....	23
2.4.1.	Selection and comparison of best interpolation approaches	23
2.4.2.	Seafloor depth and its derivatives.....	27
2.4.3.	Demersal fish species distribution models	29
2.4.4.	Variables importance.....	30
2.5.	DISCUSSION	34
2.5.1.	Selection and comparison of best interpolation approaches	34
2.5.2.	Seafloor depth and its derivatives.....	35
2.5.3.	Demersal fish species distribution models	36
2.6.	CONCLUSION	37
2.7.	ACKNOWLEDGEMENTS	38
Chapter 3	39
3.	Does the addition of seafloor backscatter data improve demersal fish distribution models based on multibeam bathymetry collected in Ningaloo Marine Park, Western Australia?.....	39
3.1.	ABSTRACT	40
3.2.	INTRODUCTION.....	41
3.3.	METHODS	42
3.3.1.	Study area	42
3.3.2.	Stereo-BRUV	45
3.3.3.	Depth and depth derivatives	45
3.3.4.	Backscatter derivative	46
3.3.5.	Angle vs. Range Analysis (ARA)	46
3.3.6.	Species distribution models	47
3.4.	RESULTS.....	49
3.4.1.	Angle vs. Range Analysis (ARA)	49
3.4.2.	Species distribution models	50
3.4.3.	Richness	52
3.4.4.	Variables importance in the distribution model	52
3.5.	DISCUSSION	54
3.5.1.	Backscatter derivatives.....	54
3.5.2.	Species distribution models	55

3.6.	CONCLUSION	57
3.7.	ACKNOWLEDGMENTS	57
Chapter 4	59
4.	Investigating the value of acoustic water column data in demersal fish assessment using historical data from Ningaloo Marine Park, Western Australia	59
4.1.	ABSTRACT	60
4.2.	INTRODUCTION.....	61
4.3.	METHODS	63
4.3.1.	Study area	63
4.3.2.	Acoustic data acquisition	64
4.3.3.	Post-processing of acoustic data.....	65
4.3.4.	Baited Remote Underwater Stereo-Video (stereo-BRUVS)	66
4.3.5.	Acoustic vs. stereo-BRUVS.....	67
4.3.6.	Models of demersal fish abundance and biomass	68
4.4.	RESULTS.....	71
4.4.1.	Spatial distribution of fish biomass and abundance	71
4.4.2.	Correlations between acoustic and stereo-BRUVS	73
4.4.3.	Model of fish biomass and abundance.....	76
4.5.	DISCUSSION	79
4.5.1.	Species distribution models	79
4.5.1.1.	Temporal difference	79
4.5.1.2.	Spatial resolution.....	80
4.5.1.3.	Broad-scale analysis.....	81
4.6.	CONCLUSION	81
4.7.	ACKNOWLEDGEMENTS	82
Chapter 5	83
5.	Investigating the temporal and spatial variation of acoustic water column data and its relationship with Baited Remote Underwater Stereo-Videos of demersal fish off the Western Australia Coast	83
5.1.	ABSTRACT	84
5.2.	INTRODUCTION.....	85
5.3.	METHODS	86
5.3.1.	Study area	86
5.3.2.	Data acquisition.....	88

5.3.3.	Data analysis	91
5.3.3.1.	Post-processing of the acoustic data	91
5.3.3.2.	Post-processing Stereo-BRUVS.....	92
5.3.3.3.	Acoustic vs. Stereo-BRUVS.....	93
5.4.	RESULTS.....	93
5.4.1.	Spatial experiments	93
5.4.1.1.	Cockburn Sound	93
5.4.1.1.	Ningaloo Marine Park	98
5.4.2.	Temporal experiments	103
5.4.2.1.	Ningaloo Marine Park	103
5.5.	Discussion	106
5.5.1.	Spatial experiments	107
5.5.1.1.	Cockburn Sound	107
5.5.1.2.	Ningaloo Marine Park	108
5.5.2.	Temporal experiment	109
5.5.3.	Limitations of the study	109
5.5.3.1.	Cockburn Sound	109
5.5.3.2.	Ningaloo Marine Park	110
5.5.3.3.	Stereo-BRUVS and echo-sounders	110
5.6.	CONCLUSION	111
Chapter 6	112
6.	General Discussion.....	112
6.1.	AIM AND OBJECTIVES OF THE THESIS	113
6.1.1.	Performance of SBES seafloor data in the construction of demersal fish distribution models compared to the results obtained by using MBES data	113
6.1.2.	Effect of adding the seafloor backscatter data as an explanatory variable to demersal fish distribution models.....	114
6.1.3.	Value of historical water column backscatter data in assessing demersal fish distribution and abundance	115
6.1.4.	Temporal and spatial variation of abundance of demersal fish using SBES water column data and stereo-BRUVS data	116
6.1.4.1.	Cockburn Sound	117
6.1.4.2.	Ningaloo Marine Park	117
6.1.4.3.	The portion of the fish sampled by acoustics vs. stereo-BRUVS.....	118

6.2. CONCLUSIONS.....	118
References	120
Publications part of this thesis.....	132
Appendix A.....	133
Appendix B.....	159
Appendix C.....	160

List of Tables

Table 2.1. Depth derivatives produced from SBES depth data.....	21
Table 2.2. Root mean squared error (RMSE) for the different combinations of powers and number of neighbours tested in the inverse distance weighting interpolation. The best interpolation is indicated by the lowest value of RMSE.....	23
Table 2.3. Root mean squared error (RMSE) for the multiquadratic (M) and completely regularized spline (CRS) radial basis functions (RBFs). Three scenarios of a maximum number of neighbours (n) are shown, and the lowest value of RMSE is shown in bold.....	24
Table 2.4. Parameters of the Gaussian models fitted to the empirical variograms comparing Ordinary, and Universal kriging first and second degree detrending, as well as isotropic and anisotropic directionality. Partial sill (psill) is the sill minus the nugget effect.	24
Table 2.5. Root mean square error (RMSE) from cross-validation for the kriging interpolations. The model with the smallest difference between the average kriging standard error (ASE) and RMSE is marked in bold.....	25
Table 2.6. Performance of the models measured by the five-fold cross-validation mean AUCs. The results for the species modelled are shown for MBES and interpolated SBES data using universal kriging with a first-degree detrending (UK1) inverse distance weighting (IDW), and radial basis function (RBF). The number of presences of the species in the study site is also shown.....	30
Table 3.1. Depth derivatives produced from bathymetry. Aspect (orientation of the slope) was divided in two variables using trigonometric transformations.....	46
Table 3.2. Habitat and feeding preference of the species included in the study.	48
Table 3.3. Mean percentage of variance explained by the Random Forest for the total richness of species in the three study sites for both the depth and depth derivatives (DV, BT+DV) and depth, depth derivatives and seafloor backscatter data (DVBS, BT+DV+BS) scenarios.	52
Table 3.4. Summary of variable importance in the construction of the distribution models for the species included in the study. Only the three variables with highest ranking of importance are included for each species and each scenario. The scenario of depth and derivatives (DV) and depth, depth derivatives and backscatter data (DVBS) scenarios are shown.	53
Table 4.1. Terrain variables used in the Random Forest models. The depth derivatives were calculated using four sizes of neighbourhoods (3, 9, 15 and 21).....	70

Table 4.2. Results of the Random Forest models for the MaxN and relative biomass from the stereo-BRUVS, using terrain variables (Table 4.1) and adding the 2008 depth-stratified NASC data averaged to create a 250 m resolution grid (WC data) in the Mandu area. The results for the model of depth-stratified NASC and depth-stratified NASC no schools 2008 using terrain variables are also show. Correlations are between the estimated and real value. 76

Table 5.1. Settings of the transducers mounted in the pontoon, for the two experiments and the two areas included in the study. 89

Table 5.2. Results of the stereo-BRUVS analysis for the three sites considered in the temporal analysis. 104

Table 5.3. Results of the post hoc Dunn test for comparison of depth-stratified NASCs medians of the three sites grouped by time: before the stereo-BRUV deployment, during the soaking time and the day after. Only the demersal layer is considered (0.5-5.05 m above the seafloor). 105

Table 5.4. Results of the post hoc Dunn test for comparison of depth-stratified NASCs medians of the three sites grouped by time: before the stereo-BRUV deployment, during the soaking time and the day after. The full water column is considered. 106

List of Figures

Figure 1.1. Study site in the Ningaloo Marine Park is a tropical area of Western Australia located 1000 km north of Perth..... 11

Figure 2.1. Map indicating (a) the study site located in the north section of the Ningaloo Marine Park, and (b) the locations of single-beam echo-sounder survey tracks shown in red and stereo BRUVS deployment sites shown with black dots..... 17

Figure 2.2. Coefficient of determination (R^2) between best SBES the interpolated surfaces and the multibeam data (MBES). Five intervals of distance from the original SBES track are shown for universal kriging with a first-degree of detrending (UK1), inverse distance weighting (IDW), and radial basis function (RBF). In all cases, the linear relationship was significant ($p < 0.001$)..... 26

Figure 2.3. Bathymetry of the study site using a 3D projection for a) MBES and the best SBES data interpolations in this study using: b) universal kriging with first degree of detrending, c) inverse distance weighting, and d) radial basis function..... 26

Figure 2.4 Mean and standard deviation (as error bar) of the depth derivatives based on the MBES and interpolated SBES data using universal kriging with a first-degree detrending (UK1), inverse distance weighting (IDW), and radial basis function (RBF). The four resolutions included in the analysis are shown. a) slope measured in degrees, b) mean curvature (MNC), c) northness (slopes facing north (NS=1), south (NS=-1)), d) topographic position index (TPI), e) eastness (slopes facing east (WE=1), or west (WE=-1)), f) terrain ruggedness index (TRI), g) standard deviation of depth (SD), and h) roughness. 28

Figure 2.5 3D projection of the roughness derivate from the MBES and interpolated SBES data using universal kriging with a first-degree detrending (UK1), inverse distance weighting (IDW), and radial basis function (RBF). The four resolutions included in the analysis are shown. 29

Figure 2.6 Variables importance in the construction of the Random Forest models using MBES and SBES interpolated data with Universal Kriging with first degree of detrending (UK1), Inverse distance weighting (IDW), and Radial Basis Function (RBF) for a) *A. stellatus*, b) *G. grandoculis*, c) *L. scleratus*, d) *L. macrorhinus*, e) *P. multidentis*, and f) *P. typus*. For brevety, only the 20 most important variables (according to the MBES model) are shown. 32

Figure 2.7. Maps of probability of occurrence of *P. typus* based on depth and depth derivatives of the MBES and the three interpolation techniques tested: Universal Kriging with first degree of detrending (UK1), inverse distance weighting (IDW) and radial basis function (RBF). 33

Figure 2.8. Spatial distribution of the residuals of the Random Forest predicting the testing portion of the *P. typus* data. Positive values corresponds to under predictions while negative values represent over predictions. 34

Figure 3.1. Study site. a) Mandu in the northern area of the NMP, b) Point Cloates in the central area and c) Gnaraloo in the southern area of the NMP. The deployment location of the stereo-BRUVS is shown as red stars, and the backscatter mosaics are shown as black and white images. 44

Figure 3.2. Linear regression between the grain size calculated with the ARA analysis and the phi size calculated from the ground-truth samples. 50

Figure 3.3. Mean AUC and standard error of the Random Forest distribution models for *A. stellatus*, *G. grandoculis*, *L. sceleratus*, *L. miniatus*, *L. macrorhinus*, *L. sebae* and *S. queenslandicus* in the three study sites of the Ningaloo Marine Park. The depth and depth derivative scenario (DV), and the depth, depth derivatives plus the backscatter data (DVBS) scenario are shown. 51

Figure 4.1. Study site, a) Location of the two study sites in the Ningaloo Marine Park, b) Zoom to the Mandu area with the acoustic survey showed in brown and the location of the stereo-BRUVS deployments showed as black dots, c) Zoom to the Point Cloates area. 64

Figure 4.2. Example of the extraction of acoustic data to be compared with the stereo-BRUVS data. On the left side, an S_v mean echogram where the acoustic energy was exported using a grid with Intervals 50 m long and 5 m depth Layers. Each interval is represented on the right side as a blue dot. Different radii of search around the stereo-BRUVS were used to extract the acoustic data, a 150 m radius is shown as an example. 68

Figure 4.3. The abundance fish (MaxN) register by the stereo-BRUVS is shown in the left side for both the Mandu area (top) and the Pt Cloates (bottom). The number of acoustic targets for 2006 and 2008 for both areas are also shown at the centre and right of the figure. 72

Figure 4.4. The relative biomass from the stereo-BRUVS is shown on the left side for both the Mandu area (top row) and the Pt Cloates (bottom row). The depth-stratified NASC for 2006 and 2008 in the two areas is also shown at the centre and right of the figure. 73

Figure 4.5. Summary of correlations between the relative biomass of the stereo-BRUVS and acoustic variables including a) $NASC_{BRUV-mean}$ 2006, b) $NASC_{BRUV-mean}$ 2008, c) $NASC_{BRUV-mean}$ no schools 2006, d) $NASC_{BRUV-mean}$ no schools 2008, e) Number of targets 2006, and f) Number of targets 2008). At different radii of search distance around the stereo-BRUVS (50-1500 steps of 50 m), and including different Layers of water column (5 m depth each) where Layer 0 = 1-6 m above the seafloor. 74

Figure 4.6. Summary of correlations between the MaxN of the stereo-BRUVS and acoustic variables including a) $NASC_{BRUV-mean}$ 2006, b) $NASC_{BRUV-mean}$ 2008, c) $NASC_{BRUV-mean}$ no schools 2006, d) $NASC_{BRUV-mean}$ no schools 2008, e) Number of targets 2006, and f) Number of targets 2008). At different radii of search distance around the stereo-BRUVS (50-1500 steps of 50 m), and including different Layers of water column (5 m depth each) where Layer 0 = 1-6 m above the seafloor..... 75

Figure 4.7. Importance of terrain variables in the Random Forest model of the distribution of 2008 depth-stratified NASC no schools. Variables names according to Table 4.1, the number in the names of the variables corresponds to the neighbourhood used in its calculation. 77

Figure 4.8. Percentage of biomass as recorded by the stereo-BRUVS (relative biomass, blue) and acoustics ($NASC_{BRUV-mean}$, red) in relation to the: depth gradient for a) 2006 data, and b) 2008. Percentage of biomass and mean NASC compared to a gradient of phi sediment size estimated using the seafloor backscatter for: c) 2006, and d) 2008..... 78

Figure 4.9. Percentage of biomass as recorded by the stereo-BRUVS (relative biomass, blue) and acoustics ($NASC_{BRUV}$, red) in relation to the depth gradient of phi sediment size estimated using the seafloor backscatter for: a) 2006, and b) 2008..... 79

Figure 5.1. Cockburn Sound study site off the South-West coast of Australia, b) Stereo-BRUVS deployment sites (black star) and echo-sounder transects (continuous line). The benthic habitat classification is an adapted version of (Cockburn Sound Management Council, 2004). 87

Figure 5.2. a) Map of Australia with a magnification of the Exmouth peninsula, delineating areas of the Commonwealth Marine Reserve and the Ningaloo Marine Park. b) Expansion of the study site within the Marine Park with the locations of the temporal and spatial study locations marked. c) Expansion of the spatial site with seafloor E1 (coloured areas), together with deployment locations of stereo-BRUVS (red stars) and echo-sounder transects conducted (black dots). 88

Figure 5.3. Three echo-sounders were mounted in a pontoon which was towed on the side of the vessel (left and centre). One of the Stereo-BRUVS used in the experiments is shown on the right of the figure. 89

Figure 5.4. The three echo-sounders mounted in the pontoon and the GPS antenna in the centre, towed by the vessel..... 91

Figure 5.5. a) Abundance and b) relative biomass from the stereo-BRUVS in the Cockburn Sound area laid over the benthic habitat map. c) Total number of acoustic targets and d) depth-stratified NASC are shown with the stereo-BRUVS data showed as graduated circles..... 94

Figure 5.6. a) Correlations between the $NASC_{BRUV-mean}$ and relative biomass recorded by the stereo-BRUVS, and b) $NASC_{BRUV-mean}$ without schools and relative biomass at different radius of search around the stereo-BRUVS and depth Layers. 95

Figure 5.7. Correlations between the relative biomass from the stereo-BRUVS and a) $NASC_{BRUV-mean}$ no schools, and b) acoustic targets using a 300 m radius of search around the stereo-BRUVS and including acoustic data from 15.5 and 10.5 m above the seafloor respectively. The standard errors are shown as error bars. 96

Figure 5.8. Correlations between the relative biomass without rays from the stereo-BRUVS and the $NASC_{BRUV-mean}$ no schools (left), and acoustic targets (right) using a 250 m and 400 m radii of search respectively around the stereo-BRUVS and including 10.5 m above the seafloor. The standard error is shown in the error bars, and the number of acoustic samples is also shown. 97

Figure 5.9. Boxplot of the MaxN, relative biomass, $NASC_{BRUV-mean}$, $NASC_{BRUV-mean}$ no schools and acoustic targets grouped by benthic habitat class. 97

Figure 5.10. Spatial distribution of the relative biomass a) and MaxN c) with the acoustic classification of the seafloor. The results of the acoustic analysis are shown in the right side of the figure depth-stratified $NASC$ with the relative biomass (b) and MaxN (d) from the stereo-BRUVS data shown as graduate circles. 98

Figure 5.11. Correlations between the $NASC_{BRUV-mean}$ and the relative biomass (left) and MaxN (right) from the stereo-BRUVS using different radii of search around the stereo-BRUV, and including different Layers of the water column. Layer 0 represents the interval 0.5-5.5 m above the seafloor. 99

Figure 5.12. Correlations between the abundance (MaxN) from the stereo-BRUVS and the $NASC_{BRUV-mean}$ using different radii of search around the stereo-BRUVS and including different Layers of the water column starting from the surface (left). Layer 0 represents the interval 0.5-5.5 m above the seafloor. Correlation between MaxN and the $NASC_{BRUV-mean}$ using a radius of search of 250 m and excluding 40.5 m closer to the bottom (right), the number of acoustic samples (intervals) considered in the calculation of the $NASC_{BRUV-mean}$ and the standard error are shown. 100

Figure 5.13. Spatial distribution of the depth-stratified $NASC$ excluding the 40.5 m closer to the bottom with the relative abundance from the stereo-BRUVS (MaxN) plotted as graduated circles. 100

Figure 5.14. Correlation between the $NASC_{BRUV-mean}$ and the relative biomass from the stereo-BRUVS excluding the sharks and rays using different radii of search around the stereo-BRUV and including different Layers of the water column starting from the bottom (left) and top (right). 101

Figure 5.15. Benthic habitats present in the sampling points. a) Classification of the benthic habitats based on the stereo-BRUVS data over the seafloor backscatter. b) Example of the bottoms classified as “Sand”. c) Example of benthic habitat classified as “Reef” in the spatial experiment at Ningaloo Marine Park..... 102

Figure 5.16. Box plots of the abundance (MaxN) and relative biomass from the stereo-BRUVS, $NASC_{BRUV-mean}$, and $NASC_{BRUV-mean}$ no schools grouped by the benthic habitat observed in the stereo-BRUVS. . 103

Figure 5.17. Box plots of the acoustic variables $NASC_{BRUV-mean}$, and $NASC_{BRUV-mean}$ without schools grouped by benthic habitats excluding the 40.5 m of water column above the seafloor. 103

Figure 5.18. Temporal 1 had predominately sandy bottom with some algae (left), the Temporal 2 (centre) was located in a sandy bottom, and the Temporal 3 had a sandy bottom with the presence of sponges and soft corals (right). 104

Figure 5.19. Distribution of depth-stratified NASC in the demersal layer (5 m above the seafloor) of the temporal 1 (left) temporal 2 (centre) and temporal 3 (right) sites before, during and a day after the deployment of the stereo-BRUV. Each point in the plot represents one 50 m Interval of depth-stratified NASC. 105

Figure 5.20. Distribution of the depth-stratified NASC in the second (left) and third (right) sites of the temporal experiment considering the full water column. Each point in the plot represents one 50 m Interval..... 106

Chapter 1

1. General introduction

Coral reefs are a highly biodiverse ecosystems (Sheppard et al., 2009) and provide a variety of ecological services and habitat for many biologically and economically important fish species (Sale, 2002). However, coral reefs are one of the most fragile habitats facing increasing human pressure (Hughes et al., 2003, Pandolfi et al., 2011). The increasing efforts to conserve coral reef communities in the face of local and global threats rely predominantly on the establishment of Marine Protected Areas (MPAs). It is expected that such MPAs can increase the spatial resilience of reef ecosystems by protecting populations that can reseed the affected areas (Hughes et al., 2003).

To measure the impact of MPAs on fish species abundance and spatial distribution, it is necessary to develop effective species population monitoring programs (Hill et al., 2014a, Young et al., 2017). This requires the production of spatially explicitly information of coral reef fish assemblage distribution and abundance, for successful management in a changing environment (Sequeira et al., 2018, Galaiduk et al., 2017b).

The use of environmental variables combined with biological data to produce models of fish species distribution can assist in the elucidation of spatial patterns necessary to guide conservation efforts (Haggarty and Yamanaka, 2018, Monk et al., 2011). However, the success of modelling species distribution depends on the inclusion of variables closely related to direct factors driving their distribution (Schultz et al., 2014). Depth is considered an indirect surrogate of fish distribution as it is associated with variables such as temperature and light availability which can influence the distribution of the species (Sih et al., 2017, Hill et al., 2014b). Depth derivatives related to seafloor complexity (e.g., roughness) have also been linked to fish distribution and are now commonly used in models of fish distribution (Young and Carr, 2015). The production of full-coverage bathymetries used to produce depth derivatives included in models of species distribution is usually based on multibeam echo-sounders (MBES) data. MBES data collection and processing are expensive and logistically demanding. The use of single-beam echo-sounder (SBES) data to produce species distribution models with similar levels of accuracy to the ones produced with MBES data offers an attractive alternative, to significantly reduce the cost, of producing spatially explicit information on demersal fish distribution.

The reflectivity of the seafloor (backscatter) is a variable that can be used to approximate the seafloor roughness and hardness, which can indirectly affect fish distributions (Monk et al., 2011, Monk et al., 2010). However, the use of seafloor backscatter and in particular the use of the Angle vs Range Analysis (ARA) in the study of demersal fish distribution models have been scarce (Monk et al., 2010, Young et al., 2010). An improvement of demersal fish distribution model's accuracy by adding seafloor backscatter data

already available would represent a benefit in the predictive power of the models, without increasing the cost in the data collection.

Fish biomass and density are two critical variables that can be used as indicators of the MPAs performance. However, some of the most common techniques used to monitor demersal fish assemblages in coral reef areas, including underwater visual census, baited/unbaited underwater videos, and acoustics have their own limitations and bias. For example, visual census can produce estimates of fish density, but the assessments can be biased depending on the strength of fish behavioural response (i.e. avoidance, attraction) to the presence of divers (Willis et al., 2000), and are restricted in the spatial area that can be covered (Andrefouet and Riegl, 2004, Irigoyen et al., 2013). Baited underwater videos, on the other hand, can produce a characterization of the assemblage of species. However, the estimation of density requires a measure of the area of influence of the bait-plume which varies depending on the seafloor structure, currents and species-specific response to the bait plume, and soak time (Cappo et al., 2004). Consequently, the estimation of density is rarely done and relative biomass and abundance are reported (Ellis and Demartini, 1995, Cappo et al., 2004). The use of acoustics in the estimation of fish density and biomass is a common practice in temperate regions but is more limited in coral reef areas with complex bottoms where the collection of ground-truth information has not been standardised (Zenone et al., 2017). Therefore, previous studies have suggested the use of more than one method can help to have a better understanding of the fish density and biomass at a MPA level (Murphy and Jenkins, 2010, Willis et al., 2000). The combination of data collected with stereo-BRUVS, including abundance and biomass, with historical SBES water column data could improve our ability to monitor these two important parameters (Halpern, 2003). The potential to apply such models to historical data, where only SBES could be afforded (financially, logistically or technically) holds the potential to develop comparative distribution maps for a given area through time.

1.1. Random Forest

Random Forest (RF) as proposed by (Breiman, 2001) was used in this study to model the distribution of demersal species of fish. RF is a machine-learning technique which has been shown to outperform conventional statistical techniques such as linear and generalized additive regression models when used to model the distribution and diversity of demersal fish (Knudby et al., 2010, Smolinski and Radtke, 2017). RF can be used for both regression and classification problems and is based on growing many classification or regression de-correlated trees and then averaging their predictions (Liaw and Wiener, 2002). The algorithm starts by selecting bootstraps samples n_{tree} from the original data. Usually, 63% of the original

observations are included at least once in the bootstrapped samples, the observations not included in the bootstrap sample are called the out-of-bag (OOB) observations. An unpruned classification or regression tree is fully grown for each bootstrap sample. However, at each node of the trees, a randomly selected sample of explanatory variables m_{try} is used to select the best split instead of including the full set of variables. Usually m_{try} is the square root of the number of explanatory variables for classification and the number of variables divided by three for regression. The final prediction for the new data is based on the aggregation of the predictions of the n_{tree} trees, the majority votes in the classification case and the average for regression (Liaw and Wiener, 2002).

The grown trees are used to predict the OOB observations, and the accuracies and error rate are calculated for each OOB prediction. The estimated error can be seen as a cross-validated accuracy estimate as the OOB observations were not used during the fitting of the trees. The importance of the explanatory variables is estimated based on changes in the error rate when a modified version of the explanatory variable with randomly selected values is used to fit the trees. The difference in the error rate of each tree between the original and modified OOB data, divided by the standard error, is a measure of the variable importance. If a variable is critical in the prediction, changes in this particular variable would have a significant impact on the error rate of the prediction (Liaw and Wiener, 2002).

1.2. Collecting species biological data

1.2.1. Baited Remote Underwater Stereo-Videos: stereo-BRUVS

The use of underwater cameras in the study of fish abundance and species richness has been present since 1902 (Hardinge et al., 2013). The use of these techniques has grown as they offer a series of advantages compared to other methods. Underwater cameras can operate at a wider depth range compared to visual census and can be used to sample deeper areas. They can also be used in non-trawling grounds, and are particularly useful to sample no-take areas like marine parks (Watson et al., 2010). A decrease in the price of high-resolution cameras has led to the increase in the use of this technology, and the development of standardized calibration procedures (Fitzpatrick et al., 2012). Stereo-BRUVS, in particular, has become one of the preferred methods to assess demersal species assemblages in coral reef areas (Cappo et al., 2004). Stereo-BRUVS have shown to be well suited to sample large predatory species (Moore et al., 2010, Bouchet et al., 2018), however, they are less effective in sampling small cryptic species, compared to diver operated stereo systems. A conservative measurement of abundance is obtained by counting the maximum number of organisms of the same species present in a frame at one time during the period being analysed (MaxN; Watson et al., 2010). The possibility to measure fish length

with high levels of precision allows the scientist to estimate the biomass of the organisms based on the weight-length relationship (Harvey et al., 2003). However, the main disadvantage of the stereo-BRUVS is the unknown area of influence of the bait-plume which can vary based on the topography, currents, soak time and the swimming speed of species (Ellis and Demartini, 1995, Cappo et al., 2004). Therefore, the biomass estimated with the stereo-BRUVS cannot be transformed into a density of fish, and relative biomass is reported instead (Cappo et al., 2004). In their original design, stereo-BRUVS were deployed on the seafloor with the focus on sampling the demersal and semi-demersal species, but the presence of pelagic species in the recording are not uncommon (Cappo et al., 2004).

1.3. Collecting environmental data to predict the presence of species where biological data is not available

1.3.1. Using acoustics to characterise the seafloor

Seafloor characteristics, including rugosity, hardness, percentage of vegetation coverage among others have been linked to the occurrence of demersal fish species (Becker et al., 2009, Demestre et al., 2000, Lucieer and Pederson, 2008, Ierodiaconou et al., 2011, Galaiduk et al., 2017a, Young et al., 2010). The geomorphology, in particular, has been recognised as an important factor influencing the distribution of demersal species at different scales (Demestre et al., 2000, Monk et al., 2011, Pierdomenico et al., 2015, Moore et al., 2011). However, mapping the seafloor can be technically challenging, expensive and time-consuming. Therefore, despite the recognition of seafloor importance, only between 5-10% of the world's seafloor has been mapped at fine resolution e.g., meters to decimetres (Wright and Heyman, 2008, Jones and Brewer, 2012).

The development of underwater acoustic mapping technology in the last two decades has enabled scientists to collect accurate information of the seafloor geomorphology and substrate characteristics. Underwater acoustic systems can operate in a wide range of depths, beyond the limits of the satellite remote sensing techniques, and in some cases, with resolution comparable to terrestrial studies (Bartholomae et al., 2011). During an acoustic survey by an active sonar, acoustic energy is transmitted into the water, the delay between transmission and reception of the reflected wave is used to estimate depth (bathymetry). The amount of energy reflected by the seafloor (backscatter) can be used to infer the acoustic 'roughness' and 'hardness' of the bottom (Brown et al., 2011). Strong targets present in the water column, e.g., fish, can also reflect part of the acoustic energy producing water column backscatter. Active sonars include single-beam echo-sounders (SBES), multibeam echo-sounders (MBES), and side scan sonars. SBES usually operate in lower frequencies between 17 and 200 kHz, while MBES normally operate

at higher frequencies between 12 kHz and 700 kHz. Higher frequencies produce higher resolution data but suffer from higher attenuation and low penetration in the seafloor (Schneider von Deimling et al., 2013).

SBES are one of the simplest echo-sounders capable of collecting bathymetry and backscatter data. During an SBES survey, a transducer is typically mounted on a vessel facing down, and the acoustic energy is transmitted downwards insonifying the area under the transducer. The size of the insonified area will depend on the beam angle and depth (Foster-Smith and Sotheran, 2003). The first (E1), and second (E2) echos produced by the seafloor in an SBES survey have been used to classify seafloors with higher levels of backscatter as 'acoustically hard' (i.e. dense, consolidate) or 'acoustically rough' (relative to the acoustic wavelength). Low levels of backscatter are usually associated with flat, silty sand (Foster-Smith and Sotheran, 2003). However, the second echo can also be hard to interpret and utilise, as the propagation geometry is not trivial.

MBES systems consist of acoustic transducers to transmit and receive sound waves to and from the seafloor, which result in a fan of narrow beams (typically 100s) covering a swath area perpendicular to the route of the vessel (Pandian et al., 2009, Lurton, 2002). MBES are usually used to produce full-coverage maps of bathymetry and seafloor backscatter with high resolution. As with the SBES, the backscatter data can be used to infer acoustic roughness and hardness of the seafloor (Innangi et al., 2015). The seafloor backscatter recorded in an MBES survey is usually used to produce a mosaic with the same resolution of the bathymetry. In the mosaic approach, the backscattered energy received from different grazing angles is normalised for a certain angle or a range of angles. However, for certain frequencies, the relationship between grazing angle and intensity of backscatter can be used to infer more information about the seafloor properties (Fonseca and Mayer, 2007). In an Angle vs Range Analysis (ARA) the pattern of backscatter response at a range of grazing angles is compared to expected acoustic response curves for various substrate types, based on a mathematical model, the Jackson Model (Jackson et al., 1986). The ARA can be used to estimate the sediment grain size (Fonseca and Mayer, 2007), which has been shown in some demersal species to be a driver of distribution, or at least a correlate (McConnaughey and Smith, 2000). The use of seafloor backscatter mosaic in modelling the distribution of benthic habitats has increased in the last decade (Ierodiaconou et al., 2007, Brown et al., 2012, Hasan et al., 2012a). Less attention has been placed on using the angular response data in models of demersal fish distribution which traditionally included the mosaic image and derivatives e.g., texture features (Monk et al., 2011, Monk et al., 2010, Young et al., 2010).

Because of its high resolution and swath coverage, MBES has become a popular method for characterising the seafloor. However, the use of MBES typically requires much greater financial and technical resources for operation and data analysis than SBES. In contrast, SBES is usually the simplest and cheapest system for collecting bathymetric information. The main disadvantage of SBES is its limited coverage; therefore, interpolation is required to fill the gaps to make up a continuous seafloor map.

1.3.2. Water column acoustic data

Scientific echo-sounders are capable of recording the water column backscatter, which is produced by any object or organism present in the water column with a different density than the surrounding medium. The magnitude of the echo produced by a 'target', such as fish or other marine organisms, ('target strength') can be used to infer characteristics of the target. However, the target strength is a stochastic variable, with a range of values described by a probability of distribution (Simmonds and MacLennan, 2008). The species, size, morphology (e.g., presence or absence of a swim bladder), depth, swimming angle among other variables can affect the target strength. Therefore, the conversion of acoustic energy into species-specific biomass is not a straight-forward process. Ground-truth information is needed to inform on the species being insonified, along with length distribution of the targets. In temperate regions, the use of acoustics in fish-stock assessment is a well-established method, and ground-truth data is normally obtained by using nets (Kloser et al., 2002). Also, a limited number of species typically present in temperate regions reduce, partially, the complexity of transforming the acoustic energy into biomass.

The use of acoustics for monitoring fish biomass has many advantages, including the possibility of covering large areas in a short period, and the opportunity of gather information about different components of the ecosystem sampled in the water column (e.g., zooplankton). However, the main disadvantage for using acoustics in coral reef areas is the need of ground-truth data which is harder to collect in no-trawling diverse areas. Therefore, the use of optic methods to provided ground-truth data is proposed as an alternative (Boswell et al., 2010, Costa et al., 2014, Campanella and Taylor, 2016).

1.4. Key knowledge gaps

Although an increasing number of studies have been produced relating the distribution of demersal fish to MBES bathymetry and depth derivatives (Galaiduk et al., 2017b, Ierodiaconou et al., 2011, Monk et al., 2011, Monk et al., 2012, Monk et al., 2010), it is unclear if the high resolution produced by MBES is required to produce reliable models of demersal fish distribution. The potential of using accurate seafloor

maps using SBES interpolated data would reduce the cost of producing demersal fish distribution models needed for conservation and management.

MBES surveys main focus is usually collecting bathymetric data, although, seafloor backscatter data has increasingly been collected, it is not necessarily an objective of the surveys. A possible benefit of including seafloor backscatter data in demersal fish distribution models has been proposed (Schultz et al., 2014), yet the number of publications in which the backscatter is included in demersal fish distribution models has grown slowly (Monk et al., 2010, Young et al., 2010). This is due to the complexity of data processing and in part, a current lack of standardisation in acquisition and data pre-processing. In instances in which the seafloor backscatter has been added, the angular information contained in the seafloor backscatter, which might be more related to the distribution of species is usually discarded and the backscatter is only included as a mosaic in which the angular responses are normalised (Monk et al., 2010). Using the seafloor backscatter that has already been collected in the construction of demersal fish distribution models has the potential of improving the models without increasing the cost of data collection.

The estimation of demersal fish biomass in coral reef areas is a fundamental question that remains harder to estimate using traditional methods designed to assess the assemblage of fish in coral reef areas (Cappo et al., 2004). Fisheries acoustics methods have been used to monitor the fish stocks in some of the most important fisheries in temperate regions around the world (Simmonds and MacLennan, 2008). The use of water column backscatter collected with either SBES or MBES could add to the successful modelling of the biomass distribution of species in coral reef areas. However, the necessity of collecting ground-truth information for transforming the water column backscatter into species-specific biomass has been one of the main limitations for using acoustics in coral reef areas with high species heterogeneity. Though, the use of underwater acoustics in coral reefs is increasing with visual techniques providing the complementary source of validation data (Boswell et al., 2010, Costa et al., 2014, Campanella and Taylor, 2016).

1.5. Aims and objectives

This thesis aimed to evaluate the performance of demersal fish distribution models based on underwater acoustic and stereo-BRUVS data, in suitable areas of the Western Australia coast. This was evaluated with four specific objectives:

1. To use SBES seafloor data in the construction of demersal fish distribution models based on stereo-BRUVS data, and to compare the accuracy of the models obtained by using MBES data.

2. Measure the effects of adding seafloor backscatter data as an explanatory variable to demersal fish distribution models in terms of the accuracy.
3. Elucidate the value and requirements of the use of historical water column backscatter data in assessing demersal fish abundance and biomass distribution.
4. Investigate the temporal and spatial variation of the abundance of demersal fish using SBES water column data and stereo-BRUVS data.

1.6. Research significance

Effective conservation and management of the marine environments require information about distribution and abundance of different fauna, such as fish. However, collecting detailed and frequent data from the marine environment's fauna can be costly. Therefore, the development and validation of cost-effective methods that provide spatially explicit information of demersal fish distribution would be a positive outcome for conservation managers and marine scientists. In addition, the integration and comparison of acoustic and video techniques, will further assist in the understanding and improve the assessment of demersal fish abundance and biomass in coral reef areas, which will be significant for fisheries research.

1.7. Study site

To achieve the objectives of this thesis, the Ningaloo Marine Park (NMP) was used as the main study site based on the ecological importance of the site, but also in the availability of both acoustic and stereo-BRUVS data.

Located off the coast of north-western Australia, Ningaloo Reef (NR) is the longest fringing coral reef in Australia and is recognised as a global biodiversity hotspot, as it is home to a wide variety of wildlife, including many endangered species (Gazzani and Marinova, 2007, Schonberg and Fromont, 2012). The established NMP protects 260 of the 290-km-long NR.

NR is considered a well-preserved reef area. A stable average coral coverage of around 28% have been reported across NR for a period of 25 years (1987-2012; Speed et al., 2013). However, particular areas of the NR including the north-eastern and southern have experienced a decline in overall coverage. Periodic disturbances including severe bleaching events in 2010-2011 and 2012-2013, and several cyclones have been linked to the declining in the coral coverage in particular areas of the NR (Depczynski et al., 2009, Moore et al., 2012).

The general trend of stable mean coral coverage observed in NR is probably related to the lack of long term anthropogenic pressure including agricultural runoff and intense commercial fishing during the last 25 years. The apparent stability of the NR contrast with the general trend of declining of coral reef systems around the globe including the GBR. Nevertheless, NR is facing an increasing human pressure, mainly through a significant growth in tourism. The number of people participating in whale shark tours, for example, increased from around 2,000 in 1996 to more than double that by 2006 and continues to increase (Catlin and Jones, 2010). The local pressures, in addition to the global changing environment that coral reefs are facing around the world, make the NR potentially at risk of degradation.

To obtain knowledge on the ecology and biodiversity of NMP, a multi-institutional research program was conducted by Western Australia Marine Science Institute (WAMSI) partners between 2006 and 2009 (Waples and Hollander, 2008). As part of this program, SBES data were collected between 2006 and 2008 (Colquhoun et al., 2007). The assemblage and relative abundance of demersal fish were surveyed using stereo-BRUVS (Simpson and Waples, 2012) in three different locations of the NMP including Mandu, Point Cloates and Gnarlou in 2009 (Figure 1.1). Another project carried out by Geoscience Australia (GA) collected MBES data in some areas of the NMP in 2008 (Brooke et al., 2009).

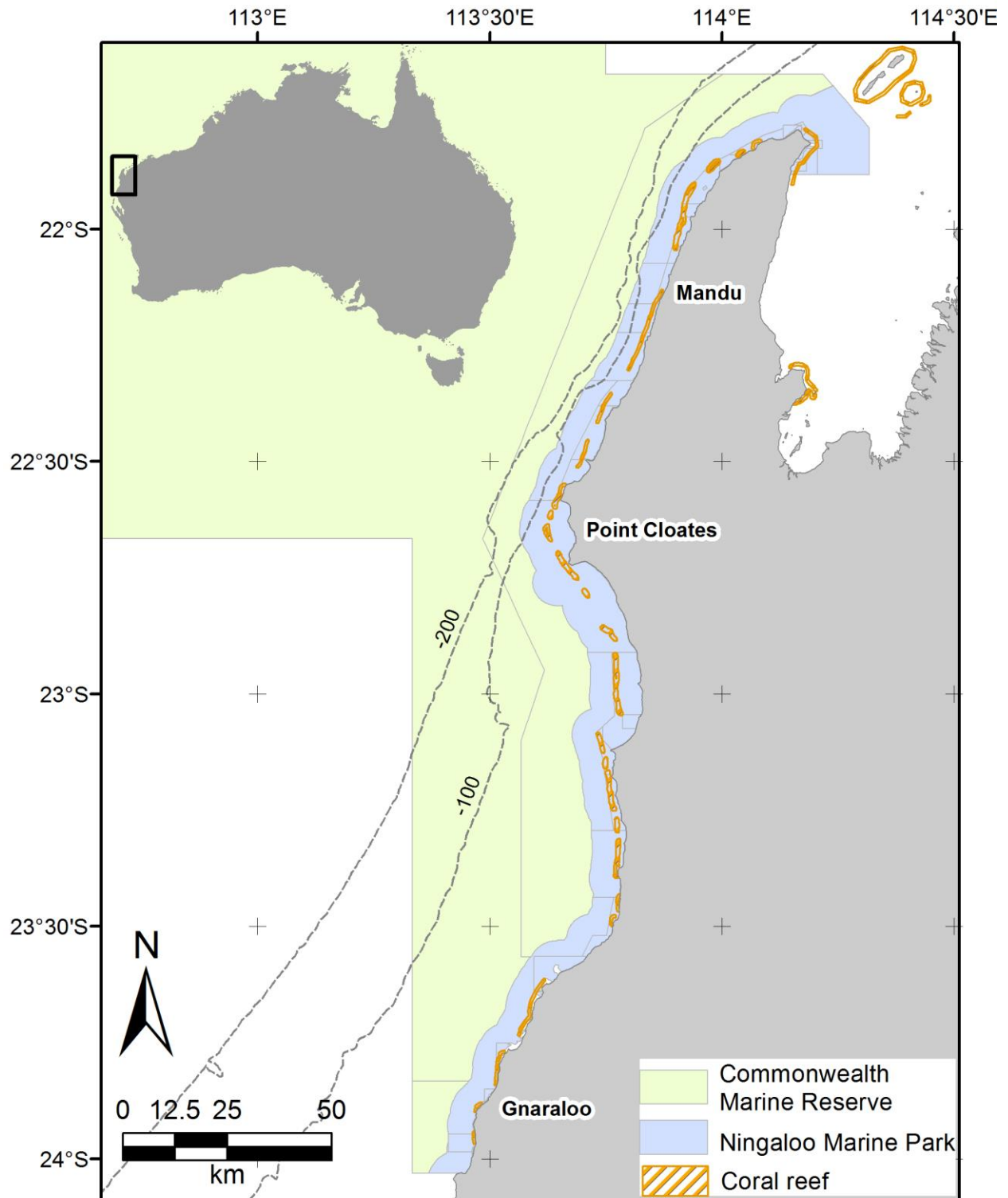


Figure 1.1. Study site in the Ningaloo Marine Park is a tropical area of Western Australia located 1000 km north of Perth.

1.8. Thesis structural overview

This thesis is presented as a compilation of four data chapters, each of them addressing one of the thesis objectives and written in the format of a journal paper. Inevitable repetition between chapters' introductions and this chapter were minimised; however, some repetition persists.

Chapter 2. Can single-beam echo-sounder depth data be used to produce models of demersal fish distribution that are comparable to models produced using multibeam echo-sounder depth data in Ningaloo Marine Park, Western Australia?

The possibility of using SBES data in the production of demersal fish distribution models was tested in the Mandu area of the NMP using six species recorded in the stereo-BRUVS as examples.

Chapter 3. Does the addition of seafloor backscatter data improve demersal fish distribution models based on multibeam bathymetry collected in Ningaloo Marine Park, Western Australia?

The value of adding the seafloor backscatter of MBES data into demersal species distribution models was evaluated in three areas of the NMP using seven species of coral reef fishes. The backscatter data were added to the models in the traditional format of mosaic but also as an approximation of grain size which can be more related to the distribution of species.

Chapter 4. Investigating the value of acoustic water column data in demersal fish assessment using historical data from Ningaloo Marine Park, Western Australia.

Historical data were used in Chapter 4 to test the possible improvement of models of total abundance and biomass of demersal species in the Mandu area of NMP.

Chapter 5. Investigate the temporal and spatial variation of acoustic water column data and their relationship with demersal stereo-BRUVS.

As the assessment of acoustic water column data in Chapter 4 was conducted using historic data that were not collected with comparison with BRUVS in mind, Chapter 5 presents two experiments purposely designed to examine the relationship between the spatial distribution of coral reef fishes assessed by acoustics and stereo-BRUVS. This was first carried out locally in Cockburn Sound, Western Australia to test methods and experiment design. Then this was replicated in NMP. Although Cockburn Sound is not a tropical environment, it was considered it was best to include all data collected as part of the study to maximise the results.

The thesis concludes with a general discussion reviewing the original objectives and the main findings of the research, limitations and future work.

Chapter 2

2. Can single-beam echo-sounder depth data be used to produce models of demersal fish distribution that are comparable to models produced using multibeam echo-sounder depth data in Ningaloo Marine Park, Western Australia?

2.1. ABSTRACT

Seafloor characteristics, such as depth and complexity, have a significant influence on the distribution of demersal fish. Consequently, seafloor characteristics can help in the prediction of fish distribution, which is required for fisheries and conservation management. Despite this, only 5-10% of the world's seafloor has been mapped at high resolution as it is a time-consuming and expensive process. Multibeam echo-sounders (MBES) can produce high-resolution bathymetry and a broad swath coverage of the seafloor, but requires greater financial and technical resources for operation and data analysis than single-beam echo-sounders (SBES). The main disadvantage of SBES is its comparatively limited spatial coverage, as only the area insonified directly under the echo-sounder is mapped. As a result, interpolation is usually required to fill gaps between echo-sounder transects to produce a continuous map. This study focuses on comparing the accuracy of demersal fish species distribution models by comparing interpolated SBES with full-coverage MBES distribution models. A Random Forest classifier was used to model the distribution of *Abalistes stellatus*, *Gymnocranius grandoculis*, *Lagocephalus sceleratus*, *Loxodon macrorhinus*, *Pristipomoides multidentis* and *Pristipomoides typus*, with depth and depth derivatives, including slope, aspect, standard deviation of depth, terrain ruggedness index, mean curvature and topographic position index as explanatory variables. The results indicated that distribution models for *A. stellatus*, *G. grandoculis*, *L. sceleratus*, and *L. macrorhinus* performed poorly for MBES and SBES data with AUCs below 0.7. Consequently, the distribution of these species could not be predicted by seafloor characteristics produced from either echo-sounder type. Distribution models for *P. multidentis* and *P. typus* performed well for MBES and the SBES data with accuracies above 0.8. Depth was the most important variable explaining the distribution of *P. multidentis* and *P. typus* in both MBES and SBES models. In conclusion, this study is indicative that in resource limited scenarios, SBES can produce comparable results to MBES for use in demersal fish management and conservation. However, further studies including a wide range of species are recommended to further corroborate findings from this study.

2.2. INTRODUCTION

Seafloor geomorphology has been recognised as an important factor influencing demersal fish distribution both at broad (kilometres) and fine (tens of metres) scales (Demestre et al., 2000, Monk et al., 2011, Pierdomenico et al., 2015, Moore et al., 2011). Hence, various terrain parameters that quantify the geomorphology of the seafloor such as slope, aspect, curvature, and rugosity have been included in distribution models of demersal fish (Becker et al., 2009, Demestre et al., 2000, Lucieer and Pederson, 2008, Ierodiaconou et al., 2011, Young and Carr, 2015, Young et al., 2010). These terrain parameters can be derived from acoustic depth surveys, and are commonly referred to as depth derivatives (Garcia-Alegre et al., 2014). Broad-scale depth derivatives can help to explain the distribution of species with a preference for large scale features (Wilson et al., 2007). However, the fine-scale associations within the landscape context are also important in structuring demersal species distribution (Anderson et al., 2009). In this context, consideration of habitat associations at different scales is recommended when modelling habitat availability for species (Anderson et al., 2009, Monk et al., 2011, Pittman and Brown, 2011, Garcia-Alegre et al., 2014, Jones and Brewer, 2012).

Despite the importance of the seafloor geomorphology in determining habitat for application in fisheries and conservation management, only 5-10 % of the world's seafloor has been mapped at fine resolution (meters to decimetres). This low percentage is because accurate characterization is usually time-consuming, expensive and technically challenging; especially in deep areas where remotely operated vehicles (ROVs) or autonomous underwater vehicles (AUVs) are needed to collect high-resolution seafloor mapping data (Wright and Heyman, 2008, Jones and Brewer, 2012). Since their invention in 1913, echo-sounders have become one of the most effective methods to map the seafloor, especially in deep and/or turbid waters where sound can penetrate the seawater to significantly greater depths than satellite remote sensing techniques (Rhoads et al., 2001, Mitchell, 2016). There are two main types of echo-sounders used in seafloor mapping: multibeam and single-beam. Multibeam echo-sounders (MBESs) collect high-resolution bathymetric information, cover a wide swath area on either side of the platform they operate from (typically a survey vessel), and usually acquire an almost continuous coverage of the study area. For these reasons, MBES has become a standard method for characterising the seafloor. However, the use of MBES typically requires greater financial and technical resources for operation and data analysis than single-beam echo-sounders (SBESs). In contrast, SBES is usually the simplest and cheapest system for collecting bathymetric information. The main disadvantage of SBES is its limited coverage, which is only the area insonified directly under the echo-sounder during the survey. Therefore,

interpolation is required to fill the gaps to make up a continuous seafloor map. If accurate seafloor maps could be produced from SBES interpolated data, the cost to produce accurate demersal fish distribution models for conservation and management would be significantly reduced.

While there are numerous interpolation methods available to produce continuous bathymetry data from sparse datasets, no consensus has been reached on a single-method as the most accurate to answer ecological questions like habitats, species and communities' distributions (Bello-Pineda and Hernández-Stefanoni, 2007, Arun, 2013, Curtarelli et al., 2015). In other disciplines like navigation charts, protocols and requirements are well established to fulfil legal requirements of scale and accuracy (Mills, 2015). The performance of different interpolation methods depends upon the seabed characteristics, density and distribution of measurement points (Erdogan, 2009, Arun, 2013, Moskalik et al., 2013). This study compared the accuracy of three methods commonly used that have been proven to model bathymetry effectively. The three methods include: inverse distance weighting (IDW), radial basis function (RBF) and Kriging (Moskalik et al., 2013, Sanchez-Carnero et al., 2012). Kriging included testing three variations; ordinary (OK) and universal with a first and second-degree de-trending (UK1 and UK2).

The overall aim of this study was to test the ability of cost-effective methods (i.e. SBES derived depth data) for modelling demersal fish species distributions. This study compares the accuracy of models using SBES bathymetry and depth derivatives at different scales with those derived from MBES data. Specifically, this study had the following objectives: (1) evaluate and compare the accuracy of the three common SBES interpolation methods (inverse distance weighting, radial basis function and Kriging) in producing continuous bathymetry using SBES data using a leave-one-out cross-validation test; (2) compare resulting interpolated SBES bathymetries and depth derivatives with the MBES bathymetry and depth derivatives; and (3) compare the accuracy of demersal fish predictive distribution models constructed using SBES and MBES bathymetry and depth derivatives at different scales.

2.3. METHODS

2.3.1. Study area and data collection

Located off the coast of north-western Australia, Ningaloo Reef (NR) is the longest fringing coral reef in Australia and is recognised as a global biodiversity hotspot, as it is home to a wide variety of wildlife, including many endangered species (Gazzani and Marinova, 2007, Schonberg and Fromont, 2012). The established Ningaloo Marine Park (NMP) protects 260 of the 290-km-long NR system. To obtain knowledge on the ecology and biodiversity of NMP, a multi-institutional research program was conducted

by Western Australia Marine Science Institute (WAMSI) partners between 2006 and 2009 (Waples and Hollander, 2008). As part of this program, SBES data were collected between 2006 and 2008 (Colquhoun et al., 2007), and the assemblage and relative abundance of demersal fish were surveyed using Baited Remote Underwater Stereo-Video (stereo-BRUVS) in 2008, and 2009.

Another project carried out by Geoscience Australia (GA) collected MBES data in particular areas of the NMP in 2008 (Brooke et al., 2009). To achieve the objectives of this study, an area of NMP where SBES, MBES and stereo-BRUVS data overlapped was selected as the study site (Figure 2.1). The study site was located 2.5 km from the mainland coast to 7.5 km offshore. The area extended approximately 35 km parallel and 5 km perpendicular to the coast, with seafloor depths ranging from approximately 20 to 130 m.

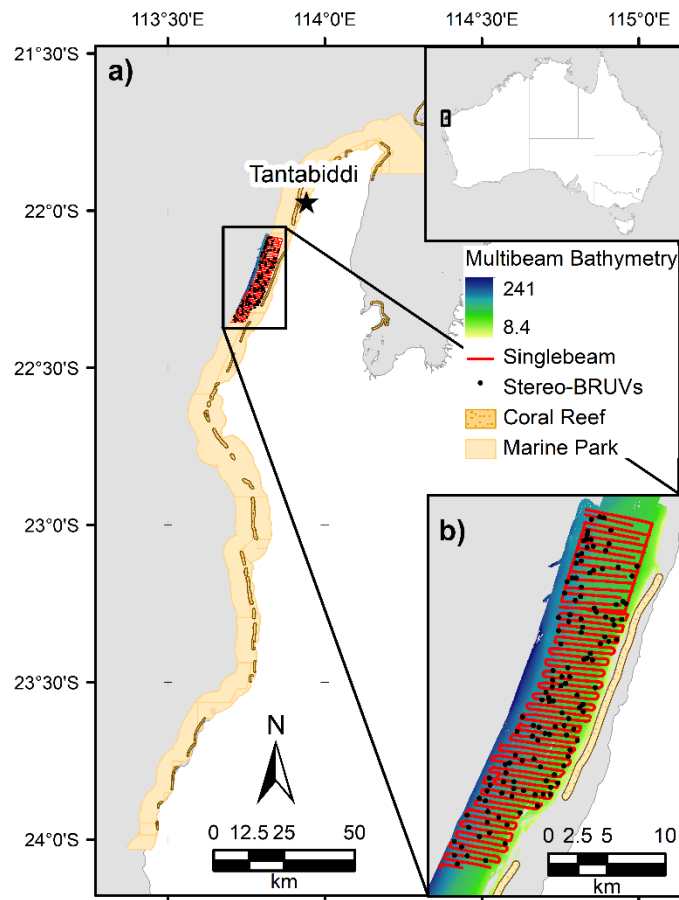


Figure 2.1. Map indicating (a) the study site located in the north section of the Ningaloo Marine Park, and (b) the locations of single-beam echo-sounder survey tracks shown in red and stereo BRUVS deployment sites shown with black dots.

Stereo-BRUVS data were collected between 26th March and 6th May 2009 as part of WAMSI Ningaloo Reef Marine Park deepwater benthic biodiversity survey project 3.1.1 (Colquhoun et al., 2007). A full

description of the methods for collection and processing of the stereo-BRUVS data can be found in Harvey et al. (2007). The resulting presence and absence records of different fish species at each stereo-BRUVS station during a period of an hour were used in this study.

SBES bathymetric data were collected with a Simrad EQ60 echo-sounder (38 and 200 kHz frequencies) mounted on the RV Cape Ferguson and RV Solander vessels for the 2006 and 2008 surveys respectively (Colquhoun et al., 2007). The spacing of the transects in the SBES survey was approximately 500 m; more details of the SBES analysis are provided in the next section.

The MBES bathymetric data covering the area of interest for this study was downloaded as a 3 metres resolution grid from the GA website (Figure 2.1).

2.3.2. SBES data processing

Depths values from the SBES acoustic data were extracted using the readEKraw MATLAB toolkit (by Rick Towler, NOAA Alaska Fisheries Science Centre, Seattle, WA, USA). The depth was estimated for 10 averaged pings to improve the signal-to-noise ratio with a mean distance of 40 m between the averaged pings. Depth values were corrected for tidal height using the predicted values of tide for Tantabiddi provided by the department of transport (Copyright. Dept. for Planning and Infrastructure, Western Australia) and adjusted so that they were relative to the Australian Height Datum (AHD 0.30 m above Chart datum). Quality control was conducted manually by removing erroneous depth values, including those that were positive and those that were unrealistic in relation to surrounding values. Text files were exported for further analysis including depth, latitude, and longitude.

2.3.3. Spatial interpolation methods

Text files containing depth and location were process using the three methods described below, and more thoroughly in (Mitas and Mitasova, 1999). All the analysis were carried out in R (R Development Core Team, 2017):

Inverse distance weighting (IDW): IDW interpolation is an exact interpolation technique, which means, the interpolated surface will have the same values in the measured sampling points while producing an estimation for the unsampled areas. The values at unsampled points are estimated based on the weighted average of known points within a searching neighbourhood. The weighting is based on the proximity of known points (the inverse of the distances). IDW requires the selection of neighbourhood size and a power parameter which determines the weight of the surrounding points with greater values of p corresponding

to greater influence close to the unknown point being interpolated. In this study, different powers (ranging from 0.5 – 6 in 0.5 increments) and selected neighbourhoods (50, 100 and 150 raster's cells) were tested using the gstat package (Pebesma, 2004).

Radial Basis Functions (RBFs): RBFs are in the group of exact interpolation methods, however, the estimation in the unsampled areas can variate depending on the basis function used (Buhmann, 2003). The algorithm behind RBFs can be visualized as fitting an elastic surface through the measured sample values while creating a surface as smooth as possible by minimising its total curvature (Erdogan, 2009). There are five basis functions: thin-plate spline, spline with tension, completely regularised spline, and inverse multiquadratic function. In this study, we used the completely regularised spline (CRS) and multiquadratic (M) RBFs which have been found accurate in the production of depth interpolation. The RBFs functions use a smoothness and robustness parameters to control the level of smoothness and stability of the interpolation. These two parameters were optimised using the optimisation algorithm in the geospt package (Melo, 2012) which is based on minimising the root-mean-square prediction errors using cross-validation. The performance of CRS and M with neighbours set at 50, 100 and 150 raster's cells was tested.

Kriging: Kriging is an interpolation method that assumes that sample points are spatially correlated, and uses a fitted mathematical model that explains the correlation as a function of distance and/or direction to produce a predicted surface. The spatial autocorrelation (or dependency) is estimated by creating a semi-variogram (commonly called a variogram) using empirical sample points. A model is then fitted to the points (in this study a Gaussian model; Cressie, 1993). Unmeasured locations on the surface are then predicted by weighted measures surrounding values based on the semi-variogram function. For each predicted value, uncertainty is also estimated. Isotropic (uniform values in all directions) and anisotropic (different values in different directions) variograms for ordinary (assumes an unknown constant mean) and universal kriging (assumes a prevailing trend in the data) with a first and second-degree detrending with 100 and 150 neighbourhoods were tested using the gstat package (Pebesma, 2004).

2.3.4. Selection and comparison of best interpolation approaches

For each scenario of IDW and RBF the best method was selected based on minimising the root mean squared error (RMSE) using leave-one-out cross-validation (Hengl, 2009). The best model among the kriging scenarios was based on the (RMSE) and the average kriging standard error (ASE; Asa et al., 2012). The difference between ASE and RMSE is indicative of how accurately the model is capturing the variability

in the interpolated values (Asa et al., 2012). When the ASE is greater than the RMSE, the model is underestimating the variability while greater values of RMSE than ASE indicate an overestimate of the variability. In an ideal interpolation, the difference between ASE and RMSE would be zero.

The interpolated surfaces from the best IDW, RBF, and kriging methods selected were compared with the MBES surface using correlation and regression analyses. The relationship between the overall surfaces (interpolated vs MBES) rather than absolute values was considered to be important in predicting fish distribution. Therefore, correlation and regression tests were considered appropriate. The correlation and regression analyses were undertaken for subsets of raster pixel values corresponding to different buffer distance (intervals) around the original SBES track. Distances were split into four intervals, including 0-100, 101-200, 201-300 and 301-400 m perpendicular from the track. The pixels values of the interpolated SBES contained in each interval were compared to the MBES pixel of the same interval using correlation and regression analysis. Values closer to the original SBES data (e.g., 0-100 m) were expected to be accurate regardless of interpolation techniques, while the accuracy of values further away (e.g., 301-400 m) were expected to depend upon interpolation technique. The significance of the correlation coefficient r and the coefficient of determination R^2 was also tested.

2.3.5. Digital Elevation Models

A Digital Elevation Model (DEM) in which each pixel corresponds to the interpolated values, was produced using the best interpolation method, considering the RMSE metric. Additional DEMs were produced at resolutions of 9, 15, and 25 meters. To achieve this, a Gaussian filter (kernel size 5x5) was first applied to the interpolated bathymetry to reduce the effect of noise which can be particularly problematic at the edges of overlapping transects (Stephens and Diesing, 2014). Then, the DEM was resampled at the corresponding resolutions using a bilinear method with the raster package (Hijmans, 2016). DEMs were also produced from MBES data. MBES were filtered in the same way as SBES data.

2.3.6. Seafloor depth and its derivatives

Depth derivatives including slope, aspect, terrain ruggedness index (TRI), standard deviation of depth (SD), topographic position index (TPI), roughness, and mean curvature (MNC) were calculated using a 3x3 windows analysis at four different resolutions (Table 2.1). The finest scale of analysis was fixed by the resolution of the MBES data (3 m) while the other three were chosen based on the spatial dependence of species. A variogram analysis was used to identify the maximum distance at which the species present spatial dependency which is called the range (> 4 km). The scales were chosen to cover the span between

the 3 m resolution and the range of species (Holmes et al., 2008). Therefore, the resolutions were set at 3, 9, 15 and 25 m. Depth derivatives were produced for SBES and MBES DEMs at the four resolutions.

Table 2.1. Depth derivatives produced from SBES depth data

Variable	Abbreviation	Software	Reference
Slope	slope	R (raster)	(Horn, 1981)
Aspect	Northness	R (raster)	(Horn, 1981)
	Eastness	R (raster)	(Horn, 1981)
Standard deviation of depth	SD	R	(Lecours et al., 2016)
Terrain ruggedness index	TRI	R (raster)	(Wilson et al., 2007)
Topographic position Index	TPI	R (raster)	(Wilson et al., 2007)
Roughness	Roughness	R (raster)	(Wilson et al., 2007)
Mean curvature	MNC	Landserf v 2.3	(Wood, 1996)

The gradient of change in depth (slope) and orientation of this gradient (aspect) were calculated using (Horn, 1981) approach, implemented in the raster package (Hijmans, 2016). Because aspect is a circular variable calculated as degrees clockwise from 0 to 360, values close to north (0° or 360°) are taken as very different in the analysis when in fact they are close to each other. Previous studies have proposed to split aspect into two variables using trigonometric functions: northness (NS) and eastness (WE), where NS is the cosine of aspect and WE is the sine of aspect. The values for NS and WE range from -1 to 1; slopes facing north (NS=1), south (NS=-1), east (WE=1), or west (WE=-1; Deng et al., 2007;). This approach was applied here.

The TPI was calculated as the vertical position of a particular raster pixel in relation to its eight surrounding neighbours, where positive values corresponded to crest areas and negative values are associated with troughs (Wilson et al., 2007). The TRI was calculated as the mean of the absolute differences between the value of a raster pixel and that of each eight surrounding pixels (Wilson et al., 2007). Roughness was the difference between the maximum and the minimum value of a pixel and its eight neighbouring pixels. The mean curvature (MNC) was calculated using a fitted polynomial expression following the approach described by (Wood, 1996), where curvature is the second derivative of the modelled depth, MNC was calculated using Landserf Version 2.3 (Wood, 2009).

2.3.7. Demersal fish species distribution models

The distribution of the Starry Triggerfish (*Abalistes stellatus*), Robinson's Seabream (*Gymnocranius grandoculis*), Silver Toadfish (*Lagocephalus sceleratus*), Sliteye Shark (*Loxodon macrorhinus*), Goldband Snapper (*Pristipomoides multidentis*), and the Sharptooth Snapper (*Pristipomoides typus*), was modelled using seafloor depth and its derivatives from SBES and MBES. While fish species with high commercial

value were prioritised, the low number of presences of these species in stereo-BRUVS in the study area did not allow accurate models to be produced. Consequently, the species chosen for these analyses have minor commercial value, with the exception of *P. multidentis*, *P. typus* which are considered as an important component of commercial and recreational fisheries in Western Australia, and had a minimum of 35 presences in the study area. The species distribution models were constructed using presence/absences records from stereo-BRUVS data. The species included in the analysis are considered to be reef associated with a habitat generalist's relatively broad distribution (Fitzpatrick et al., 2012, Kalogirou, 2013, Randall, 1967). Depth derivatives included in the species distribution model are listed in Table 2.1. Four distribution models were created for each of the six species using MBES data and SBES, including depth and its derivatives (24 models in total).

Random Forest (RF) was used in this study to model the distribution of *A. stellatus*, *G. grandoculis*, *L. scleratus*, *L. macrorhinus*, *P. multidentis*, and *P. typus*. RF is based on growing many classification trees using random subsets of the input data and variables then averaging or voting over all the trees to provide predictions. More detail of the method can be found in (Breiman, 2001). The performance of the models was evaluated using the Area Under the Receiver Operator Curve (AUC), which summarises the sensitivity and specificity of the model. Higher AUC values (towards 1) correspond to models that are highly sensitive and specific (Manel et al., 2001). Seventy per cent of the data was used to train the RF, and the rest was used to test the accuracy of predictions from the model. The trained RF was used to predict the probability of presence of the species in the 30 % reserved for testing. The residuals were then calculated. The accuracy of the models was tested using a five-fold cross-validation procedure, an AUC is obtained for each fold, and the average of the five-fold AUCs is reported for each model. The significance of the difference in mean AUC between the interpolated SBES and the MBES models was tested using a T-test.

The relationship between the terrain variables and the presence of the species can be explored using partial dependence plots in a RF. Partial dependence plots give a graphical representation of the marginal effect of a variable on the selection of a class (Friedman, 2001). Each point on the partial dependence plot is the average vote percentage in favour of the "presence" class across all observations, given a fixed level of the variable. The vote percentage is expressed as logits (log of a fraction of votes). Logits will be referred to as the probability of occurrence, as it is easier to understand in the partial dependence analysis, but this metric cannot be directly translated to likelihood.

2.4. RESULTS

After the filtering and averaging process, 11,122 depth records of the SBES survey were included. The maximum depth in the study site was 127 m with a mean of 77.26 and a minimum of 18 m. The coefficient of skewness, was below the threshold of ± 1 (0.14), indicating the data had a symmetrical normal distribution, and so no transformation was required for geostatistical analysis (Kerry and Oliver, 2007). The average distance between the points that were analysed was 39 m. For this reason, interpolation over a regular 40 m resolution grid was considered appropriate.

2.4.1. Selection and comparison of best interpolation approaches

Inverse distance weighting: The best IDW method based on minimising the RMSE was one with a power parameter of three, although very similar values were observed for powers between 3 and 3.5, at a higher precision the 3 power scenario presented a slightly lower RMSE values (Table 2.2). Lower levels of RMSE were found when the number of neighbours was decreased.

Table 2.2. Root mean squared error (RMSE) for the different combinations of powers and number of neighbours tested in the inverse distance weighting interpolation. The best interpolation is indicated by the lowest value of RMSE.

Power	RMSE		
	Neighbours		
	50	100	150
2	0.477	0.559	0.621
2.5	0.410	0.425	0.434
3	0.398	0.400	0.401
3.5	0.398	0.398	0.398
4	0.401	0.401	0.401
4.5	0.404	0.404	0.404
5	0.406	0.406	0.406
5.5	0.409	0.409	0.409
6	0.411	0.411	0.411

Radial Basis Function: The best RBF based on the lowest RMSE had a multiquadratic function (M). Completely regularized spline (CRS) had greater associated error. No differences were observed when the number of neighbours was increased (Table 2.3).

Table 2.3. Root mean squared error (RMSE) for the multiquadratic (M) and completely regularized spline (CRS) radial basis functions (RBFs). Three scenarios of a maximum number of neighbours (n) are shown, and the lowest value of RMSE is shown in bold.

Type	RMSE		
	Neighbours		
	50	100	150
M	0.397	0.397	0.397
CRS	0.456	0.459	0.460

Kriging: The initial analysis of the variograms showed the presence of spatial structure in the data which made the data suitable for geostatistical analysis. An anisotropy was found in the data with a major axis parallel to the coast where less variation was observed and a minor axis perpendicular to the coast in which much more rapid changes in depth occurred. The anisotropy persisted after a first and second-degree detrending. When fitting a theoretical model to the empirical variograms, Gaussian variograms had the best fit. The distance at which the spatial autocorrelation reached the sill (called the range) was between 430 and 720 m (Table 2.4).

Table 2.4. Parameters of the Gaussian models fitted to the empirical variograms comparing Ordinary, and Universal kriging first and second degree detrending, as well as isotropic and anisotropic directionality. Partial sill (psill) is the sill minus the nugget effect.

Type	Directionality	psill	range
Ordinary Kriging	Isotropic	28	617
	Anisotropic	24	720
Universal Kriging 1	Isotropic	8	464
	Anisotropic	7	519
Universal Kriging 2	Isotropic	6	428
	Anisotropic	6	492

The best fit kriging interpolation based on minimising the difference between ASEs and RMSEs was the universal kriging with a first-degree detrending (UK1) using anisotropic variograms. In most cases, interpolation using anisotropic variograms had lower RMSEs over those using isotropic variograms. Ordinary Kriging (OK) and universal kriging with a first-degree detrending (UK1) performed similarly with low values of RMSE. For OK and UK1 higher ASEs than RMSEs were estimated when an anisotropic variogram was used, indicating an underestimation of the variability. Higher values of RMSE than ASE indicate an overestimate of the variability which was the case for OK and UK1 when an isotropic variogram was used (Table 2.5). Universal kriging with a second-degree detrending (UK2) with an isotropic and anisotropic variogram also overestimates the variability. A slightly lower value of ASE-RMSE was observed

for OK and UK1 when an anisotropic variogram was used. Universal kriging with second-degree detrending (UK2) had, in general, the worst performance, with higher values of RMSE and a greater difference between ASE and RMSE.

Table 2.5. Root mean square error (RMSE) from cross-validation for the kriging interpolations. The model with the smallest difference between the average kriging standard error (ASE) and RMSE is marked in bold.

Type	Directionality	Neighbours					
		100			150		
		RMSE	ASE	ASE-RMSE	RMSE	ASE	ASE-RMSE
Ordinary Kriging	Isotropic	0.418	0.360	-0.058	0.420	0.359	-0.061
	Anisotropic	0.342	0.381	0.039	0.343	0.381	0.038
Universal Kriging 1	Isotropic	0.387	0.342	-0.045	0.388	0.342	-0.046
	Anisotropic	0.331	0.366	0.034	0.332	0.366	0.034
Universal Kriging 2	Isotropic	4.604	0.341	-4.263	19.802	0.341	-19.461
	Anisotropic	3.151	0.366	-2.785	3.645	0.366	-3.279

In comparing the best methods for all three interpolation techniques based on reducing the RMSEs, kriging had the better performance with the lowest value (0.332) than IDW and RBF (0.398 and 0.397, respectively).

When comparing the SBES interpolated surfaces with the gridded depth surface from the MBES data, a good correlation (all coefficients of determination were $> .99$) was found between the MBES data and the three SBES interpolated DEMs. Significant linear relationships between the MBES data and the interpolated data were found for all methods ($p < 0.001$). A decrease in the coefficient of determination (R^2) was observed when the distance from the original SBES track was increased (Figure 2.2). UK1 had the highest R^2 for all intervals of distance, closely followed by RBF. IDW had the lowest values of R^2 for all the distances and particularly for the areas further away from the SBES data (400 m). The MBES and SBES interpolated surfaces are comparable with some artefacts visible, particularly for the IDW and RBF surfaces (Figure 2.3).

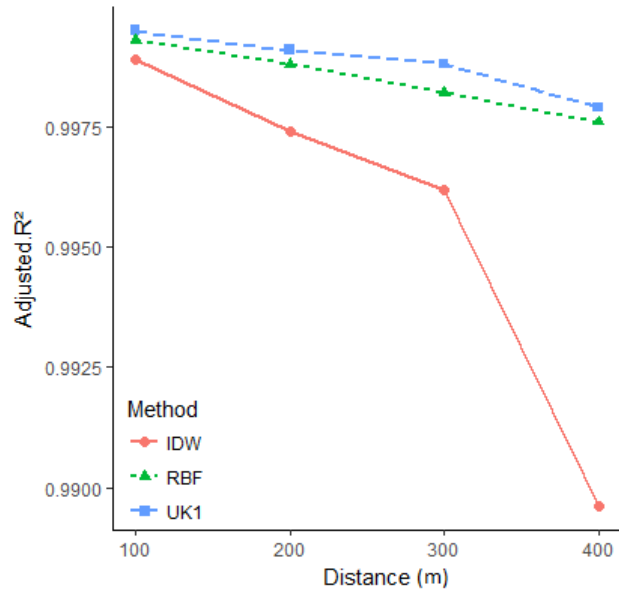


Figure 2.2. Coefficient of determination (R^2) between best SBES the interpolated surfaces and the multibeam data (MBES). Five intervals of distance from the original SBES track are shown for universal kriging with a first-degree of detrending (UK1), inverse distance weighting (IDW), and radial basis function (RBF). In all cases, the linear relationship was significant ($p < 0.001$).

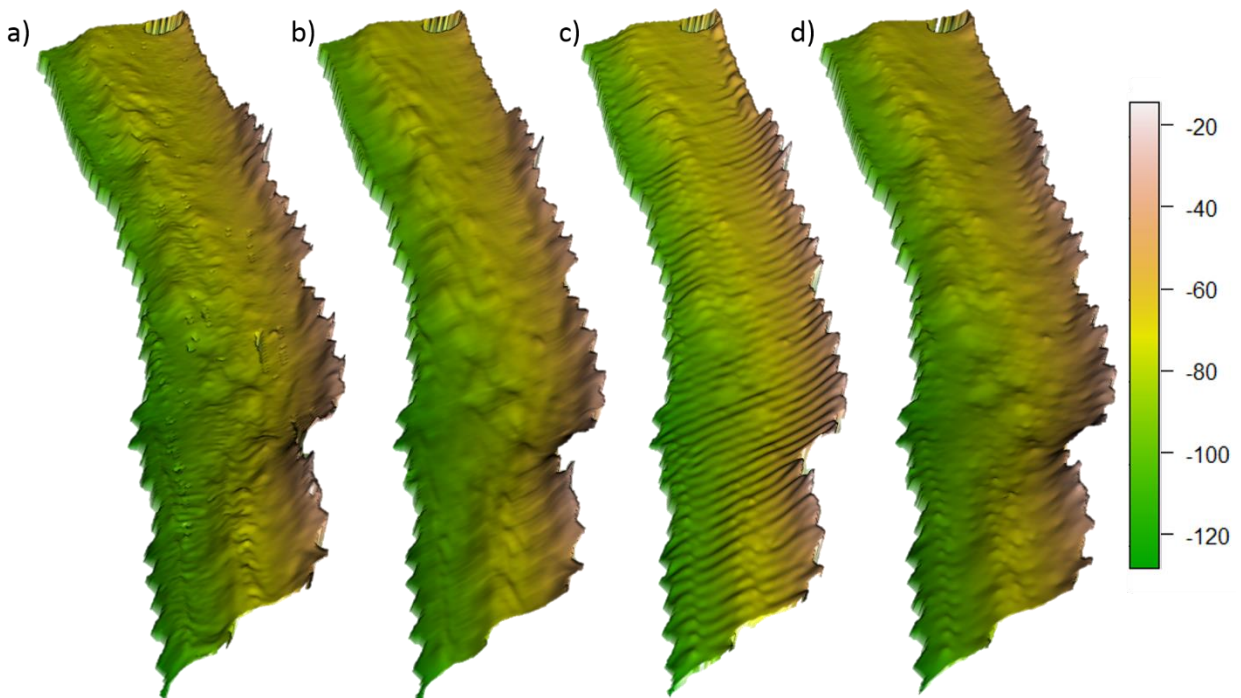


Figure 2.3. Bathymetry of the study site using a 3D projection for a) MBES and the best SBES data interpolations in this study using: b) universal kriging with first degree of detrending, c) inverse distance weighting, and d) radial basis function.

2.4.2. Seafloor depth and its derivatives

In general, a larger variation was found in the depth derivatives based on the MBES data compared to the SBES interpolated data; this was particularly true for the derivatives based on the highest resolution bathymetry (3 m, Figure 2.4). The derivatives based on the interpolated SBES data had similar means and standard deviations to the MBES derivatives at a broader scale (25 m resolution).

A gentle slope was found in the study area with a mean of around 1 degree. The orientation of the slope was mainly north-west, as shown by the predominately positive NS and negative WE values. High variation in the orientation of the slope was observed, particularly for the MBES data, at the 3 m resolution. The mean curvature had in all cases slightly negative values associated with concave areas in the terrain. However, both positive and negative MNC were observed. The standard deviation of depth, terrain ruggedness, TPI and roughness, all of them measures of terrain variability, presented a mean close to zero at the highest resolution indicating a low variability at a fine scale. Higher means and standard deviations were observed for the MBES data, and the interpolated surfaces as the resolution decreased (i.e. the cell size increased).

The derivatives based on the interpolated bathymetries presented different levels of artefacts associated with inaccuracies in the interpolation process. Pronounced artefacts were observed, particularly in the derivatives based on the IDW interpolated bathymetry (Figure 2.3). Roughness derivate from the MBES data and the three interpolation methods are shown as an example (Figure 2.5), similar effects were observed for the rest of the derivatives based on the different interpolation methods (Not shown).

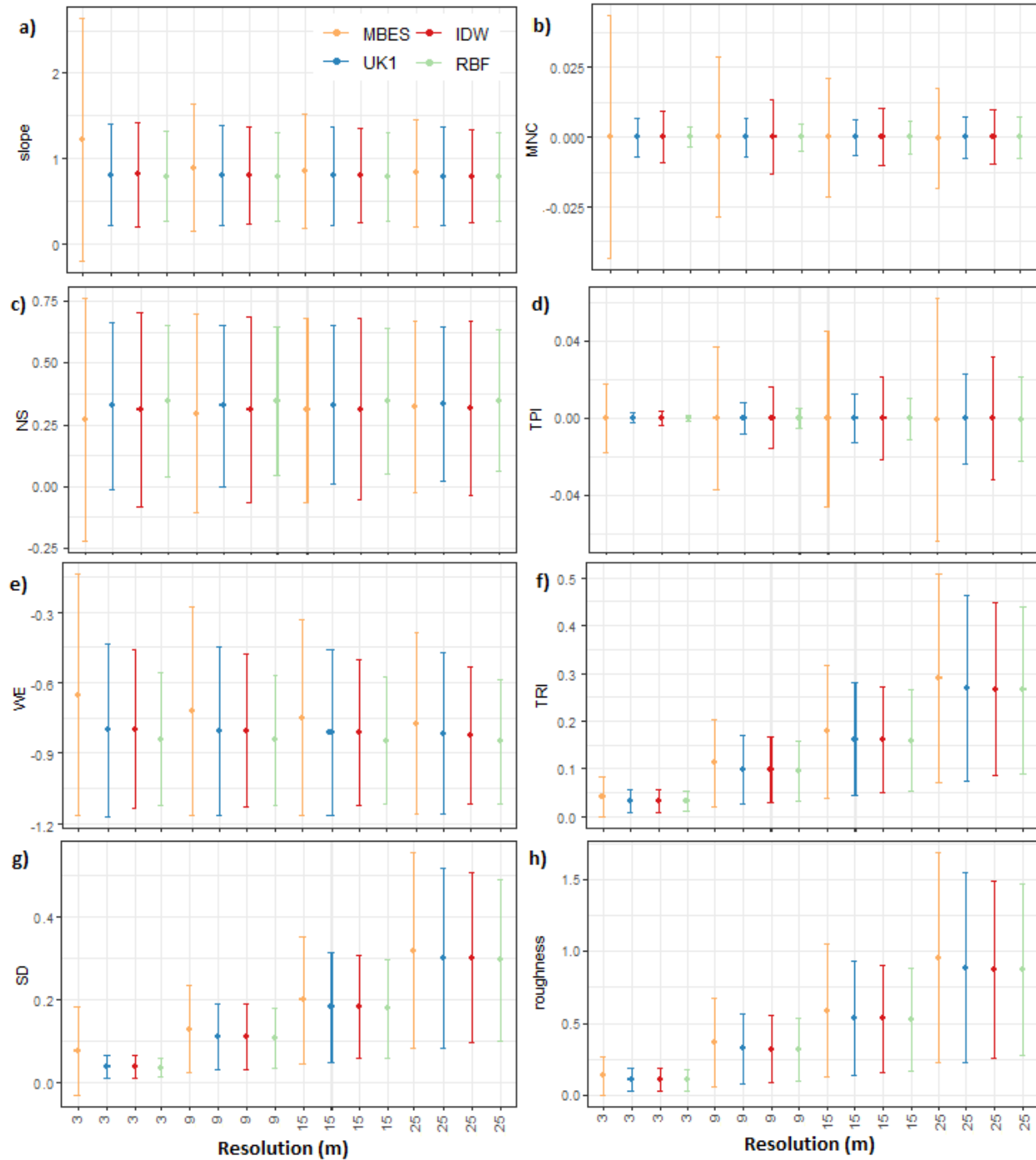


Figure 2.4 Mean and standard deviation (as error bar) of the depth derivatives based on the MBES and interpolated SBES data using universal kriging with a first-degree detrending (UK1), inverse distance weighting (IDW), and radial basis function (RBF). The four resolutions included in the analysis are shown. a) slope measured in degrees, b) mean curvature (MNC), c) northness (slopes facing north (NS=1), south (NS=-1)), d) topographic position index (TPI), e) eastness (slopes facing east (WE=1), or west (WE=-1)), f) terrain ruggedness index (TRI), g) standard deviation of depth (SD), and h) roughness.

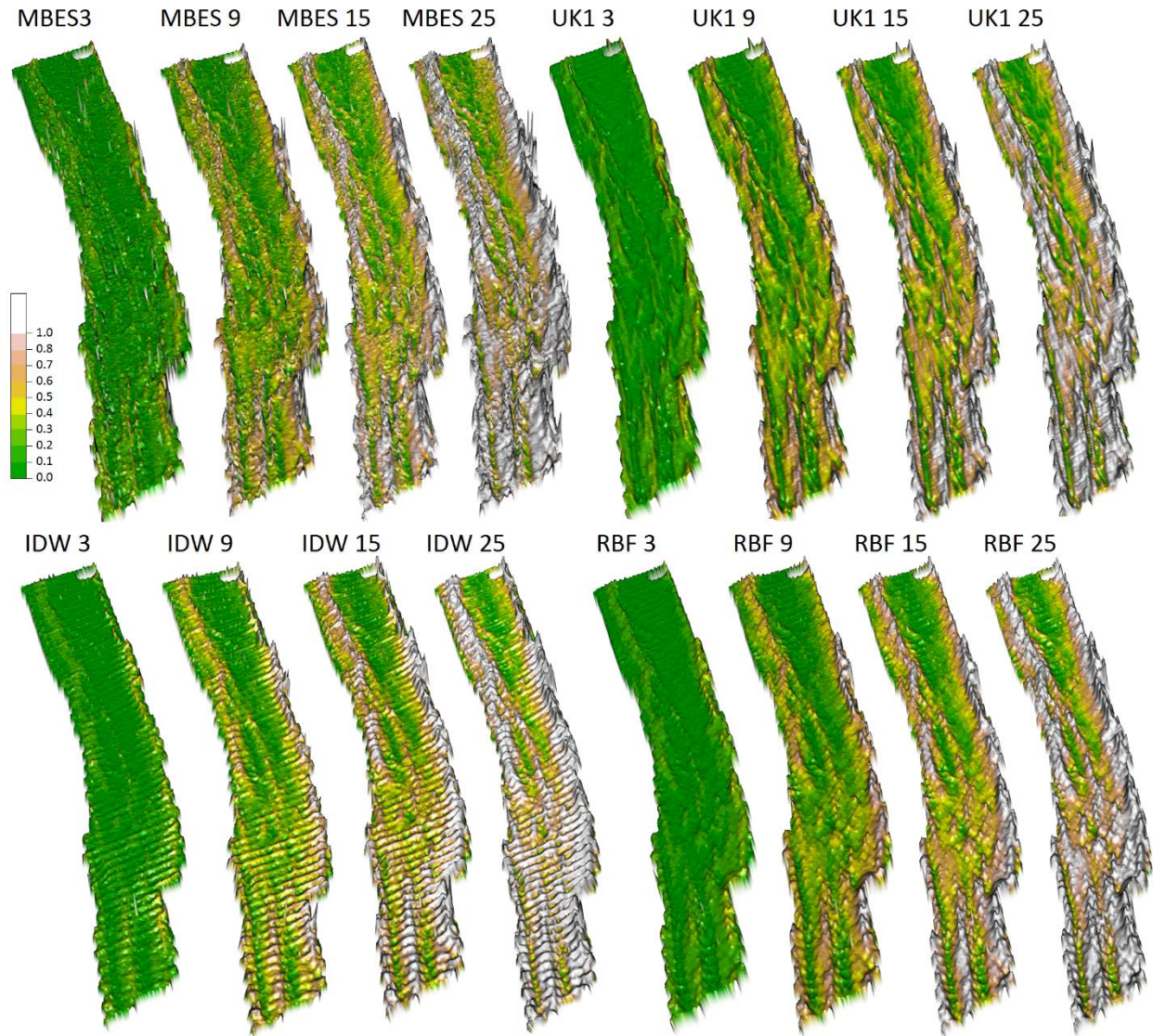


Figure 2.5 3D projection of the roughness derivative from the MBES and interpolated SBES data using universal kriging with a first-degree detrending (UK1), inverse distance weighting (IDW), and radial basis function (RBF). The four resolutions included in the analysis are shown.

2.4.3. Demersal fish species distribution models

Demersal fish distribution modelling based on depth and its derivatives varied in its performance, depending upon fish species. The distribution of *A. stellatus*, *G. grandoculis*, *L. scleratus*, and *L. macrorhinus* was poorly modelled by the MBES and interpolated SBES data (Table 2.6) with mean AUCs below 0.7, which is considered the threshold for an acceptable level of accuracy (Hosmer Jr et al., 2013). The distribution of *P. multidentis* and *P. typus* was well modelled using the variables included in the analysis, with AUCs above 0.8 for both the MBES and SBES interpolated models. No significant differences were

observed between the mean AUCs of the models produced using MBES data compared to the SBES models ($p < 0.05$).

Table 2.6. Performance of the models measured by the five-fold cross-validation mean AUCs. The results for the species modelled are shown for MBES and interpolated SBES data using universal kriging with a first-degree detrending (UK1) inverse distance weighting (IDW), and radial basis function (RBF). The number of presences of the species in the study site is also shown.

Species	Mean AUC				Presences
	MBES	UK1	IDW	RBF	
<i>A. stellatus</i>	0.48	0.40	0.44	0.45	99
<i>G. grandoculis</i>	0.57	0.58	0.56	0.64	78
<i>L. sceleratus</i>	0.54	0.58	0.54	0.69	55
<i>L. macrorhinus</i>	0.53	0.69	0.53	0.57	35
<i>P. multidentis</i>	0.94	0.92	0.92	0.91	36
<i>P. typus</i>	0.87	0.84	0.84	0.84	38

2.4.4. Variables importance

Even though the accuracy of the models for *A. stellatus*, *G. grandoculis*, *L. sceleratus* and *L. macrorhinus* was below the acceptable level, the analysis of the variables importance can give some insight of the factors affecting their distribution. For *G. grandoculis* and *L. sceleratus*, depth was the most important variable in the MBES and SBES models (Figure 2.6). TRI and MNC at a fine-medium scale were also important in the *L. sceleratus* MBES model, however, in the SBES models these variables had only a marginal contribution. Variables related to terrain variability such as roughness, standard deviation of depth (SD) and terrain ruggedness index (TRI) were important in the *A. stellatus* model, at both broad and fine-scale for both the MBES and SBES models. The slope orientation in both the northness and eastness components were also important in the MBES model but at specific scales of analysis with eastness being more important at the finest scale (3 m resolution) while northness was relevant at medium to large scale (9-25 m resolution). For the *L. macrorhinus* model, depth had slightly higher importance followed by roughness, SD, TRI and slope at both fine and broad resolutions for the MBES and the SBES UK1 model. Mean curvature was important at a broad scale (25 m) while northness was relevant at a fine scale (3-9 m).

Depth was the most critical variable in modelling the distribution of both *P. multidentis* and *P. typus* for the MBES data, and the models based on the interpolated SBES data (e and f in Figure 2.6). For *P. multidentis*, roughness, slope, SD and TRI, followed depth in importance at both fine and broad scale, MNC had also a significant contribution but only at a medium scale (15 m). In the *P. typus* model, the eastness component of slope orientation was important at a fine scale (3 m) with the rest of the variables having a lower

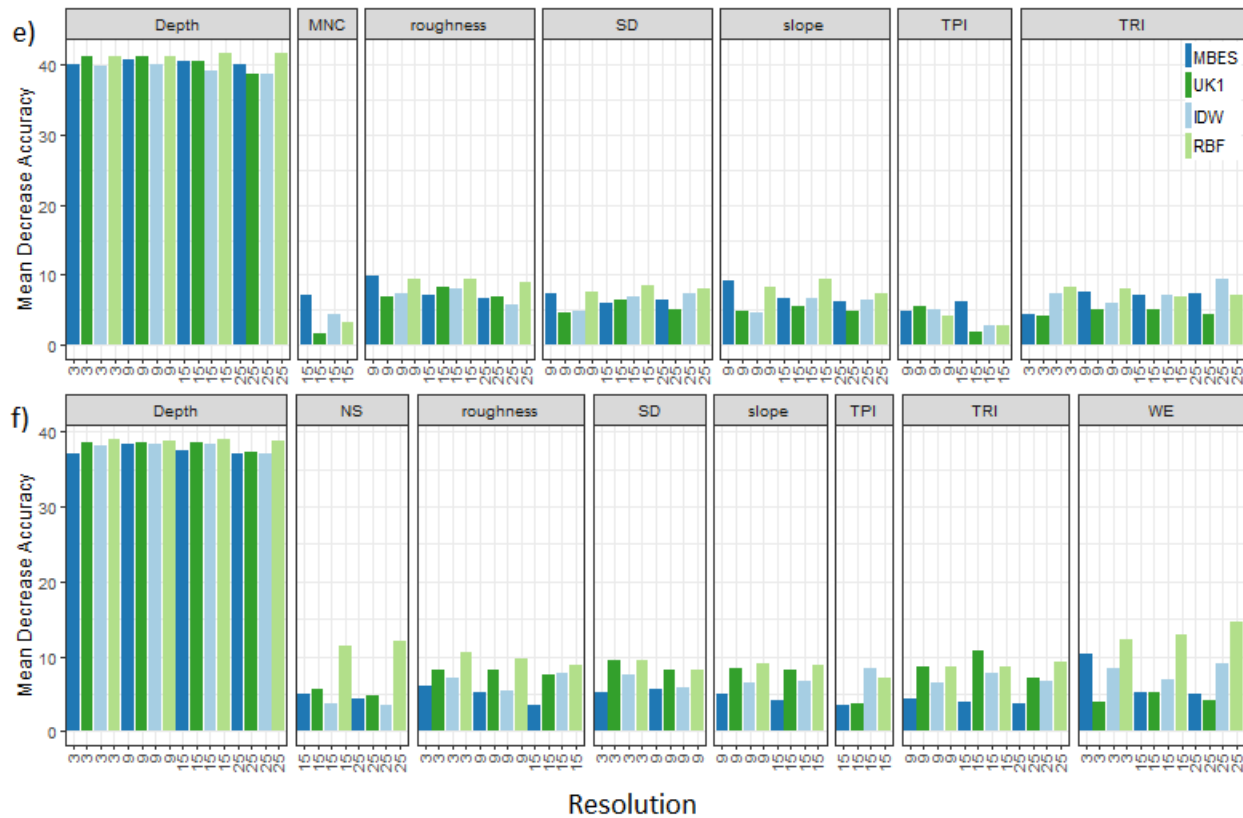


Figure 2.6 Variables importance in the construction of the Random Forest models using MBES and SBES interpolated data with Universal Kriging with first degree of detrending (UK1), Inverse distance weighting (IDW), and Radial Basis Function (RBF) for a) *A. stellatus*, b) *G. grandoculis*, c) *L. sceleratus*, d) *L. macrorhinus*, e) *P. multidentis*, and f) *P. typus*. For brevity, only the 20 most important variables (according to the MBES model) are shown.

Probability of occurrence of *P. typus*

P. multidentis and *P. typus* have a very similar habitat distribution with a preference for deeper areas. The map of probability of occurrence of the models are shown only for *P. typus* as both maps were very similar. The map of probability of occurrence of *P. typus* showed higher probabilities of occurrence in deeper areas and lower in the rest of the study area for both MBES and SBES models (Figure 2.7). Similar spatial patterns were observed for all the models, however, the SBES models presented visually recognisable artefacts in the probability of occurrence derived from errors in the interpolations (Figure 2.7). In particular, the model created using the SBES interpolated by RBF presented a more evident pattern of artefacts in the areas of high probability of occurrence.

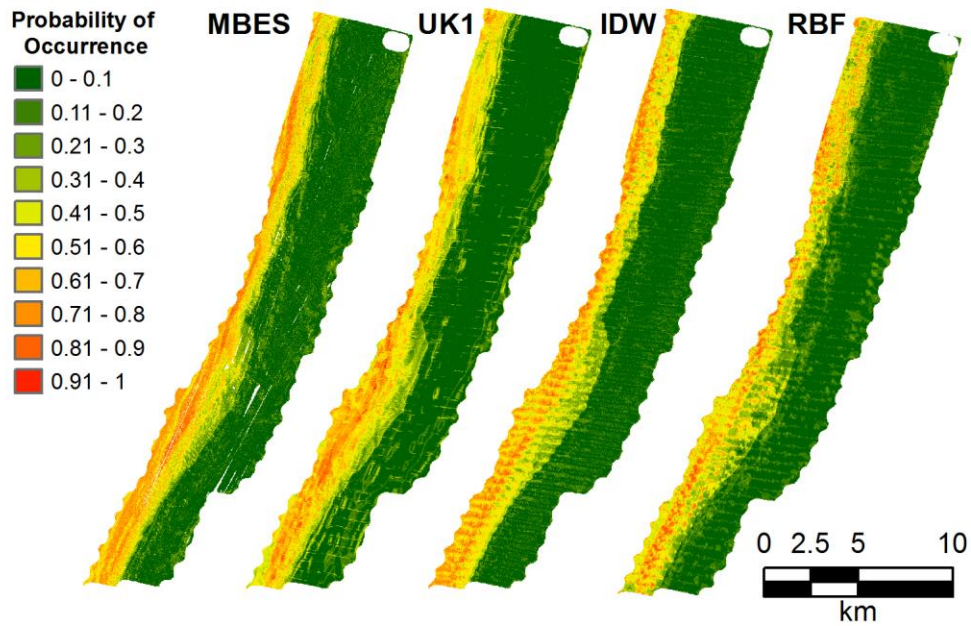


Figure 2.7. Maps of probability of occurrence of *P. typus* based on depth and depth derivatives of the MBES and the three interpolation techniques tested: Universal Kriging with first degree of detrending (UK1), inverse distance weighting (IDW) and radial basis function (RBF).

Spatial clustering of the residuals were observed in all the models of *P. typus* including the MBES model. In general an under prediction was observed in the deeper areas and over prediction in the shallows (Figure 2.8). However, over prediction in the shallower areas was less pronounced in the MBES model compared to the interpolated models.

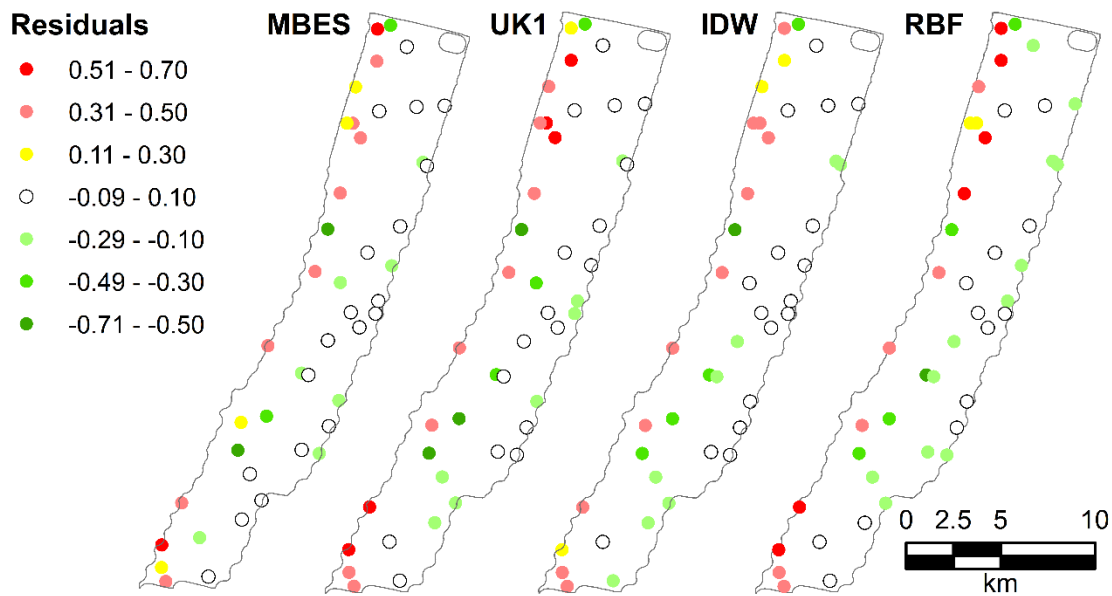


Figure 2.8. Spatial distribution of the residuals of the Random Forest predicting the testing portion of the *P. typus* data. Positive values corresponds to under predictions while negative values represent over predictions.

2.5. DISCUSSION

The possibility of using interpolated SBES depth and depth derivatives to produce species distribution models of six species of fish with comparable accuracies to the ones produced using MBES data was explored. Three interpolation methods were used to produce continuous bathymetries using SBES data. Kriging was found to be the most accurate method to interpolate the SBES depth data, compared to IDW and RBF. Similar accuracies (AUCs) were found in the modelling of species distribution using MBES and SBES interpolated data with no significant differences between them. However, the derivatives based on the SBES data failed to accurately represent the fine scale variability. Therefore, it is possible that species with habitat distribution influenced by fine scale variability, will not be model accurately using SBES interpolated data.

2.5.1. Selection and comparison of best interpolation approaches

In this study, Universal Kriging with a first order detrending (UK1) was found to be the method of choice to interpolate the SBES depth data, over Inverse Distance Weighting (IDW) and Radial basis functions (RBFs). This was based on the surface produced by UK1 having the lowest RMSE in the leave-one-out cross-validation test and the highest correlation with the MBES data. Similar results of Kriging outperforming IDW and RBF have been reported before when modelling elevation data (Moskalik et al., 2013, Curtarelli et al., 2015, Zimmermann and Kienast, 1999, Arun, 2013, Bello-Pineda and Hernández-

Stefanoni, 2007). The better performance of kriging in this study, could have been related to the sampling design as geostatistical methods are best suited for modelling irregularly distributed data (Curtarelli et al., 2015). The data analysed here were not equally spaced, as there was a high density of data in the transects, but also significant areas without any data between the transects. One of the disadvantages of kriging, is that some knowledge of geostatistics is needed to produce the best possible result. For instance, an exploration of the (variogram) model needs to be carried out to determine which theoretical variogram should be used and if a detrending process or the use of an anisotropic variogram is required. However, there is well-established software and guidance available to carry these steps out (Glenn et al., 2016).

2.5.2. Seafloor depth and its derivatives

Sampling areas with sparse data in the form of single-beam lines, produce track line artefacts when interpolated (Hell and Jakobsson, 2011). These artefacts affect the depth derivatives which reflect not only real variations in the DEM, but also false variations. In this study, all the interpolation methods were found to produce artefacts, which affected the depth derivatives. Hell and Jakobsson (2011) proposed gridding with minimum curvatures splines in tension at multiple grid resolutions to overcome this issue. Therefore, using a high-resolution grid in the areas with high volumes of data and lower resolution in no data areas. The use of different resolutions could reduce the artefacts produced during the interpolation, between the areas with high density of data and absence of it, which affected the accuracy of the derivatives. A practical limitation of the Hell and Jakobsson (2011) approach is the large computational requirements.

Changes in resolution had different effects in the depth derivatives, related to the specific terrain under study (Deng et al., 2007). Slope, for example, has the general pattern of a decrease as the resolution decreases (Wilson et al., 2007). The degree of the change in slope will depend on the specific type of terrain form with flat areas being less affected and regions with higher relief being more affected (Dolan and Lucieer, 2014). While slope usually decreases as the resolution decreases, the derivatives measuring terrain variability (TRI, roughness and SD) had the opposite trend. Terrain variability was less effectively captured by high resolution bathymetries while an exaggerated reduction of the resolution produced a spatial smoothing of the results (Friedman et al., 2012).

The inclusion of different resolutions of derivatives can increase the possibilities of having relevant information at the correct scale for the species under study. However, the fine resolution derivatives based on the SBES data, failed to capture the fine scale variability observed in the high resolution MBES

derivatives. Therefore, species whose distribution is influenced by terrain variability at a fine scale are less likely to be well modelled by SBES interpolated data.

2.5.3. Demersal fish species distribution models

The performance of the distribution models varied depending on the species, but no significant difference was observed between the accuracy of the models constructed using MBES and SBES data. The species included in this study are demersal carnivores with a certain degree of generalist and/or opportunistic feeding behaviour (Randall, 1967, Carpenter and Niem, 2001, Rousou et al., 2014, Gutteridge et al., 2011). Four of them including *G. grandoculis*, *L. macrorhinus*, *P. multidentis*, and *P. typus* belong to families that have been found in a variety of benthic habitats and classified as habitat generalist with relatively broad cross-shelf distribution in a previous study in the NMP (Fitzpatrick et al., 2012). However, the difference between habitat-generalist and habitat-specialist species is related to the ratio of occurrence extent occupied to the extent of the study area (Jarnevich et al., 2015). In the present study, three species including *A. stellatus*, *G. grandoculis*, and *L. sceleratus* had a generalist behaviour with high prevalence in the sampling points (> 40%), the models of these species had poor performance for both MBES data and SBES data. Previous studies, have found that generalist species are harder to model while specialist species are usually better modelled using environmental variables (Franklin et al., 2009). In this study we found this pattern to be particularly true in the two extremes of the prevalence scale with *A. stellatus* having the highest prevalence (> 70%) and its models having the lowest accuracy (AUCs <0.5), while *P. multidentis*, had a low prevalence (< 30%) and had the highest accuracy (AUCs >0.9). The generalist behaviour of *A. stellatus*, *G. grandoculis*, and *L. sceleratus* might be due to the extent and the temporal resolution of the study, for example, some species might use specific feeding habitats at night while using different habitats during the day (Harvey et al., 2012). *L. macrorhinus*, on the other hand, had the lowest prevalence in the study site, but its distribution was poorly modelled by depth and its derivatives, a possible explanation for this results can be that other variables related to the water column and not terrain variables are more related to its distribution. A previous study by (Gutteridge et al., 2011) found that *L. macrorhinus* prefers areas with clear water when compared to other areas, therefore, the inclusion of water column variables could improve the performance of the models for this species.

The RF models showed that both *P. multidentis* and *P. typus* prefer deep waters with some level of bottom complexity. *P. multidentis* is a schooling deeper-water demersal species that feeds on fishes, and benthic invertebrates. *P. multidentis* inhabits tropical and subtropical waters in the Indo-Pacific and is usually found

in depths between 40 and 245 m (Allen, 1985). It can be found in rocky reefs, coral reef areas, and loose rock/pebble/gravel areas close to steep drop-offs (Allen, 1985).

For *P. typus*, the preference of deeper areas has been supported by other studies, which indicate a preference for non-flat sea floors (Parrish, 1987a) and specific depth ranges (Fry et al., 2006). Fry et al. (2006) found a preference of *P. typus* for deeper areas with more fish caught in depth ranges between 125-150 m. In a more recent study in the Great Barrier Reef, a series of stereo-BRUVS were deployed along the shelf-edge and found *P. typus* was only present in sampling stations between 115-250 m (Sih et al., 2017). The high importance of depth as a variable to explain *P. typus* distribution could not *per se* be the primary factor driving its distribution. Depth is a variable correlated with a combination of biotic and abiotic environmental conditions that might be more related to the distribution of *P. typus* (Sih et al., 2017). The preference of *P. typus* for deep and non-flat areas was identified by the MBES model, and was captured by the model based on the interpolated DEM. For the MBES model and the interpolated model, the medium and broader scale variables had higher importance in the construction of the models. There was a general trend across models for an association between the presence of *P. typus* and areas with increased complexity. The final prediction of the probability of occurrence for *P. multidentis* and *P. typus* based on the MBES and interpolated models was similar. However, under and overestimation of probability of occurrence were present in all the models while spatial clustering of the residuals was more evident in the RBS interpolated model.

2.6. CONCLUSION

Kriging was the best model to interpolate the SBES data in the study site with lower errors compared to the other two interpolation methods and higher correlations with the MBES data. For the six studied species, the general pattern of relationship or absence of a relationship between depth and the depth derivatives was found using the MBES data and also using interpolated SBES data. *P. multidentis* and *P. typus* were successfully modelled by both the MBES and the SBES data, probably because key variables directly or indirectly related with their distribution were included in the analysis (e.g. depth). While it is evident that MBES produces a much higher resolution DEM than SBES, it also comes at a higher cost and requires more advanced training and experienced staff to operate and process data. In marine surveys, though, vessel costs can be very high, so the comparative cost of MBES is reduced. When vessel costs are very high there is an incentive to make the most of the vessel time and acquire data at the highest possible resolution (e.g. collecting MBES data). So where possible, I advocate the collection of MBES data. However, the possibility of using a low cost readily available equipment for modelling species distribution

at a comparable accuracy to the MBES data can be particularly useful for shallow turbid areas where satellite derived bathymetry is not suitable and the use of MBES offers little advantage because of its narrow coverage. A limitation of using interpolated SBES data to produce depth derivatives is the failure to capture fine scale variation of the terrain complexity. Therefore, the use of SBES depth and depth derivatives for modelling species distribution is expected to be less successful than MBES in modelling the distribution of species affected by fine scale variation of the terrain. The intrinsic characteristics of the seafloor (e.g. pronounced relief) can also limit the success of the SBES interpolation, as less variation would be captured by the interpolated surface. Further studies including a wide range of species and terrains with different levels of complexity are needed to confirm the findings of the present study. Different species with specific levels of habitat specialization and relationship with the environmental variables might respond differently. The inclusion of other variables like backscatter of the seafloor may help to increase the accuracy of the models for some species.

2.7. ACKNOWLEDGEMENTS

Stereo-BRUVS data were collected through the Western Australian Marine Science Institute (WAMSI) node 3 project 1 subproject 3.1.1: deepwater communities at Ningaloo Marine Park.

Chapter 3

3. Does the addition of seafloor backscatter data improve demersal fish distribution models based on multibeam bathymetry collected in Ningaloo Marine Park, Western Australia?

3.1. ABSTRACT

Demersal fish species constitute an essential component of the continental shelf ecosystem, and a significant element of fisheries catches around the world. However, collecting distribution and abundance data of demersal fish, necessary for their conservation and management, is usually expensive and logistically complex. The increasing availability of seafloor mapping technologies has led to the opportunity to exploit the strong relationship demersal fish exhibit with seafloor morphology to model their distribution. Multibeam echo-sounder (MBES) systems are a standard method to map seafloor morphology. The amount of acoustic energy reflected by the seafloor (backscatter) is used to estimate specific characteristics of the seafloor, including acoustic hardness and roughness. MBES data including bathymetry and depth derivatives were used to model the distribution of *Abalistes stellatus*, *Gymnocranius grandoculis*, *Lagocephalus sceleratus*, *Lethrinus miniatus*, *Loxodon macrorhinus*, *Lutjanus sebae*, and *Scomberomorus queenslandicus*. The possible improvement of models accuracies by adding the seafloor backscatter was tested in three different areas of the Ningaloo Marine Park off the west coast of Australia. For the majority of species, depth was a primary variable explaining their distribution in the three study sites. Backscatter was identified to be an important variable in the models, but did not necessarily lead to a significant improvement in the demersal fish distribution models accuracy. Possible reasons for that include: the depth and derivatives were capturing the significant changes in the habitat; the substrate was not a significant driver for the species distribution. The improvement in the accuracy of the models for certain species using data already available is an encouraging result, which can have a direct impact in our ability to monitor these species.

3.2. INTRODUCTION

Coral reef fish constitute an essential component of the continental shelf ecosystem, and a significant element of fisheries catches around the world (Anderson et al., 2009). Successful management and conservation of demersal fish rely on our ability to monitor their abundance and distribution. However, collecting distribution and abundance data is often expensive and logistically complex (Anderson et al., 2009). Increasing availability of seafloor mapping technologies has led to the opportunity to exploit the strong relationship demersal fish species exhibit with seafloor morphology to model their distribution in a cost-effective manner (Brown et al., 2012).

Multibeam echo-sounders (MBES) have become the standard method to map seafloor morphology. During an MBES survey, acoustic energy is transmitted by a transducer, towards the seafloor, over a swath that is wide across-track (120-150°) and narrow along-track ($\approx 1^\circ$). A portion of the emitted energy is scattered by the seafloor back towards a receiver array (commonly referred to as backscatter). The two-way travel time of this energy, to and from the transducer, combined with the angle of its travel, is used to determine the depth (bathymetry). The amount of acoustic energy reflected by the seafloor (backscatter) is used to estimate specific characteristics of the seafloor, including acoustic hardness and roughness (Fonseca and Mayer, 2007). Currently, a wide variety of MBES are available using frequencies between 12 kHz and 700 kHz. Higher frequencies produce higher resolution data but suffer from higher attenuation and low penetration in the seafloor (Schneider von Deimling et al., 2013).

The importance of depth to the assemblage of demersal fish has been well established (Fitzpatrick et al., 2012, Garcia-Alegre et al., 2014). As well as the direct influence depth has on demersal fish, it is also seen as a proxy for a broader set of variables involved in processes that occur at different levels of the water column which are usually harder to sample (e.g. temperature and light; Sih et al., 2017). Depth derivatives (e.g., ruggedness) are used to describe the complexity of the seafloor which can also influence the distribution of demersal fish at a variety of scales (Monk et al., 2011). Differences in the seafloor backscatter are used to help discriminate between benthic habitats, which can be closely related to the distribution of demersal species (e.g. sand vs rock bottom; Monk et al., 2011, Monk et al., 2010). Therefore, the inclusion of seafloor backscatter data in demersal fish distribution models is becoming a common practice. However, multiple descriptors can be derived from the original backscatter data adding more or less useful information for the species distribution modelling (Hasan et al., 2012a).

One of the most common products derived from the raw backscatter data is a mosaic, where the backscattered energy (measured as the backscatter strength on the dB scale, and backscatter intensity on

the linear scale) received from different grazing angles is normalised for a certain angle or a range of angles. This method produces a regular grid usually with a resolution equal to the bathymetry layer (Fonseca et al., 2009). However, the relationship between the backscatter strength/intensity and grazing angle is related, for certain frequencies, to particular properties of the seafloor (Fonseca and Mayer, 2007). Normalising the data to a specific angle dismisses valuable information contained in the angular response curve. Another approach is to characterize the seafloor using the Angle vs Range Analysis (ARA) (Fonseca et al., 2009). During the ARA analysis, the backscatter response observed is compared to expected acoustic response curves based on a mathematical model, the Jackson Model (Jackson et al., 1986). In particular, the ARA analysis can be used to estimate the sediment grain size, which has been shown in some demersal species to be a driver of distribution, or at least a correlate. Previous studies have focused on testing the relevance of including the backscatter and its derivatives to model the distribution of benthic habitat classes (Ierodiaconou et al., 2007, Brown et al., 2012, Hasan et al., 2012a). Less attention has been placed in testing the benefit of adding the angular response data in modelling the distribution of demersal fish which traditionally included the mosaic image and derivatives e.g., texture features (Hasan et al., 2014). In the present study, terrain variables were used to model the distribution of fish data derived from Baited Remote Underwater Stereo-Video (stereo-BRUVS). The overarching aim was to test the possible improvement of a model's accuracy if the backscatter data is included. This was tested in three areas of the Ningaloo Marine Park (NMP) with different bathymetry and levels of terrain complexity. Seven species were chosen as an indicative evaluation of the accuracy of species distribution models: starry triggerfish (*Abalistes stellatus*), Robinson's seabream (*Gymnocranius grandoculis*), silver toadfish (*Lagocephalus sceleratus*), red throat emperor (*Lethrinus miniatus*), sliteye shark (*Loxodon macrorhinus*), red emperor (*Lutjanus sebae*), and school mackerel (*Scomberomorus queenslandicus*). The probability of presence of each of these species was modelled using depth, depth derivatives and backscatter (mosaic and angular response curve) data as explanatory variables.

3.3. METHODS

3.3.1. Study area

Ningaloo Reef (NR) is the longest fringing coral reef in Australia, and is considered a biodiversity hotspot and to be in a good state of conservation compared with other coral reefs (Gazzani and Marinova, 2007, Schonberg and Fromont, 2012). The NMP was designed to protect 90% of these iconic waters (MPRA, 2005). A biodiversity analysis of different phyla including demersal fish, sponges, and soft corals showed the NMP is a biogeographical overlap zone, where more tropical species occur in the northern section and

both tropical and temperate species are present in the southern area (Simpson and Waples, 2012). In the present study, three areas of the NMP were used to model the distribution of demersal species of fish using depth derivatives and backscatter information. Mandu in the northern area, Point Cloates in the central area and Gnaraloo in the southern zone (Figure 3.1).

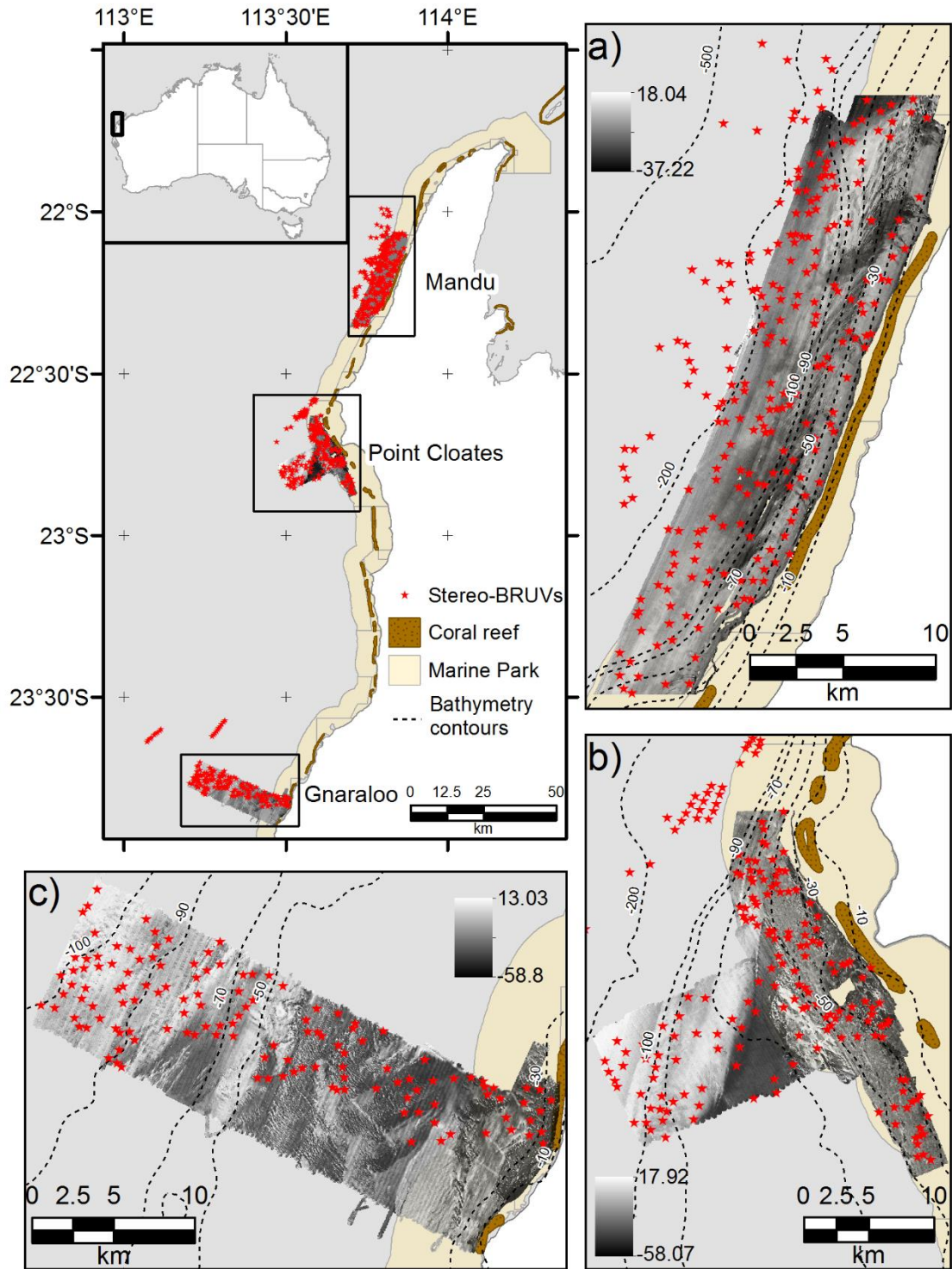


Figure 3.1. Study site. a) Mandu in the northern area of the NMP, b) Point Cloates in the central area and c) Gnaraloo in the southern area of the NMP. The deployment location of the stereo-BRUVS is shown as red stars, and the backscatter mosaics are shown as black and white images.

3.3.2. Stereo-BRUV

A multidisciplinary project was conducted in NMP between 2006 and 2009 by the Western Australia Marine Science Institution (WAMSI) and associates (Waples and Hollander, 2008). As part of this project, many aspects of the NMP were studied, including the demersal fish composition using Baited Remote Underwater Stereo-Video (stereo-BRUVS). A total of 656 stereo-BRUVS were deployed across the areas in Figure 1 in March-May 2009 between depths of 15 and 350 m. The stereo-BRUVS data included 239 deployments in Mandu, 185 in Pt Cloates and 155 in Gnarlou (Simpson and Waples, 2012). A database that included relative abundance, produced by the Australian Institute of Marine Science (AIMS), was used in the present study. The commonly used metric, MaxN, corresponds to the maximum number of individuals of the same species observed together in one frame at any one time, during the analysed period of the video, and has been shown to provide a conservative estimate of relative abundance (Willis et al., 2000, Cappo et al., 2003). The original video recorded by the stereo-BRUVs was divided in segments of an hour. Only the first hour of recording was used for the MaxN estimation analysis, which commences the moment the cameras touch the bottom. More details on the collection and analysis of the stereo-BRUVS can be found in Harvey et al. (2007).

3.3.3. Depth and depth derivatives

MBES surveys of the study areas were conducted in 2008 by Geoscience Australia and AIMS, using a Kongsberg EM3002, operating at 300 kHz. The MBES bathymetry was downloaded from the Geoscience Australia (GA) website as a raster with 3 m resolution. Ten depth derivatives were calculated from the bathymetry as shown in Table 3.1 (Moore et al., 2010, Moore et al., 2011). Some of the derivatives were produced using the raster package (Hijmans, 2016) of the free software R (R Development Core Team, 2017) and the rest were produced using Landserf v2.3 as specify in Table 3.1. Ecological processes occurring at different scales can affect the distribution and abundance of demersal fishes. Therefore, four different windows sizes were used in the production of the derivatives. The finest scale of analysis was fixed by the resolution of the MBES data (3m) and a 3x3 window of analysis, while the other three were chosen based on the spatial dependence of the species. A variogram analysis was used to identify the maximum distance at which the species display spatial dependency (the range) (Holmes et al., 2008). For the species with spatial dependency, the range was above 4 km. Therefore, the scales were chosen to cover the span between the finest resolution and the ~ 4 km range of the species using four windows sizes of analysis 3x3m (81m²), 9x9 (729m²), 15x15 (2025m²), and 21x21 (3969m²). For the fractal dimension

calculation, the smallest windows size allowed in Landsfer is 9x9. Therefore, the 3x3 window analysis was not used for this variable.

Table 3.1. Depth derivatives produced from bathymetry. Aspect (orientation of the slope) was divided in two variables using trigonometric transformations.

Variable	Abbreviation	Description	Software	Reference
Slope	slope	Rate of change in elevation over the analysis windows express in degrees.	Landsfer v2.3	Wood (1996)
Aspect	Northness	Cosine of aspect where slopes facing north (NS=1), or south (NS=-1).	Landsfer v2.3	Wood (1996)
	Eastness	Sine of aspect where slopes facing east (WE=1), or west (WE=-1).	Landsfer v2.3	Wood (1996)
Curvature	Profile	Curvature of a line formed by intersecting the vertical plane oriented in the direction of the steepest slope with the terrain surface.	Landsfer v2.3	Wood (1996)
	Plan	Curvature of a line formed by intersecting the horizontal plane oriented in the direction of the steepest slope with the terrain surface.	Landsfer v2.3	Wood (1996)
	Mean	Mean curvature in any plane.	Landsfer v2.3	Wood (1996)
Fractal dimension	fractal	Indicates how surface roughness changes over space with a minimum value of 2.0 indicating smooth, scale invariant behaviour and a theoretical maximum of 3.0 indicating a space filling rough surface.	Landsfer v2.3	Wood (1996)
Standard deviation of depth	SD	Standard deviation of depth.	R raster package	Holmes et al., 2008
Benthic position index	BTI	Measure of the position of a particular pixel concerning the average depth of its surrounding neighbours. Positive values showing depth above the average (ridges), and negative values for pixels below the average (troughs).	R raster package	Wilson et al. (2007)
Terrain ruggedness Index	TRI	Mean of the absolute differences between the value of a cell and its neighbouring cells.	R raster package	Wilson et al. (2007)
Roughness	rough	Difference between the maximum and the minimum depth of a cell and its neighbouring cells.	R raster package	Wilson et al. (2007)

3.3.4. Backscatter derivative

The backscatter information was included in the models as two different layers. The first one was the full-coverage, 3-m resolution mosaic, downloaded from the GA website. The second one is an approximation of the sediment phi size estimated using the ARA (Fonseca et al., 2009), applied to the raw files.

3.3.5. Angle vs. Range Analysis (ARA)

The relationship between the backscatter strength and the grazing angle is commonly known as the angular response curve (ARC). ARC is related, for certain frequencies, to particular properties of the seafloor (Hasan et al., 2014). Therefore, the angular response curve can be used to infer characteristics of the seafloor using the Angle vs Range Analysis (ARA; Fonseca et al., 2009). In this study, we used the FMGT

software (version 7.8) to conduct an ARA analysis using the raw MBES backscatter data. A full description of the method followed during the ARA analysis in FMGT can be found in (Fonseca and Mayer, 2007), a brief description of the method is given here.

The backscatter angular response is first corrected for radiometric and geometric distortions to locate each ping to its correct angular position. In the next step, a group of consecutive pings is stacked in the along-track direction, 30 pings were stacked. The stack of the pings produces two seafloor patches, one for the port side and another for the starboard side. The size of the patch being analysed is approximately half of the swath of the MBES system coverage. The stacking of the pings in a patch has the effect of reducing the resolution of the final layer, but it is a necessary step to reduce the speckle noise, typical to any acoustic method. An average angular response curve calculated for each patch is then compared to a formal mathematical model which relates the observed backscatter with seafloor properties in a process called the ARA-inversion. During the inversion, the model is used to produce an approximation of the acoustic impedance, roughness and consequently the mean grain size of the patch under analysis. An ARA-inversion analysis was conducted for all the patches in the three studied sites to obtain maps of the distribution of grain size, with a resolution of 60 m. During the analysis, only incidence angles between 20-60° were included, as the angles in the near nadir and outer angle regions tend to be noisy with less power of discrimination between different types of substrate (Hasan et al., 2012b).

As part of the WAMSI project, 290 sediment samples were collected using a Van-Veen grab sampler for surface and subsurface material between 2007-2006 (Colquhoun et al., 2007). The grain size estimated for this ground-truth data was compared with sediment phi size estimated using the ARA analysis, correlation and regression was used to test the relationship between them.

3.3.6. Species distribution models

The environmental variables including depth, depth derivatives, and the backscatter data were used as explanatory variables to explain the probability of presence of *A. stellatus*, *G. grandoculis*, *L. sceleratus*, *L. miniatus*, *L. macrorhinus*, *L. sebae*, and *S. queenslandicus*. The species were selected based on a minimum 25 presence in each of the sampled areas. All the species included in the present study are carnivores with different degrees of generalist feeding behaviour using a variety of benthic habitats (Table 3.2). Lutjanids and lethrinids including *G. grandoculis*, *L. miniatus*, and *L. sebae* have a strong association to hard bottom or substrate with a certain degree of vertical relief (Parrish, 1987b). *L. sceleratus* and *A. stellatus*, on the other hand, have a preference for sandy bottoms (Rousou et al., 2014, Randall, 1967). Considering that

seafloor backscatter can help to differentiate hard from sandy bottoms; this study has the hypothesis that the inclusion of seafloor backscatter will improve the accuracy of the models for the lutjanids and lethrinids species. For *S. queenslandicus* and *L. macrorhinus*, water column variables may be more important in explaining their distribution (Collette and Nauen, 1983, Gutteridge et al., 2011), and it is expected that the inclusion of seafloor backscatter data to have a marginal effect on their models.

Table 3.2. Habitat and feeding preference of the species included in the study.

Species	Habitat	Feeding preferences	Reference
<i>Gymnocranius grandoculis</i> <i>Lethrinus miniatus</i> <i>Lutjanus sebae</i>	Hard substrata or substrata having some vertical relief.	Benthic invertebrates and small fishes.	Parrish, 1987
<i>Scomberomorus queenslandicus</i>	Pelagic in bays and around islands and coastal reefs.	Neritic species.	Collette et al., 1983
<i>Lagocephalus sceleratus</i>	Sandy, rocky substrates and seagrass meadows.	Benthic invertebrates.	Rousou et al., 2014
<i>Loxodon macrorhinus</i>	Inshore habitats with clear waters.	Benthic invertebrates and small fishes.	Gutteridge et al., 2011
<i>Abalistes stellatus</i>	Sand, sponge, and weed areas on deep slopes.	Feeds on benthic animals.	Randal, 1967

Random Forest (RF) is a robust statistical method with many advantages to solving ecological problems, including high classification accuracy and particularly high capacity to model complex interactions without statistical pre-assumptions like normality (Breiman, 2001). The algorithm begins by selecting a bootstrap sample from the data, approximately 63% of the original observations are used at least once in the bootstrap sample. The rest of the observations not selected for the bootstrap sample are called out-of-bag (OOB) observations. RF fits a tree to each bootstrap sample, but in each node, only a subsample of the variables is available for the binary partitioning (one-third of the total number of variables in the case of regression and the square root in the case of classification). All the trees are fully grown and used to predict the OOB observations. The predicted value for each observation is based on the average value predicted by the trees (Breiman, 2001). In this study, we used RF classification to model the presence/absence of the nine selected species and RF regression for the richness of species.

For the RF classification, the sensitivity and specificity were evaluated using the Area Under the Curve (AUC) of the Receiver Operator Curve. The AUC varies between 0 and 1. Values higher than 0.9 are considered outstanding whereas values between 0.9 and 0.7 indicate good performance. Values lower than 0.7 indicate poor prediction and values lower than 0.5 indicate that the model is not better than a

random classification (Hosmer et al., 2013). The effect of including the backscatter data as explanatory variables in the accuracy of the models was examined using two scenarios, the first one including depth and depth derivatives (DV) and in the second one the two backscatter variables were added (DVBS). A five-fold cross-validation procedure was used, for each fold 65 percent of the data was used to train the model and the rest to test it, an AUC was obtain for each fold and the mean AUC is reported. The difference in the mean AUC for the DV and DVBS scenarios was tested using a t-test in R.

For the RF regression the accuracy was measured by the mean square error (MSE), and also the percentage of variance explained by the model is reported.

3.4. RESULTS

3.4.1. Angle vs. Range Analysis (ARA)

A significant correlation was found in the Mandu area between the phi sediment size estimated using the backscatter data in the ARA analysis and the ground-truth sediment samples grain size ($r=0.59$, $p<0.001$, $r^2=0.25$, $p<0.001$). A significant correlation was also found in the Pt Cloates area between the phi sediment size estimated using the backscatter data in the ARA analysis and the ground-truth sediment samples grain size ($r=0.47$, $p=0.003$, $r^2=0.22$, $p<0.001$). The relationship between the grab grain size and the ARA-phi for the full data combined was also significant ($p<0.001$, Figure 3.2). No significant correlation was found for the Gnaraloo site.

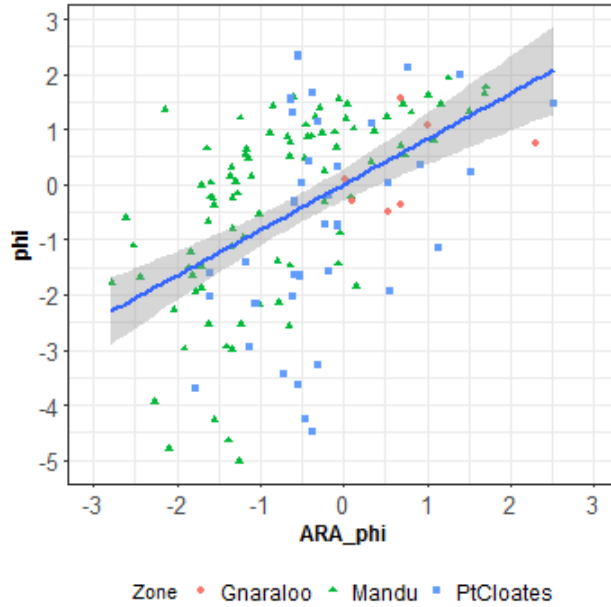


Figure 3.2. Linear regression between the grain size calculated with the ARA analysis and the phi size calculated from the ground-truth samples.

3.4.2. Species distribution models

The performance of the models was species and area dependent with some species being better modelled in some areas than others and all species models having acceptable levels of accuracy (above 0.7) in at least one of the studied sites (Figure 3.3). The effect of adding the backscatter data (DVBS) also varied by species and study site with no consistent improvement in the accuracy of the models. The Mandu area had fewer models of species with acceptable levels of accuracy (above 0.7) while Pt Cloates had only one species with model accuracy consistently below 0.7.

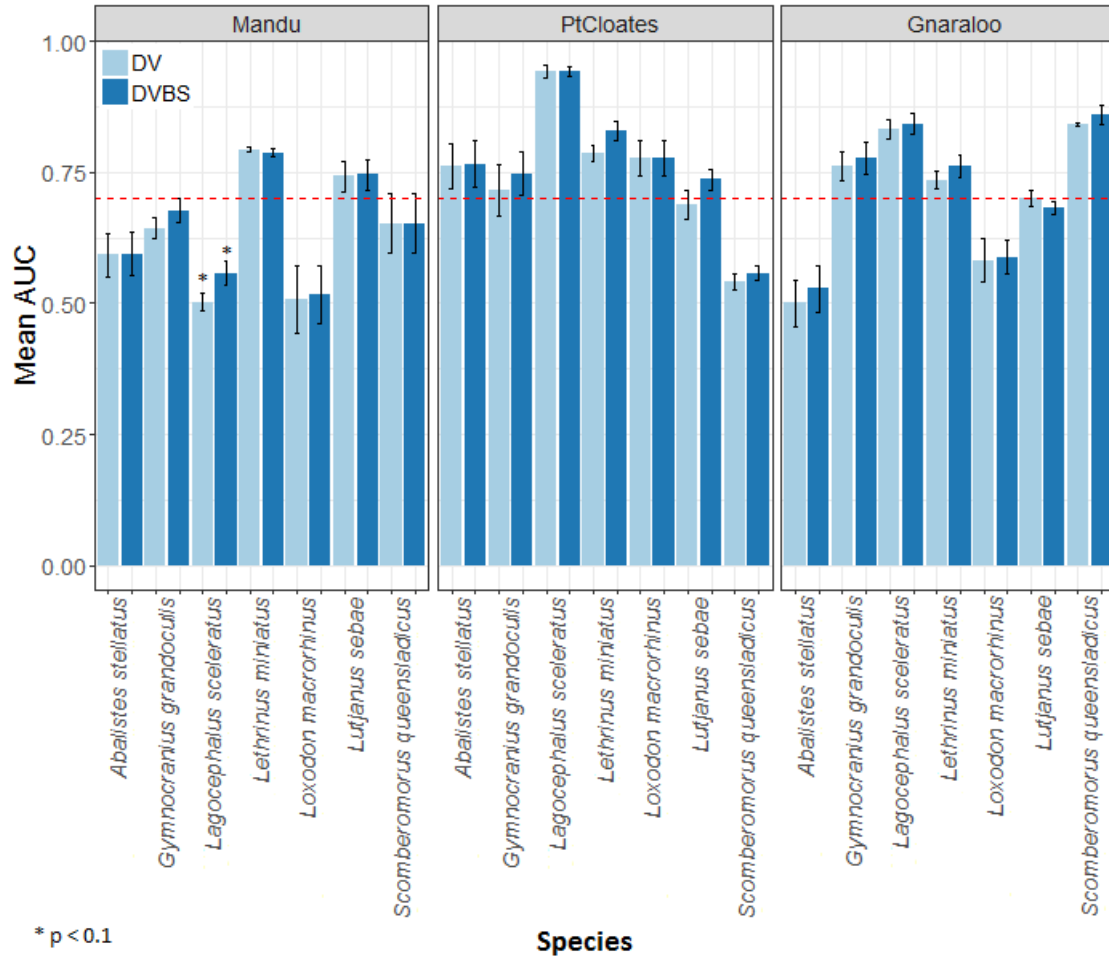


Figure 3.3. Mean AUC and standard error of the Random Forest distribution models for *A. stellatus*, *G. grandoculis*, *L. sceleratus*, *L. miniatus*, *L. macrorhinus*, *L. sebae* and *S. queenslandicus* in the three study sites of the Ningaloo Marine Park. The depth and depth derivative scenario (DV), and the depth, depth derivatives plus the backscatter data (DVBS) scenario are shown.

For *G. grandoculis*, the inclusion of the seafloor backscatter had a positive effect on the performance of the models increasing the mean AUC in all the three study sites. Although the increase of the mean accuracy in the *G. grandoculis* models was not significant, the mean AUC (\pm se) for Pt Cloates area was above the 0.7 threshold after the inclusion of the seafloor backscatter data (Figure 3.3). The DVBS scenario had a better performance in the models of *L. miniatus*, *L. macrorhinus*, and *S. queenslandicus* in at least two of the study sites, with different levels of improvement. A significant increase in the mean AUC was observed for the *L. sceleratus* model (Figure 3.3) in the Mandu area when the seafloor backscatter was included; however, the performance of the model was still below the 0.7 threshold. The addition of the seafloor backscatter data improved the accuracy of the *L. sebae* model in the Pt Cloates area to a mean accuracy above the 0.7 threshold.

3.4.3. Richness

The RF for the richness of demersal species explained different level of variance in the three study sites (Table 3.3). The model with the lowest level of mean explained variance was at Gnaraloo, although, the DVBS scenario produced a significant increase of explained variance by 5 % ($P < 0.05$). In the Mandu area, a significant portion of variance was explained by the models, with more than 25% of mean explained variance. However, no change in explained variance was observed in the DVBS scenario. The richness of demersal fish species was particularly well modelled in the Pt Cloates area with variance explained of greater than 40%. The importance of the backscatter data was evident with an increase of the explained variance in the DVBS scenario, although the increase was not significant (Table 3.3).

Table 3.3. Mean percentage of variance explained by the Random Forest for the total richness of species in the three study sites for both the depth and depth derivatives (DV, BT+DV) and depth, depth derivatives and seafloor backscatter data (DVBS, BT+DV+BS) scenarios.

Variable	Scenario	Variance explained		
		Mandu	Pt Cloates	Gnaraloo
Richness	DV	26%	42%	2%
	DVBS	26%	46%	7% **

3.4.4. Variables importance in the distribution model

A summary of the most important variables explaining the distribution of the species is shown in Table 3.4. Only the three most important variables are shown for brevity, a full table is presented in Appendix A. Depth and seafloor backscatter were the most important variables in the construction of the models for the majority of the species in the three study sites (Table 3.4). Depth was key for the majority of the species in the three study areas, with some exceptions. Variables related to terrain variability including roughness, TRI, and standard deviation of depth were important for many of the species, in particular at a broad scale (15 -21 neighbours). For the models of *L. sceleratus*, *L. macrorhinus*, and *S. queenlandicus*, for example, the terrain variability variables had higher importance than depth in the Pt Cloates area.

The seafloor backscatter, and the ARA-phi layer, were among the three most important variables in the models of six of the seven studied species in at least one of the study areas. For *G. grandoculis*, the ARA-phi was the second most important variable in the models of the three study sites, confirming its importance for this species as shown by higher mean AUC of the DVBS models compared to the DV scenario. For *L. sceleratus* DVBS models in both the Mandu and Gnaraloo areas the ARA-phi and the backscatter mosaic ranked among the three most important variables in the models. The ARA-phi variable was identified as one of the three most important variables in the models of *L. miniatus*, *S. queenlandicus*,

in both Pt Cloates and Gnaraloo areas. For the *L. macrorhinus* and *L. sebae* model, the ARA-Phi was important in the Gnaraloo and Pt Cloates areas respectively.

Depth was the most important variable in the construction of the model for the richness of species in the Mandu area, in both DV and DVBS scenarios. For the Pt Cloates area, TRI, followed by the profile curvature were the most important variables explaining the richness of species. The ARA-phi layer was also considered important when included in the model for Pt Cloates, although with a lower ranking. For the Gnaraloo area, slope, profile curvature and depth were the most important variables in the DV model, while for the DVBS model, both the ARA-phi layer and backscatter mosaic were second and third in importance.

Table 3.4. Summary of variable importance in the construction of the distribution models for the species included in the study. Only the three variables with highest ranking of importance are included for each species and each scenario. The scenario of depth and derivatives (DV) and depth, depth derivatives and backscatter data (DVBS) scenarios are shown.

Species	Importance	Area/Scenario					
		Mandu		Pt Cloates		Gnaraloo	
		DV	DVBS	DV	DVBS	DV	DVBS
<i>A. stellatus</i>	1	Depth	Depth	Depth	Depth	NS9	NS9
	2	rough21	rough21	TRI21	TRI21	Depth	Depth
	3	slope15	slope15	slope21	slope21	BPI9	profc15
<i>G. grandoculis</i>	1	Depth	Depth	Depth	Depth	Depth	Depth
	2	rough9	ARA_Phi	slope15	ARA_Phi	meanc21	ARA_Phi
	3	BPI3	TRI15	SD15	BS	fractal21	profc15
<i>L. sceleratus</i>	1	Depth	ARA_Phi	TRI21	TRI21	Depth	Depth
	2	NS3	Depth	SD21	SD21	WE21	ARA_Phi
	3	planc9	BS	TRI15	TRI15	NS21	WE21
<i>L. miniatus</i>	1	rough15	rough15	Depth	ARA_Phi	Depth	Depth
	2	profc15	profc15	SD9	SD9	TRI9	BS
	3	Depth	rough21	rough9	Depth	profc3	TRI9
<i>L. macrorhinus</i>	1	Depth	Depth	TRI9	TRI9	TRI15	TRI15
	2	rough3	rough3	TRI15	TRI15	TRI21	TRI21
	3	TRI21	TRI3	SD9	SD9	SD3	ARA_Phi
<i>L. sebae</i>	1	Depth	Depth	Depth	Depth	slope9	slope9
	2	profc21	profc21	rough21	rough21	rough21	rough21
	3	SD3	rough3	SD21	ARA_Phi	Depth	Depth
<i>S. queenslandicus</i>	1	fractal9	fractal9	planc15	ARA_Phi	Depth	Depth
	2	fractal21	fractal21	profc15	profc15	WE21	ARA_Phi
	3	fractal15	Depth	profc21	planc15	NS21	WE21
Richness	1	Depth	Depth	TRI15	TRI15	slope9	Depth
	2	slope15	slope15	profc21	profc21	profc9	BS
	3	SD9	slope9	SD15	ARA_Phi	Depth	ARA_Phi

3.5. DISCUSSION

The accuracy of the species distribution models based on depth and depth derivatives varied among species and study sites. Higher accuracies were observed, in general, for the species in the Pt Cloates area, which is considered to have a complex seafloor. The terrain variables were less successful in modelling the presence of the species in the Mandu area. The addition of the seafloor backscatter in the species distribution models, did not necessarily increase the models accuracy in a significant manner, although, in the majority of the cases the ARA-phi layer was ranked as an important variable when included in the models. The ARA-phi layer was particularly important in the model of *G. grandoculis* in the three study sites, and *L. miniatus* in two areas, increasing the accuracy of the models. A significant portion of the species richness variation was explained using the terrain variables, and the addition of the seafloor backscatter improved the accuracy of the model in the Gnoraloo area.

3.5.1. Backscatter derivatives

A significant relationship was found between the phi size estimated with the ARA analysis and the grain sediment size measured from the grab samples. However, the ARA-phi analysis did not identify coarse gravel sediments (cobbles) with phi values below -3. Instead, the ARA-phi analysis classified cobbles as pebble and granule gravel. Previous studies have suggested the inclusion of backscatter, and in particular, the use of the angular response of the backscatter can add to the discrimination between benthic habitats (Hasan et al., 2014). However, the seafloor backscatter intensity can be affected in different ways by the frequency of the echo-sounder, sediment grain size, nature, and magnitude of seabed roughness, and volume scattering by subsurface scatters (Ferrini and Flood, 2006). For example, scattering register by a high-frequency echo-sounder would be related to seabed surface roughness while scattering by particles under the sediment-water interface will be relatively more important at lower frequencies (Jackson et al., 1986). The importance of the different variables influencing the backscatter of the seafloor can also vary between sampling sites (Ferrini and Flood, 2006). Therefore the seafloor backscatter on its own has limitations to predict seabed characteristics (Ferrini and Flood, 2006).

A drawback in the approach adopted in this study was using a constant number of stack pings during the ARA analysis, as the area sampled would then depend on the water depth. As a result, the sampling areas in the shallowest depths were around three times smaller than in the deepest zones. This can produce a misinterpretation of the sediment class in deeper areas, in particular, in areas of transition between two different classes. However, the vast majority of stereo-BRUVs deployments were not located in areas of

transition between different ARA-phi classes reducing the risk of mixing sediment classes. Hence, it is unlikely that the different resolutions of the ARA-phi size layer had a significant effect on the species distribution models. The high ranking of the ARA-phi in the models of species distribution, reinforce the idea that the resolution of the variable was appropriate.

A previous study compared a high (200 kHz) and low (50 kHz) frequency echo-sounders and its ability to discriminate sediment grain size and found the higher frequency system failed to differentiate between sediment grain sizes even between mud and sand (Freitas et al., 2008).

3.5.2. Species distribution models

For the majority of species, depth was a primary variable in explaining their distribution across the three study sites and for both DV and DVBS scenarios. Depth is a common variable influencing the distribution of species in coral reef areas, as it is related to the effects of light availability on community composition and function (Hill et al., 2014b).

The importance of the depth derivatives at different window sizes varied among species and study sites. For the most abundant species, such as *A. stellatus*, *L. sceleratus* and *G. grandoculis*, broader-scale variables (15x15 and 21x21 windows size) of TRI, roughness, slope and fractal dimension were considered key variables in explaining their distribution. These results agree with previous studies, showing that broad-scale variables are more relevant for species with higher mobility and larger home ranges that use a variety of benthic habitats (Tamburello et al., 2015, Franklin et al., 2009). For other species, like *L. macrorhinus*, which had the lowest prevalence in the study, the fine-scale variables were more important in two of the study areas, indicating a higher level of specialisation. For the remaining species, a mix of fine and broad-scale variables was important in the construction of the distribution models.

The ARA-phi layer which was calculated with a broad resolution of 60 m, was found to be one of the three most important variables in the species models. This reaffirms the importance of broad-scale variables for roaming species with a wide niche (Monk et al., 2011, Moore et al., 2011). The backscatter mosaic at 3 m resolution was often included as a key variable, though to a lesser extent. This study investigated the hypothesis that the addition of the seafloor backscatter would increase the accuracy of the models, in particular, for *G. grandoculis*, *L. miniatus*, *L. sebae*, *L. sceleratus* and *A. stellatus* models. Seafloor backscatter data were consistently important in the models of *G. grandoculis*, increasing the model's accuracy for the three study sites. *G. grandoculis* is a species that inhabits rocky bottoms (Dorenbosch et al., 2005), which can explain the importance of backscatter in the construction of the models as this

variable can be used to differentiate between soft/hard bottoms (Kloser et al., 2010). *L. miniatus* is associated with sand around coral reefs areas where it feeds on benthic invertebrates, which could explain the importance of the seafloor backscatter in the models of two of the study sites (Carpenter and Niem, 2001). However, results showed only an increase of between 2 and 5% in the model accuracy for *G. grandoculis*, *L. miniatus* and *L. sceleratus*, in at least two of the study sites. Also, the increase of the mean AUC was only significant for *L. sceleratus*, therefore the improvement can only be seen as indicative. One potential reason for the lack of improvement in the accuracy of the model for *L. miniatus* in the Mandu area, was a previous study showed this species to be more prevalent in shallow waters (12-18m) of the Great Barrier Reef (Newman and Williams, 2001). So, depth might play a more important role as a rapid change in bathymetry is observed in this area. *L. sceleratus*, inhabits offshore sandy bottoms in their early life stages with a habitat shift to deeper or rocky grounds for the largest individuals (Fitzpatrick et al., 2012). The inclusion of the ARA layer may, therefore, add useful information to differentiate between sandy and rocky habitats. For *L. sebae*, the inclusion of the seafloor backscatter had a positive effect on the accuracy of the models for the Pt Cloates while variables measuring the rugosity of the seafloor were particularly important for this species in the three study sites. This species is associated with exposed reef slope (Fitzpatrick et al., 2012) which could explain the importance of variables related to the complexity of the seafloor as coral reef areas have, in general, higher levels of terrain complexity and rugosity.

Depth and backscatter were not considered as important in explaining the distribution of some species. For example, *L. macrohinus* is a small species of shark whose distribution was more related to variables measuring the rugosity of the seafloor. Another species, *S. queenslandicus*, is an epipelagic neritic schooling species (Collette and Nauen, 1983, Kailola et al., 1993), which might explain the poor performance of the models for this species in two of the study sites, as variables of the terrain might not be related to its distribution.

Previous studies have found the addition of backscatter metrics can be important in the construction of models of demersal fish distribution (Monk et al., 2011) or suggested further studies were needed to assess the relationship between seafloor backscatter and the assemblage of demersal fish (Schultz et al., 2014). The results of this study showed that the seafloor backscatter was an important variable in the models of demersal fish distribution. However, the inclusion of this variable did not necessarily lead to an improvement in the accuracy of the models. Possible reasons for that may be that the depth and derivatives were capturing the significant changes in the habitat, or that the substrate was not a significant driver for the species distribution. Also, the high frequency of the MBES (300 kHz) could limit the

penetration of the acoustic energy to just a very superficial layer of the seafloor which could consequently limit its power of discrimination between benthic habitats (Schneider von Deimling et al., 2013, Boscoianu et al., 2008). Therefore, it is suggested the effect of frequency selection on model performance is investigated in future studies.

The analysis of the 656 stereo-BRUVS showed that only around 3% of the species were moderately prevalent, occurring in $\geq 20\%$ of the sampling point (Simpson and Waples, 2012). In the present study we included some of these species, those with a minimum of 25 occurrences on each of the three sites in an effort to compare the model performance in different areas of the NMP. Therefore, they all presented a certain degree of generalist behaviour which is related to less specialised habitat requirements, and as a result it is more difficult to produce well performing models of the species distributions (Wilson et al., 2008).

3.6. CONCLUSION

Demersal species were well modelled with the depth and depth derivatives in the majority of the species analysed in at least one of the study sites. The addition of the backscatter data increased the accuracy of the models for some species, in particular, a consistent positive effect was observed for *G. grandoculis*. Depth derivatives can integrate some of the seafloor roughness information which may explain the limited benefit of adding the backscatter data in some of the species distribution models. Additional information related to the hardness/roughness not included in the depth derivatives were important for some species for which the inclusion of the backscatter data had a positive effect.

For some species the mosaic backscatter layer appeared as an important variable in explaining their distribution, in general however, the ARA-layer was more important for the variables in the construction of the models. This is an encouraging result that demonstrates that the use of novel derivatives which take advantage of the angular response can produce models with higher accuracies. Although the increase in the accuracy of the models was not significant for the majority of the species, it can be considered an indicative result, but more efforts are needed to confirm this pattern.

3.7. ACKNOWLEDGMENTS

The authors would like to thank Geoscience Australia for making the bathymetry and backscatter data available and particularly Justy Siwabessy for helping provide the raw MBES data. The authors would also like to thank WAMSI for funding research and making data available from NMP.

Stereo-BRUVS data were collected through the Western Australian Marine Science Institute (WAMSI) node 3 project 1 subproject 3.1.1: deepwater communities at Ningaloo Marine Park.

Chapter 4

4. Investigating the value of acoustic water column data in demersal fish assessment using historical data from Ningaloo Marine Park, Western Australia

4.1. ABSTRACT

Conservation and management of coral reef fish require spatially explicit information of their abundance and distribution. However, collecting biological data is expensive and logistically complex. The use of non-destructive methods like underwater cameras and echo-sounders are particularly important for non-trawling areas like marine parks. Each of these methods, however, have their limitations and bias. The coordinated use of more than one technique can produce a more accurate characterization of coral reef fishes' distribution. The potential of complementary use of historical data from Baited Remote Underwater Stereo-Video (stereo-BRUVS) and acoustics in the estimation of demersal and semi-demersal fish biomass distribution is the focus of the present study. Random Forest was used to model the distribution of the relative biomass and abundance of organisms observed by the stereo-BRUVS. Acoustic data opportunistically collected in Ningaloo Marine Park (NMP) was used to estimate acoustic biomass. The value of adding the acoustic biomass in the model was tested by changes in the percentage of variance explained by the model. The addition of the acoustic biomass in the models of total abundance and relative biomass did not improve the performance of the models. Temporal differences are argued as the main reason for the lack of correlation between the two data sets. However, a broad scale analysis showed significant correlations between the acoustic and stereo-BRUVS biomass and the seafloor backscatter. This relationship needs to be further explored but suggests that broad-scale patterns could be detected using opportunistic data collected years apart.

4.2. INTRODUCTION

Coral reefs are highly productive ecosystems, supporting important commercial and recreational fisheries and providers of diverse ecological services. However, they are also increasingly vulnerable to anthropogenic impacts (Hill et al., 2014a). Conservation and management of coral reef fishes have historically been challenging, partially because they reside in and around highly structured habitats where collecting fish abundance and distribution data is a complex process.

In the last few decades, several non-destructive methods have been developed to collect fishery-independent data of coral reef fishes including visual counts by SCUBA divers (Bohnsack and Bannerot, 1986), underwater video techniques (Watson et al., 2005) and more recently, acoustics (Zenone et al., 2017). Each of these methods has bias and limitations, including spatial or temporal resolution restrictions, fish avoidance and gear selectivity (Harvey et al., 2007, Watson et al., 2005). The coordinated use of more than one technique can produce a more accurate characterization of coral reef fishes' distribution. The potential of complementary use of Baited Remote Underwater Stereo-Video (stereo-BRUVS) and acoustics in the estimation of demersal and semi-demersal fish distribution is the focus of the present study.

Since their invention, stereo-BRUVS have been increasingly used to study demersal and semi-demersal fishes in coral reef areas around the world (Cappo et al., 2004). Stereo-BRUVS can be used to sample a wider depth range than visual census, including deeper depth ranges, and also produce higher levels of accuracy in the length measurements (Harvey et al., 2003). However, the main disadvantage of the stereo-BRUVS is the unknown area of influence of the bait-plume used in the system which has the effect of attraction and concentration of fish around the cameras (Cappo et al., 2006). The area of influence of the bait-plume will depend on several factors including currents, tides, soak time and species swimming speed. Therefore, it is not possible to assess the density of fish and the estimated biomass should be considered relative biomass (Cappo et al., 2006).

Fisheries acoustics is the second non-destructive method to monitor fish distribution included in this analysis. Continuous theoretical and experimental research in the acoustic field in the 1970s and 1980s have led to increasing use of this technique as the standard method for monitoring populations of commercially important species in temperate regions (Davison et al., 2015, Kloser et al., 2016). During an acoustic survey, an echo-sounder is used to transmit acoustic energy into the water in the form of a beam. Where there is a difference in acoustic impedance between two mediums within the acoustic beam (an encountered object and surrounding water), a part of this energy is reflected back to the receiver of the

echo-sounder and recorded. The magnitude of the echo reflected to the transducer by the target, such as fish or other marine organisms, in the water ('target strength') is highly dependent on target-specific factors, including: size, morphology (e.g., presence or absence of a swim bladder), the angle in which the target was swimming when it was insonified by the echo-sounder and, the physiology of the species (Simmonds and MacLennan, 2008). The shape of the swim bladder and the tilt behaviour of the fish, in particular, are considered the most important factors determinant of the target strength (Simmonds and MacLennan, 2008).

The possibility of covering extensive areas in a relatively short period is one of the main advantages of using acoustics to monitor fish distribution. Also, during an acoustic survey, the entire water column is sampled, including different elements of the ecosystem i.e. zooplankton, pelagic and demersal species. Therefore, there is the potential of using the acoustic data to manage the ecosystem rather than target species, which complements an ecosystem-based management approach (Trenkel et al., 2011). However, the information contained in the acoustic return is limited with regard to the number and identity of potential species present and their size (many combinations of which may provide similar acoustic returns). Species identification is complex and typically unreliable when based only on the echo produced by the targets insonified (Ona, 1990). Concurrent ground-truth data is required to inform on the identity of species producing the acoustic signals recorded by the echo-sounder (Simmonds and MacLennan, 2008). While an increasing number of studies have been conducted using acoustics in reef areas (Boswell et al., 2010, Costa et al., 2014, Campanella and Taylor, 2016), the collection of ground-truth information in non-trawling diverse zones like coral reefs is in its infancy and has not been standardised.

Although mobility of coral reef fishes can vary between metres to thousands of kilometres (Green et al., 2015), a strong association between fish distribution and geomorphology, biological cover, and reef topographic complexity have been found in many areas and for many species (Gratwicke and Speight, 2005, Pittman et al., 2007, Young and Carr, 2015). The strong association between demersal species of fish and the morphology of the seafloor have been used before to approximate the distribution of species using depth, depth derivatives and more recently the backscatter of the seafloor (Monk et al., 2011, Monk et al., 2010). The backscatter level of the seafloor reflects the roughness (relative to the acoustic wavelength) and impedance contrast (sometimes referred to as acoustic softness) of the seafloor (Fonseca and Mayer, 2007).

In the present study, the hypothesis tested is that demersal and semi-demersal species of fish in coral reef areas have a strong site-fidelity that produce areas of high biomass which can be detected by both stereo-

BRUVS and hydroacoustic surveys. Therefore, these complementary data sets can be used in conjunction to better understand demersal and semi demersal fish distributions.

To test this hypothesis, the spatial distribution of demersal fish in two areas of the Ningaloo Marine Park (NMP) was evaluated using acoustic data (from two different years) and compared to stereo-BRUVS data (collected from one year). Three specific objectives of the study were:

1. Produce spatial distribution maps of acoustic variables including depth-stratified NASC and number of single targets per km.
2. Estimate correlations between the acoustic variables and stereo-BRUVS data including relative biomass and the total MaxN.
3. Model the spatial distribution of the total MaxN and relative biomass using terrain variables and test change of performance of the model when the depth-stratified NASCs data were included as an explanatory variable in one area of the NMP.

4.3. METHODS

4.3.1. Study area

Ningaloo Reef (NR) is the longest fringing coral reef of Australia and has been identified as an important marine hotspot of biodiversity of Western Australia (Schonberg and Fromont, 2012). The creation of the NMP and the establishment of the Ningaloo Research Program (NRP) had the objective of protecting and managing this iconic, highly biodiverse reef (Waples and Hollander, 2008). As part of the NRP, the Western Australian Marine Science Institution (WAMSI) and its partners carried out an extensive series of surveys to increase the scientific understanding of this vital ecosystem (Simpson and Waples, 2012).

The WAMSI project included acoustic (single-beam) and stereo-BRUVS surveys. A total of 656 stereo-BRUVS were deployed in March-May 2009 between depths of 15 and 350 metres in three different areas of the NMP (Simpson and Waples, 2012). The acoustic data were collected using a single-beam Simrad EQ60 echo-sounder (38 kHz) between 2006 and 2008 (Figure 4.1; Colquhoun et al., 2007). Acoustic data collected between April-May 2006 and February 2008 were selected for this study due to their spatially overlapping coverage with the stereo-BRUVS.

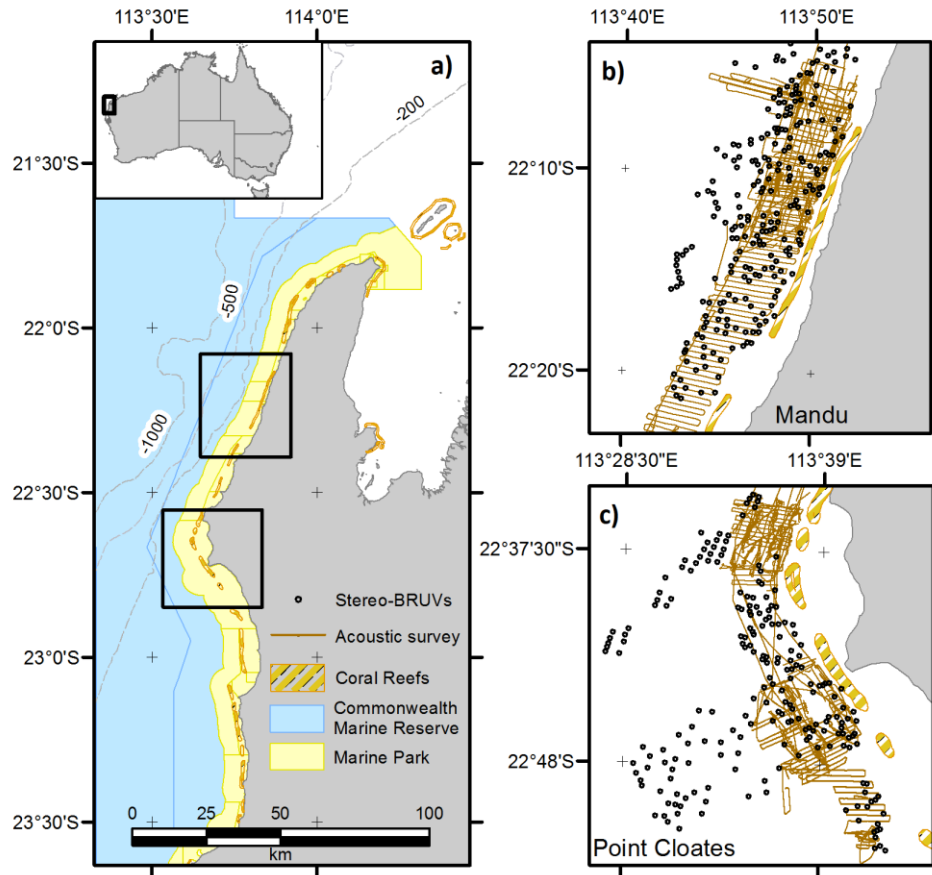


Figure 4.1. Study site, a) Location of the two study sites in the Nigaloo Marine Park, b) Zoom to the Mandu area with the acoustic survey showed in brown and the location of the stereo-BRUVS deployments showed as black dots, c) Zoom to the Point Cloates area.

4.3.2. Acoustic data acquisition

Diel cycle changes in fish behaviour have a significant effect on the estimations of fish biomass derived from the acoustics (Hjellvik et al., 2004, Lawson and Rose, 1999, Fréon et al., 1993). Consequently, long term monitoring surveys are, in general, consistently conducted either during day or night (Godlewska et al., 2011). Otherwise, the day/night data are analysed separately (Guillard and Verges, 2007). However, the acoustic data used in this study was collected by Colquhoun et al. (2007), with the objective of sampling seafloor bathymetry that is not affected by the diel cycle. Therefore, the water column data were considered opportunistically collected, during transects sampling seafloor bathymetry, and during transit time between sampling stations with other objectives such as towed-video sampling. As a consequence, the data were collected during day and night, the 2008 data, in particular, were collected mostly at night. Therefore, the separation between day and night time was not possible as it would reduce the spatial coverage of the acoustic data. The acoustic data were analysed separately by year.

4.3.3. Post-processing of acoustic data

Acoustic measurements are often quoted in decibels (dB) units rather than pressure units, this is because the range of variation in sound covers many orders of magnitude (Simmonds and MacLennan, 2008). In the acoustics field, a decibel is used to express the ratio between two intensities in a logarithmic scale, the use of dB allows us to express big changes in sound in a few decibels (Simmonds and MacLennan, 2008). To denote the different scales used when expressing fisheries acoustics data, standard terminology has been established. For example, s_v is used to define the volume backscattering coefficient in the linear domain while S_v ($S_v=10\log(s_v)$) is used for the volume backscattering strength in the logarithmic scale (Simmonds and MacLennan, 2008). Echo Integration is a common fisheries acoustics analysis based on echo integral over a volume (S_v) or area (area backscattering coefficient s_a). There are various scaled versions of s_a including the nautical area scattering coefficient (NASC) for which the accepted symbol is s_A . In this study, we used a depth-stratified NASC and when related to the stereo-BRUVS data, it will be referred to as “ $NASC_{BRUV-mean}$ ”.

The acoustic data was processed using Software Echoview (ver. 8.0; Echoview Software Pth Ltd.). The acoustic energy recorded by the echo-sounder as a function of depth and distance travelled was used to create an echogram in which each point represents the amount of energy reflected by the targets present in the water column at a particular depth and time (Simmonds and MacLennan, 2008). In Echoview, two types of echograms are created for each frequency operated. The Target Strength (TS) echogram referenced to 1 m^2 , and the Volume backscattering coefficient (S_v) echogram referenced to $1 \text{ m}^2/\text{m}^3$. The S_v echogram is usually used for echo integration analysis while the TS echograms are used to estimate the target strength of single targets.

The first five metres below the surface were excluded from the analysis to avoid the nearfield area and to evade aeration noise. Only data collected when the vessel was traveling between 3 and 12 knots was used in the analysis as part of recommended quality control (ICES, 2015). A bottom line was created using the maximum S_v algorithm in Echoview. An offset line was created to exclude a layer of a metre above the bottom to avoid including parts of the seafloor and reef as targets. A visual inspection was conducted to correct for false bottom detections and mark noisy areas as bad data which were excluded from the analysis.

In the context of fisheries acoustics, noise can be defined as an unwanted signal which can interfere with the detection of target signals (Simmonds and MacLennan, 2008). The use of filters can mitigate the effects of noise increasing the signal-to-noise ratio (SNR; Ryan et al., 2015) Two filters were applied in

both the S_v and TS echograms: an impulse (Ryan et al., 2015) and background noise filter (De Robertis and Higginbottom, 2007). The S_v filtered echogram was used in the calculation of depth-stratified NASC while the TS filtered echogram was used in the single target analysis.

Nautical area scattering coefficient

A blurring procedure was conducted in the S_v filtered echogram to create a clean S_v echogram. A -55 dB threshold was applied to the clean S_v echogram. This threshold was selected after a visual inspection of the echograms which presented strong plankton reverberation typical of surveys in the tropics (Simmonds and MacLennan, 2008). Clean S_v echograms were binned into 50 m horizontal 'Intervals' by 5 m depth 'Layers' analysis cells, and an integration per cell was conducted and exported as nautical area scattering coefficient 'depth-stratified NASC', for the different Layers. Pelagic schooling species of fish are uncommon in the stereo-BRUVS recordings; therefore, a second depth-stratified NASC value was exported for each cell where the schools were excluded. Schools were first detected using the SHAPES algorithm (Coetzee, 2000) implemented in Echoview in the clean S_v echogram. The detection parameters set to a minimum total school length of 2 m, a minimum candidate height of 1m, a minimum candidate length of 2 m, a minimum candidate height of 1 m, a maximum horizontal gap distance of 1 m, and a minimum S_v of -60 dB (Campanella and Taylor, 2016). The school areas were used to produce a 'school' mask which was applied to the clean S_v echogram to produce a S_v echogram without schools. The NASC per cell was then exported and will be referred to as 'depth-stratified NASC no schools'.

Single targets

The school mask was applied to the TS echogram to acquire an echogram excluding the schools. A second mask was created based on the S_v echogram where values below the -55 dB threshold were set to zero. This mask was applied to the TS echogram without schools to produce a clean TS echogram. A single target detection algorithm was applied in the clean TS echogram using the default values suggested by Echoview (TS threshold -50 dB, pulse length determination level 6.0, Minimum normalized pulse length 0.7, and maximum normalized pulse length: 1.5). The number of targets per cell was then exported as another acoustic variable to be referred to as 'targets'.

4.3.4. Baited Remote Underwater Stereo-Video (stereo-BRUVS)

Typical analysis of stereo-BRUV data provides information on the number, species and size of fish that are attracted to the bait on the mooring and into the field of view of the attached cameras. The maximum number of individual fish (MaxN) corresponds to the maximum number of fish of the same species

observed in one frame during an hour of video analysis. The selection of one frame avoids re-counting fish (Cappo et al., 2004). The stereo capabilities of the system allow the calculation of the fish length with millimetres of precision in most instances (Harvey et al., 2003, Boutros et al., 2015). The MaxN used in this study includes all the MaxNs of the different species observed at each sampling position, hereafter referred to as 'MaxN'. The original MaxN by species was determined in the original WAMSI program (Simpson and Waples, 2012), and the extensive description of the methods are out of the scope of the present study. Details on the calibration (Harvey and Shortis, 1995), and use of the stereo-BRUVS (Cappo et al., 2003) have been fully described elsewhere (Harvey et al., 2007).

An estimate of the relative biomass per sampling point was calculated using the length of the fish and the standard weight-length equation (Richards and Kavanagh, 1945): $W = aL^b$ where W is the weight (g), L is the length (cm), and the coefficient a and b are species-specific parameters. The parameter a is called the condition factor, and the exponent b , usually known as the allometric coefficient, can be considered as the ratio of the specific growth rates of weight and length (Huxley, 1950). The weight-length equations were used to transform the fishes lengths into grams of biomass using the a and b parameters from Fishbase (Froese and Pauly, 2012). When the a and b parameters were not available for a particular species, these parameters from a similar species within the genus were used. However, the measurement of all fish of a particular species detected in a frame is not always possible. For occasions where not all the individuals of a given species were measured, the mean length of fish of the same species at the sampling station was used to estimate the length of the unmeasured individuals (Bach et al., 2019). Individual weights of all species present in a sampling point were summed to obtain the relative biomass of that point and will be referred to as 'relative biomass'.

4.3.5. Acoustic vs. stereo-BRUVS

As an exploratory analysis, correlations between the acoustics and stereo-BRUVS data were conducted. The location of deployment (stereo-BRUVS) and the locations of each interval (acoustics) were plotted (Figure 4.2). For each deployment searches were conducted to identify the intervals that occurred within a series of ranges from the deployment location (commencing at searches up to 50 m from the stereo-BRUV and increasing by steps of 50 m up to 1 km).

The acoustic variables including depth-stratified NASC, depth-stratified NASC no schools, and targets summed among the layers to obtain a single value per Interval, the Intervals extracted for each stereo-BRUV location were then averaged. Demersal and semi-demersal species of fish are usually observed in

the stereo-BRUVS recordings, but pelagic fishes are occasionally observed (Cappo et al., 2004). A reason for this may be that the bait plume contains buoyant oils and is therefore likely to attract fishes throughout the water column. The area of attraction to the bait plume is very difficult to define and depends on seabed topography (Cappo et al., 2004, Stobart et al., 2007), behavioural responses to bait the bait plume (Bailey and Priede, 2002, Colton and Swearer, 2010) and soaking time (Harasti et al., 2015). Therefore, correlations between the stereo-BRUVS and the acoustic data were conducted across different water column layers of the intervals in an attempt to assess the effect of depth on the potential for acoustic data to correlate with stereo-BRUV data. This commenced with only the first 5 m above the seafloor (Layer 0, Figure 4.2) and moved higher into the water column by increasingly adding subsequent 5 m layers (e.g. adding Layers 1-8 in Figure 4.2).

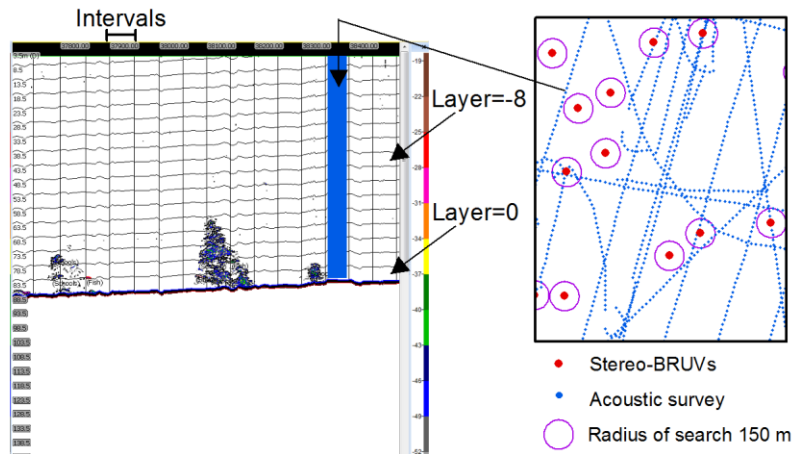


Figure 4.2. Example of the extraction of acoustic data to be compared with the stereo-BRUVS data. On the left side, an S_v mean echogram where the acoustic energy was exported using a grid with Intervals 50 m long and 5 m depth Layers. Each interval is represented on the right side as a blue dot. Different radii of search around the stereo-BRUVS were used to extract the acoustic data, a 150 m radius is shown as an example.

The “ $NASC_{BRUV-mean}$ ”, “ $NASC_{BRUV-mean}$ no schools” and $targets_{mean}$ were calculated for the corresponding stereo-BRUV position, creating matrices with the four acoustic variables and the biomass and MaxN of the stereo-BRUVS. Correlations were then tested between the acoustic data and the stereo-BRUVS. Curves of correlations were constructed to find an optimal radius of search and number of Layers.

4.3.6. Models of demersal fish abundance and biomass

The 2008 acoustic data collected in the Mandu area was used to test the effect of including water column data in a model of spatial distribution of MaxN. Random Forest (RF) was used to model the MaxN using depth, depth derivatives and seafloor backscatter as explanatory variables. A summary of the terrain variables included in the model is shown in Table 4.1. Depth derivatives were calculated using four

different neighbourhoods (3, 9, 15 and 21 raster's cells) as variables can relate to the distribution of abundance at different scales. The bathymetry and the backscatter mosaics were downloaded from the Geoscience Australia (GA) website as a raster with 3 m resolution. The seafloor backscatter can be used to approximate specific characteristics of the seafloor, including acoustic hardness and roughness (Fonseca and Mayer, 2007). The seafloor backscatter was added into the models as two different layers. The first one was the full-coverage, 3-m resolution mosaic, and the second one is an approximation of the sediment phi size estimated using the Angle vs. Range Analysis (ARA; Fonseca et al, (2009), applied to the MBES raw files.

The MaxN and relative biomass were first modelled using only the terrain variables. In a second scenario, the average depth-stratified NASC as a 250 m resolution grid was included as another explanatory variable in the MaxN and relative biomass models. Two more models were constructed using the terrain variables listed in Table 4.1, to explain the distribution of the depth-stratified NASC, and depth-stratified NASC no schools gridded at a 250 m resolution. For all models, 70% of the data was used to train the model and the remaining 30% to test it. The amount of variance explained by the model and the mean square error (MSE) were used to evaluate the performance of the model.

Table 4.1. Terrain variables used in the Random Forest models. The depth derivatives were calculated using four sizes of neighbourhoods (3, 9, 15 and 21).

Variable	Abbreviation	Description	Software	Reference
Depth derivatives				
Slope	slope	Rate of change in elevation over the analysis windows express in degrees.	Landserf v2.3	Wood (1996)
Aspect	Northness	Cosine of aspect where slopes facing north (NS=1), or south (NS=-1).	Landserf v2.3	Wood (1996)
	Eastness	Sine of aspect where slopes facing east (WE=1), or west (WE=-1).	Landserf v2.3	Wood (1996)
Curvature	Profile	Curvature of a line formed by intersecting the vertical plane oriented in the direction of the steepest slope with the terrain surface.	Landserf v2.3	Wood (1996)
	Plan	Curvature of a line formed by intersecting the horizontal plane oriented in the direction of the steepest slope with the terrain surface.	Landserf v2.3	Wood (1996)
	Mean	Mean curvature in any plane.	Landserf v2.3	Wood (1996)
Fractal dimension	fractal	Indicates how surface roughness changes over space with a minimum value of 2.0 indicating smooth, scale invariant behaviour and a theoretical maximum of 3.0 indicating a space filling rough surface.	Landserf v2.3	Wood (1996)
Standard deviation of depth	SD	Standard deviation of depth.	R raster package	Holmes et al., 2008
Benthic position index	BTI	Measure of the position of a particular pixel concerning the average depth of its surrounding neighbours. Positive values showing depth above the average (ridges), and negative values for pixels below the average (troughs).	R raster package	Wilson et al. (2007)
Terrain ruggedness Index	TRI	Mean of the absolute differences between the value of a cell and its neighbouring cells.	R raster package	Wilson et al. (2007)
Roughness	rough	Difference between the maximum and the minimum depth of a cell and its neighbouring cells.	R raster package	Wilson et al. (2007)
Seafloor backscatter derivatives				
ARA (phi)	ARA	Approximation of sediment phi size using an Angle vs Range Analysis of the backscatter.	FMGT	Fonseca et al., (2009)

4.4. RESULTS

4.4.1. Spatial distribution of fish biomass and abundance

The MaxN of demersal fish as recorded by the stereo-BRUVS did not show a clear spatial pattern, high values were observed in shallower areas less than 50 m depth, but also in deeper areas greater than 100 m for both the Mandu and Pt Cloates zones. However, in the Mandu area, the highest MaxNs were found near the 100 m depth contour (Figure 4.3, top row). The acoustic data showed highest densities of number of acoustic targets in zones between 50 and 100 m, particularly for the 2008 data in the Mandu area.

In the Pt Cloates area, the highest abundances recorded by the stereo-BRUVS were located, in general, in areas shallower than 50 m; with a few higher abundance points in areas between 50 and 100 m depth (Figure 4.3, bottom row). For the acoustic data, the highest number of acoustic targets were observed around the 50 m isobaths; in particular, in the southern part of the survey area for both the 2006 and 2008 data. Although, the spatial coverage of the acoustic data was limited to shallower areas in the Pt Cloates area.

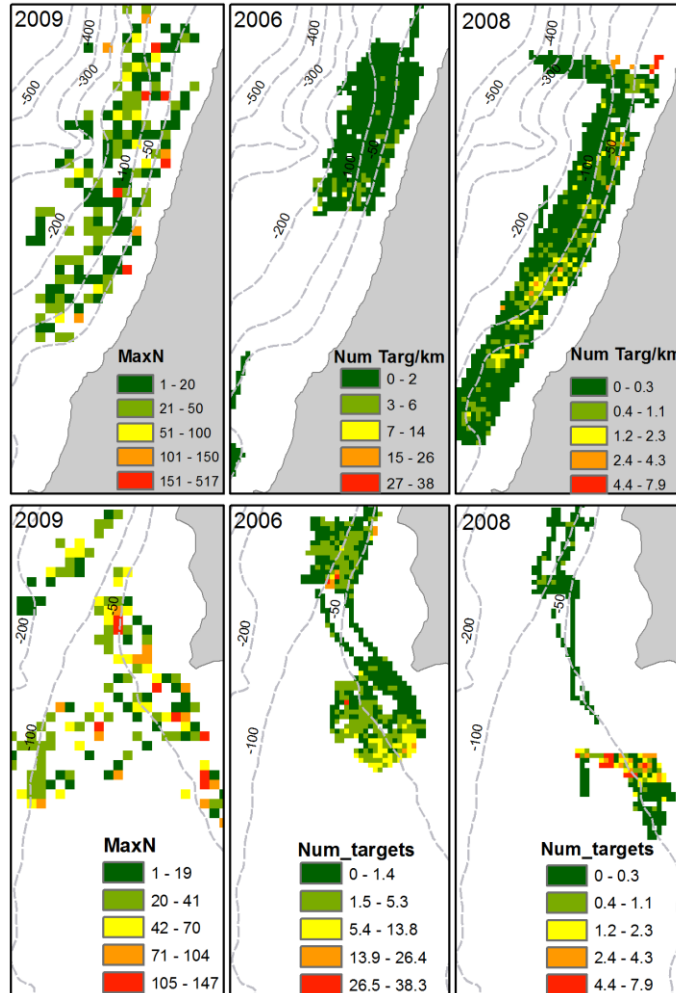


Figure 4.3. The abundance fish (MaxN) register by the stereo-BRUVS is shown in the left side for both the Mandu area (top) and the Pt Cloates (bottom). The number of acoustic targets for 2006 and 2008 for both areas are also shown at the centre and right of the figure.

In the Mandu area, the relative biomass estimated from the stereo-BRUVS did not display a clear relationship with depth, with high values observed both in deeper areas and shallower areas (Figure 4.4, top row). In the acoustic data for 2006, higher values of depth-stratified NASC were observed in deeper areas between 100 and 200 m depth in the middle of Mandu (Figure 4.4, top row). For the 2008 acoustic data, higher values were observed around the 100 isobath, particularly in the middle and south portion of the Mandu zone.

For the Pt Cloates area, the highest values of biomass derive from the stereo-BRUVS were observed around the 100 m isobath, but also some high values were observed in shallower areas (Figure 4.4 bottom row). The 2006 acoustic data, showed two areas of higher values of depth-stratified NASC, at the south-west and north of the sampled area.

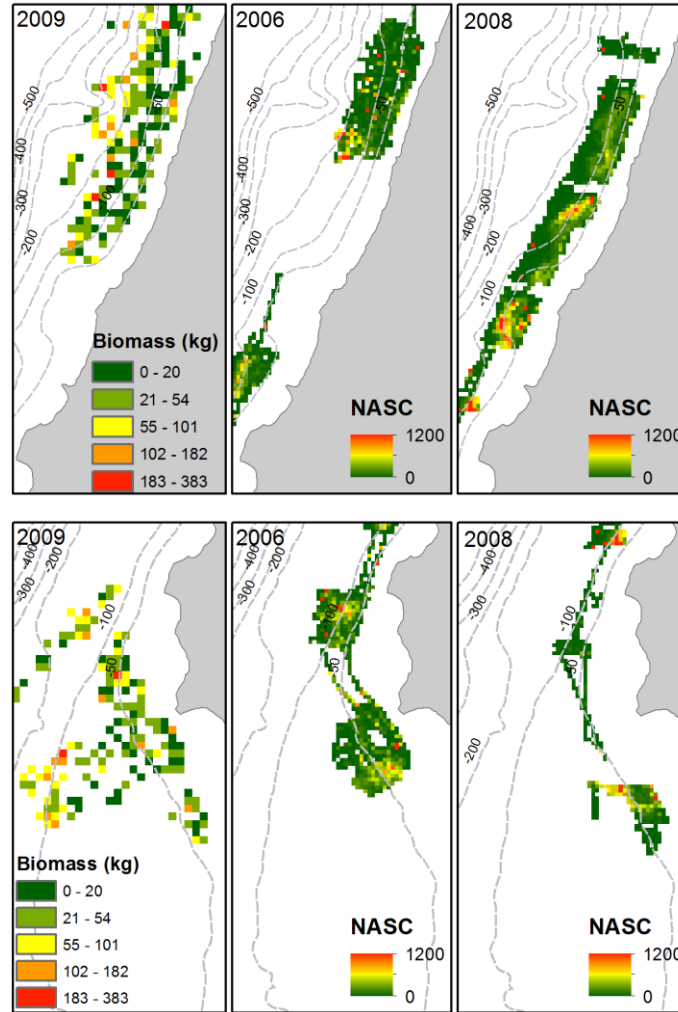


Figure 4.4. The relative biomass from the stereo-BRUVS is shown on the left side for both the Mandu area (top row) and the Pt Cloates (bottom row). The depth-stratified NASC for 2006 and 2008 in the two areas is also shown at the centre and right of the figure.

4.4.2. Correlations between acoustic and stereo-BRUVS

No significant correlation (at $\alpha = 0.05$) was found between the acoustic variables and the stereo-BRUVS data relative Biomass (Figure 4.5) and MaxN (Figure 4.6), and only low correlations were found for both years. No pattern was observed between Layers of acoustic data included and the level of correlation with the stereo-BRUVS data.

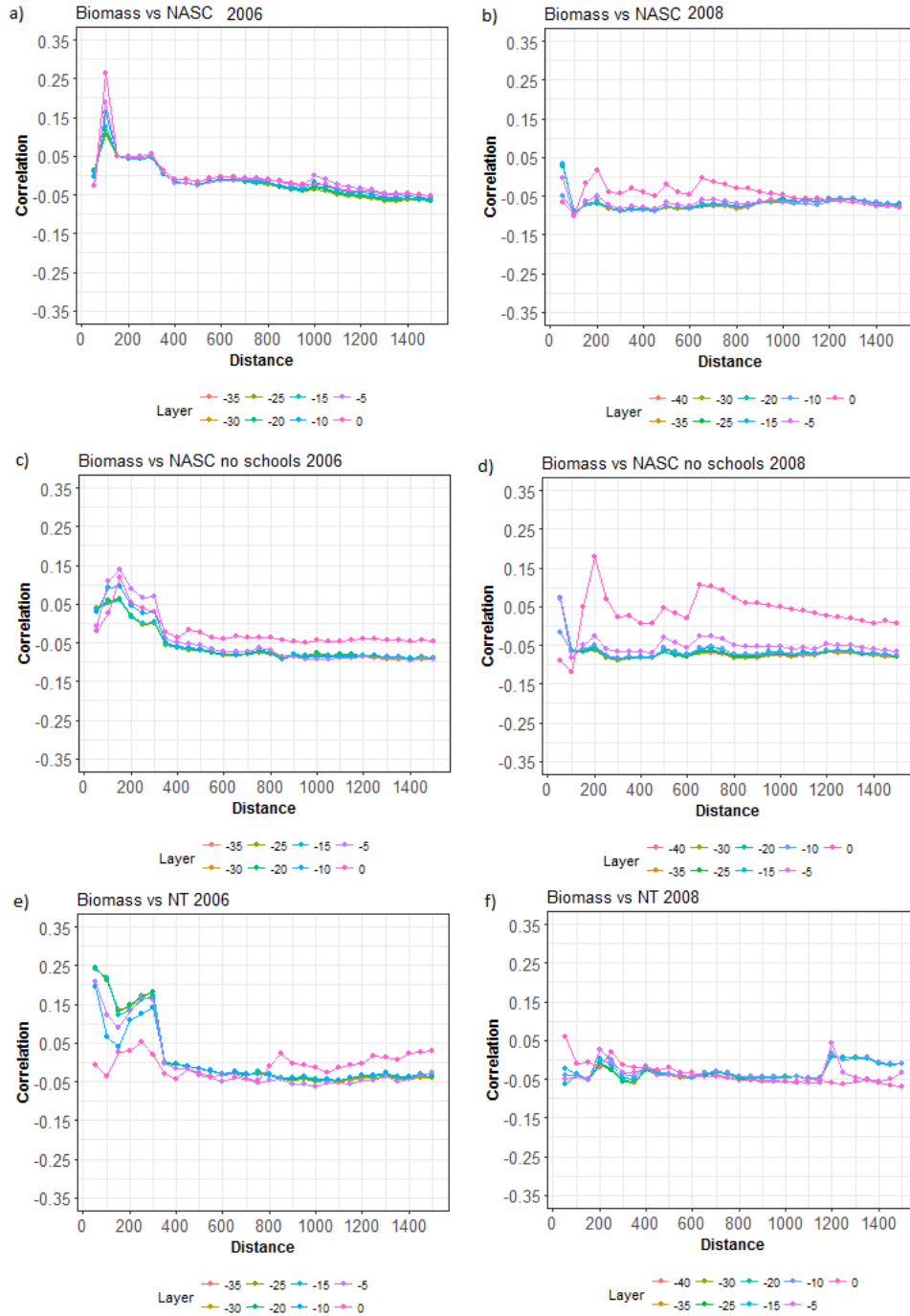


Figure 4.5. Summary of correlations between the relative biomass of the stereo-BRUVs and acoustic variables including a) $NASC_{BRUV-mean}$ 2006, b) $NASC_{BRUV-mean}$ 2008, c) $NASC_{BRUV-mean}$ no schools 2006, d) $NASC_{BRUV-mean}$ no schools 2008, e) Number of targets 2006, and f) Number of targets 2008). At different radii of search distance around the stereo-BRUVs (50-1500 steps of 50 m), and including different Layers of water column (5 m depth each) where Layer 0 = 1-6 m above the seafloor.

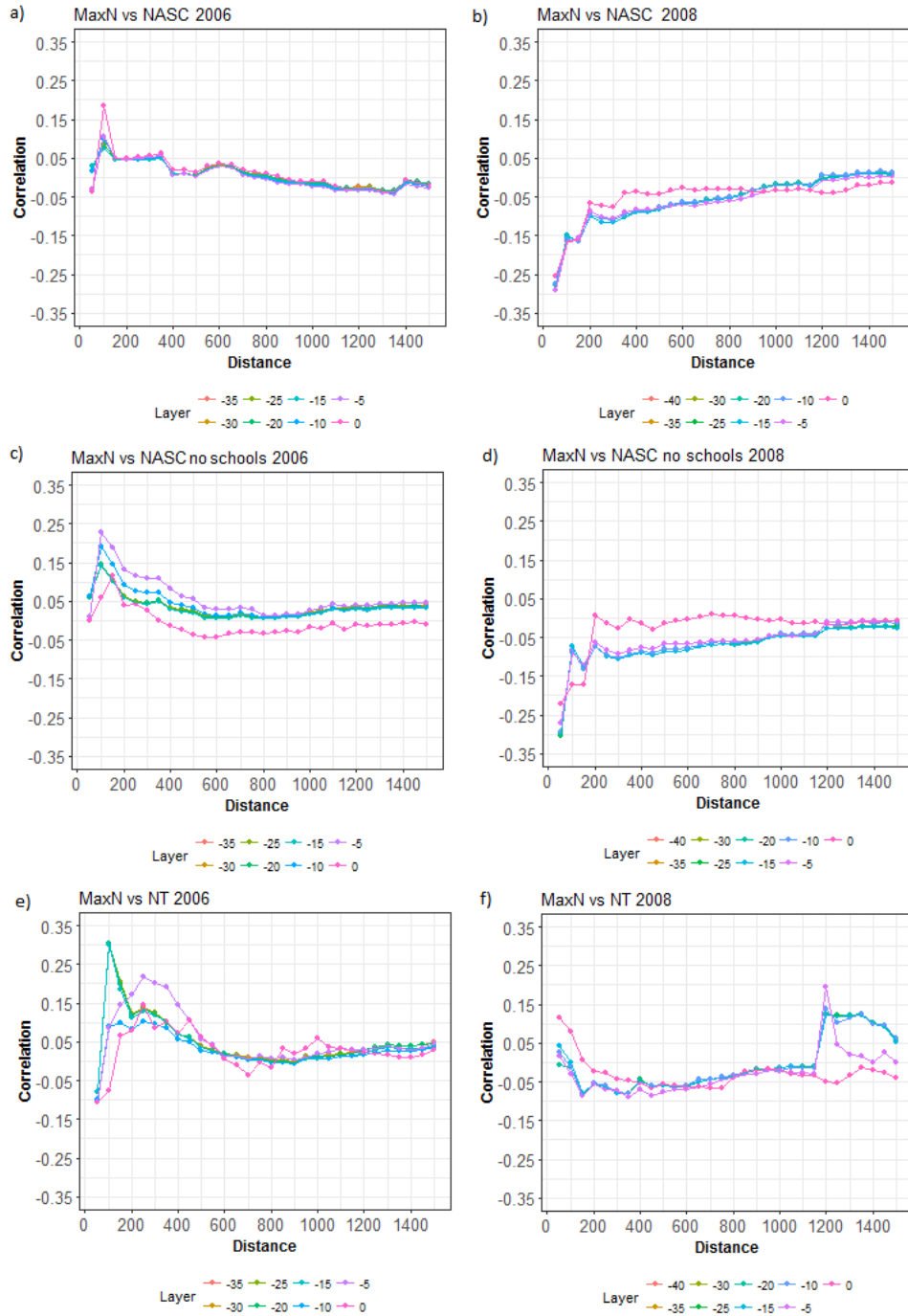


Figure 4.6. Summary of correlations between the MaxN of the stereo-BRUVs and acoustic variables including a) $NASC_{BRUV-mean}$ 2006, b) $NASC_{BRUV-mean}$ 2008, c) $NASC_{BRUV-mean}$ no schools 2006, d) $NASC_{BRUV-mean}$ no schools 2008, e) Number of targets 2006, and f) Number of targets 2008). At different radii of search distance around the stereo-BRUVs (50-1500 steps of 50 m), and including different Layers of water column (5 m depth each) where Layer 0 = 1-6 m above the seafloor.

4.4.3. Model of fish biomass and abundance

The model using only the terrain variables did not explain any variance of the distribution of MaxN or relative biomass. No improvement of the models was observed with the inclusion of the depth-stratified NASC with no variance explained by the models (Table 4.2).

Table 4.2. Results of the Random Forest models for the MaxN and relative biomass from the stereo-BRUVS, using terrain variables (Table 4.1) and adding the 2008 depth-stratified NASC data averaged to create a 250 m resolution grid (WC data) in the Mandu area. The results for the model of depth-stratified NASC and depth-stratified NASC no schools 2008 using terrain variables are also show. Correlations are between the estimated and real value.

Scenario	Variable	% Var explained	MSR	% Pearson cor	% Spearman cor
Terrain Var	MaxN	0	29876	0.5	0.5
	Biomass	0	4051	0.0	0.5
Terrain Var + WC data	MaxN	0	30201	0.7	0.0
	Biomass	0	4125	0.0	0.2
Terrain Var	NASC	22.73	1447800	23.0	31.9
	NASC no schools	23.03	708	23.1	35.1

The terrain variables explained 22% of the total 2008 depth-stratified NASC variance. A slight improvement was observed when the schools were excluded from the depth-stratified NASC (Table 4.2). The analysis of variable importance for the '2008 depth-stratified NASC no schools' model illustrated that depth was the main variable explaining the distribution of depth-stratified NASC followed by the backscatter of the seafloor (Figure 4.7).

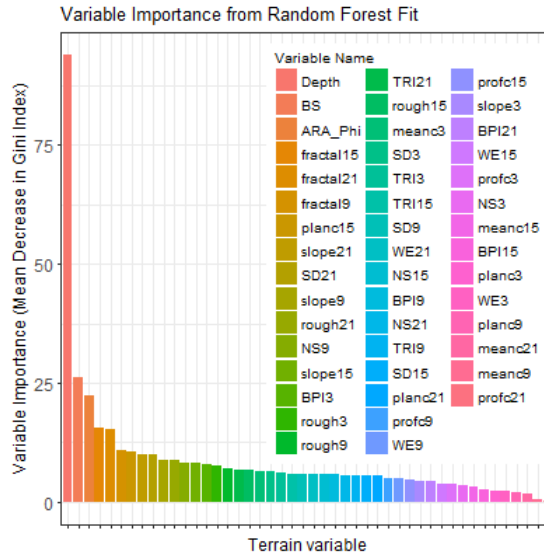


Figure 4.7. Importance of terrain variables in the Random Forest model of the distribution of 2008 depth-stratified NASC no schools. Variables names according to Table 4.1, the number in the names of the variables corresponds to the neighbourhood used in its calculation.

The relationship between the relative biomass from the stereo-BRUVS and the depth-stratified NASC with depth and seafloor backscatter was further explored as these two variables were important in the construction of the 2008 NASCs models. The seafloor backscatter mosaic and ARA-phi layer are highly correlated and were similar in importance for the construction of the model, however, grain size is easier to interpret and was used for further analysis.

The depth and the ARA-phi size were divided into intervals, and the percentage of relative biomass and depth-stratified NASC was estimated for each interval. A radius of 500 m around the stereo-BRUVS was used to extract the demersal layer (Layer 0) of the acoustic data which was averaged to obtain a value per stereo-BRUVS. Only sampling points with both acoustics and stereo-BRUVS data were included, therefore, a different number of stations were considered for each year as the coverage of the acoustic sampling varied.

The highest percentages of $NASC_{BRUV-mean}$ were found at depth intervals between 31 and 62 m for both 2006 and 2008 data, although, the percentages were also high for depths below 125 m (Figure 4.8). The relative biomass from the stereo-BRUVS had a more normal distribution with the highest biomass in the interval between 62-91 m for points with concurrent $NASC_{BRUV-mean}$ data of 2006 and 2008. Areas deeper than 125 m had lower values of relative biomass and $NASC_{BRUV-mean}$ for both years. A similar pattern was observed for both the $NASC_{BRUV-mean}$ and relative biomass in relation to different levels of seafloor backscatter (ARA-phi), in particular for the 2006 data. Areas with ARA-phi size between -2 and 0 (very fine gravel to very

coarse sand) had the highest relative biomass and $NASC_{BRUV-mean}$ for both years. For the 2006 data, a significant correlation was found between the relative biomass and $NASC_{BRUV-mean}$ ($R=0.98$, $t=11.85$, $df = 5$, $p<0.0001$). The Kruskal-Wallis rank sum test showed that no significant difference was found between $NASC_{BRUV-mean}$ and relative biomass grouped by ARA-phi size class ($\chi^2=6$, $df = 6$, $p=0.42$). For the 2008 data, a strong correlation was also found between the relative biomass and $NASC$ ($R=0.91$, $t=5.6$, $df = 6$, $p=0.0012$). The Kruskal-Wallis test shows no significant differences between them ($\chi^2=7$, $df = 7$, $p=0.42$).

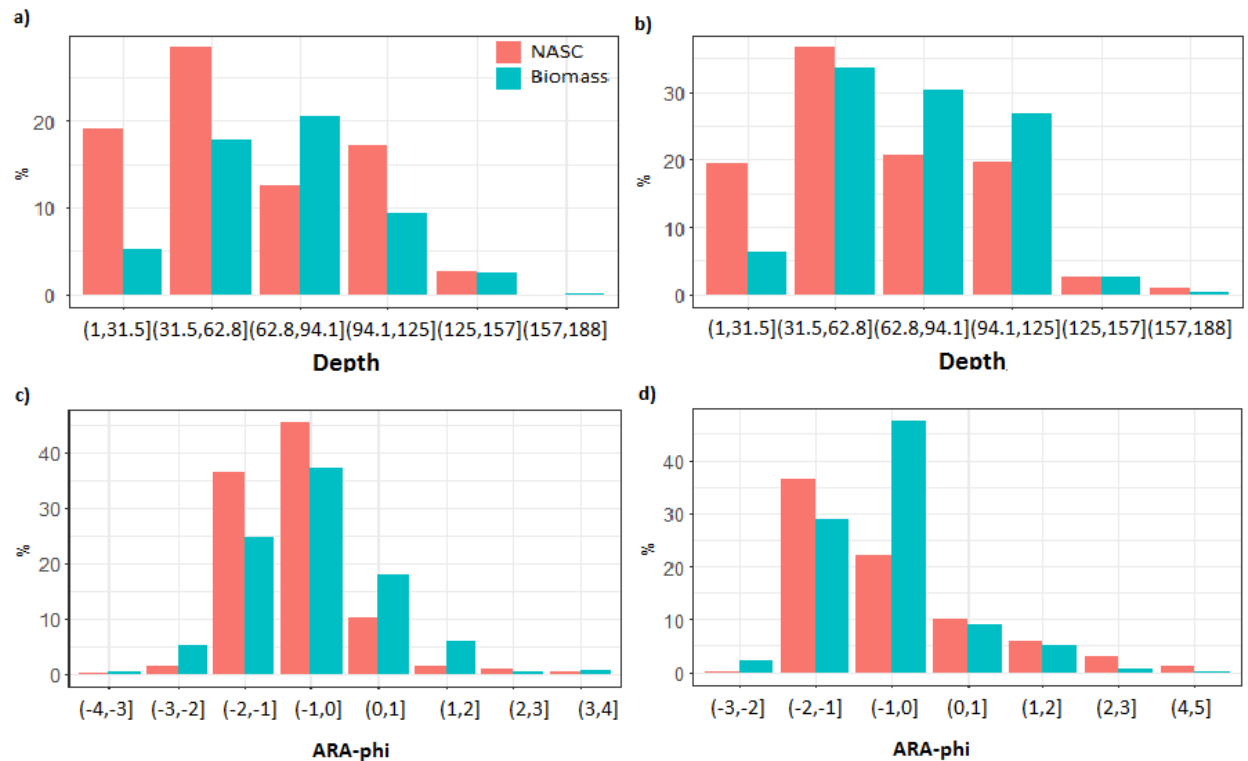


Figure 4.8. Percentage of biomass as recorded by the stereo-BRUVS (relative biomass, blue) and acoustics ($NASC_{BRUV-mean}$, red) in relation to the: depth gradient for a) 2006 data, and b) 2008. Percentage of biomass and mean $NASC$ compared to a gradient of phi sediment size estimated using the seafloor backscatter for: c) 2006, and d) 2008.

In a finer scale analysis, the acoustic data was not averaged per sampling point but instead used to get the ARA-phi value for each acoustic Interval to get a better understanding of the distribution of the depth-stratified $NASC$ in the surrounding of the stereo-BRUVS. For 2006 the results showed a very similar pattern of the percentage of distribution of relative biomass and $NASC_{BRUV}$ per class of ARA-phi size compared with the average one (Figure 4.9), the correlation was still strong, but the level of significance decreased ($R=0.87$, $t=4.5$, $df = 6$, $p=0.003$). The Kruskal-Wallis test was not significant showing no difference between the groups ($\chi^2=7$, $df = 7$, $p=0.42$). For the 2008 data, the correlation between the $NASC_{BRUV}$ and

relative biomass was not significant ($R=0.74$, $t=2.48$, $df = 5$, $p= 0.05$). However, the Kruskal-Wallis test showed no significant differences between the two groups ($\chi^2 = 6$, $df = 6$, $p = 0.42$).

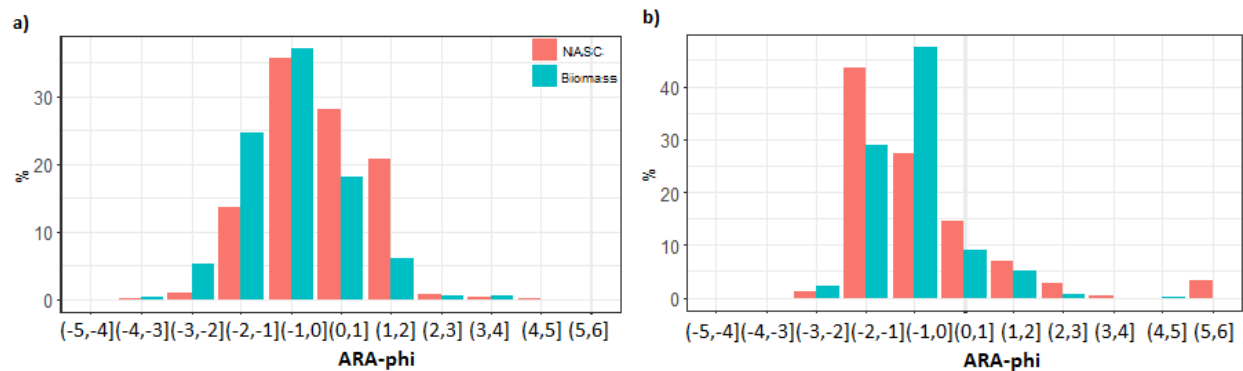


Figure 4.9. Percentage of biomass as recorded by the stereo-BRUVS (relative biomass, blue) and acoustics ($NASC_{BRUV}$, red) in relation to the depth gradient of phi sediment size estimated using the seafloor backscatter for: a) 2006, and b) 2008.

4.5. DISCUSSION

4.5.1. Species distribution models

The total MaxN and relative abundance were not well modelled by the terrain variables included in this study. Stereo-BRUVS are designed to aggregate species from an unknown area (Cappo et al., 2004) which can vary depending on the topography, currents, soak time and the swimming speed of the species (Misa et al., 2016, Cappo et al., 2004). Therefore, a wide variety of species can be attracted by the bait. The distribution of specific species would respond differently to different habitats and at different scales (Moore et al., 2010). The sum of the abundance and biomass would mask the preferences of the different species. However, it was expected that the acoustic biomass estimated with the echo-sounder could add useful information to explain the distribution of relative biomass derived from the stereo-BRUVS. The lack of relationship between the two data sets as found in the correlations and later confirmed by the RF was possibly related to a combination of temporal difference and resolution of the two methods.

4.5.1.1. Temporal difference

It is possible that the main reason for the lack of relationship between the two data sets was the temporal gap between them. Coral reef fish are hard to manage in part because they are highly mobile, their movements can respond to diel cycles (Harvey et al., 2012), seasonal (Mackie, 2007) and ontogenic shifts of habitats (Galaiduk et al., 2017b).

The acoustic data used in the RF model corresponds to the 2008 data which was collected mostly at night. Oppositely, the stereo-BRUVS data were collected during the day. The difference in fish behaviour between day and night have been largely reported (Harvey et al., 2012, Myers et al., 2016, Nagelkerken et al., 2000). Variances included the area used; some species are more mobile during the night increasing the used area (Lowry and Suthers, 1998), while others are less mobile at night (Fairclough et al., 2011). Changes to the habitat used have been associated with species differential preferences for resting and/or feeding and general use (Ferguson et al., 2013). Vertical migration and schooling is also an important component of the diel cycle with some species schooling during the day and becoming more scattered at night (Lowry and Suthers, 1998). Differences in the biomass-derived by acoustic surveys conducted during the day compared to night time has also largely been reported (O'Driscoll et al., 2009, Lawson and Rose, 1999, Fréon et al., 1993). The vertical migration of some species can affect their availability to be sampled with an echo-sounder when they migrate to the bottom into the Acoustic Dead Zone (ADZ). The ADZ is an area close to the bottom which cannot be sampled by the echo-sounder (Ona and Mitson, 1996). Vertical migration of species with swim bladders can also affect the size of the swim bladder which can impact the target strength of the species (Fréon et al., 1993).

Some reef fishes encompass seasonal migrations, related to reproductive behaviour, and usually linked to the lunar cycle (Mackie, 2007). The acoustic and stereo-BRUVS data were collected during different phases of the moon cycle which could have contributed to the lack of relationship between them (Fabi and Sala, 2002).

4.5.1.2. Spatial resolution

Differences in the spatial resolution between the two methods can also explain some of the differences in the spatial patterns detected by each of them. The acoustic data can produce an almost continuous picture of the distribution of acoustic depth-stratified NASC and targets along the ship track while the relative biomass and MaxN recorded by the stereo-BRUVS are point measurement, with an unknown sampling unit (Cappo et al., 2004). As a result, the spatial resolution of the stereo-BRUVS is coarser than acoustic data. The increase in sample size could also have contributed to a better performance of the RF in explaining the distribution of depth-stratified NASC using the terrain variables.

The exclusion of species identified by the stereo-BRUVS that might not be available to be sampled by the echo-sounder (e.g., flatfish, small fish) could contribute to obtain a better correlation between the two data sets and it is another possibility to be explored.

4.5.1.3. Broad-scale analysis

An interesting finding of the present study was the higher percentage of relative biomass from the stereo-BRUVS and the echo-sounder in two intervals of the ARA-phi layer at a broad scale. The use of seafloor backscatter in modelling the distribution of benthic habitats has risen in recent years with the increasing availability of high resolution multibeam data (Holmes et al., 2008, Hasan et al., 2012a, Hasan et al., 2014). However, fewer studies have included the seafloor backscatter in the models of the distribution of fish (Ierodiaconou et al., 2011, Monk et al., 2010, Young et al., 2010), although, they are increasing. The value of adding the seafloor backscatter in the models of demersal fish will depend on the relationship of this surrogate with direct variables affecting the distribution of the particular species (Haggarty and Yamanaka, 2018). For example, grain size has been described as strongly related to the size of the organisms living in the sediments (McArthur et al., 2010). Therefore, sediment grain size could have an indirect effect on the distribution of benthic carnivorous fishes (Platell and Potter, 2001).

The identification of a broad-scale pattern between the stereo-BRUVS and acoustic data could be related to the fact that the fine-scale patterns vary in a short temporal scale but broad-scale patterns are persistent over more extended periods unless extreme events occurred. These broad-scale patterns can be particularly useful to understand better the distribution of species with large home ranges as roaming species (Monk et al., 2011, Dagneaux et al., 2009).

4.6. CONCLUSION

The complementary use of opportunistic acoustic data and stereo-BRUVS showed limited benefits to the modelling precision. No value was added to the models of abundance and relative biomass from the stereo-BRUVS by adding the acoustic data for specific areas. The temporal difference is probably the main reason for the lack of relationship between the two data sets; therefore, the collection of acoustic data during the daytime when possible is advised. However, a broad-scale relationship between the acoustic and relative biomass with particular classes of sediment size was found. Further exploration of this relationship is needed, but it is an encouraging result that shows the possibility of detecting broad-scale drivers of fish biomass using opportunistic data. Broad-scale patterns can be particularly important for models of the distribution of species with large home ranges. A more rigorous comparison between stereo-BRUVS and acoustic techniques could be achieved in a more controlled environment in which both surveys are carried out simultaneously or at least within a shorter time gap.

4.7. ACKNOWLEDGEMENTS

Stereo-BRUVS data were collected through the Western Australian Marine Science Institute (WAMSI) node 3 project 1 subproject 3.1.1: deepwater communities at Ningaloo Marine Park.

Chapter 5

5. Investigating the temporal and spatial variation of acoustic water column data and its relationship with Baited Remote Underwater Stereo-Videos of demersal fish off the Western Australia Coast

5.1. ABSTRACT

Spatially explicit information on coral fish species abundance and distribution is required for effective management. Non-extractive techniques, including echo-sounders and video census, can be particularly useful in marine reserves where the use of extractive methods is restricted. This study investigates the use of echo-sounders and Baited Remote Underwater Stereo-Videos (stereo-BRUVS) in demersal fish assessment. Echo-sounders allow the sampling of big areas in a short period collecting data from the full water column. However, “ground-truth” data are required to transform the acoustic energy into species-specific biomass, collecting these type of information is problematic in areas with complex topography. In contrast, stereo-BRUVS can produce species identification and length measurements to be used in biomass estimates. This study aimed to investigate the possibility of combining stereo-BRUVS and echo-sounder in providing more holistic information on the distribution of demersal fish. The spatial distribution of fish biomass was assessed using both methods in two small areas, one in Cockburn Sound (CS), a temperate body of water, and other in the tropical waters of Ningaloo Marine Park (NMP). A temporal experiment was also conducted to test the temporal variation of the biomass before, during, and after the deployment of a stereo-BRUV, also in the NMP. The results showed high correlations between the acoustic and stereo-BRUVS data in the CS suggesting the potential use of both for a better estimation of biomass in the area. The results for the NMP showed weaker correlations between the two datasets, and highlighted the high variability of the system. Further studies are required, but our initial findings suggest a potential benefit of combining both techniques in the demersal fish distribution assessment.

5.2. INTRODUCTION

Coral reefs are the most biodiverse ecosystems on the ocean, providers of a variety of environmental services and home to a diverse number of species of fish (Goldman et al., 1976, Cole et al., 2008, Reaka-Kudla, 1997). Coral reef fishes are a critical source of protein for the world's tropical coast and support important commercial and artisanal fisheries (Reaka-Kudla, 1997). However, coral reefs and the species depending on them are increasingly being threatened by anthropogenic impacts both at a local (e.g., overfishing), and global scale (e.g., global warming) (Veron et al., 2009). Traditional management strategies for coral-reef fisheries, including catch quotas, size restrictions, or seasonal closures, have had poor performances. This has resulted in the implementation of marine protected areas (MPAs) as the leading tool for coral-reef fish conservation (Friedlander et al., 2003). It is expected that MPAs would reduce the pressure from direct anthropogenic impacts, allowing the species to cope with global-warming related stressors and natural disturbances (Mora et al., 2006). However, sustainable management of coral reef fishes requires spatially-explicit information on their abundance and distribution at scales relevant for MPAs monitoring (McClanahan et al., 2006). Non-destructive methods are required to collect reef fish data on MPAs, some of the methods commonly used are scuba-diving census, video-based techniques and more recently active acoustics. However, each of these methods' present limitations and bias (Logan et al., 2017, Cappo et al., 2003, Zenone et al., 2017). Two fishery-independent and non-destructive methods are the focus of this study, baited remote underwater stereo-video (stereo-BRUVS) (Cappo et al., 2003) and active acoustics (Zenone et al., 2017).

The use of cameras has been present in the study of fishes since the 1900s (Reighard, 1908). Technological advances in the last two decades have allowed scientist to use high-resolution video cameras which can be deployed to a wider depth range compared to visual census (Pelletier et al., 2011). The addition of bait in front of the cameras promotes the fishes to get close, allowing for species identification and length measurements with high levels of accuracy (Cappo et al., 2004). Stereo-BRUVS have been used successfully to estimate the effect of MPAs on the species richness and relative abundance of demersal fish inside and outside the protected areas (Cappo et al., 2003). The main disadvantage of the stereo-BRUVS is the complexity of converting the biomass estimated into density, which requires the area of influence of the bait plume to be estimated. The area of influence of the stereo-BRUVS is highly variable and can be influenced by the bottom current speed, soak time and swimming speed of the organisms (Ellis and Demartini, 1995, Cappo et al., 2004). Therefore, the biomass estimated with stereo-BRUVS should be reported as relative biomass.

On the other hand, active acoustic systems, such as echo-sounders, have become the standard method to monitor the exploited populations of some of the most commercially important fisheries of the world (Davison et al., 2015, Kloser et al., 2016). The use of active acoustics have shown particular benefit for assessing large, single-species schools of fish, and have the advantage of being able to sample large areas in a relatively short time (Simmonds and MacLennan, 2008). Echo-sounders have the potential to be used in an ecosystem-based management approach, as different components of the water column can be sampled at the same time (e.g., zooplankton, fish; Kowlow, 2009, Godo, 2009). During an acoustic survey, an echo-sounder is used to transmit acoustic energy into the water and record the echoes produced by targets present in the water. The amount of energy reflected ('backscatter') by the water column can be used as an approximation of the biomass present in the water column (Simmonds and MacLennan, 2008). The main disadvantage of acoustics, is the need of ground-truth information to convert the acoustic energy into species-specific biomass. In temperate regions, the use of nets is the usual method to collect ground-truth information. The low diversity of species present in temperate regions also contributes to making the conversion from backscatter to species-specific biomass a straightforward procedure. However, the use of underwater acoustics in coral reefs is increasing with visual techniques providing the complementary source of validation data (Boswell et al., 2010, Costa et al., 2014, Campanella and Taylor, 2016).

This study aimed to investigate the possibility of combining stereo-BRUVS and echo-sounder data in providing more holistic information of the distribution of demersal fish with a general hypothesis: The spatial distribution of biomass captured by stereo-BRUVS is highly correlated with the spatial distribution of the acoustic biomass estimated based on the echo-sounder. And two particular objectives:

1. Evaluate the spatial distribution of demersal and semi demersal fish using both methods in a near concurrent timeframe in a temperate area close to Perth WA and in the Ningaloo Marine Park.
2. Evaluate the relative biomass for demersal and semi demersal fish using an echo-sounder and stereo-BRUVS in three small areas before, during and after the deployment of the stereo-BRUV.

5.3. METHODS

5.3.1. Study area

Cockburn Sound

The first spatial experiment was conducted in CS, a body of water off the southwest coast of Perth, Western Australia (Figure 5.1). At the study area, different benthic habitats including cobble reef and high relief reef have been described (Cockburn Sound Management Council, 2004). CS provided an accessible site with known habitats and previously studied fish assemblage from which hypotheses could be test.

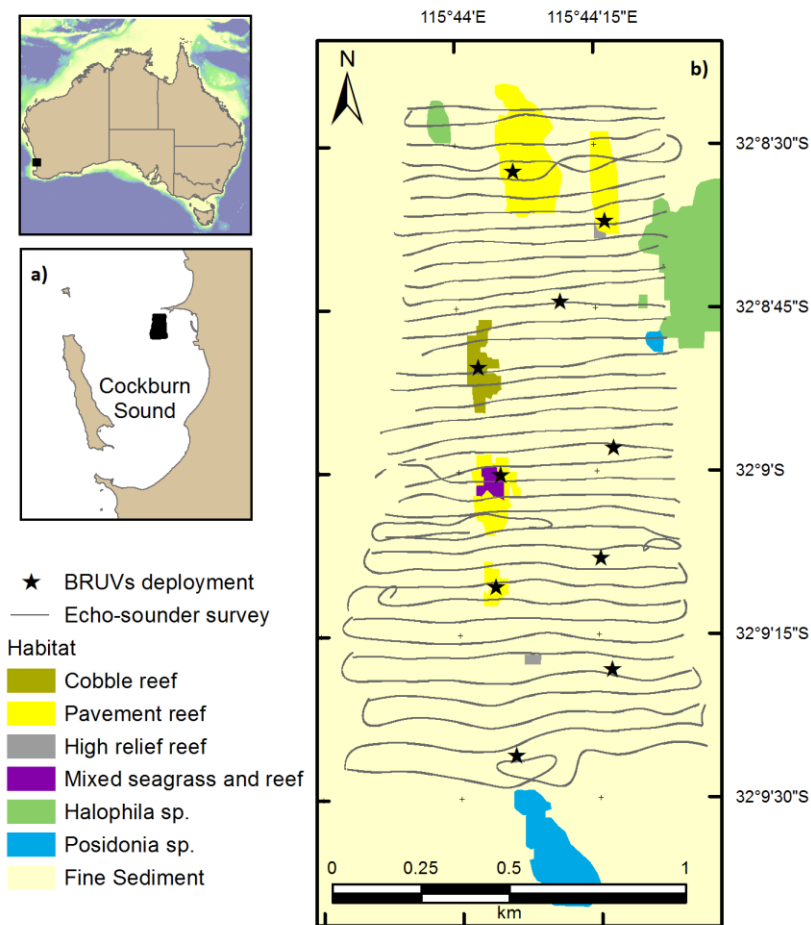


Figure 5.1. Cockburn Sound study site off the South-West coast of Australia, b) Stereo-BRUVS deployment sites (black star) and echo-sounder transects (continuous line). The benthic habitat classification is an adapted version of (Cockburn Sound Management Council, 2004).

Ningaloo Marine Park

The second area of study was located in the Ningaloo Marine Park (NMP) in a tropical area of Western Australia (Figure 5.2). NMP is recognised as a highly diverse ecosystem and is considered as an emblematic area of the WA (Waples and Hollander, 2008). As part of a previous study in the NMP, an acoustic survey was conducted using a single-beam echo-sounder which was used to produce a seafloor classification. The tail of the first echo (E1) returning from the seafloor can be used to estimate the acoustic “roughness”

while the second echo (E2) is related to the acoustic “hardness” (Foster-Smith and Sotheran, 2003). Two classes were detected using the E1 metric (smooth and rough), and used to select the sites for the deployment of the stereo-BRUVS (Siwabessy, 2001).

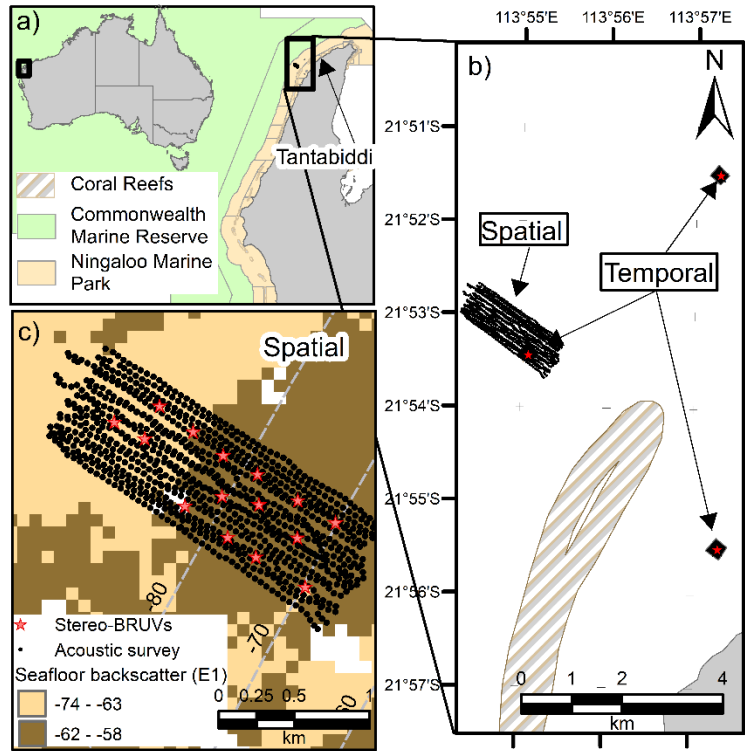


Figure 5.2. a) Map of Australia with a magnification of the Exmouth peninsula, delineating areas of the Commonwealth Marine Reserve and the Ningaloo Marine Park. b) Expansion of the study site within the Marine Park with the locations of the temporal and spatial study locations marked. c) Expansion of the spatial site with seafloor E1 (coloured areas), together with deployment locations of stereo-BRUVS (red stars) and echo-sounder transects conducted (black dots).

5.3.2. Data acquisition

Acoustics

For all areas in all the experiments, both the acoustic and stereo-BRUVS surveys were conducted between 9 am and 4 pm to avoid differential behaviour of fish between day and night time and the diel migration at dusk time.

Three Biosonics single-beam transducers (38, 120 and 420 kHz) were mounted on a small pontoon which was towed alongside a vessel (Figure 5.3). The 120 kHz transducer was at the front of the pontoon followed by the 38 kHz (0.33 cm of separation) with the GPS antenna attached, and the 420 kHz at the end (0.26 cm of separation). The settings of the echo-sounder are shown in Table 5.1. Calibration was

conducted posteriori in the CS; each transducer was calibrated following the recommendations of (Foote 1987).

Table 5.1. Settings of the transducers mounted in the pontoon, for the two experiments and the two areas included in the study.

Frequency (kHz)	Beam width	NMP Spatial		NMP Temporal 1		NMP Temporal 2 and 3		Cockburn Sound	
		Pulse length (ms)	Ping rate (pings s ⁻¹)	Pulse length (ms)	Ping rate (pings s ⁻¹)	Pulse length (ms)	Ping rate (pings s ⁻¹)	Pulse length (ms)	Ping rate (pings s ⁻¹)
38	9.8°	0.8	1.9	0.2	5	0.7	1.9	0.3	9.2
120	7.8°	0.5	1.9	0.2	5	0.4	1.9	0.2	9.2
420	6.8°	0.5	1.9	0.1	5	0.4	1.9	0.1	9.2

Stereo-BRUVS

The stereo-BRUVS systems consist of two video cameras mounted in a metallic frame which hold them at an inward convergence of 8° so both cameras had a common area of view (Figure 5.3). In the centre of the frame, an arm suspends a bait bag between cameras. Each video camera was equipped with an SD card with enough memory to record for at least 2 hours. The stereo-BRUVS technique used in this study was conducted following the same process reported by Harvey et al. (2007).



Figure 5.3. Three echo-sounders were mounted in a pontoon which was towed on the side of the vessel (left and centre). One of the Stereo-BRUVS used in the experiments is shown on the right of the figure.

Cockburn Sound

Two small vessels were used during the survey, one collecting acoustic data at an average speed of 4 knots and another vessel deploying and retrieving the stereo-BRUVS. The acoustic survey was conducted following transects perpendicular to the coast, with successive transects separated by approximately 50 m (Figure 5.1). Ten stereo-BRUVS were deployed in two main benthic habitats, five in sand and five in 'reefs' areas which included pavement reef, cobble reef, and mixed seagrass and reef (Figure 5.1). A minimum of 250 m of separation between them was used to minimise the possibility of mixing bait plumes and reduce the likelihood of fish moving between sites within the sampling period (Watson et al., 2007).

The acoustic survey was conducted either before the stereo-BRUVS were deployed or at least 1 hour after their removal.

Ningaloo Marine Park

Spatial experiment

A 7.9 m vessel was used to conduct the acoustic survey and the deployment of 14 stereo-BRUVS. The acoustic survey and deployment/recovery of the stereo-BRUVS in one day was not logistically possible as a second vessel would be required. Therefore, the acoustic survey was carried out on the 5th of October 2016 while the deployment and recovery of the stereo-BRUVS were conducted the next day within the same moon and similar tidal phase. During the acoustic survey, the Biosonics echo-sounder was towed on the side of the vessel in the same arrangement used in CS. Transects 2 km long and 50 m apart from each other were followed to cover an area of 800 m width and 2 km length at an average speed of 7 knots.

The selection of the stereo-BRUVS deployment locations was based on differences on the seafloor backscatter (E1) such that at least two areas with different levels of seafloor backscatter were included. The same criteria of 250 m as a minimum distance between stereo-BRUVS was applied.

Temporal experiment

An area close to the Tantabiddi ramp (Figure 5.2) was used to assess the temporal distribution of fish in two different benthic habitats: “rough” and “smooth” bottoms. Three small areas of 250 m by 250 m were used to test the effect on the acoustic variables before, during, and a day after the deployment of a stereo-BRUV. In each of the three 250 m² areas, six parallel acoustics transects were conducted, using a 50 m separation with the vessel that towed the pontoon with the echo-sounders approximately 1 m from the starboard side (Figure 5.4). On completion of the acoustic survey, a stereo-BRUV was deployed in the centre of the square, and the acoustic transects repeated in the same square while the stereo-BRUV was recording. Once the transects were completed, the stereo-BRUV was recovered. The following day, a third acoustic survey was conducted at the location, in the same manner.



Figure 5.4. The three echo-sounders mounted in the pontoon and the GPS antenna in the centre, towed by the vessel.

5.3.3. Data analysis

5.3.3.1. Post-processing of the acoustic data

The Software Echoview (ver. 8.0; Echoview Software Pty Ltd.) was used for the post-processing of the acoustic data. The offsets between the physical location of the GPS antenna and the 120 and 430 kHz transducers were added to the Echoview transducers configuration to correct the spatial information of the acoustic data. In Echoview, two types of echograms are created for each frequency register by the echo-sounder. The TS echogram, in which each data point represents a Target Strength measured in decibels referenced to 1 m^2 and the S_v echogram in which each point represents the Volume backscattering coefficient in decibels referred to $1 \text{ m}^2/\text{m}^3$. The acoustic analysis was carried out using the 38 kHz frequency, and the 120 kHz data were used only for classification purposes.

A bottom detection algorithm was applied to detect the bottom line (best candidate) in the 38 kHz S_v echogram. Two metres from the surface were excluded from the analysis to avoid the near-field in which the acoustic data is unreliable. Also, an area of 0.5 m above the seafloor was excluded to avoid integrating parts of the seafloor or reef as targets. A visual inspection of the echograms was conducted to correct for wrong detections of the bottom and to mark noise areas as bad data which were excluded from the analysis.

Different types of unwanted signals 'noise' can be found in acoustic data. Background noise is a combination of attenuation of the signal caused by transmission loss, and other noise sources, including vessel noise (De Robertis and Higginbottom, 2007). Impulse noise is generally caused by interference with other unsynchronized acoustic instruments operating simultaneously (Ryan et al., 2015). Two noise filters

were applied in both the 38 kHz and 120 kHz S_v echograms to reduce the effect of unwanted signals in the data: an impulse noise removal filter (Ryan et al., 2015) and background noise filter (De Robertis and Higginbottom, 2007). The 'dB difference' method developed by (Ballon et al., 2011) was used to separate fish with swim bladder from zooplankton and fluid-like organisms using the 38 and 120 kHz frequencies. Therefore, the ping time and geometry of the two frequencies were matched to be compatible.

Nautical area scattering coefficient

For a pixel to be classified as fish, the sum of 120 and 38 kHz S_v echograms has to be higher than -122 dB, and the difference between 120 and 38 kHz S_v has to be less than 3 dB. A threshold of -60 dB was applied to remove no-fish targets (Parker-Stetter, 2009). Then a blurring was applied using a 3x3 convolution matrix (1,2,1;2,1,2;1,2,1). The resulting echogram was gridded and the integrated 'depth-stratified NASC' (m^2/nmi^2) exported in cells 50 m long and 5 m deep. A second estimation of depth-stratified NASC was also exported in which the schools of fish were excluded. The SHAPES algorithm (Coetzee, 2000) implemented in Echoview was used to detect the schools with detection parameters set to a minimum total school length of 2 m, a minimum school height of 1m, a minimum candidate length of 2 m, a minimum candidate height of 1 m, a vertical linking distance of 1 m, a maximum horizontal gap distance of 1 m, and a minimum volume backscattering coefficient (S_v) of -60 dB (Campanella and Taylor, 2016). The schools' areas were used to create a mask which was applied to the clean S_v echogram. The 'depth-stratified NASC no schools' were then exported using the same vertical and horizontal grid of 5 m by 50 m. The results for both depth-stratified NASC and depth-stratified NASC no schools were exported into R (R Development Core Team, 2017) for further analysis.

5.3.3.2. Post-processing Stereo-BRUVS

The two video recordings (left and right cameras from each deployment) were synchronised and analysed using the 'EventMeasure Stereo' (SeaGIS, 2011) software. An hour of the recording time was analysed, starting from the moment the stereo-BRUV reaches the seafloor. The reviewing process involved identifying the fish present in the videos and selecting the frame with the higher abundance of each particular species to count and measure the individuals. The selection of only one frame prevents recounting. This approach is known as 'MaxN' and is considered a conservative measure of abundance. The analysis procedure was also conducted following (Harvey et al., 2007).

The fork length of the fish counted in the MaxN frame visible in both cameras was measured. For the majority of the sampling points, the length of all the fish considered in the MaxN were measured.

However, in some instances, the measurement of all fish was not possible (e.g., overlapping in the view of the cameras). In those cases, the average length of the measured fish was used to estimate the length of the unmeasured ones. The length-weight relationship per species was used to convert the length measurements to biomass using Fishbase data (Froese and Pauly, 2012) . When a species length-weight relationship was not available, the parameters of a species within the same genus was used. The weight of individual fish was summed to estimate the ‘relative biomass’ for each sampling point.

5.3.3.3. Acoustic vs. Stereo-BRUVS

Correlations between acoustic variables and stereo-BRUVS variables were explored. The location of the stereo-BRUVS deployments was used to extract the acoustic data in the surrounding areas. Different radii of search were tested from 50 m and increasing in 50 m steps to 1500 m (as explained in section 4.3.7). The acoustic data were then averaged among the sampling points in the corresponding radius of search.

Demersal and semi demersal species were anticipated to be present in the stereo-BRUVS, however, it is not clear the area of influence of the bait-plume in the water column. For this reason, the different layers of the water column as exported from Echoview were included, one by one, starting from Layer 0, which corresponds to 0.5 to 5.5 m above the seafloor. This was particularly important in the NMP spatial experiment in which there was a significant change in depth across the sampling area, compared to CS where only two Layers were sampled. The possible correlation between the water column acoustic data with the stereo-BRUVS was also tested by summing the acoustic Layers starting from the top, and adding Layers until the one above the seafloor.

A Wilcoxon rank sum test was used to compare the mean relative biomass, MaxN, $NASC_{BRUV-mean}$, and $NASC_{BRUV-mean}$ no schools between benthic habitat (sand/ reef). For the temporal experiment, the depth-stratified NASC before, during and after the deployment of the stereo-BRUV were compared using a Kruskal-Wallis rank sum test and the Dunn post hoc test to identify differences between the groups.

5.4. RESULTS

5.4.1. Spatial experiments

5.4.1.1. Cockburn Sound

Stereo-BRUVS

Higher levels of relative biomass were observed in the pavement reef, and cobble reef areas (Figure 5.5).

The sampling points located in the sandy bottoms had, in general, lower levels of relative biomass with few exceptions in which rays were observed, increasing the biomass for those sampling points. The total abundance (MaxN) was also lower in areas with benthic habitats defined as sand.

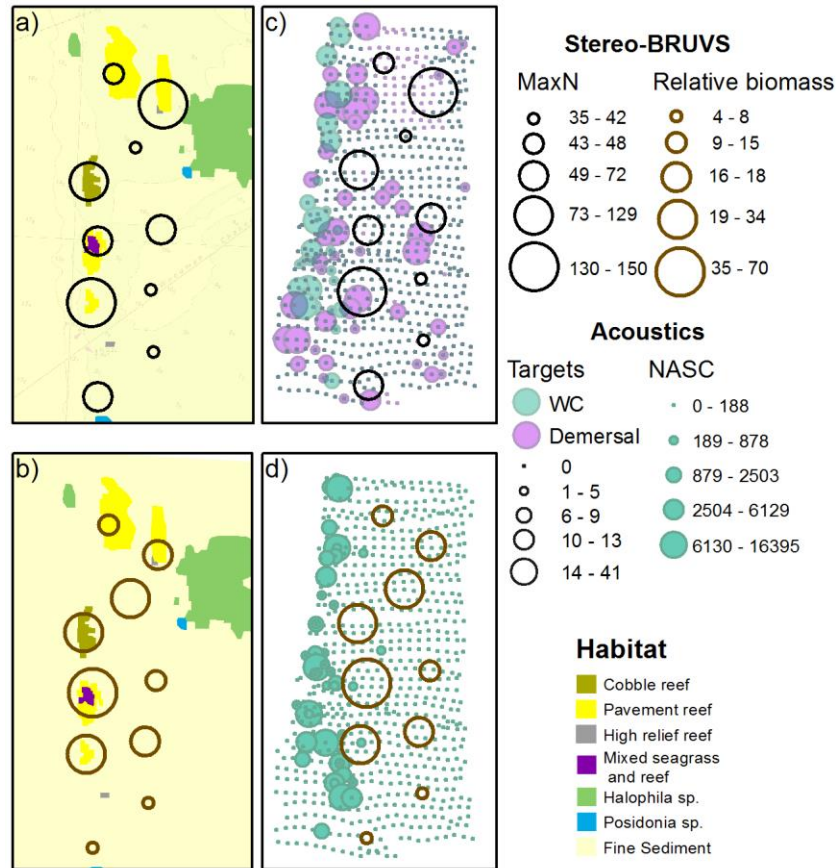


Figure 5.5. a) Abundance and b) relative biomass from the stereo-BRUVS in the Cockburn Sound area laid over the benthic habitat map. c) Total number of acoustic targets and d) depth-stratified NASC are shown with the stereo-BRUVS data showed as graduated circles.

Acoustics

Higher values of acoustic backscatter were found on the west side of the study site where there is a greater variety of benthic habitats and also a change in the depth (Figure 5.5). Lower levels of backscatter were observed in the eastern part of the study area.

Acoustics vs. Stereo-BRUVS

The best correlation between the acoustic and stereo-BRUVS data was for the relative biomass from the stereo-BRUVS and the $NASC_{BRUV-mean}$ no schools using a radius of 300 m around the stereo-BRUVS and summing three Layers (0.5 to 15.5 m) above the seafloor ($R=0.85$, $p<0.0001$, $R^2=0.8$, $p<0.0001$, Figure 5.6).

The high correlation between the $NASC_{BRUV-mean}$ and the relative biomass was only observed when the schools were excluded (Figure 5.6).

The correlation between the number of acoustic targets and relative biomass from the stereo-BRUVS was also highly significant with the same 300 m radius of search but including only two Layers (0.5-10.5 m) above the seafloor ($R=0.908$, $p<0.0014$, $R^2=0.7$, $p<0.001$, Figure 5.7). No difference was observed in the levels of correlation when the integration started from the bottom or surface.

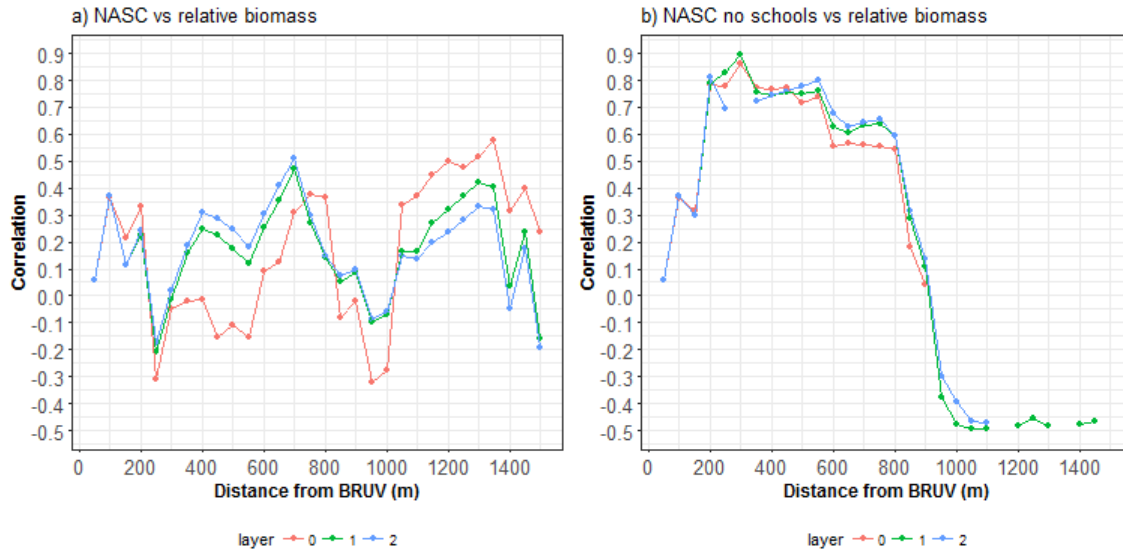


Figure 5.6. a) Correlations between the $NASC_{BRUV-mean}$ and relative biomass recorded by the stereo-BRUVS, and b) $NASC_{BRUV-mean}$ without schools and relative biomass at different radius of search around the stereo-BRUVS and depth Layers.

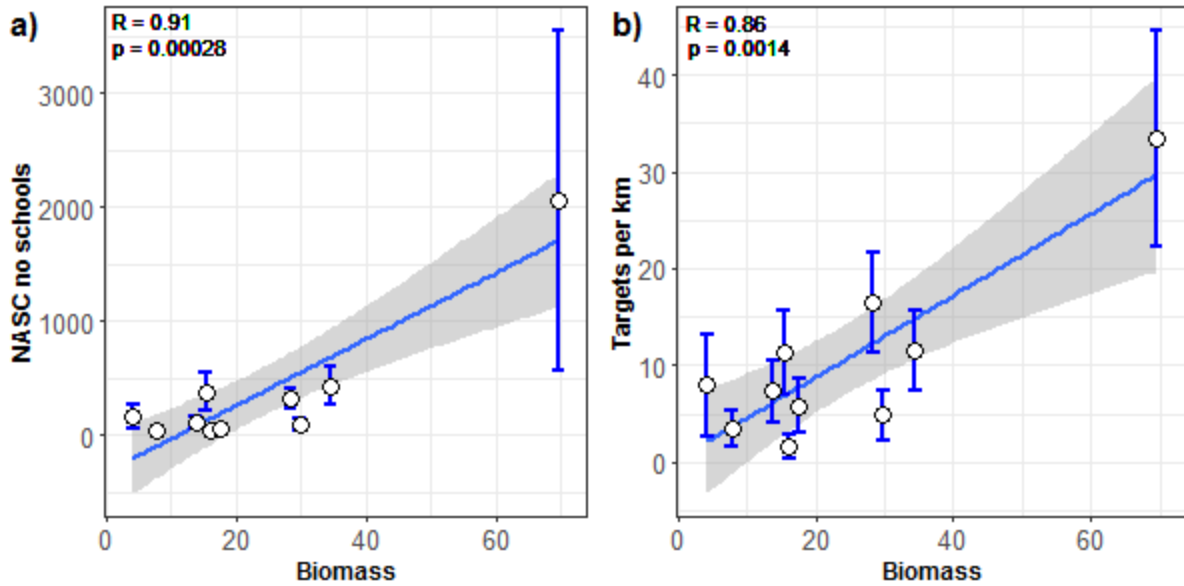


Figure 5.7. Correlations between the relative biomass from the stereo-BRUVS and a) $NASC_{BRUV-mean}$ no schools, and b) acoustic targets using a 300 m radius of search around the stereo-BRUVS and including acoustic data from 15.5 and 10.5 m above the seafloor respectively. The standard errors are shown as error bars.

The correlation between acoustic variables and the biomass of the stereo-BRUVS removing the rays was also explored. These organisms are usually very close to the bottom (Thrush et al., 1991), and are unlikely to be resolved by the echo-sounder. When excluding the rays, the best correlation was found between the number of acoustic targets and the relative biomass with an almost linear relationship between the two variables (Figure 5.8). A strong and significant correlation was also found for the $NASC_{BRUV-mean}$ no schools and the relative biomass without rays (Figure 5.8).

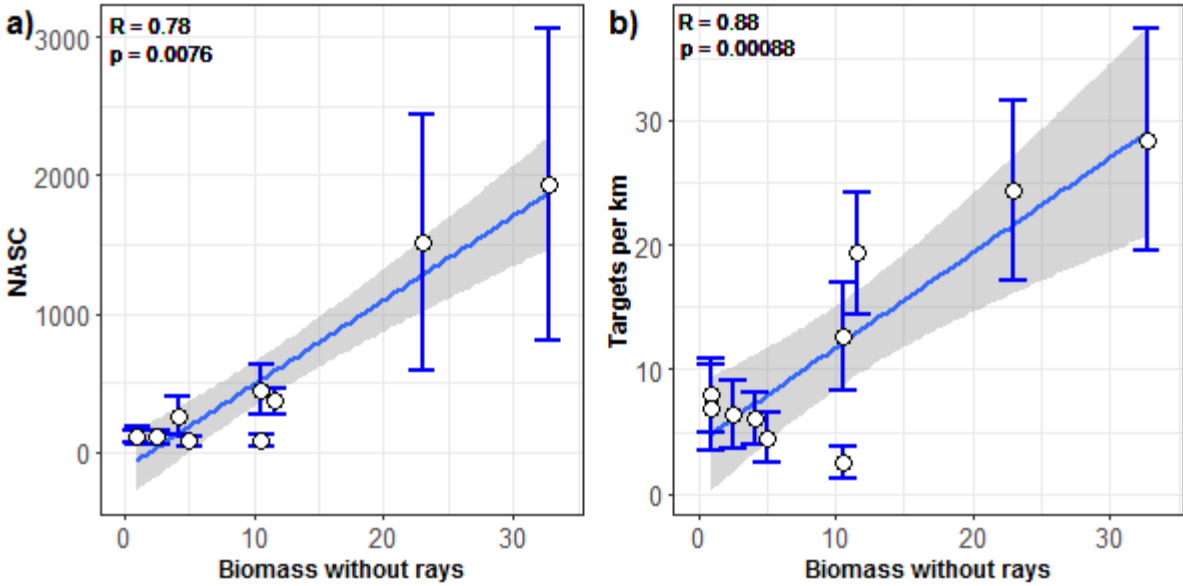


Figure 5.8. Correlations between the relative biomass without rays from the stereo-BRUVS and the $NASC_{BRUV-mean}$ no schools (left), and acoustic targets (right) using a 250 m and 400 m radii of search respectively around the stereo-BRUVS and including 10.5 m above the seafloor. The standard error is shown in the error bars, and the number of acoustic samples is also shown.

Benthic habitats

The classification of benthic habitats in two classes: reef and sand showed a consistent pattern of higher levels of relative biomass and MaxN in the areas with reef habitats and was also reflected in the $NASC_{BRUV-mean}$ and number of acoustic targets (Figure 5.9). However, the difference between benthic classes was not significant for $NASC_{BRUV-mean}$ and number of acoustic targets ($\alpha < 0.05$), and was only indicative for MaxN ($W = 3, p = 0.05, power = 0.52$).

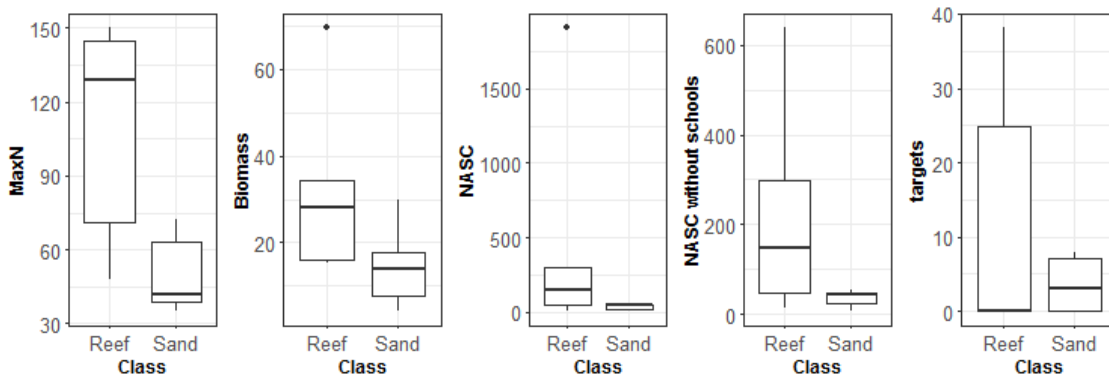


Figure 5.9. Boxplot of the MaxN, relative biomass, $NASC_{BRUV-mean}$, $NASC_{BRUV-mean}$ no schools and acoustic targets grouped by benthic habitat class.

5.4.1.1. Ningaloo Marine Park

Stereo-BRUVS

A spatial pattern of higher levels of abundance (MaxN) was observed in the central-south section of the study area characterised by “hard” acoustic seafloor and shallower depths (Figure 5.10). A similar pattern was observed to a lesser extent in the relative biomass. In the sandy bottoms, higher values of biomass but less abundance suggest less number of individual but larger while in the south some sampling points had higher abundance but lower biomass which corresponds to smaller individuals.

Acoustics

Areas of high acoustic biomass were observed at the east edge of the sampled area and in some particular areas in the central portion of the study site (Figure 5.10). No apparent difference was observed between the depth-stratified NASC with and without schools of fish, therefore only the total depth-stratified NASC is shown.

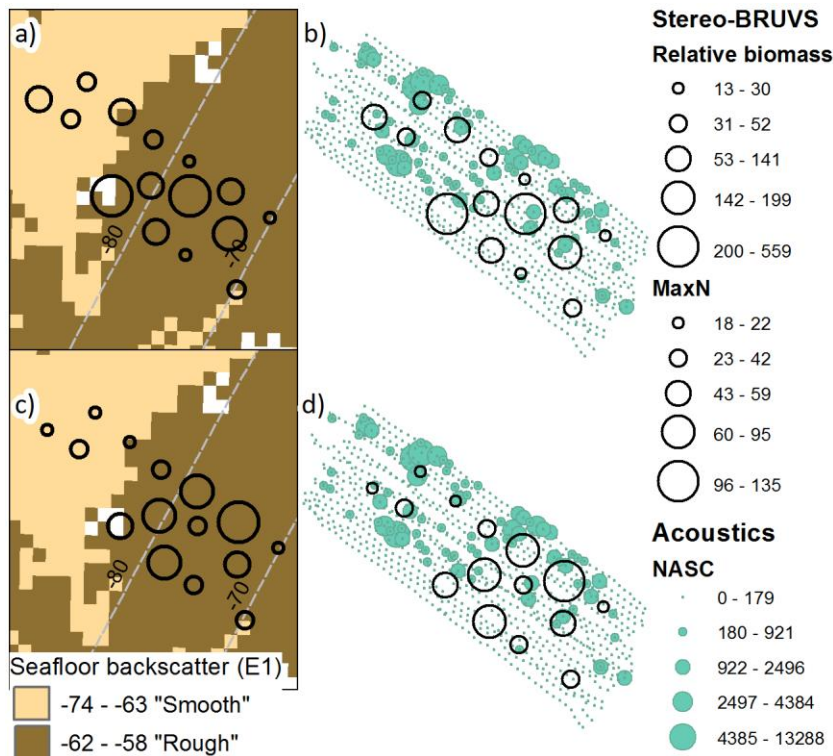


Figure 5.10. Spatial distribution of the relative biomass a) and MaxN c) with the acoustic classification of the seafloor. The results of the acoustic analysis are shown in the right side of the figure depth-stratified NASC with the relative biomass (b) and MaxN (d) from the stereo-BRUVS data shown as graduate circles.

Acoustics vs. Stereo-BRUVS

Low correlations were found between the relative biomass from the stereo-BRUVS and the $NASC_{BRUV-mean}$ (Figure 5.11), the removal of the schools did not change the correlation between them, and the curve has an almost identical shape, therefore, only the $NASC_{BRUV-mean}$ is shown. Low correlations were also found between the MaxN and the $NASC_{BRUV-mean}$, only the 50 m radius around the stereo-BRUVS produce a correlation of $R=0.6$, but it was not significant (at $\alpha = 0.05$).

When the Layers were integrated starting from the surface, a strong correlation was found between the MaxN from the stereo-BRUVS and the $NASC_{BRUV-mean}$ ($R=0.855$, $p<0.001$, $R^2=0.71$, $p<0.001$) when only the 35 m closest to the surface were included (Figure 5.12).

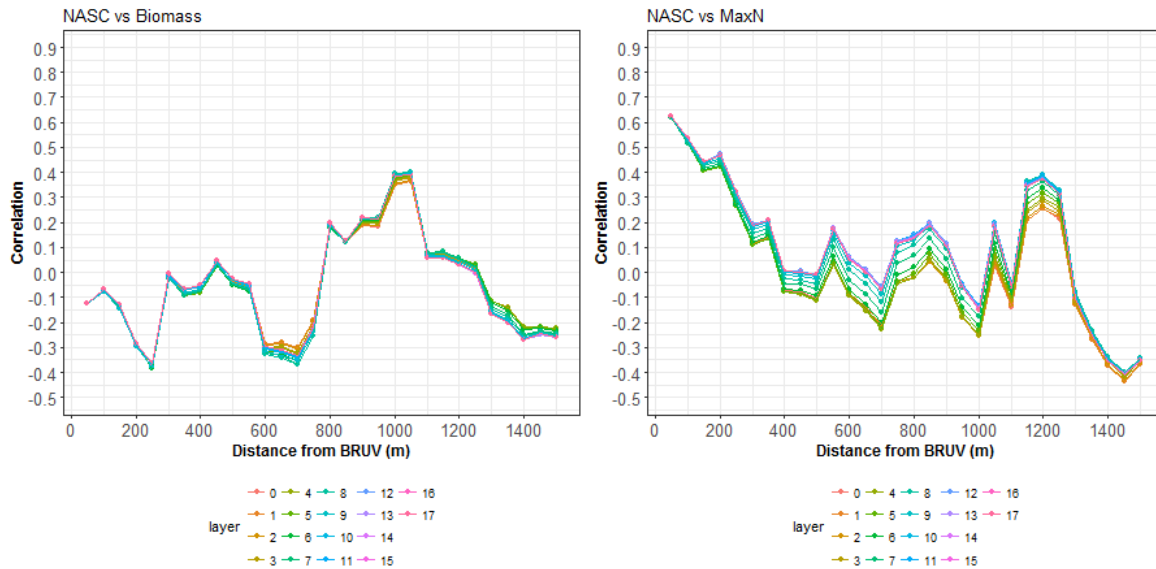


Figure 5.11. Correlations between the $NASC_{BRUV-mean}$ and the relative biomass (left) and MaxN (right) from the stereo-BRUVS using different radii of search around the stereo-BRUV, and including different Layers of the water column. Layer 0 represents the interval 0.5-5.5 m above the seafloor.

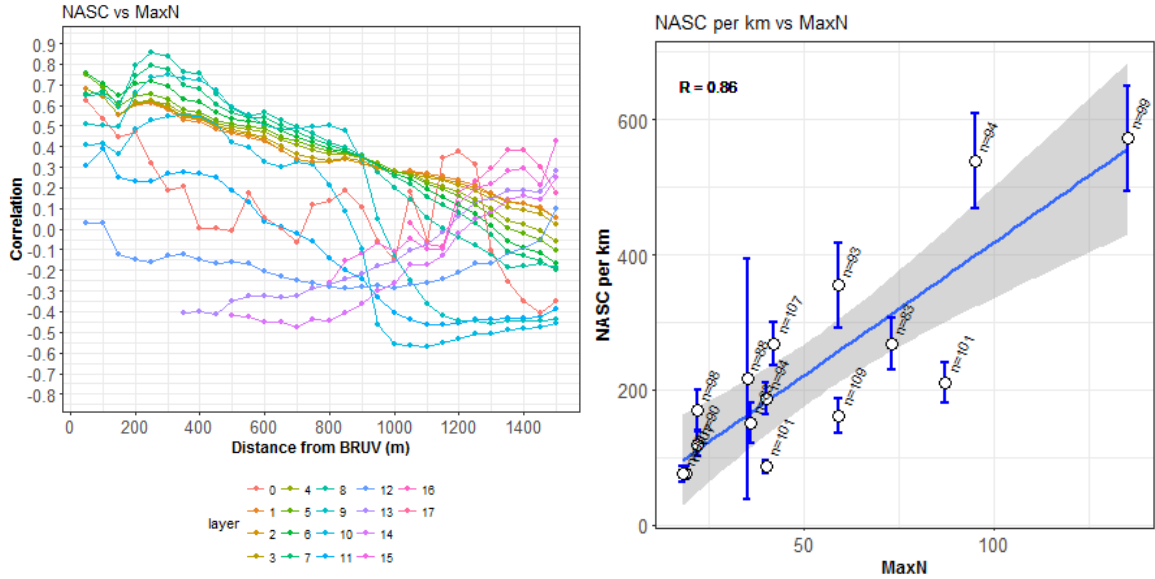


Figure 5.12. Correlations between the abundance (MaxN) from the stereo-BRUVS and the $NASC_{BRUV-mean}$ using different radii of search around the stereo-BRUVS and including different Layers of the water column starting from the surface (left). Layer 0 represents the interval 0.5-5.5 m above the seafloor. Correlation between MaxN and the $NASC_{BRUV-mean}$ using a radius of search of 250 m and excluding 40.5 m closer to the bottom (right), the number of acoustic samples (intervals) considered in the calculation of the $NASC_{BRUV-mean}$ and the standard error are shown.

The spatial distribution of the depth-stratified NASC when the 40.5 m closest to the seabed were excluded presented a pattern of higher values in the east edge of the sampling areas and also at the west edge. A similar pattern was observed for the MaxN of the stereo-BRUVS (Figure 5.13).

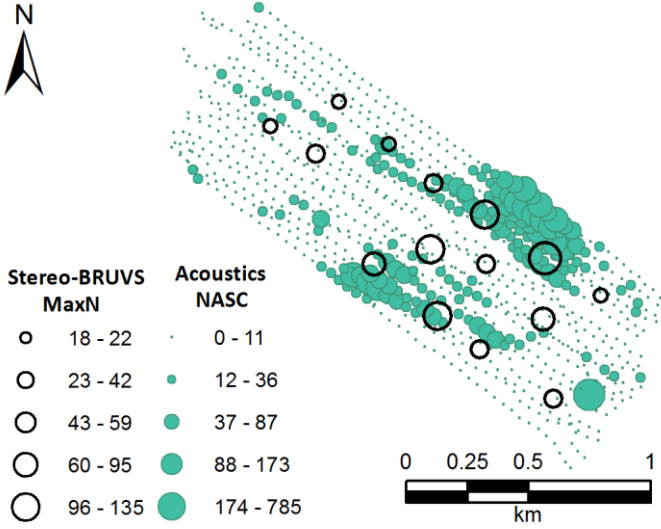


Figure 5.13. Spatial distribution of the depth-stratified NASC excluding the 40.5 m closer to the bottom with the relative abundance from the stereo-BRUVS (MaxN) plotted as graduated circles.

In some of the stations, the presence of one shark can increase the biomass by hundreds of kilograms, while it is unlikely that the narrow beam of the echo-sounder would have insonified it. Hence, the

correlation between the acoustic variables and the relative biomass without sharks and rays was also tested. However, the exclusion of the sharks did not improve the correlation between the acoustic $NASC_{BRUV-mean}$ and the relative biomass from the stereo-BRUVS. Both the bottom to top and top to bottom summing Layers approaches were tested (Figure 5.14).

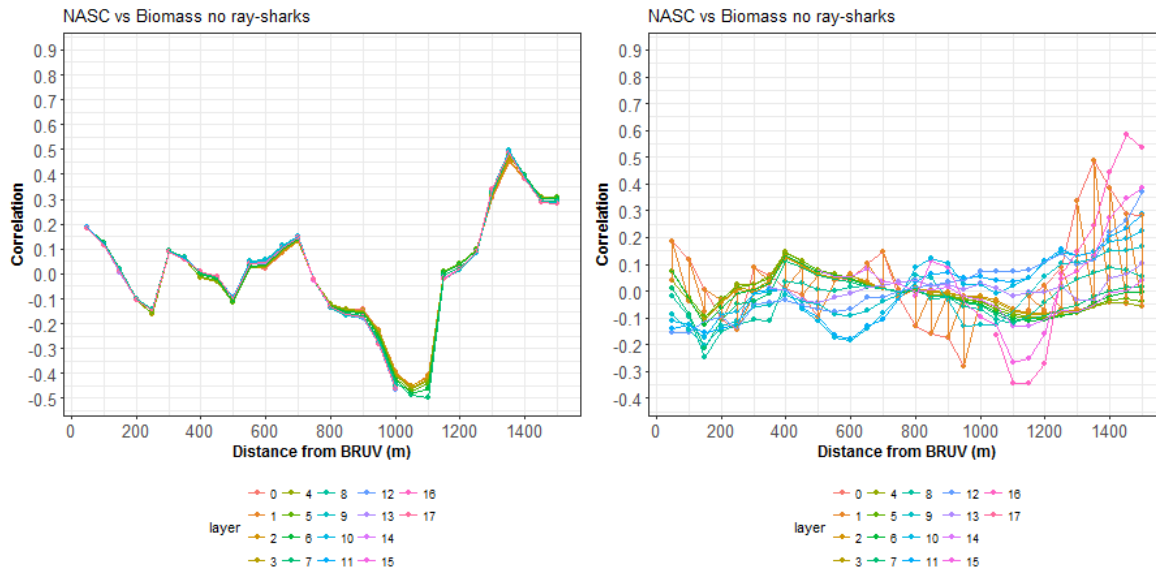


Figure 5.14. Correlation between the $NASC_{BRUV-mean}$ and the relative biomass from the stereo-BRUVS excluding the sharks and rays using different radii of search around the stereo-BRUV and including different Layers of the water column starting from the bottom (left) and top (right).

Benthic habitats

The seafloor classification based on acoustic roughness (E1) was useful to differentiate between sandy bottoms and areas with the presences of sponges and soft corals which were denominated reef habitat (Figure 5.15). Out of the 15 sampling points, only two were misclassified by using the E1 parameter. In all cases sandy bottoms were classified as smooth bottoms using the E1.

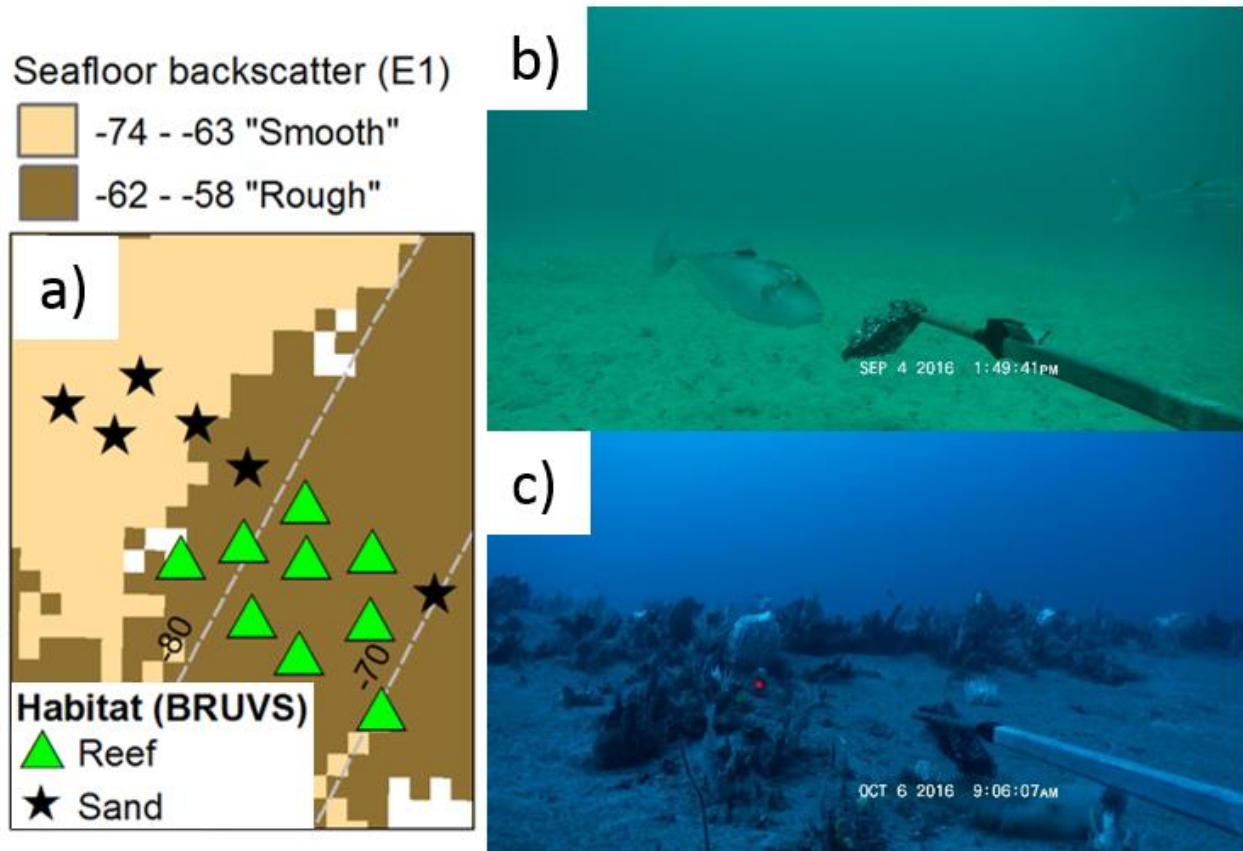


Figure 5.15. Benthic habitats present in the sampling points. a) Classification of the benthic habitats based on the stereo-BRUVS data over the seafloor backscatter. b) Example of the bottoms classified as "Sand". c) Example of benthic habitat classified as "Reef" in the spatial experiment at Ningaloo Marine Park.

A significant difference was found between the MaxN in sampling points with 'rough' and 'smooth' bottom classified using the seafloor backscatter ($W = 4$, $p = 0.021$, power = 0.57). A much stronger difference was found using the benthic habitat classification based on a visual assessment from the stereo-BRUVS ($W = 4$, $p = 0.007$, power = 0.81; Figure 5.16). No differences were observed between the $NASC_{BRUV-mean}$ with or without schools between the benthic habitats for the full water column in a 150 m radius around the stereo-BRUVS (Figure 5.16). An apparent pattern of higher values of depth-stratified NASC both with and without schools was observed in the reef areas when only the water column above 40.5 m was included. However, the differences were not significant ($W = 20$, $p = 0.45$, power = 0.21; Figure 5.17).

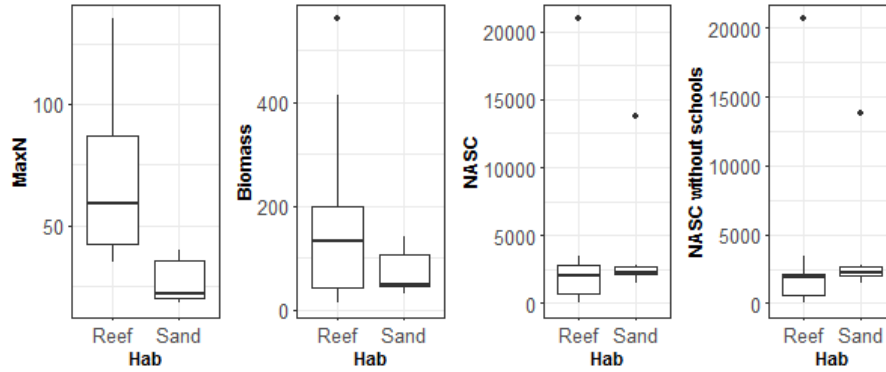


Figure 5.16. Box plots of the abundance (MaxN) and relative biomass from the stereo-BRUVS, $NASC_{BRUV-mean}$, and $NASC_{BRUV-mean}$ no schools grouped by the benthic habitat observed in the stereo-BRUVS.

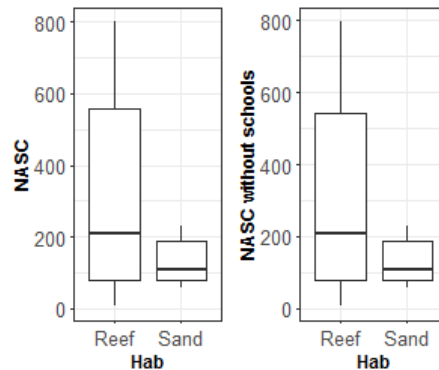


Figure 5.17. Box plots of the acoustic variables $NASC_{BRUV-mean}$, and $NASC_{BRUV-mean}$ without schools grouped by benthic habitats excluding the 40.5 m of water column above the seafloor.

5.4.2. Temporal experiments

5.4.2.1. Ningaloo Marine Park

Stereo-BRUVS

Two of the temporal experiments were conducted in benthic habitats classified as ‘sand’ while the deeper Temporal 3 was located in a ‘reef’ habitat. The total MaxN was higher in the shallowest Temporal 1 site located inside the reef lagoon while the other two sites located outside the lagoon and deeper had similar MaxNs (Table 5.2). The relative biomass was also higher in the Temporal 1 site, where the presence of a tiger shark increased the biomass (Figure 5.18).



Figure 5.18. Temporal 1 had predominately sandy bottom with some algae (left), the Temporal 2 (centre) was located in a sandy bottom, and the Temporal 3 had a sandy bottom with the presence of sponges and soft corals (right).

Table 5.2. Results of the stereo-BRUVS analysis for the three sites considered in the temporal analysis.

Station	Biomass	MaxN	Richness	Depth
Temporal01	105.9	52	19	4
Temporal02	17.5	32	10	60
Temporal03	45.5	33	14	75

Acoustics

The difference between the depth-stratified NASC before, during and after the deployment of the stereo-BRUV varied between areas. The water column was divided in two categories the ‘demersal layer’ which corresponds to the 5.5 m above the seafloor and the ‘water column’ in which all the Layers were summed. For the shallow Temporal 1 site (4 m), only a demersal layer was available as it is also the total water column.

Acoustics demersal

In the first area, which was the shallowest and located in the reef lagoon, the depth-stratified NASC was low before the deployment of the stereo-BRUV, increased during the soaking time and decreased again the day after (Figure 5.19). The depth-stratified NASC was significantly different the day after from the one measured the first day before the stereo-BRUV was deployed (Table 5.3).

Table 5.3. Results of the post hoc Dunn test for comparison of depth-stratified NASCs medians of the three sites grouped by time: before the stereo-BRUV deployment, during the soaking time and the day after. Only the demersal layer is considered (0.5-5.05 m above the seafloor).

Site	Comparison	Z	P.adj
Temporal 1	1.Before-2.During	-11.4568	0.0000
	1.Before-3.After	-9.2138	0.0000
	2.During-3.After	1.4409	0.1496
Temporal 2	1.Before-2.During	0.2295	0.8185
	1.Before-3.After	-8.6869	0.0000
	2.During-3.After	-11.4956	0.0000
Temporal 3	1.Before-2.During	1.6766	0.0936
	1.Before-3.After	-2.0722	0.0574
	2.During-3.After	-3.8857	0.0003

For the Temporal 2 and Temporal 3 sites, the depth-stratified NASC in the demersal layer was higher the day after the deployment of the stereo-BRUV, the differences were significant in both cases (Table 5.4).

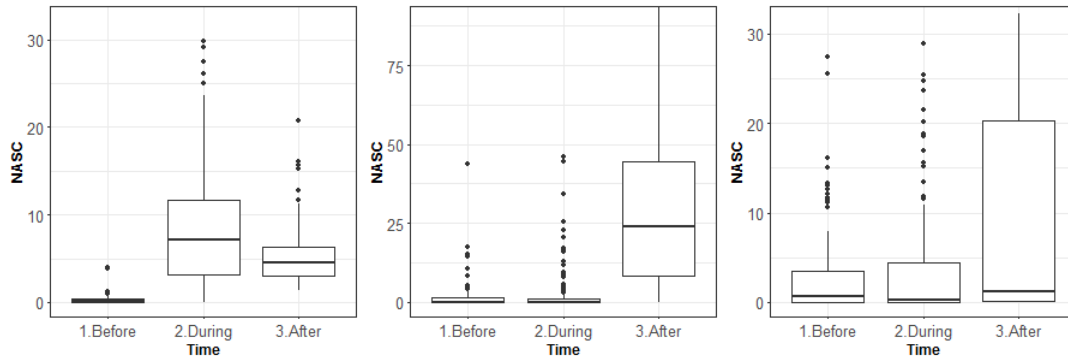


Figure 5.19. Distribution of depth-stratified NASC in the demersal layer (5 m above the seafloor) of the temporal 1 (left) temporal 2 (centre) and temporal 3 (right) sites before, during and a day after the deployment of the stereo-BRUV. Each point in the plot represents one 50 m Interval of depth-stratified NASC.

Water column

For the Temporal 2 site the water column depth-stratified NASC increased during the soaking time and presented similar values the next day (Figure 5.20).

Table 5.4. Results of the post hoc Dunn test for comparison of depth-stratified NASCs medians of the three sites grouped by time: before the stereo-BRUV deployment, during the soaking time and the day after. The full water column is considered.

Site	Comparison	Z	P.adj
Temporal 2	1.Before-2.During	-7.9169	0.0000
	1.Before-3.After	-8.1617	0.0000
	2.During-3.After	0.6732	0.5008
Temporal 3	1.Before-2.During	0.1575	0.8748
	1.Before-3.After	-3.6530	0.0004
	2.During-3.After	-4.1942	0.0001

For the Temporal 3 site, the depth-stratified NASC was significantly different the day after the deployment of the stereo-BRUV while no change was observed before and during the soaking time (Table 5.4).

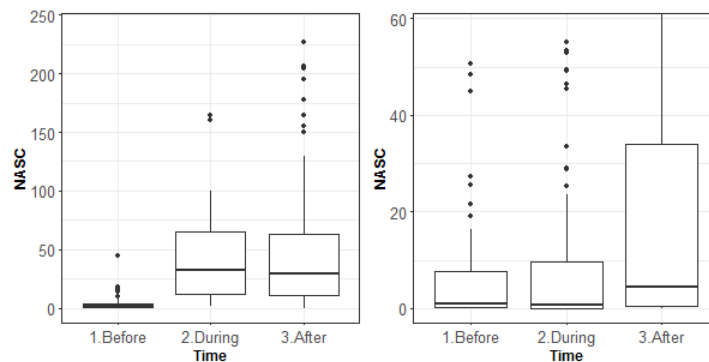


Figure 5.20. Distribution of the depth-stratified NASC in the second (left) and third (right) sites of the temporal experiment considering the full water column. Each point in the plot represents one 50 m Interval.

5.5. Discussion

Two study sites off the coast of WA were used to explore the possibility of combining stereo-BRUVS and echo-sounder data in the assessment of demersal fish in reef areas. The results in the CS area showed a strong correlation between the spatial distribution acoustic biomass and the relative biomass recorded by the stereo-BRUVS, in particular when the pelagic schools were excluded from the analysis. For the NMP, on the other hand, significant but not strong correlations were found between the demersal acoustic biomass and the stereo-BRUVS. The higher variability of the NMP system was evident in both the spatial and temporal experiments, highlighting the importance of collecting the acoustic and stereo-BRUVS data as close in time as possible.

5.5.1. Spatial experiments

5.5.1.1. Cockburn Sound

Areas of higher abundance (MaxN) from the stereo-BRUVS were associated with reef benthic habitats. A similar pattern was observed in the number of acoustic targets and $NASC_{BRUV-mean}$ to a lesser extent. Although, these differences were not statistically significant, perhaps the low sample size was the main reason of this indicative, but not significant, relationship as shown by the power analysis. Previous studies in the nearshore waters of Western Australia, have shown the importance of seagrass and limestone reef areas, with higher levels of fish biomass and richness when compared to flat sand or silt substrate (Howard, 1989, Wakefield and Johnston, 2009).

The highest values of depth-stratified NASC were associated with pelagic schools located in the west edge of the study site where there is a rapid change in depth. The exclusion of the depth-stratified NASC from the schools had the effect of increasing the correlation between the acoustic and stereo-BRUVS data. Therefore, it appears that the pelagic schools recorded by the echo-sounder were not observed in the stereo-BRUVS. Demersal stereo-BRUVS can sample demersal, semi-demersal and pelagic species (Cappo et al., 2004), however, recent studies using pelagic stereo-BRUVS in a tropical area showed significant differences between the assemblages of species at two different depths in the water column (Santana-Garcon et al., 2014). The differences between depths in Santana-Garcon (2014) study, were mainly driven by species which were only recorded in the superficial or deeper deployment. Some of the species only recorded in the superficial stereo-BRUVS in Santana-Garcon (2014) study usually form big pelagic schools. It is possible that the schooling species recorded by the echo-sounder were not observed with the stereo-BRUVS.

An almost linear relationship between the $NASC_{BRUV-mean}$ without schools and the biomass from the stereo-BRUVS, suggest that the acoustic biomass of the non-schooling targets was a good indicator of the relative biomass as observed by the stereo-BRUVS. The exclusion of the rays, which spend most of the time very close to the bottom (Thrush et al., 1991), and are probably not detected by the echo-sounder, reduced the correlation but the relationship was still strong which supports the idea that the depth-stratified NASC is a good indicator of the relative biomass from the stereo-BRUVS in this study site.

An increase in the number of acoustic targets was related to an increase of relative biomass from the stereo-BRUVS, which indicates low variability in the length of the fish. This was supported by the stereo-BRUVS results, which showed less variability in the length distribution on the fish recorded in CS with

respect to the NMP area. The relationship was stronger when the rays were excluded from the biomass of the stereo-BRUVS. These results suggest a potential combination of the echo-sounder and stereo-BRUVS can improve the estimations of spatial distribution of demersal fish biomass in CS.

5.5.1.2. Ningaloo Marine Park

The benthic classification based on the E1 acoustic metric was able to discriminate the sandy bottoms from the sand with sponges and corals, with some two exceptions. The E1 metric is more influenced by the “roughness” of the seafloor, which can explain the misclassification of the two sampling points as areas with sand waves and sand ripples are considered soft rough (Siwabessy, 2001).

A combination of benthic habitats and depth were the possible cause of higher MaxN record by the stereo-BRUVS in shallow areas of reef, although, the relative biomass was also high in some areas of the sandy deeper bottom. The presence of sharks and bigger fish in the deeper areas created this pattern of less abundance but high biomass. A previous study conducted in the NMP reported less abundance and richness of species in deeper areas, but larger individuals, related to ontogenic habitat changes for many species (Fitzpatrick et al., 2012). Low correlations were found between the $NASC_{BRUV-mean}$ with and without schools, and the acoustic data when the layers were summed from bottom to top, and the exclusion of the sharks and rays did not increase the relationship. Unlike what was observed in CS, the exclusion of the schools of fish did not affect the relationship between the acoustics and the stereo-BRUVS data, as the depth-stratified NASC concentrated in the schools was low.

An unexpected result was the strong correlation (the highest) between the relative biomass of the stereo-BRUVS with the $NASC_{BRUV-mean}$ in the water column when the 40 m closer to the bottom were excluded. Although the presence of pelagic species in the recordings of the stereo-BRUVS is not unusual (Cappo et al., 2004), the field of view in the stereo-BRUVS will not cover areas so far from the seafloor. Therefore, one of the possible explanations for this correlation would be that the high productivity in the surface might be related to schools of midwater fishes like *Sphyraena obtusata* and pelagic species like *Sarda orientalis* which were observed in sampling points with high levels of MaxN in the stereo-BRUVS. However, it is possible that the observed correlations between acoustic variables and BRUVS derived data could have been anomalies. Further experiments are required to determine if this is a real effect or not.

CS presented higher levels of acoustic biomass, most of which was concentrated in pelagic schools located in the slope of the study area. In the NMP, on the other hand, hotspots of biomass were found in different areas of the study site with smaller schools occurring at different levels of the water column. These results

are in accordance with the literature which suggests temperate reef fishes are more likely to form dense schools than tropical ones (Hixon, 1991). Higher levels of diversity are normally observed in tropical areas compared to temperate ones, as was observed by the higher richness of species observed in NMP, but also a wider range of lengths in the species recorded (Holmes et al., 2013). Considering the wider range of species and high variability of the ecosystem observed in the NMP, it is recommended the acoustic and video recording are conducted as close as possible in time. Also, the use of pelagic stereo-BRUVS (Bouchet and Meeuwig, 2015) could be used to add information on the species composition in pelagic species.

5.5.2. Temporal experiment

High variability was found between the acoustic biomass depth-stratified NASC before, during and after the deployment of the stereo-BRUVS. The depth-stratified NASC of the first day was significantly different from the second day of the survey, for both the water column and the demersal layer with only one exception. High variability in the stereo-BRUVS MaxN in sandy areas has been reported before, where the first day of sampling was significantly different from the following two days of deployments, compared with a more stable behaviour around reef bottoms (McIlwain et al., 2011). In this study, two of the sampling points were located in sandy bottoms, and only Temporal 3 was located in a sandy bottom with sponges. These results give us evidence of the highly variable the acoustic biomass can be in the NMP. Although, the low number of samples without replicates do not allow for a final conclusion.

5.5.3. Limitations of the study

5.5.3.1. Cockburn Sound

A point of concern in the results of the CS experiment was the timing between the acoustic survey and the deployment of the stereo-BRUVS. Due to an unexpected delay in the sampling, the deployment of half of the stereo-BRUVS were conducted before the acoustic survey. In the rest of the sampling stations in CS and the totality of the NMP area, the acoustic survey was conducted before the deployment of the stereo-BRUVS. The response of fish to baited equipment can be species-specific and affected by a number of factors, including individuals response time, feeding behaviours, current activity, schooling behaviour and propagation of the bait plume (Sheaves, 1995, Cappo et al., 2006), thus soak time is a factor in numbers of fishes present at any given time. Similarly, after the stereo-BRUVS has been retrieved, there may be a period while species abundance is affected by prior presence of the bait and the remaining bait plume. As a result, when the acoustic transects were conducted post stereo-BRUVS deployment, a minimum time of 1 hour was allowed before the transect commenced, to minimise any bias. However, the length of the

bait effect in the water column has not been well studied. A separate experiment needs to be considered to investigate the effect of the bait in the water column which might last longer than an hour, increasing the correlation with the acoustic data in those sampling points.

5.5.3.2. Ningaloo Marine Park

The echo-sounders were mounted in a pontoon which was originally designed to be used in a shallow protected area. However, the pontoon was very unstable under the conditions of stronger wind and current that we experienced in the deeper areas outside the lagoon in the NMP. As a result, the echograms presented high levels of noise and a long pulse length was used for the deeper areas. The use of a long pulse-lengths can help to increase the signal to noise ratio (SNR; Godlewska (2011)), and the probability of detect targets, at the cost of losing vertical resolution (Simmonds and MacLennan, 2008). Therefore, the use of long pulse lengths can lead to under estimations of single targets and for that reason only depth-stratified NASC, which is less affected by long pulse lengths (Godlewska et al., 2011), was used for the NMP study site.

Considering the results from the experiment conducted in CS, it was expected that eight stereo-BRUVS in each benthic habitat would be sufficient to detect differences in the MaxN, and 15 for NASC with a 0.8 power. However, the higher variability observed in NMP, indicated that a larger sample was needed to achieve similar levels of power. This variability may be one explanation for the low correlations observed between the acoustics and the stereo-BRUVS. In addition, the temporal experiment demonstrated that the high variability of the ecosystem in a short time (e.g., next day), can have a significant effect on the correlations between the two data sets in the demersal layer sampled by the stereo-BRUVS. Previous knowledge of this information would have been useful to improve the sampling design by collecting both stereo-BRUVS and acoustics on the same day. It is recommend for future studies that combine acoustics and stereo-BRUVS to sample both methods simultaneously, or on the same day if possible. Alternatively such studies could include a small temporal experiment like the one conducted in this study. This would allow the temporal variability to be assessed, and validation of the assumptions intrinsic in the sampling design.

5.5.3.3. Stereo-BRUVS and echo-sounders

The two different methods used in the present study have their own limitations and bias in the portion of the fish they can sample (Harvey et al., 2007, Lawson and Rose, 1999). For instance, the stereo-BRUVS are located on the seafloor with a field of view limited to a few metres above the bottom (Harvey et al., 2002).

The presence of pelagic species is not uncommon but schooling pelagic species are not usually observed in the stereo-BRUVS (Cappo et al., 2004). The echo-sounders on the other hand, cannot get reliable measurements in area closer to the surface (near-field), so a couple of metres have to be excluded. Also, the geometry of the beam of the echo-sounder produces a blind area closer to the bottom known as the Acoustic Dead Zone (ADZ). The size of the ADZ will vary depending on the depth, pulse length (increasing as the pulse length increases) and speed of sound in water (Ona and Mitson, 1996). Therefore, the area closer to the bottom might not be available to be sampled by the echo-sounder while the stereo-BRUVS are very efficient in sampling that area. The algorithm used to separate fish from zooplankton, and fluid-like organisms in the acoustic data (Ballon et al., 2011), exclude species which do not have a swim bladder, while the stereo-BRUVS can efficiently be used to measure all the species in the field of view of both cameras. Splitting the species by morphology is an option that was not explored in the present study, but it could improve the relationship between the two data sets in particular for the NMP as in the CS area, almost all the species recorded had a swim bladder.

5.6. CONCLUSION

The results of this study showed a significant correlation between the acoustic data and the relative biomass recorded by the stereo-BRUVS, in particular with the number of acoustic targets and biomass without schools in the CS area. Suggesting the possibility of combining both methods to estimate spatial patterns of biomass in the area, supporting the original hypothesis of this study. However, this strong relationship was not observed in the NMP where the correlations between the demersal layers of the acoustic data and the stereo-BRUVS were weak. Although the results showed significant relationships between the acoustic biomass in superficial layers of the water column and the stereo-BRUVS, our results suggest the system is highly variable, and we recommend reducing the time gap between the collection of the two data sets. Future directions for this research, included: increasing the area covered with the echo-sounder and the number of sampling points for the stereo-BRUVS to increase the power of our hypothesis testing. The use of pelagic stereo-BRUVS could also help to elucidate the species present in the water column which are not recorded by the demersal stereo-BRUVS.

Chapter 6

6. General Discussion

6.1. AIM AND OBJECTIVES OF THE THESIS

This thesis aimed to evaluate the performance of demersal fish distribution models based on underwater acoustic and stereo-BRUVS data, in suitable areas of the Western Australia coast. This was evaluated with four specific objectives:

1. To use SBES seafloor data in the construction of demersal fish distribution models based on stereo-BRUVS data, and to compare the results obtained by using MBES data.
2. Measure the effect of adding MBES seafloor backscatter data as an explanatory variable to demersal fish distribution models.
3. Elucidate the value and requirements of the use of historical water column backscatter data in assessing demersal fish abundance and biomass distribution.
4. Investigate the temporal and spatial variation of the abundance of demersal fish using SBES water column data and stereo-BRUVS data.

6.1.1. Performance of SBES seafloor data in the construction of demersal fish distribution models compared to the results obtained by using MBES data

In the present study, it was found that the species distribution models for six demersal species analysed had comparable performances using SBES and MBES data. The spacing of the SBES survey (500 m) was enough to produce an interpolated surface with a good agreement with the MBES. Kriging, using a first-degree detrending and an anisotropic variogram, produced the best result regarding reducing the error in unsampled areas. Kriging had been used before to successfully interpolate elevation data (Moskalik et al., 2013, Curtarelli et al., 2015, Zimmermann and Kienast, 1999, Arun, 2013, Bello-Pineda and Hernández-Stefanoni, 2007).

For *Abalistes stellatus*, *Gymnocranius grandoculis*, *Lagocephalus sceleratus*, and *Loxodon macrorhinus*, both the SBES and MBES models had poor performance which indicates that the variables included in the analysis were not enough to detect relevant variation influencing their distribution. *A. stellatus*, *G. grandoculis*, and *L. sceleratus*, presented a wide distribution through the study site, and were present in more than 40% of the sampling points including all ranges of depths. Generalist species can be difficult to model as they can have a broad tolerance to changes in environmental variables (Devictor et al., 2008).

For *P. multidentis* and *Pristipomoides typus*, both SBES and MBES produced acceptable levels of accuracy although some spatial clustering in the residuals indicates some under and over-prediction in the testing data set. An increase in the spatial clustering of the residuals of the models based on SBES data

interpolated using radial basic function suggests that the selection on the interpolation method had implications in the accuracy of the models.

The strong preference of *P. multidentis* and *P. typus* for deep waters could explain the success in modelling their distribution using depth and depth derivatives as explanatory variables. MBES bathymetry was strongly correlated with the SBES interpolated bathymetry, therefore, is not surprising that similar results of accuracy could be achieved using both data sets. Depth is an indirect surrogate of biotic and abiotic environmental variables that can influence the distribution of species (Sih et al., 2017). The depth derivatives included in this analysis were more important in the construction of the models at a medium or broad scale. *P. multidentis* and *P. typus* are roaming carnivorous species feeding on benthic invertebrates and fishes (Parrish, 1987a). Broad-scale variables might be better suited to explain the distribution of roaming species with variables affecting their distribution occurring at a large-scale. Broad-scale variables have shown to better explain the distribution of another demersal carnivores species with a relatively wide niche (Monk et al., 2011). However, fine-scale variables might be more important for more sedentary species, and it is possible that SBES data cannot produce relevant models for them. Only six species were included in the analysis. Therefore, the results should be taken with caution as a larger number of species of varying known behaviours must be tested to be able to provide a full assessment.

This study has shown the utility of applying SBES to acquire results in the same order of quality as MBES. This has positive implications for using such techniques to develop species distribution models in i) less affluent areas where MBES expertise and operation are not affordable and ii) historical data to assess how the models change over time.

6.1.2. Effect of adding the seafloor backscatter data as an explanatory variable to demersal fish distribution models

The addition of the seafloor backscatter did not have a consistent effect of improving the performance of the models of the distribution of the species included in the analysis. The performance of the models was species and study site dependent. Depth was the most important variable in the majority of the models and study sites. Depth is usually an important variable explaining the distribution of coral reef fishes because it is a surrogate for other variables including temperature and light availability which affect the community composition and function (Hill et al., 2014b).

The addition of seafloor backscatter had a marginal effect on the models. For *Lagocephalus sceleratus*, and *Abalistes stellatus* with a preference for sandy bottoms and roaming habits (Wahab et al., 2018), the

performance of the models were site dependent. In the sites where the models had a good performance for these two species, the addition of the seafloor backscatter produced only a marginal increase in the models accuracy.

For the models of *Lethrinus miniatus*, and *Lutjanus sebae*, the addition of the seafloor backscatter in Pt Cloates, in particular, increased the performance of the models. These two carnivorous species feed on a broad array of prey items showing opportunistic behaviours (Parrish, 1987a). The models of *G. grandoculis* distribution were the only case in which the inclusion of the seafloor backscatter consistently improved the performance of the model in the three study sites. It is possible that the acoustic 'hardness' was a good proxy of the rocky bottoms preferred by *G. grandoculis* (Dorenbosch et al., 2005).

The use of high frequencies typical in MBES systems has the disadvantage of a low penetration into the seafloor (Schneider von Deimling et al., 2013). It is possible that the acoustic signal of the superficial layer of the seafloor does not have a strong relationship with the characteristics of the benthic habitats selected by the demersal fish. Although, in a previous study using a 300 kHz echo-sounder, it was possible to detect sand with hard surface underneath (Huang et al., 2012). The potential of using SBES backscatter data with lower frequencies is a question that can be addressed in a future project.

All the species considered in this study had at least a 10 percent of presence in three study sites with a different set of environmental conditions including depth gradient, and shift of species from more tropicals in Mandu and a combination of temperate and tropical in Gnaraloo. Consequently, all the species included in this study can be considered generalistic at the scale of the study. They are all also carnivorous roaming species feeding on demersal animals (Carpenter and Niem, 2001, Sommer, 1996, Aydın, 2011, Compagno, 1984, Parrish, 1987a). Therefore, it is not surprising that broad-scale depth derivatives were usually more important in the construction of their models.

6.1.3. Value of historical water column backscatter data in assessing demersal fish distribution and abundance

The total abundance and relative biomass of all species recorded by the stereo-BRUVS were not well modelled using terrain variables, which is expected as different species would have specific habitat requirements (Moore et al., 2010). However, it was anticipated that the addition of water column data in the form of acoustic biomass could increase the variance explained by the model, in particular, for the relative biomass. However, the lack of relationship between the two data sets as found in the correlations

analysis and later confirmed by the Random Forest was possibly related to the time difference between the two datasets.

Coral reef fishes can be highly mobile; their movements can respond to the diel cycle, seasonal migrations and ontogenic shifts of habitats. The acoustic data use in the Random Forest was mostly collected at night in contrary to the stereo-BRUVS which were sampled during the day. The difference in fish behaviour between day and night have been largely reported (Harvey et al., 2012, Myers et al., 2016, Nagelkerken et al., 2000). Differences in the habitats that some species occupy during the day and night can contribute to observing a different spatial distribution of the species between day and night (O'Driscoll et al., 2009, Lawson and Rose, 1999, Fréon et al., 1993). Differences in the season and phase of the moon cycle can also have contributed to observed a different pattern of distribution in the two data sets (Fabi and Sala, 2002).

Interestingly, an analysis at a broad-scale showed a similar pattern of association between the ARA-phi grain size estimated using seafloor backscatter and the biomass recorded by the stereo-BRUVS and the acoustics. In particular, two classes of sediment grain size appear to have higher values of biomass for the 2006, and 2008 acoustic data and also for the stereo-BRUVS, considering only the sampling points with both stereo-BRUVS and acoustic data. Sediment grain size can act as an indirect surrogate of the distribution of certain species of fish, for example by affecting the size and distribution of the infauna on which many species of carnivorous fishes feed on (Platell and Potter, 2001, McArthur et al., 2010).

The identification of a broad-scale pattern of distribution of the fish biomass with the sediment ARA-phi layer indicates that broad-scale patterns could be persistent over time unless an extreme event occurred. These broad-scale patterns might be particularly useful to understand the distribution of species with wide niches while it might be less relevant for sedentary species. Further exploration of this relationship is needed, but it is an encouraging result that shows the possibility of detecting broad-scale drivers of fish biomass using opportunistic data.

6.1.4. Temporal and spatial variation of abundance of demersal fish using SBES water column data and stereo-BRUVS data

A significant correlation was found between the acoustic data and the stereo-BRUVS data collected in two small areas, one located in CS WA and the second one in a north section of the NMP. However, the relationship was not always between the same acoustic and stereo-BRUVS variables.

6.1.4.1. Cockburn Sound

In the CS area, the highest correlation was found between the $NASC_{BRUV-mean}$ no schools and the relative biomass from the stereo-BRUVS. Demersal stereo-BRUVS such as the ones used in the present study are designed to sample demersal and semi-demersal fish, however, some pelagic species are commonly observed (Cappo et al., 2004). A recent study using pelagic stereo-BRUVS showed significant differences between the assemblages of fish at different depths (Santana-Garcon et al., 2014), in particular, some pelagic schooling species were only present in the superficial deployments. It is possible that the species present in the water column during the acoustic sampling were not observed with the stereo-BRUVS. Therefore, the exclusion of the schools from the $NASC_{BRUV-mean}$ increased the correlation between the two biomasses.

The correlation between the number of acoustic targets and relative biomass from the stereo-BRUVS was very strong with an almost linear relationship between them. These results suggest a consistent size of the fish sampled in CS. The length measurements of the stereo-BRUVS confirmed these results with less variation in the length distribution of the fish in CS compared to the NMP area. CS is a temperate embayment with small patches of limestone reef and seagrass beds, which supports a variety of species of fish (Wakefield and Johnston, 2009), however, it is less diverse than the tropical area of NMP. The relationship between the number of acoustic targets and the relative biomass of the stereo-BRUVS was stronger when the rays, which spend most of the time very close to the bottom (Thrush et al., 1991), were excluded from the relative biomass.

6.1.4.2. Ningaloo Marine Park

No correlation was found between the $NASC_{BRUV-mean}$ and relative biomass from the stereo-BRUVS, and the exclusion of the schools did not increase the correlation, unlike the CS area. Only a few schools of fish were observed in the acoustic data from the NMP data, and the exclusion of them did not make a difference in the general pattern of distribution of the depth-stratified NASC. Although schooling species are not uncommon in coral reef areas (Campanella and Taylor, 2016), in a highly diverse ecosystem, they might not represent a significant portion of the biomass. Something similar was observed in another coral reef area using acoustics and visual census, where schools of fish were uncommon, therefore excluded from their analysis (Zenone et al., 2017).

In contrary to what we expected, the best correlation between the stereo-BRUVS and the acoustics was found between the relative abundance of the stereo-BRUVS and the $NASC_{BRUV-mean}$, but considering only

the superficial layers of the water column. A possible explanation for this correlation would be that the high productivity occurring at the surface, could attract midwater species such as *Sphyraena obtusata* and pelagic species including *Sarda orientalis*. These two species were present in the sampling points where higher abundance in the stereo-BRUVS and high levels of depth-stratified NASC were recorded. However, without further replication of experiments like this, it is hard to draw any conclusive findings.

The high variability of the system as observed in the temporal experiment could be responsible for the weak correlation between the demersal $NASC_{BRUV-mean}$ and stereo-BRUVS data. The two dataset were collected in consecutive days in an attempt for minimising the variation. However, as the temporal experiment showed, the biomass can variate significantly in consecutive days. High variability in the assemblage of reef fishes, particularly in sandy bottoms, has been reported before in consecutive sampling days (McIlwain et al., 2011). We suggest that better results could be obtained if the sampling of both techniques were carried out the same day as close as possible in time.

6.1.4.3. The portion of the fish sampled by acoustics vs. stereo-BRUVS

In the present study, the 'dB difference' method developed by (Ballon et al., 2011) was used to exclude the zooplankton from the acoustic analysis, and theoretically, only fish with swim bladders were included. Although the majority of the species registered with the stereo-BRUVS had a swim bladder, the exclusion of the species without swim bladder from the stereo-BRUVS data, could potentially increase the relationship between the two data sets.

The Acoustic Dead Zone (ADZ) is an area close to the bottom which is not sampled during the acoustic survey, the size of the ADZ varied depending on the depth, pulse duration, and speed of the sound in water (Ona and Mitson, 1996). Therefore, the possibility of sampling species near the seafloor using acoustics will be limited by the ADZ. Also, the acoustic analysis in this study excluded 0.5 m above the seafloor to avoid the integration of seafloor elements or parts of the reef. The exclusion of this area could also have an impact on the number of targets that can be detected for the acoustics in the demersal layer.

6.2. CONCLUSIONS

Species distribution models of demersal species of fish with wide niches which distribution might be influenced by broad-scale variables could be well modelled using SBES data with comparable results to the ones obtained with MBES data. This can reduce the cost of producing useful information for conservation and management. The performance of species distribution models using MBES seafloor

backscatter can variate depending on the species and specific sampling site. However, the MBES seafloor backscatter can be particularly valuable in the models of roaming species associated with rocky bottoms. The use of historical stereo-BRUVS and SBES data, separated by a three years gap might not be suitable to understand fine-scale patterns of distribution of fish biomass. Though, broad-scale patterns could be found which could be relevant for roaming species.

The spatial experiments conducted in two small areas, one in CS and the other in a northern section of the NMP showed significant correlations between the acoustics and stereo-BRUVS. These results indicate that similar spatial distributions patterns of fish biomass were observed with both the acoustic and stereo-BRUVS. Therefore, the combination of the two techniques would allow the transformation of the point samples of the stereo-BRUVS into maps of biomass in areas covered with the echo-sounder. However, the possibility of combining these two methods in a highly variable ecosystem such as coral reef areas could require a simultaneous data collection and possibly the use of both demersal and pelagic stereo-BRUVS.

References

- ALLEN, G. R. 1985. *Snappers of the world: an annotated and illustrated catalogue of lutjanid species known to date*.
- ANDERSON, T. J., SYMS, C., ROBERTS, D. A. & HOWARD, D. F. 2009. Multi-scale fish-habitat associations and the use of habitat surrogates to predict the organisation and abundance of deep-water fish assemblages. *Journal of Experimental Marine Biology and Ecology*, 379, 34-42.
- ANDREFOUET, S. & RIEGL, B. 2004. Remote sensing: a key tool for interdisciplinary assessment of coral reef processes. *Coral Reefs*, 23, 1-4.
- ARUN, P. V. 2013. A comparative analysis of different DEM interpolation methods. *The Egyptian Journal of Remote Sensing and Space Science*, 16, 133-139.
- ASA, E., SAAFI, M., MEMBAH, J. & BILLA, A. 2012. Comparison of Linear and Nonlinear Kriging Methods for Characterization and Interpolation of Soil Data. *Journal of Computing in Civil Engineering*, 26, 11-18.
- AYDIN, M. 2011. Growth, reproduction and diet of pufferfish (*Lagocephalus sceleratus* Gmelin, 1789) from Turkey's Mediterranean sea coast. *Turkish Journal of Fisheries and Aquatic Sciences*, 11.
- BACH, L. L., SAUNDERS, B. J., NEWMAN, S. J., HOLMES, T. H. & HARVEY, E. S. 2019. Cross and long-shore variations in reef fish assemblage structure and implications for biodiversity management. *Estuarine Coastal and Shelf Science*, 218, 246-257.
- BAILEY, D. M. & PRIEDE, I. G. 2002. Predicting fish behaviour in response to abyssal food falls. *Marine Biology*, 141, 831-840.
- BALLON, M., BERTRAND, A., LÉBOURGÈS-DHAUSSY, A., GUTIERREZ, M., AYON, P., GRADOS, D. & GERLOTTO, F. 2011. Is there enough zooplankton to feed forage fish populations off Peru? An acoustic (positive) answer. *Progress in Oceanography*, 91, 360-381.
- BARTHOLOMAE, A., HOLLER, P., SCHROTTKE, K. & KUBICKI, A. 2011. Acoustic habitat mapping in the German Wadden Sea - Comparison of hydro-acoustic devices. *Journal of Coastal Research*, 1-5.
- BECKER, J. J., SANDWELL, D. T., SMITH, W. H. F., BRAUD, J., BINDER, B., DEPNER, J., FABRE, D., FACTOR, J., INGALLS, S., KIM, S. H., LADNER, R., MARKS, K., NELSON, S., PHARAOH, A., TRIMMER, R., VON ROSENBERG, J., WALLACE, G. & WEATHERALL, P. 2009. Global Bathymetry and Elevation Data at 30 Arc Seconds Resolution: SRTM30_PLUS. *Marine Geodesy*, 32, 355-371.
- BELLO-PINEDA, J. & HERNÁNDEZ-STEFANONI, J. L. 2007. Comparing the performance of two spatial interpolation methods for creating a digital bathymetric model of the Yucatan submerged platform. *Pan-American Journal of Aquatic Sciences*, 2, 247-254.
- BOHNSACK, J. A. & BANNEROT, S. P. 1986. A stationary visual census technique for quantitatively assessing community structure of coral reef fishes.
- BOSCOIANU, M., MOLDER, C., ARHIP, J., STANCIU, M. I. & VIZITIU, I. C. 2008. *Feature sets based on fuzzy reasoning for automatic sea floor characterization*.
- BOSWELL, K. M., WELLS, R. J. D., COWAN, J. H., JR. & WILSON, C. A. 2010. Biomass, density, and size distribution of fishes associated with a large-scale artificial reef complex in the Gulf of Mexico. *Bulletin of Marine Science*, 86, 879-889.
- BOUCHET, P., PHILLIPS, C., HUANG, Z., MEEUWIG, J., FOSTER, S. & PRZESLAWSKI, R. 2018. Comparative assessment of pelagic sampling methods used in marine monitoring.
- BOUCHET, P. J. & MEEUWIG, J. J. 2015. Drifting baited stereo-videography: a novel sampling tool for surveying pelagic wildlife in offshore marine reserves. *Ecosphere*, 6.
- BOUTROS, N., SHORTIS, M. R. & HARVEY, E. S. 2015. A comparison of calibration methods and system configurations of underwater stereo-video systems for applications in marine ecology. *Limnology and Oceanography-Methods*, 13, 224-236.

- BREIMAN, L. 2001. Random forests. *Machine learning*, 45, 5-32.
- BROOKE, B., NICHOL, S., HUGHES, M., MCARTHUR, M., ANDERSON, T., PRZESLAWSKI, R., SIWABESSY, J., HEYWARD, A., BATTERSHILL, C. & COLQUHOUN, J. 2009. Carnarvon Shelf Survey Post-Survey Report. *Geoscience Australia Record*, 2.
- BROWN, C. J., SAMEOTO, J. A. & SMITH, S. J. 2012. Multiple methods, maps, and management applications: Purpose made seafloor maps in support of ocean management. *Journal of Sea Research*, 72, 1-13.
- BROWN, C. J., SMITH, S. J., LAWTON, P. & ANDERSON, J. T. 2011. Benthic habitat mapping: A review of progress towards improved understanding of the spatial ecology of the seafloor using acoustic techniques. *Estuarine Coastal and Shelf Science*, 92, 502-520.
- BUHMANN, M. D. 2003. *Radial basis functions: theory and implementations*, Cambridge university press.
- CAMPANELLA, F. & TAYLOR, J. C. 2016. Investigating acoustic diversity of fish aggregations in coral reef ecosystems from multifrequency fishery sonar surveys. *Fisheries Research*, 181, 63-76.
- CAPPO, M., HARVEY, E., MALCOLM, H. & SPEARE, P. 2003. Potential of video techniques to monitor diversity, abundance and size of fish in studies of marine protected areas. *Aquatic Protected Areas-what works best and how do we know*, 455-464.
- CAPPO, M., HARVEY, E. & SHORTIS, M. Counting and measuring fish with baited video techniques-an overview. Australian Society for Fish Biology Workshop Proceedings, 2006. 101-114.
- CAPPO, M., SPEARE, P. & DE'ATH, G. 2004. Comparison of baited remote underwater video stations (BRUVS) and prawn (shrimp) trawls for assessments of fish biodiversity in inter-reefal areas of the Great Barrier Reef Marine Park. *Journal of Experimental Marine Biology and Ecology*, 302, 123-152.
- CARPENTER, K. E. & NIEM, V. H. 2001. *FAO species identification guide for fishery purposes. The living marine resources of the Western Central Pacific. Volume 6. Bony fishes part 4 (Labridae to Latimeriidae), estuarine crocodiles, sea turtles, sea snakes and marine mammals*, FAO Library.
- CATLIN, J. & JONES, R. 2010. Whale shark tourism at Ningaloo Marine Park: A longitudinal study of wildlife tourism. *Tourism Management*, 31, 386-394.
- COCKBURN SOUND MANAGEMENT COUNCIL 2004. Benthic Habitat mapping of the Eastern Shelf of Cockburn Sound.
- COETZEE, J. 2000. Use of a shoal analysis and patch estimation system (SHAPES) to characterise sardine schools. *Aquatic Living Resources*, 13, 1-10.
- COLE, A. J., PRATCHETT, M. S. & JONES, G. P. 2008. Diversity and functional importance of coral-feeding fishes on tropical coral reefs. *Fish and Fisheries*, 9, 286-307.
- COLLETTE, B. B. & NAUEN, C. E. 1983. *FAO species catalogue. Volume 2. Scombrids of the world. An annotated and illustrated catalogue of tunas, mackerels, bonitos and related species known to date*.
- COLQUHOUN, J., HEYWARD, A., REES, M., TWIGGS, E., FITZPATRICK, B., MCALLISTER, F. & SPEARE, P. 2007. Ningaloo Reef Marine Park deepwater benthic biodiversity survey. *Perth, Western Australia*.
- COLTON, M. A. & SWEARER, S. E. 2010. A comparison of two survey methods: differences between underwater visual census and baited remote underwater video. *Marine Ecology Progress Series*, 400, 19-36.
- COMPAGNO, L. J. 1984. *Sharks of the world: an annotated and illustrated catalogue of shark species known to date*.
- COSTA, B., TAYLOR, J. C., KRACKER, L., BATTISTA, T. & PITTMAN, S. 2014. Mapping Reef Fish and the Seascape: Using Acoustics and Spatial Modeling to Guide Coastal Management. *Plos One*, 9.
- CRESSIE, N. A. 1993. *Statistics for spatial data*, Wiley Online Library.

- CURTARELLI, M., LEAO, J., OGASHAWARA, I., LORENZZETTI, J. & STECH, J. 2015. Assessment of Spatial Interpolation Methods to Map the Bathymetry of an Amazonian Hydroelectric Reservoir to Aid in Decision Making for Water Management. *Isprs International Journal of Geo-Information*, 4, 220-235.
- DAGNEAUX, D., BOSCHETTI, F., BABCOCK, R. & VANDERKLIFT, M. 2009. Detecting general patterns in fish movement from the analysis of fish tagging data. *18th World Imacs Congress and Modsim09 International Congress on Modelling and Simulation: Interfacing Modelling and Simulation with Mathematical and Computational Sciences*, 2094-2100.
- DAVISON, P. C., KOSLOW, J. A. & KLOSER, R. J. 2015. Acoustic biomass estimation of mesopelagic fish: backscattering from individuals, populations, and communities. *ICES Journal of Marine Science*, 72, 1413-1424.
- DE ROBERTIS, A. & HIGGINBOTTOM, I. 2007. A post-processing technique to estimate the signal-to-noise ratio and remove echosounder background noise. *ICES Journal of Marine Science*, 64, 1282-1291.
- DEMESTRE, M., SANCHEZ, P. & ABELLO, P. 2000. Demersal fish assemblages and habitat characteristics on the continental shelf and upper slope of the north-western Mediterranean. *Journal of the Marine Biological Association of the United Kingdom*, 80, 981-988.
- DENG, Y., WILSON, J. P. & BAUER, B. O. 2007. DEM resolution dependencies of terrain attributes across a landscape. *International Journal of Geographical Information Science*, 21, 187-213.
- DEPCZYNSKI, M. M., HEYWARD, A. A., RADFORD, B. B., BABCOCK, R. R., HAYWOOD, M. M. & THOMSON, D. D. 2009. Stock Assessment of targeted invertebrates at Ningaloo Reef. Final Report for WAMSI Node 3 Project 3.1. 3.
- DEVICTOR, V., JULLIARD, R. & JIGUET, F. 2008. Distribution of specialist and generalist species along spatial gradients of habitat disturbance and fragmentation. *Oikos*, 117, 507-514.
- DOLAN, M. F. J. & LUCIEER, V. L. 2014. Variation and Uncertainty in Bathymetric Slope Calculations Using Geographic Information Systems. *Marine Geodesy*, 37, 187-219.
- DORENBOSCH, M., GROL, M. G. G., CHRISTIANEN, M. J. A., NAGELKERKEN, I. & VAN DER VELDE, G. 2005. Indo-Pacific seagrass beds and mangroves contribute to fish density coral and diversity on adjacent reefs. *Marine Ecology Progress Series*, 302, 63-76.
- ELLIS, D. M. & DEMARTINI, E. E. 1995. Evaluation of a video camera technique for indexing abundances of juvenile pink snapper, *Pristimomoides filamentosus*, and other Hawaiian insular shelf fishes. *Fishery Bulletin*, 93, 67-77.
- ERDOGAN, S. 2009. A comparison of interpolation methods for producing digital elevation models at the field scale. *Earth Surface Processes and Landforms*, 34, 366-376.
- FABI, G. & SALA, A. 2002. An assessment of biomass and diel activity of fish at an artificial reef (Adriatic sea) using a stationary hydroacoustic technique. *ICES Journal of Marine Science*, 59, 411-420.
- FAIRCLOUGH, D., POTTER, I., LEK, E., BIVOLTSIS, A. & BABCOCK, R. 2011. The fish communities and main fish populations of the Jurien Bay Marine Park.
- FERGUSON, A. M., HARVEY, E. S., TAYLOR, M. D. & KNOTT, N. A. 2013. A herbivore knows its patch: luderick, *Girella tricuspidata*, exhibit strong site fidelity on shallow subtidal reefs in a temperate marine park. *PloS one*, 8, e65838.
- FERRINI, V. L. & FLOOD, R. D. 2006. The effects of fine-scale surface roughness and grain size on 300 kHz multibeam backscatter intensity in sandy marine sedimentary environments. *Marine Geology*, 228, 153-172.
- FITZPATRICK, B. M., HARVEY, E. S., HEYWARD, A. J., TWIGGS, E. J. & COLQUHOUN, J. 2012. Habitat Specialization in Tropical Continental Shelf Demersal Fish Assemblages. *Plos One*, 7.

- FONSECA, L., BROWN, C., CALDER, B., MAYER, L. & RZHANOV, Y. 2009. Angular range analysis of acoustic themes from Stanton Banks Ireland: A link between visual interpretation and multibeam echosounder angular signatures. *Applied Acoustics*, 70, 1298-1304.
- FONSECA, L. & MAYER, L. 2007. Remote estimation of surficial seafloor properties through the application Angular Range Analysis to multibeam sonar data. *Marine Geophysical Researches*, 28, 119-126.
- FOSTER-SMITH, R. L. & SOTHERAN, I. S. 2003. Mapping marine benthic biotopes using acoustic ground discrimination systems. *International Journal of Remote Sensing*, 24, 2761-2784.
- FRANKLIN, J., WEJNERT, K. E., HATHAWAY, S. A., ROCHESTER, C. J. & FISHER, R. N. 2009. Effect of species rarity on the accuracy of species distribution models for reptiles and amphibians in southern California. *Diversity and Distributions*, 15, 167-177.
- FREITAS, R., RODRIGUES, A. M., MORRIS, E., LUCAS PEREZ-LLORENS, J. & QUINTINO, V. 2008. Single-beam acoustic ground discrimination of shallow water habitats: 50 kHz or 200 kHz frequency, survey? *Estuarine Coastal and Shelf Science*, 78, 613-622.
- FRÉON, P., GERLOTTO, F. & MISUND, O. A. Consequences of fish behaviour for stock assessment. ICES Marine Science Symposia, 1993. 190-195.
- FRIEDLANDER, A. M., BROWN, E. K., JOKIEL, P. L., SMITH, W. R. & RODGERS, K. S. 2003. Effects of habitat, wave exposure, and marine protected area status on coral reef fish assemblages in the Hawaiian archipelago. *Coral Reefs*, 22, 291-305.
- FRIEDMAN, A., PIZARRO, O., WILLIAMS, S. B. & JOHNSON-ROBERSON, M. 2012. Multi-Scale Measures of Rugosity, Slope and Aspect from Benthic Stereo Image Reconstructions. *Plos One*, 7.
- FRIEDMAN, J. H. 2001. Greedy function approximation: a gradient boosting machine. *Annals of statistics*, 1189-1232.
- FROESE, R. & PAULY, D. 2012. FishBase World Wide Web electronic publication, Version (09/2010). URL [Www Fishbase Org](http://www.fishbase.org) Accessed, 1.
- FRY, G. C., BREWER, D. T. & VENABLES, W. N. 2006. Vulnerability of deepwater demersal fishes to commercial fishing: Evidence from a study around a tropical volcanic seamount in Papua New Guinea. *Fisheries Research*, 81, 126-141.
- GALAUDUK, R., HALFORD, A. R., RADFORD, B. T., MOORE, C. H. & HARVEY, E. S. 2017a. Regional-scale environmental drivers of highly endemic temperate fish communities located within a climate change hotspot. *Diversity and Distributions*, 23, 1256-1267.
- GALAUDUK, R., RADFORD, B. T., SAUNDERS, B. J., NEWMAN, S. J. & HARVEY, E. S. 2017b. Characterizing ontogenetic habitat shifts in marine fishes: advancing nascent methods for marine spatial management. *Ecological Applications*, 27, 1776-1788.
- GARCIA-ALEGRE, A., SANCHEZ, F., GOMEZ-BALLESTEROS, M., HINZ, H., SERRANO, A. & PARRA, S. 2014. Modelling and mapping the local distribution of representative species on the Le Danois Bank, El Cachucho Marine Protected Area (Cantabrian Sea). *Deep-Sea Research Part II-Topical Studies in Oceanography*, 106, 151-164.
- GAZZANI, F. & MARINOVA, D. 2007. *Using Choice Modelling to Account for Biodiversity Conservation: Non-use Value for Ningaloo Reef*.
- GLENN, J., TONINA, D., MOREHEAD, M. D., FIEDLER, F. & BENJANKAR, R. 2016. Effect of transect location, transect spacing and interpolation methods on river bathymetry accuracy. *Earth Surface Processes and Landforms*, 41, 1185-1198.
- GODLEWSKA, M., COLON, M., JOZWIK, A. & GUILLARD, J. 2011. How pulse lengths impact fish stock estimations during hydroacoustic measurements at 70 kHz. *Aquatic Living Resources*, 24, 71-78.
- GODO, O. R. 2009. *Technology Answers to the Requirements Set by the Ecosystem Approach*.
- GOLDMAN, B., TALBOT, F. H., JONES, O. & ENDEAN, R. 1976. Aspects of the ecology of coral reef fishes. *Biology and geology of coral reefs*, 3, 125-154.

- GRATWICKE, B. & SPEIGHT, M. R. 2005. Effects of habitat complexity on Caribbean marine fish assemblages. *Marine Ecology Progress Series*, 292, 301-310.
- GREEN, A. L., MAYPA, A. P., ALMANY, G. R., RHODES, K. L., WEEKS, R., ABESAMIS, R. A., GLEASON, M. G., MUMBY, P. J. & WHITE, A. T. 2015. Larval dispersal and movement patterns of coral reef fishes, and implications for marine reserve network design. *Biological Reviews*, 90, 1215-1247.
- GUILLARD, J. & VERGES, C. 2007. The repeatability of fish biomass and size distribution estimates obtained by hydroacoustic surveys using various sampling strategies and statistical analyses. *International Review of Hydrobiology*, 92, 605-617.
- GUTTERIDGE, A., BENNETT, M., HUVENEERS, C. & TIBBETTS, I. 2011. Assessing the overlap between the diet of a coastal shark and the surrounding prey communities in a sub-tropical embayment. *Journal of Fish Biology*, 78, 1405-1422.
- HAGGARTY, D. & YAMANAKA, L. 2018. Evaluating Rockfish Conservation Areas in southern British Columbia, Canada using a Random Forest model of rocky reef habitat. *Estuarine, Coastal and Shelf Science*, 208, 191-204.
- HALPERN, B. S. 2003. The impact of marine reserves: do reserves work and does reserve size matter? *Ecological Applications*, 13, 117-137.
- HARASTI, D., MALCOLM, H., GALLEN, C., COLEMAN, M. A., JORDAN, A. & KNOTT, N. A. 2015. Appropriate set times to represent patterns of rocky reef fishes using baited video. *Journal of Experimental Marine Biology and Ecology*, 463, 173-180.
- HARDINGE, J., HARVEY, E. S., SAUNDERS, B. J. & NEWMAN, S. J. 2013. A little bait goes a long way: The influence of bait quantity on a temperate fish assemblage sampled using stereo-BRUVs. *Journal of Experimental Marine Biology and Ecology*, 449, 250-260.
- HARVEY, E., CAPPO, M., SHORTIS, M., ROBSON, S., BUCHANAN, J. & SPEARE, P. 2003. The accuracy and precision of underwater measurements of length and maximum body depth of southern bluefin tuna (*Thunnus maccoyii*) with a stereo-video camera system. *Fisheries Research*, 63, 315-326.
- HARVEY, E., FLETCHER, D. & SHORTIS, M. 2002. Estimation of reef fish length by divers and by stereo-video - A first comparison of the accuracy and precision in the field on living fish under operational conditions. *Fisheries Research*, 57, 255-265.
- HARVEY, E. & SHORTIS, M. 1995. A system for stereo-video measurement of sub-tidal organisms. *Marine Technology Society Journal*, 29, 10-22.
- HARVEY, E. S., BUTLER, J. J., MCLEAN, D. L. & SHAND, J. 2012. Contrasting habitat use of diurnal and nocturnal fish assemblages in temperate Western Australia. *Journal of Experimental Marine Biology and Ecology*, 426, 78-86.
- HARVEY, E. S., CAPPO, M., BUTLER, J. J., HALL, N. & KENDRICK, G. A. 2007. Bait attraction affects the performance of remote underwater video stations in assessment of demersal fish community structure. *Marine Ecology Progress Series*, 350, 245-254.
- HASAN, R. C., IERODIACONOU, D. & LAURENSEN, L. 2012a. Combining angular response classification and backscatter imagery segmentation for benthic biological habitat mapping. *Estuarine Coastal and Shelf Science*, 97, 1-9.
- HASAN, R. C., IERODIACONOU, D., LAURENSEN, L. & SCHIMEL, A. 2014. Integrating Multibeam Backscatter Angular Response, Mosaic and Bathymetry Data for Benthic Habitat Mapping. *Plos One*, 9.
- HASAN, R. C., IERODIACONOU, D. & MONK, J. 2012b. Evaluation of Four Supervised Learning Methods for Benthic Habitat Mapping Using Backscatter from Multi-Beam Sonar. *Remote Sensing*, 4, 3427-3443.
- HELL, B. & JAKOBSSON, M. 2011. Gridding heterogeneous bathymetric data sets with stacked continuous curvature splines in tension. *Marine Geophysical Research*, 32, 493-501.
- HENGL, T. 2009. *A practical guide to geostatistical mapping*, Hengl.

- HIJMANS, R. J. 2016. raster: Geographic Data Analysis and Modeling. R package version 2.5-8 ed.
- HILL, N. A., BARRETT, N., LAWRENCE, E., HULLS, J., DAMBACHER, J. M., NICHOL, S., WILLIAMS, A. & HAYES, K. R. 2014a. Quantifying Fish Assemblages in Large, Offshore Marine Protected Areas: An Australian Case Study. *Plos One*, 9.
- HILL, N. A., LUCIEER, V., BARRETT, N. S., ANDERSON, T. J. & WILLIAMS, S. B. 2014b. Filling the gaps: Predicting the distribution of temperate reef biota using high resolution biological and acoustic data. *Estuarine Coastal and Shelf Science*, 147, 137-147.
- HIXON, M. 1991. Tropical and temperate reef fishes: comparison of community structures. Academic Press: New York.
- HJELLVIK, V., GODØ, O. R. & TJØSTHEIM, D. 2004. Diurnal variation in acoustic densities: why do we see less in the dark? *Canadian Journal of Fisheries and Aquatic Sciences*, 61, 2237-2254.
- HOLMES, K. W., VAN NIEL, K. P., RADFORD, B., KENDRICK, G. A. & GROVE, S. L. 2008. Modelling distribution of marine benthos from hydroacoustics and underwater video. *Continental Shelf Research*, 28, 1800-1810.
- HOLMES, T. H., WILSON, S. K., TRAVERS, M. J., LANGLOIS, T. J., EVANS, R. D., MOORE, G. I., DOUGLAS, R. A., SHEDRAWI, G., HARVEY, E. S. & HICKEY, K. 2013. A comparison of visual-and stereo-video based fish community assessment methods in tropical and temperate marine waters of Western Australia. *Limnology and Oceanography: Methods*, 11, 337-350.
- HORN, B. K. 1981. Hill shading and the reflectance map. *Proceedings of the IEEE*, 69, 14-47.
- HOSMER, D. W., LEMESHOW, S. & STURDIVANT, R. X. 2013. *Applied logistic regression*, John Wiley & Sons.
- HOSMER JR, D. W., LEMESHOW, S. & STURDIVANT, R. X. 2013. *Applied logistic regression*, John Wiley & Sons.
- HOWARD, R. K. 1989. The structure of a nearshore fish community of Western-Australia - diel patterns and the habitat role of limestone reefs. *Environmental Biology of Fishes*, 24, 93-104.
- HUANG, Z., NICHOL, S. L., SIWABESSY, J. P., DANIELL, J. & BROOKE, B. P. 2012. Predictive modelling of seabed sediment parameters using multibeam acoustic data: a case study on the Carnarvon Shelf, Western Australia. *International Journal of Geographical Information Science*, 26, 283-307.
- HUGHES, T. P., BAIRD, A. H., BELLWOOD, D. R., CARD, M., CONNOLLY, S. R., FOLKE, C., GROSBURG, R., HOEGH-GULDBERG, O., JACKSON, J. B. C., KLEYPAS, J., LOUGH, J. M., MARSHALL, P., NYSTRÖM, M., PALUMBI, S. R., PANDOLFI, J. M., ROSEN, B. & ROUGHGARDEN, J. 2003. Climate Change, Human Impacts, and the Resilience of Coral Reefs. *Science*, 301, 929-933.
- HUXLEY, J. S. 1950. Relative growth and form transformation. *Proceedings of the Royal Society of London. Series B-Biological Sciences*, 137, 465-469.
- ICES 2015. Manual for International Pelagic Surveys (IPS). Series of ICES Survey Protocols SISP 9–IPS.
- IERODIACONU, D., LAURENSEN, L., BURQ, S. & RESTON, M. 2007. Marine benthic habitat mapping using Multibeam data, georeferenced video and image classification techniques in Victoria, Australia. *Journal of Spatial Science*, 52, 93-104.
- IERODIACONU, D., MONK, J., RATTRAY, A., LAURENSEN, L. & VERSACE, V. L. 2011. Comparison of automated classification techniques for predicting benthic biological communities using hydroacoustics and video observations. *Continental Shelf Research*, 31, S28-S38.
- INNANGI, S., BARRA, M., DI MARTINO, G., PARNUM, I. M., TONIELLI, R. & MAZZOLA, S. 2015. Reson SeaBat 8125 backscatter data as a tool for seabed characterization (Central Mediterranean, Southern Italy): Results from different processing approaches. *Applied Acoustics*, 87, 109-122.
- IRIGOYEN, A. J., GALVÁN, D. E., VENERUS, L. A. & PARMA, A. M. 2013. Variability in Abundance of Temperate Reef Fishes Estimated by Visual Census. *PLOS ONE*, 8, e61072.

- JACKSON, D. R., WINEBRENNER, D. P. & ISHIMARU, A. 1986. Application of the composite roughness model to high-frequency bottom backscattering. *The Journal of the Acoustical Society of America*, 79, 1410-1422.
- JARNEVICH, C. S., STOHLGREN, T. J., KUMAR, S., MORISETTE, J. T. & HOLCOMBE, T. R. 2015. Caveats for correlative species distribution modeling. *Ecological Informatics*, 29, 6-15.
- JONES, D. O. B. & BREWER, M. E. 2012. Response of megabenthic assemblages to different scales of habitat heterogeneity on the Mauritanian slope. *Deep-Sea Research Part I-Oceanographic Research Papers*, 67, 98-110.
- KAILOLA, P., WILLIAMS, M., STEWART, P., REICHEL, R., MCNEE, A. & GRIEVE, C. 1993. Australian fisheries resources. Bureau of resource sciences, department of primary industries and energy. *Fisheries Research and Development Corporation, Canberra, Australia*.
- KALOGIROU, S. 2013. Ecological characteristics of the invasive pufferfish *Lagocephalus sceleratus* (Gmelin, 1789) in the eastern Mediterranean Sea—a case study from Rhodes. *Mediterranean Marine Science*, 14, 251-260.
- KERRY, R. & OLIVER, M. A. 2007. Determining the effect of asymmetric data on the variogram. I. Underlying asymmetry. *Computers & Geosciences*, 33, 1212-1232.
- KLOSER, R. J., PENROSE, J. D. & BUTLER, A. J. 2010. Multi-beam backscatter measurements used to infer seabed habitats. *Continental Shelf Research*, 30, 1772-1782.
- KLOSER, R. J., RYAN, T., SAKOV, P., WILLIAMS, A. & KOSLOW, J. A. 2002. Species identification in deep water using multiple acoustic frequencies. *Canadian Journal of Fisheries and Aquatic Sciences*, 59, 1065-1077.
- KLOSER, R. J., RYAN, T. E., TUCK, G. N. & GEEN, G. 2016. Influence on management advice of fishers acoustics-10 year review of blue grenadier monitoring. *Fisheries Research*, 178, 82-92.
- KNUDBY, A., BRENNING, A. & LEDREW, E. 2010. New approaches to modelling fish-habitat relationships. *Ecological Modelling*, 221, 503-511.
- KOSLOW, J. A. 2009. The role of acoustics in ecosystem-based fishery management. *Ices Journal of Marine Science*, 66, 966-973.
- LAWSON, G. L. & ROSE, G. A. 1999. The importance of detectability to acoustic surveys of semi-demersal fish. *ICES Journal of Marine Science*, 56, 370-380.
- LECOURS, V., BROWN, C. J., DEVILLERS, R., LUCIEER, V. L. & EDINGER, E. N. 2016. Comparing Selections of Environmental Variables for Ecological Studies: A Focus on Terrain Attributes. *Plos One*, 11.
- LIAW, A. & WIENER, M. 2002. Classification and regression by randomForest. *R news*, 2, 18-22.
- LOGAN, J. M., YOUNG, M. A., HARVEY, E. S., SCHIMEL, A. C. G. & IERODIACONOU, D. 2017. Combining underwater video methods improves effectiveness of demersal fish assemblage surveys across habitats. *Marine Ecology Progress Series*, 582, 181-200.
- LOWRY, M. & SUTHERS, I. 1998. Home range, activity and distribution patterns of a temperate rocky-reef fish, *Cheilodactylus fuscus*. *Marine Biology*, 132, 569-578.
- LUCIEER, V. & PEDERSON, H. 2008. Linking morphometric characterisation of rocky reef with fine scale lobster movement. *Isprs Journal of Photogrammetry and Remote Sensing*, 63, 496-509.
- LURTON, X. 2002. *An introduction to underwater acoustics: principles and applications*, Springer Science & Business Media.
- MACKIE, M. 2007. Reproductive behavior of the halfmoon grouper, *Epinephelus rivulatus*, at Ningaloo Reef, Western Australia. *Ichthyological Research*, 54, 213-220.
- MANEL, S., WILLIAMS, H. C. & ORMEROD, S. J. 2001. Evaluating presence-absence models in ecology: the need to account for prevalence. *Journal of Applied Ecology*, 38, 921-931.
- MCARTHUR, M. A., BROOKE, B. P., PRZESLAWSKI, R., RYAN, D. A., LUCIEER, V. L., NICHOL, S., MCCALLUM, A. W., MELLIN, C., CRESSWELL, I. D. & RADKE, L. C. 2010. On the use of abiotic surrogates to describe marine benthic biodiversity. *Estuarine Coastal and Shelf Science*, 88, 21-32.

- MCCLANAHAN, T. R., MARNANE, M. J., CINNER, J. E. & KIENE, W. E. 2006. A Comparison of Marine Protected Areas and Alternative Approaches to Coral-Reef Management. *Current Biology*, 16, 1408-1413.
- MCCONNAUGHEY, R. A. & SMITH, K. R. 2000. Associations between flatfish abundance and surficial sediments in the eastern Bering Sea. *Canadian Journal of Fisheries and Aquatic Sciences*, 57, 2410-2419.
- MCILWAIN, J. L., HARVEY, E. S., GROVE, S., SHIELL, G., AL OUF, H. & AL JARDANI, N. 2011. Seasonal changes in a deep-water fish assemblage in response to monsoon-generated upwelling events. *Fisheries Oceanography*, 20, 497-516.
- MELO, C., SANTACRUZ, A., MELO, O. 2012. geospt: An R package for spatial statistics. R package version 1.0-0 ed.: geospt.r-forge.r-project.org/.
- MILLS, G. B. 2015. International hydrographic survey standards. *The International Hydrographic Review*, 75.
- MISA, W. F. X. E., RICHARDS, B. L., DINARDO, G. T., KELLEY, C. D., MORIWAKE, V. N. & DRAZEN, J. C. 2016. Evaluating the effect of soak time on bottomfish abundance and length data from stereo-video surveys. *Journal of Experimental Marine Biology and Ecology*, 479, 20-34.
- MITAS, L. & MITASOVA, H. 1999. Spatial interpolation. *Geographical information systems: principles, techniques, management and applications*, 1, 481-492.
- MITCHELL, T. J. 2016. *Selecting the Right Technology: A Comparative Look at Remote Sensing Bathymetric Technologies for Nearshore Surveys*.
- MONK, J., IERODIACONOU, D., BELLGROVE, A., HARVEY, E. & LAURENSEN, L. 2011. Remotely sensed hydroacoustics and observation data for predicting fish habitat suitability. *Continental Shelf Research*, 31, S17-S27.
- MONK, J., IERODIACONOU, D., HARVEY, E., RATTRAY, A. & VERSACE, V. L. 2012. Are We Predicting the Actual or Apparent Distribution of Temperate Marine Fishes? *Plos One*, 7.
- MONK, J., IERODIACONOU, D., VERSACE, V. L., BELLGROVE, A., HARVEY, E., RATTRAY, A., LAURENSEN, L. & QUINN, G. P. 2010. Habitat suitability for marine fishes using presence-only modelling and multibeam sonar. *Marine Ecology Progress Series*, 420, 157-174.
- MOORE, C. H., HARVEY, E. S. & VAN NIEL, K. 2010. The application of predicted habitat models to investigate the spatial ecology of demersal fish assemblages. *Marine Biology*, 157, 2717-2729.
- MOORE, C. H., VAN NIEL, K. & HARVEY, E. S. 2011. The effect of landscape composition and configuration on the spatial distribution of temperate demersal fish. *Ecography*, 34, 425-435.
- MOORE, J. A. Y., BELLCHAMBERS, L. M., DEPCZYNSKI, M. R., EVANS, R. D., EVANS, S. N., FIELD, S. N., FRIEDMAN, K. J., GILMOUR, J. P., HOLMES, T. H., MIDDLEBROOK, R., RADFORD, B. T., RIDGWAY, T., SHEDRAWI, G., TAYLOR, H., THOMSON, D. P. & WILSON, S. K. 2012. Unprecedented Mass Bleaching and Loss of Coral across 12° of Latitude in Western Australia in 2010–11. *PLOS ONE*, 7, e51807.
- MORA, C., ANDRÉFOUËT, S., COSTELLO, M. J., KRANENBURG, C., ROLLO, A., VERON, J., GASTON, K. J. & MYERS, R. A. 2006. Coral Reefs and the Global Network of Marine Protected Areas. *Science*, 312, 1750-1751.
- MOSKALIK, M., GRABOWIECKI, P., TEGOWSKI, J. & ZULICHOWSKA, M. 2013. Bathymetry and geographical regionalization of Brepollen (Hornsund, Spitsbergen) based on bathymetric profiles interpolations. *Polish Polar Research*, 34, 1-22.
- MPRA, C. 2005. Management plan for the Ningaloo Marine Park and Muiron Islands Marine Management Area 2005–2015. *Perth, Western Australia: Conservation and Land Management and Marine Parks and Reserves Authority, Government of Western Australia*, 111.
- MURPHY, H. M. & JENKINS, G. P. 2010. Observational methods used in marine spatial monitoring of fishes and associated habitats: a review. *Marine and Freshwater Research*, 61, 236-252.

- MYERS, E. M. V., HARVEY, E. S., SAUNDERS, B. J. & TRAVERS, M. J. 2016. Fine-scale patterns in the day, night and crepuscular composition of a temperate reef fish assemblage. *Marine Ecology-an Evolutionary Perspective*, 37, 668-678.
- NAGELKERKEN, I., DORENBOSCH, M., VERBERK, W., DE LA MORINIÈRE, E. C. & VAN DER VELDE, G. 2000. Day-night shifts of fishes between shallow-water biotopes of a Caribbean bay, with emphasis on the nocturnal feeding of Haemulidae and Lutjanidae. *Marine Ecology Progress Series*, 194, 55-64.
- NEWMAN, S. J. & WILLIAMS, D. M. 2001. Spatial and temporal variation in assemblages of Lutjanidae, Lethrinidae and associated fish species among mid-continental shelf reefs in the central Great Barrier Reef. *Marine and Freshwater Research*, 52, 843-851.
- O'DRISCOLL, R. L., GAUTHIER, S. & DEVINE, J. A. 2009. Acoustic estimates of mesopelagic fish: as clear as day and night? *Ices Journal of Marine Science*, 66, 1310-1317.
- ONA, E. 1990. Physiological factors causing natural variations in acoustic target strength of fish. *Journal of the Marine Biological Association of the United Kingdom*, 70, 107-127.
- ONA, E. & MITSON, R. B. 1996. Acoustic sampling and signal processing near the seabed: The deadzone revisited. *Ices Journal of Marine Science*, 53, 677-690.
- PANDIAN, P. K., RUSCOE, J. P., SHIELDS, M., SIDE, J. C., HARRIS, R. E., KERR, S. A. & BULLEN, C. R. 2009. Seabed habitat mapping techniques: an overview of the performance of various systems. *Mediterranean Marine Science*, 10, 29-43.
- PANDOLFI, J. M., CONNOLLY, S. R., MARSHALL, D. J. & COHEN, A. L. 2011. Projecting Coral Reef Futures Under Global Warming and Ocean Acidification. *Science*, 333, 418-422.
- PARKER-STETTER, S. L. 2009. Standard operating procedures for fisheries acoustic surveys in the Great Lakes.
- PARRISH, J. 1987a. The trophic biology of snappers and groupers. In 'Tropical Snappers and Groupers: Biology and Fisheries Management'. (Eds JJ Polovina and S. Ralston.) pp. 405-463. Westview Press: Boulder, CO, USA.
- PARRISH, J. D. 1987b. The trophic biology of snappers and groupers. *Tropical snappers and groupers: biology and fisheries management*, 405-463.
- PEBESMA, E. J. 2004. Multivariable geostatistics in S: the gstat package. *Computers & Geosciences*, 30, 683-691.
- PELLETIER, D., LELEU, K., MOU-THAM, G., GUILLEMOT, N. & CHABANET, P. 2011. Comparison of visual census and high definition video transects for monitoring coral reef fish assemblages. *Fisheries Research*, 107, 84-93.
- PIERDOMENICO, M., GUIDA, V. G., MACELLONI, L., CHIOCCI, F. L., RONA, P. A., SCRANTON, M. I., ASPER, V. & DIERCKX, A. 2015. Sedimentary facies, geomorphic features and habitat distribution at the Hudson Canyon head from AUV multibeam data. *Deep-Sea Research Part II-Topical Studies in Oceanography*, 121, 112-125.
- PITTMAN, S. J. & BROWN, K. A. 2011. Multi-Scale Approach for Predicting Fish Species Distributions across Coral Reef Seascapes. *Plos One*, 6.
- PITTMAN, S. J., CHRISTENSEN, J. D., CALDOW, C., MENZA, C. & MONACO, M. E. 2007. Predictive mapping of fish species richness across shallow-water seascapes in the Caribbean. *Ecological Modelling*, 204, 9-21.
- PLATELL, M. & POTTER, I. 2001. Partitioning of food resources amongst 18 abundant benthic carnivorous fish species in marine waters on the lower west coast of Australia. *Journal of Experimental Marine Biology and Ecology*, 261, 31-54.
- R DEVELOPMENT CORE TEAM 2017. R: A language and environment for statistical computing. Vienna, Austria: R Foundation for Statistical Computing.
- RANDALL, J. E. 1967. Food habits of reef fishes of the West Indies. *Stud. Trop. Oceanogr.*, 5, 665-847.

- REAKA-KUDLA, M. L. 1997. The global biodiversity of coral reefs: a comparison with rain forests. *Biodiversity II: Understanding and protecting our biological resources*, 2, 551.
- REIGHARD, J. 1908. *The photography of aquatic animals in their natural environment*, US Government Printing Office.
- RHOADS, D. C., WARD, R., ALLER, J. & ALLER, R. 2001. *The importance of technology in benthic research and monitoring: Looking back to see ahead*.
- RICHARDS, O. W. & KAVANAGH, A. J. 1945. The analysis of growing form. *Essays in Growth and Form*, 188-230.
- ROUSOU, M., GANIAS, K., KLETOU, D., LOUCAIDES, A. & TSINGANIS, M. 2014. Maturity of the pufferfish *Lagocephalus sceleratus* in the southeastern Mediterranean Sea. *Sexuality and early development in Aquatic organisms*, 1, 35-44.
- RYAN, T. E., DOWNIE, R. A., KLOSER, R. J. & KEITH, G. 2015. Reducing bias due to noise and attenuation in open-ocean echo integration data. *Ices Journal of Marine Science*, 72, 2482-2493.
- SALE, P. F. 2002. *Coral reef fishes: dynamics and diversity in a complex ecosystem*, Academic Press.
- SANCHEZ-CARNERO, N., ACENA, S., RODRIGUEZ-PEREZ, D., COUNAGO, E., FRAILE, P. & FREIRE, J. 2012. Fast and low-cost method for VBES bathymetry generation in coastal areas. *Estuarine Coastal and Shelf Science*, 114, 175-182.
- SANTANA-GARCON, J., NEWMAN, S. J. & HARVEY, E. S. 2014. Development and validation of a mid-water baited stereo-video technique for investigating pelagic fish assemblages. *Journal of Experimental Marine Biology and Ecology*, 452, 82-90.
- SCHNEIDER VON DEIMLING, J., WEINREBE, W., TÓTH, Z., FOSSING, H., ENDLER, R., REHDER, G. & SPIEB, V. 2013. A low frequency multibeam assessment: Spatial mapping of shallow gas by enhanced penetration and angular response anomaly. *Marine and Petroleum Geology*, 44, 217-222.
- SCHONBERG, C. H. L. & FROMONT, J. 2012. Sponge gardens of Ningaloo Reef (Carnarvon Shelf, Western Australia) are biodiversity hotspots. *Hydrobiologia*, 687, 143-161.
- SCHULTZ, A. L., MALCOLM, H. A., BUCHER, D. J., LINKLATER, M. & SMITH, S. D. A. 2014. Depth and Medium-Scale Spatial Processes Influence Fish Assemblage Structure of Unconsolidated Habitats in a Subtropical Marine Park. *Plos One*, 9.
- SEAGIS, P. L. 2011. EventMeasure - event logging & 3D measurement.
- SEQUEIRA, A. M. M., MELLIN, C., LOZANO-MONTES, H. M., MEEUWIG, J. J., VANDERKLIFT, M. A., HAYWOOD, M. D. E., BABCOCK, R. C. & CALEY, M. J. 2018. Challenges of transferring models of fish abundance between coral reefs. *Peerj*, 6.
- SHEAVES, M. J. 1995. Effect of design modifications and soak time variations on Antillean-Z fish trap performance in a tropical estuary. *Bulletin of marine science*, 56, 475-489.
- SHEPPARD, C. R. C., DAVY, S. K., PILLING, G. M., SHEPPARD, C. R. C., DAVY, S. K. & PILLING, G. M. 2009. *The Biology of Coral Reefs*.
- SIH, T. L., CAPPO, M. & KINGSFORD, M. 2017. Deep-reef fish assemblages of the Great Barrier Reef shelf-break (Australia). *Scientific Reports*, 7.
- SIMMONDS, J. & MACLENNAN, D. N. 2008. *Fisheries acoustics: theory and practice*, John Wiley & Sons.
- SIMPSON, C. & WAPLES, K. 2012. Node 3: Managing and conserving the marine state. Western Australian Marine Science Institution.
- SIWABESSY, P. J. W. 2001. *An investigation of the relationship between seabed type and benthic and benthic-pelagic biota using acoustic techniques*. Curtin University.
- SMOLINSKI, S. & RADTKE, K. 2017. Spatial prediction of demersal fish diversity in the Baltic Sea: comparison of machine learning and regression-based techniques. *Ices Journal of Marine Science*, 74, 102-111.
- SOMMER, C. 1996. *The living marine resources of Somalia*, Food & Agriculture Org.

- SPEED, C. W., BABCOCK, R. C., BANCROFT, K. P., BECKLEY, L. E., BELLCHAMBERS, L. M., DEPCZYNSKI, M., FIELD, S. N., FRIEDMAN, K. J., GILMOUR, J. P., HOBBS, J.-P. A., KOBRYN, H. T., MOORE, J. A. Y., NUTT, C. D., SHEDRAWI, G., THOMSON, D. P. & WILSON, S. K. 2013. Dynamic Stability of Coral Reefs on the West Australian Coast. *Plos One*, 8.
- STEPHENS, D. & DIESING, M. 2014. A Comparison of Supervised Classification Methods for the Prediction of Substrate Type Using Multibeam Acoustic and Legacy Grain-Size Data. *Plos One*, 9.
- STOBART, B., GARCIA-CHARTON, J. A., ESPEJO, C., ROCHEL, E., GONI, R., RENONES, O., HERRERO, A., CREC'HRIOU, R., POLTI, S., MARCOS, C., PLANES, S. & PEREZ-RUZAFI, A. 2007. A baited underwater video technique to assess shallow-water Mediterranean fish assemblages: Methodological evaluation. *Journal of Experimental Marine Biology and Ecology*, 345, 158-174.
- TAMBURELLO, N., CÔTÉ, I. M. & DULVY, N. K. 2015. Energy and the scaling of animal space use. *The American Naturalist*, 186, 196-211.
- THRUSH, S., PRIDMORE, R., HEWITT, J. & CUMMINGS, V. 1991. Impact of ray feeding disturbances on sandflat macrobenthos: Do communities dominated by polychaetes or shellfish respond differently? *Marine ecology progress series. Oldendorf*, 69, 245-252.
- TRENKEL, V. M., RESSLER, P. H., JECH, M., GIANNOULAKI, M. & TAYLOR, C. 2011. Underwater acoustics for ecosystem-based management: state of the science and proposals for ecosystem indicators. *Marine Ecology Progress Series*, 442, 285-301.
- VERON, J. E. N., HOEGH-GULDBERG, O., LENTON, T. M., LOUGH, J. M., OBURA, D. O., PEARCE-KELLY, P., SHEPPARD, C. R. C., SPALDING, M., STAFFORD-SMITH, M. G. & ROGERS, A. D. 2009. The coral reef crisis: The critical importance of <350ppm CO₂. *Marine Pollution Bulletin*, 58, 1428-1436.
- WAHAB, M. A. A., RADFORD, B., CAPPO, M., COLQUHOUN, J., STOWAR, M., DEPCZYNSKI, M., MILLER, K. & HEYWARD, A. 2018. Biodiversity and spatial patterns of benthic habitat and associated demersal fish communities at two tropical submerged reef ecosystems. *Coral Reefs*, 37, 327-343.
- WAKEFIELD, C. B. & JOHNSTON, D. 2009. A preliminary investigation of the potential impacts of the proposed Kwinana Quays development on the commercially and recreationally important fish and crab species in Cockburn Sound. Fisheries Research Report No. 186.
- WAPLES, K. & HOLLANDER, E. 2008. Ningaloo Research Progress Report: Discovering Ningaloo—latest findings and their implications for management. *Ningaloo Research Coordinating Committee. Department of Environment and Conservation, Western Australia*, 114.
- WATSON, D. L., HARVEY, E. S., ANDERSON, M. J. & KENDRICK, G. A. 2005. A comparison of temperate reef fish assemblages recorded by three underwater stereo-video techniques. *Marine Biology*, 148, 415-425.
- WATSON, D. L., HARVEY, E. S., FITZPATRICK, B. M., LANGLOIS, T. J. & SHEDRAWI, G. 2010. Assessing reef fish assemblage structure: how do different stereo-video techniques compare? *Marine Biology*, 157, 1237-1250.
- WATSON, D. L., HARVEY, E. S., KENDRICK, G. A., NARDI, K. & ANDERSON, M. J. 2007. Protection from fishing alters the species composition of fish assemblages in a temperate-tropical transition zone. *Marine Biology*, 152, 1197-1206.
- WILLIS, T. J., MILLAR, R. B. & BABCOCK, R. C. 2000. Detection of spatial variability in relative density of fishes: comparison of visual census, angling, and baited underwater video. *Marine Ecology Progress Series*, 198, 249-260.
- WILSON, M. F. J., O'CONNELL, B., BROWN, C., GUINAN, J. C. & GREHAN, A. J. 2007. Multiscale terrain analysis of multibeam bathymetry data for habitat mapping on the continental slope. *Marine Geodesy*, 30, 3-35.

- WILSON, S. K., BURGESS, S. C., CHEAL, A. J., EMSLIE, M., FISHER, R., MILLER, I., POLUNIN, N. V. C. & SWEATMAN, H. P. A. 2008. Habitat utilization by coral reef fish: implications for specialists vs. generalists in a changing environment. *Journal of Animal Ecology*, 77, 220-228.
- WOOD, J. 1996. *The geomorphological characterisation of digital elevation models*. UNIVERSITY OF LEICESTER (UNITED KINGDOM).
- WOOD, J. 2009. Geomorphometry in LandSerf. *Developments in soil science*, 33, 333-349.
- WRIGHT, D. J. & HEYMAN, W. D. 2008. Introduction to the Special Issue: Marine and Coastal GIS for Geomorphology, Habitat Mapping, and Marine Reserves. *Marine Geodesy*, 31, 223-230.
- YOUNG, M. & CARR, M. H. 2015. Application of species distribution models to explain and predict the distribution, abundance and assemblage structure of nearshore temperate reef fishes. *Diversity and Distributions*, 21, 1428-1440.
- YOUNG, M. A., IAMPIETRO, P. J., KVITEK, R. G. & GARZA, C. D. 2010. Multivariate bathymetry-derived generalized linear model accurately predicts rockfish distribution on Cordell Bank, California, USA. *Marine Ecology Progress Series*, 415, 247-261.
- YOUNG, M. A., WEDDING, L. M. & CARR, M. H. 2017. Applying Landscape Ecology for the Design and Evaluation of Marine Protected Area Networks. *Seascape Ecology*, 429-462.
- ZENONE, A. M., BURKEPILE, D. E. & BOSWELL, K. M. 2017. A comparison of diver vs. acoustic methodologies for surveying fishes in a shallow water coral reef ecosystem. *Fisheries Research*, 189, 62-66.
- ZIMMERMANN, N. E. & KIENAST, F. 1999. Predictive mapping of alpine grasslands in Switzerland: Species versus community approach. *Journal of Vegetation Science*, 10, 469-482.

“Every reasonable effort has been made to acknowledge the owners of copyright material. I would be pleased to hear from any copyright owner who has been omitted or incorrectly acknowledge”.

Publications part of this thesis

Landero, M., I. Parnum, et al. (2016). Integrating echo-sounder and underwater video data for demersal fish assessment. Proceedings of Acoustics2016-The Second Australasian Acoustical Societies Conference.

Appendix A

Importance of variables in the Random Forest for the nine species and the three locations. Two scenarios are considered, BT+DV corresponds to the models produced using bathymetry and depth derivatives. The BT+DV+BS corresponds to the model with backscatter data.

Variable	MeanDecrease Accuracy	MeanDecreaseGini	Location	Scenario	Species
Depth	33.48285304	6.215885709	Mandu	BT+DV	<i>Abalistes stellatus</i>
rough21	19.43573286	3.249241677	Mandu	BT+DV	<i>Abalistes stellatus</i>
planc21	9.293956789	2.825665624	Mandu	BT+DV	<i>Abalistes stellatus</i>
rough9	11.72406266	2.155671504	Mandu	BT+DV	<i>Abalistes stellatus</i>
rough15	7.714231069	1.919781858	Mandu	BT+DV	<i>Abalistes stellatus</i>
slope15	8.36788572	1.746318551	Mandu	BT+DV	<i>Abalistes stellatus</i>
SD15	7.806752924	1.726613213	Mandu	BT+DV	<i>Abalistes stellatus</i>
slope9	8.514467098	1.721651188	Mandu	BT+DV	<i>Abalistes stellatus</i>
SD21	7.097181149	1.643009223	Mandu	BT+DV	<i>Abalistes stellatus</i>
TRI15	6.851199961	1.457315202	Mandu	BT+DV	<i>Abalistes stellatus</i>
slope21	7.126603027	1.373862428	Mandu	BT+DV	<i>Abalistes stellatus</i>
TRI21	7.777436382	1.327426991	Mandu	BT+DV	<i>Abalistes stellatus</i>
Depth	10.12699522	5.977567592	Mandu	BT+DV+BS	<i>Abalistes stellatus</i>
planc21	2.345521129	2.751479056	Mandu	BT+DV+BS	<i>Abalistes stellatus</i>
rough21	6.629733887	2.74472135	Mandu	BT+DV+BS	<i>Abalistes stellatus</i>
NS3	2.845533453	2.655656147	Mandu	BT+DV+BS	<i>Abalistes stellatus</i>
WE3	2.846560093	2.501676996	Mandu	BT+DV+BS	<i>Abalistes stellatus</i>
rough9	4.543960129	2.13006568	Mandu	BT+DV+BS	<i>Abalistes stellatus</i>
rough15	2.846768833	1.796408969	Mandu	BT+DV+BS	<i>Abalistes stellatus</i>
slope9	2.596527226	1.776433173	Mandu	BT+DV+BS	<i>Abalistes stellatus</i>
BPI21	2.246024962	1.559474135	Mandu	BT+DV+BS	<i>Abalistes stellatus</i>
TRI15	2.10856929	1.530614774	Mandu	BT+DV+BS	<i>Abalistes stellatus</i>
Depth	50.7305654	8.311839706	PtCloates	BT+DV	<i>Abalistes stellatus</i>
TRI21	28.91783604	4.35917879	PtCloates	BT+DV	<i>Abalistes stellatus</i>
SD21	23.44237018	3.138031043	PtCloates	BT+DV	<i>Abalistes stellatus</i>
slope21	20.64351671	3.0578207	PtCloates	BT+DV	<i>Abalistes stellatus</i>
TRI15	21.53192438	2.718971794	PtCloates	BT+DV	<i>Abalistes stellatus</i>
rough21	22.00161297	2.685028784	PtCloates	BT+DV	<i>Abalistes stellatus</i>
slope15	16.76156958	2.562984483	PtCloates	BT+DV	<i>Abalistes stellatus</i>
SD15	15.4335727	2.168339379	PtCloates	BT+DV	<i>Abalistes stellatus</i>
TRI9	18.0034641	1.862812015	PtCloates	BT+DV	<i>Abalistes stellatus</i>
rough9	13.91007806	1.795062898	PtCloates	BT+DV	<i>Abalistes stellatus</i>
SD9	18.44427958	1.77939338	PtCloates	BT+DV	<i>Abalistes stellatus</i>
rough15	15.34811621	1.775182004	PtCloates	BT+DV	<i>Abalistes stellatus</i>
meanc9	13.89310362	1.496527174	PtCloates	BT+DV	<i>Abalistes stellatus</i>
Depth	16.39151899	7.890536587	PtCloates	BT+DV+BS	<i>Abalistes stellatus</i>
TRI21	10.11815316	4.215356147	PtCloates	BT+DV+BS	<i>Abalistes stellatus</i>
slope21	6.368865241	3.353654244	PtCloates	BT+DV+BS	<i>Abalistes stellatus</i>
SD21	7.221438422	3.114541597	PtCloates	BT+DV+BS	<i>Abalistes stellatus</i>
rough21	7.375232345	2.717355438	PtCloates	BT+DV+BS	<i>Abalistes stellatus</i>
slope15	5.225237531	2.651012603	PtCloates	BT+DV+BS	<i>Abalistes stellatus</i>
TRI15	7.049753785	2.633322434	PtCloates	BT+DV+BS	<i>Abalistes stellatus</i>
rough9	5.574370401	1.929186693	PtCloates	BT+DV+BS	<i>Abalistes stellatus</i>
ARA_Phi	4.252632967	1.921641935	PtCloates	BT+DV+BS	<i>Abalistes stellatus</i>
SD9	5.283443979	1.827907816	PtCloates	BT+DV+BS	<i>Abalistes stellatus</i>
rough15	4.230498536	1.766150317	PtCloates	BT+DV+BS	<i>Abalistes stellatus</i>
SD15	5.798232426	1.649181067	PtCloates	BT+DV+BS	<i>Abalistes stellatus</i>
TRI9	5.160511276	1.600229085	PtCloates	BT+DV+BS	<i>Abalistes stellatus</i>
meanc9	3.52453962	1.377220741	PtCloates	BT+DV+BS	<i>Abalistes stellatus</i>
profc9	3.641265523	1.187066519	PtCloates	BT+DV+BS	<i>Abalistes stellatus</i>
BPI9	3.391550211	1.128857616	PtCloates	BT+DV+BS	<i>Abalistes stellatus</i>
meanc15	3.512855176	0.962154865	PtCloates	BT+DV+BS	<i>Abalistes stellatus</i>
Depth	18.84327811	4.142860628	Gnaraloo	BT+DV	<i>Abalistes stellatus</i>
NS9	11.86855555	2.898279346	Gnaraloo	BT+DV	<i>Abalistes stellatus</i>
WE3	3.98145357	2.094015726	Gnaraloo	BT+DV	<i>Abalistes stellatus</i>

Variable	MeanDecrease Accuracy	MeanDecreaseGini	Location	Scenario	Species
slope21	3.929806235	1.888908438	Gnaraloo	BT+DV	<i>Abalistes stellatus</i>
BPI21	4.675388485	1.732644455	Gnaraloo	BT+DV	<i>Abalistes stellatus</i>
BPI9	4.76686935	1.490858388	Gnaraloo	BT+DV	<i>Abalistes stellatus</i>
BPI15	5.494113365	1.380016454	Gnaraloo	BT+DV	<i>Abalistes stellatus</i>
SD15	5.007536836	1.212080202	Gnaraloo	BT+DV	<i>Abalistes stellatus</i>
Depth	4.596145012	3.500520219	Gnaraloo	BT+DV+BS	<i>Abalistes stellatus</i>
NS9	3.536874971	2.715744267	Gnaraloo	BT+DV+BS	<i>Abalistes stellatus</i>
ARA_Phi	2.102252137	2.35844745	Gnaraloo	BT+DV+BS	<i>Abalistes stellatus</i>
slope21	1.946959428	2.03286092	Gnaraloo	BT+DV+BS	<i>Abalistes stellatus</i>
WE3	1.601314952	1.805214464	Gnaraloo	BT+DV+BS	<i>Abalistes stellatus</i>
rough21	1.139768901	1.688186764	Gnaraloo	BT+DV+BS	<i>Abalistes stellatus</i>
profc3	1.192358788	1.634596031	Gnaraloo	BT+DV+BS	<i>Abalistes stellatus</i>
BPI21	1.220223648	1.570770525	Gnaraloo	BT+DV+BS	<i>Abalistes stellatus</i>
BPI15	2.845845491	1.332587391	Gnaraloo	BT+DV+BS	<i>Abalistes stellatus</i>
TRI3	1.07602741	1.263613055	Gnaraloo	BT+DV+BS	<i>Abalistes stellatus</i>
SD3	1.616303813	1.238015352	Gnaraloo	BT+DV+BS	<i>Abalistes stellatus</i>
BPI9	2.397979802	1.219706871	Gnaraloo	BT+DV+BS	<i>Abalistes stellatus</i>
planc21	2.240720936	1.192114116	Gnaraloo	BT+DV+BS	<i>Abalistes stellatus</i>
rough15	1.930529185	1.190013937	Gnaraloo	BT+DV+BS	<i>Abalistes stellatus</i>
SD9	1.697070684	1.189333181	Gnaraloo	BT+DV+BS	<i>Abalistes stellatus</i>
rough9	1.921155502	1.175043995	Gnaraloo	BT+DV+BS	<i>Abalistes stellatus</i>
SD15	1.939764749	0.99981671	Gnaraloo	BT+DV+BS	<i>Abalistes stellatus</i>

Variable	Mean Decrease Accuracy	Mean Decrease Gini	Location	Scenario	Species
Depth	42.38788226	8.055196182	Mandu	BT+DV	<i>Gymnocranius grandoculis</i>
fractal9	9.673733595	2.38481722	Mandu	BT+DV	<i>Gymnocranius grandoculis</i>
slope3	8.886613924	2.064394685	Mandu	BT+DV	<i>Gymnocranius grandoculis</i>
slope15	13.12896541	1.875223205	Mandu	BT+DV	<i>Gymnocranius grandoculis</i>
TRI15	9.304928388	1.811006312	Mandu	BT+DV	<i>Gymnocranius grandoculis</i>
TRI21	9.654318664	1.761289617	Mandu	BT+DV	<i>Gymnocranius grandoculis</i>
SD21	9.75579345	1.594381051	Mandu	BT+DV	<i>Gymnocranius grandoculis</i>
Depth	14.84793524	7.759502454	Mandu	BT+DV+BS	<i>Gymnocranius grandoculis</i>
ARA_Phi	6.697313386	4.541780176	Mandu	BT+DV+BS	<i>Gymnocranius grandoculis</i>
fractal9	4.128283834	2.129342874	Mandu	BT+DV+BS	<i>Gymnocranius grandoculis</i>
BPI21	3.448001294	1.991620731	Mandu	BT+DV+BS	<i>Gymnocranius grandoculis</i>
slope15	4.095779696	1.803225431	Mandu	BT+DV+BS	<i>Gymnocranius grandoculis</i>
TRI15	4.517496385	1.753233429	Mandu	BT+DV+BS	<i>Gymnocranius grandoculis</i>
slope21	4.169023819	1.655799291	Mandu	BT+DV+BS	<i>Gymnocranius grandoculis</i>
SD21	5.19883558	1.568752416	Mandu	BT+DV+BS	<i>Gymnocranius grandoculis</i>
Depth	46.77897	8.984455171	PtCloates	BT+DV	<i>Gymnocranius grandoculis</i>
NS3	10.23818068	2.59322569	PtCloates	BT+DV	<i>Gymnocranius grandoculis</i>
WE21	14.58669501	2.530211383	PtCloates	BT+DV	<i>Gymnocranius grandoculis</i>
WE15	11.04499	2.495978204	PtCloates	BT+DV	<i>Gymnocranius grandoculis</i>
SD21	12.96754123	2.341466063	PtCloates	BT+DV	<i>Gymnocranius grandoculis</i>
fractal15	10.16231504	2.26060289	PtCloates	BT+DV	<i>Gymnocranius grandoculis</i>
TRI21	14.41163774	2.247255273	PtCloates	BT+DV	<i>Gymnocranius grandoculis</i>
slope15	14.522175	2.187234747	PtCloates	BT+DV	<i>Gymnocranius grandoculis</i>
TRI15	13.94442947	1.973775568	PtCloates	BT+DV	<i>Gymnocranius grandoculis</i>
SD9	15.46379643	1.941813829	PtCloates	BT+DV	<i>Gymnocranius grandoculis</i>
rough15	11.03978357	1.758404321	PtCloates	BT+DV	<i>Gymnocranius grandoculis</i>
SD15	13.56982095	1.749008693	PtCloates	BT+DV	<i>Gymnocranius grandoculis</i>
TRI9	11.42430579	1.748764993	PtCloates	BT+DV	<i>Gymnocranius grandoculis</i>
Depth	13.50481667	7.719126395	PtCloates	BT+DV+BS	<i>Gymnocranius grandoculis</i>
ARA_Phi	7.449927623	4.842953004	PtCloates	BT+DV+BS	<i>Gymnocranius grandoculis</i>
BS	9.23237767	4.80836999	PtCloates	BT+DV+BS	<i>Gymnocranius grandoculis</i>
TRI21	5.925888445	2.060987675	PtCloates	BT+DV+BS	<i>Gymnocranius grandoculis</i>
slope15	4.149102884	2.050886303	PtCloates	BT+DV+BS	<i>Gymnocranius grandoculis</i>
fractal15	2.924803004	1.985816481	PtCloates	BT+DV+BS	<i>Gymnocranius grandoculis</i>
SD21	4.887391183	1.953024954	PtCloates	BT+DV+BS	<i>Gymnocranius grandoculis</i>
rough15	4.592135814	1.848174379	PtCloates	BT+DV+BS	<i>Gymnocranius grandoculis</i>
SD15	4.526517761	1.705481404	PtCloates	BT+DV+BS	<i>Gymnocranius grandoculis</i>
TRI15	3.756098965	1.663778808	PtCloates	BT+DV+BS	<i>Gymnocranius grandoculis</i>
SD9	4.207096282	1.602825379	PtCloates	BT+DV+BS	<i>Gymnocranius grandoculis</i>
slope9	2.947453217	1.533983167	PtCloates	BT+DV+BS	<i>Gymnocranius grandoculis</i>
rough9	3.324867178	1.267518519	PtCloates	BT+DV+BS	<i>Gymnocranius grandoculis</i>
Depth	59.2745043	9.937719689	Gnaraloo	BT+DV	<i>Gymnocranius grandoculis</i>
meanc21	17.18560994	2.361972466	Gnaraloo	BT+DV	<i>Gymnocranius grandoculis</i>

Variable	Mean Decrease Accuracy	Mean Decrease Gini	Location	Scenario	Species
Depth	16.30401347	8.291990131	Gnaraloo	BT+DV+BS	<i>Gymnocranius grandoculis</i>
ARA_Phi	9.67276341	4.575199028	Gnaraloo	BT+DV+BS	<i>Gymnocranius grandoculis</i>
BS	3.598829472	2.692249348	Gnaraloo	BT+DV+BS	<i>Gymnocranius grandoculis</i>
meanc21	4.957318241	1.89764186	Gnaraloo	BT+DV+BS	<i>Gymnocranius grandoculis</i>
WE21	3.458716744	1.746371588	Gnaraloo	BT+DV+BS	<i>Gymnocranius grandoculis</i>
NS21	3.430865566	1.706611168	Gnaraloo	BT+DV+BS	<i>Gymnocranius grandoculis</i>
prof3	3.825846622	1.642459268	Gnaraloo	BT+DV+BS	<i>Gymnocranius grandoculis</i>
meanc15	3.357493642	0.773841168	Gnaraloo	BT+DV+BS	<i>Gymnocranius grandoculis</i>

Variable	Mean Decrease Accuracy	Mean Decrease Gini	Location	Scenario	Species
Depth	12.44776758	3.838197823	Mandu	BT+DV	<i>Lagocephalus sceleratus</i>
NS3	3.922512191	3.1479687	Mandu	BT+DV	<i>Lagocephalus sceleratus</i>
planc3	2.609002062	2.553161977	Mandu	BT+DV	<i>Lagocephalus sceleratus</i>
rough21	4.189696466	2.241972346	Mandu	BT+DV	<i>Lagocephalus sceleratus</i>
slope3	3.389473805	2.232283652	Mandu	BT+DV	<i>Lagocephalus sceleratus</i>
planc9	2.817587729	2.056290012	Mandu	BT+DV	<i>Lagocephalus sceleratus</i>
profc9	4.159682472	1.94366125	Mandu	BT+DV	<i>Lagocephalus sceleratus</i>
TRI3	9.623103255	1.929516483	Mandu	BT+DV	<i>Lagocephalus sceleratus</i>
meanc9	2.880249143	1.88364746	Mandu	BT+DV	<i>Lagocephalus sceleratus</i>
SD21	5.956238595	1.788296476	Mandu	BT+DV	<i>Lagocephalus sceleratus</i>
TRI21	5.950747737	1.605285826	Mandu	BT+DV	<i>Lagocephalus sceleratus</i>
ARA_Phi	6.005396962	4.808407031	Mandu	BT+DV+BS	<i>Lagocephalus sceleratus</i>
Depth	4.874684094	3.318762199	Mandu	BT+DV+BS	<i>Lagocephalus sceleratus</i>
BS	2.279576073	2.908396387	Mandu	BT+DV+BS	<i>Lagocephalus sceleratus</i>
planc3	1.497949232	2.272181954	Mandu	BT+DV+BS	<i>Lagocephalus sceleratus</i>
slope3	1.21066466	2.127309381	Mandu	BT+DV+BS	<i>Lagocephalus sceleratus</i>
rough21	2.418297259	2.084356144	Mandu	BT+DV+BS	<i>Lagocephalus sceleratus</i>
TRI3	1.268607584	1.833838706	Mandu	BT+DV+BS	<i>Lagocephalus sceleratus</i>
BPI9	2.012079539	1.821262214	Mandu	BT+DV+BS	<i>Lagocephalus sceleratus</i>
profc9	2.971583923	1.757905705	Mandu	BT+DV+BS	<i>Lagocephalus sceleratus</i>
planc9	1.324245118	1.627787021	Mandu	BT+DV+BS	<i>Lagocephalus sceleratus</i>
slope21	1.76631262	1.535589649	Mandu	BT+DV+BS	<i>Lagocephalus sceleratus</i>
SD21	1.411162883	1.488800271	Mandu	BT+DV+BS	<i>Lagocephalus sceleratus</i>
SD3	1.207333101	1.451073121	Mandu	BT+DV+BS	<i>Lagocephalus sceleratus</i>
TRI9	1.223803901	1.354228917	Mandu	BT+DV+BS	<i>Lagocephalus sceleratus</i>
TRI21	37.35480159	5.325138573	PtCloates	BT+DV	<i>Lagocephalus sceleratus</i>
SD21	34.92933288	4.554139251	PtCloates	BT+DV	<i>Lagocephalus sceleratus</i>
TRI15	28.72927594	3.772966654	PtCloates	BT+DV	<i>Lagocephalus sceleratus</i>
slope21	25.68592526	3.199897745	PtCloates	BT+DV	<i>Lagocephalus sceleratus</i>
SD15	27.37074909	3.170566663	PtCloates	BT+DV	<i>Lagocephalus sceleratus</i>
Depth	26.77259483	2.844956372	PtCloates	BT+DV	<i>Lagocephalus sceleratus</i>
slope15	21.67332802	2.607891916	PtCloates	BT+DV	<i>Lagocephalus sceleratus</i>
slope9	18.96151277	2.428705595	PtCloates	BT+DV	<i>Lagocephalus sceleratus</i>
rough15	23.66061145	1.899299181	PtCloates	BT+DV	<i>Lagocephalus sceleratus</i>
TRI9	19.19650214	1.878049197	PtCloates	BT+DV	<i>Lagocephalus sceleratus</i>
SD9	18.07892736	1.830781956	PtCloates	BT+DV	<i>Lagocephalus sceleratus</i>
rough21	23.8987992	1.713125727	PtCloates	BT+DV	<i>Lagocephalus sceleratus</i>
rough9	14.59178106	1.329393732	PtCloates	BT+DV	<i>Lagocephalus sceleratus</i>
fractal15	8.057301044	0.897298402	PtCloates	BT+DV	<i>Lagocephalus sceleratus</i>
TRI3	16.47305119	0.855933318	PtCloates	BT+DV	<i>Lagocephalus sceleratus</i>
fractal21	7.632644131	0.82438412	PtCloates	BT+DV	<i>Lagocephalus sceleratus</i>
planc21	11.1784911	0.820545949	PtCloates	BT+DV	<i>Lagocephalus sceleratus</i>
profc9	10.04506362	0.758850129	PtCloates	BT+DV	<i>Lagocephalus sceleratus</i>
meanc21	11.73215141	0.745736797	PtCloates	BT+DV	<i>Lagocephalus sceleratus</i>
slope3	9.32154107	0.733285549	PtCloates	BT+DV	<i>Lagocephalus sceleratus</i>
BPI21	10.30358	0.677405834	PtCloates	BT+DV	<i>Lagocephalus sceleratus</i>
profc15	8.056927151	0.676574782	PtCloates	BT+DV	<i>Lagocephalus sceleratus</i>
WE9	7.50619666	0.666780638	PtCloates	BT+DV	<i>Lagocephalus sceleratus</i>
BPI15	8.654141772	0.658680583	PtCloates	BT+DV	<i>Lagocephalus sceleratus</i>
meanc15	8.479145937	0.592983033	PtCloates	BT+DV	<i>Lagocephalus sceleratus</i>
SD3	9.377967642	0.575985749	PtCloates	BT+DV	<i>Lagocephalus sceleratus</i>
rough3	9.143663077	0.570843839	PtCloates	BT+DV	<i>Lagocephalus sceleratus</i>

Variable	Mean Decrease Accuracy	Mean Decrease Gini	Location	Scenario	Species
TRI21	12.41325229	5.275851795	PtCloates	BT+DV+BS	<i>Lagocephalus sceleratus</i>
SD21	11.88403797	4.691668339	PtCloates	BT+DV+BS	<i>Lagocephalus sceleratus</i>
TRI15	9.621318853	3.773296069	PtCloates	BT+DV+BS	<i>Lagocephalus sceleratus</i>
SD15	8.658940192	3.507755175	PtCloates	BT+DV+BS	<i>Lagocephalus sceleratus</i>
slope21	7.711444994	3.425753702	PtCloates	BT+DV+BS	<i>Lagocephalus sceleratus</i>
Depth	7.514265393	2.636842828	PtCloates	BT+DV+BS	<i>Lagocephalus sceleratus</i>
slope15	7.730430996	2.381663111	PtCloates	BT+DV+BS	<i>Lagocephalus sceleratus</i>
slope9	5.439249116	2.360381163	PtCloates	BT+DV+BS	<i>Lagocephalus sceleratus</i>
SD9	4.856376564	1.96219584	PtCloates	BT+DV+BS	<i>Lagocephalus sceleratus</i>
rough15	6.766132715	1.960198832	PtCloates	BT+DV+BS	<i>Lagocephalus sceleratus</i>
rough21	7.240006864	1.798737471	PtCloates	BT+DV+BS	<i>Lagocephalus sceleratus</i>
TRI9	5.773485076	1.453668522	PtCloates	BT+DV+BS	<i>Lagocephalus sceleratus</i>
rough9	4.232530166	1.15001576	PtCloates	BT+DV+BS	<i>Lagocephalus sceleratus</i>
BPI15	2.953516493	0.783094593	PtCloates	BT+DV+BS	<i>Lagocephalus sceleratus</i>
profc21	2.567683834	0.770405218	PtCloates	BT+DV+BS	<i>Lagocephalus sceleratus</i>
planc21	2.955994068	0.751411278	PtCloates	BT+DV+BS	<i>Lagocephalus sceleratus</i>
meanc21	4.514706628	0.741188483	PtCloates	BT+DV+BS	<i>Lagocephalus sceleratus</i>
fractal9	2.654437782	0.726133832	PtCloates	BT+DV+BS	<i>Lagocephalus sceleratus</i>
profc9	2.998010001	0.710365155	PtCloates	BT+DV+BS	<i>Lagocephalus sceleratus</i>
TRI3	4.405844358	0.708396492	PtCloates	BT+DV+BS	<i>Lagocephalus sceleratus</i>
ARA_Phi	2.553218451	0.679465559	PtCloates	BT+DV+BS	<i>Lagocephalus sceleratus</i>
BPI21	3.216014914	0.636278792	PtCloates	BT+DV+BS	<i>Lagocephalus sceleratus</i>
meanc9	3.482821222	0.626633572	PtCloates	BT+DV+BS	<i>Lagocephalus sceleratus</i>
BPI3	2.763064315	0.611666503	PtCloates	BT+DV+BS	<i>Lagocephalus sceleratus</i>
rough3	3.272760633	0.569879278	PtCloates	BT+DV+BS	<i>Lagocephalus sceleratus</i>
profc15	3.722407011	0.564352612	PtCloates	BT+DV+BS	<i>Lagocephalus sceleratus</i>
meanc15	3.160521681	0.54082921	PtCloates	BT+DV+BS	<i>Lagocephalus sceleratus</i>
Depth	64.91784922	13.4104662	Gnaraloo	BT+DV	<i>Lagocephalus sceleratus</i>
NS21	18.23131252	3.482595034	Gnaraloo	BT+DV	<i>Lagocephalus sceleratus</i>
WE21	22.81443626	3.226378262	Gnaraloo	BT+DV	<i>Lagocephalus sceleratus</i>
NS9	14.08304421	2.70832183	Gnaraloo	BT+DV	<i>Lagocephalus sceleratus</i>
Depth	19.28919542	11.80142648	Gnaraloo	BT+DV+BS	<i>Lagocephalus sceleratus</i>
ARA_Phi	14.32401808	7.698438501	Gnaraloo	BT+DV+BS	<i>Lagocephalus sceleratus</i>
WE21	5.417497813	2.49058346	Gnaraloo	BT+DV+BS	<i>Lagocephalus sceleratus</i>

Variable	Mean Decrease Accuracy	Mean Decrease Gini	Location	Scenario	Species
Depth	29.5220254	2.861694519	Mandu	BT+DV	<i>Lethrinus miniatus</i>
rough15	29.25205532	2.799261945	Mandu	BT+DV	<i>Lethrinus miniatus</i>
profc15	23.2129605	2.448978178	Mandu	BT+DV	<i>Lethrinus miniatus</i>
rough21	21.40025562	2.016300704	Mandu	BT+DV	<i>Lethrinus miniatus</i>
profc21	13.76550637	1.493638679	Mandu	BT+DV	<i>Lethrinus miniatus</i>
meanc21	15.70126336	1.428733266	Mandu	BT+DV	<i>Lethrinus miniatus</i>
NS3	8.040759673	1.424196195	Mandu	BT+DV	<i>Lethrinus miniatus</i>
fractal21	21.1716371	1.419999453	Mandu	BT+DV	<i>Lethrinus miniatus</i>
slope3	12.22401063	1.377317546	Mandu	BT+DV	<i>Lethrinus miniatus</i>
meanc15	12.37624946	1.36566299	Mandu	BT+DV	<i>Lethrinus miniatus</i>
SD21	17.20591986	1.290366097	Mandu	BT+DV	<i>Lethrinus miniatus</i>
rough9	15.31339195	1.281702531	Mandu	BT+DV	<i>Lethrinus miniatus</i>
rough3	10.51445575	1.253929708	Mandu	BT+DV	<i>Lethrinus miniatus</i>
SD15	16.21673525	1.230931973	Mandu	BT+DV	<i>Lethrinus miniatus</i>
profc3	7.084448164	1.148949381	Mandu	BT+DV	<i>Lethrinus miniatus</i>
SD3	10.74477094	1.143420322	Mandu	BT+DV	<i>Lethrinus miniatus</i>
profc9	5.965778429	1.141548445	Mandu	BT+DV	<i>Lethrinus miniatus</i>
TRI15	16.64226793	1.128054821	Mandu	BT+DV	<i>Lethrinus miniatus</i>
TRI9	12.85853424	1.124496612	Mandu	BT+DV	<i>Lethrinus miniatus</i>
SD9	14.60259978	1.119421969	Mandu	BT+DV	<i>Lethrinus miniatus</i>
meanc9	7.422234159	1.054963265	Mandu	BT+DV	<i>Lethrinus miniatus</i>
TRI21	14.95065151	1.049041824	Mandu	BT+DV	<i>Lethrinus miniatus</i>
slope15	13.95613398	1.047406289	Mandu	BT+DV	<i>Lethrinus miniatus</i>
BPI9	10.48404786	1.027989617	Mandu	BT+DV	<i>Lethrinus miniatus</i>
fractal15	14.77230112	1.001011412	Mandu	BT+DV	<i>Lethrinus miniatus</i>
BPI15	11.48615735	1.001006641	Mandu	BT+DV	<i>Lethrinus miniatus</i>
fractal9	14.87113296	0.989145216	Mandu	BT+DV	<i>Lethrinus miniatus</i>
slope9	11.48601789	0.946988412	Mandu	BT+DV	<i>Lethrinus miniatus</i>
slope21	13.67853752	0.945700424	Mandu	BT+DV	<i>Lethrinus miniatus</i>
meanc3	6.542708997	0.924551431	Mandu	BT+DV	<i>Lethrinus miniatus</i>
BPI21	7.965924402	0.853588822	Mandu	BT+DV	<i>Lethrinus miniatus</i>
BPI3	7.67374561	0.806613955	Mandu	BT+DV	<i>Lethrinus miniatus</i>
Depth	8.691476298	2.802477142	Mandu	BT+DV+BS	<i>Lethrinus miniatus</i>
rough15	7.905592556	2.603601249	Mandu	BT+DV+BS	<i>Lethrinus miniatus</i>
profc15	6.013769168	2.424640585	Mandu	BT+DV+BS	<i>Lethrinus miniatus</i>
rough21	5.540432248	1.905265217	Mandu	BT+DV+BS	<i>Lethrinus miniatus</i>
slope3	3.499671229	1.550826589	Mandu	BT+DV+BS	<i>Lethrinus miniatus</i>
fractal21	6.301790691	1.436004564	Mandu	BT+DV+BS	<i>Lethrinus miniatus</i>
profc21	3.117231854	1.411446064	Mandu	BT+DV+BS	<i>Lethrinus miniatus</i>
rough3	4.490741807	1.361892348	Mandu	BT+DV+BS	<i>Lethrinus miniatus</i>
SD15	6.43796252	1.35372018	Mandu	BT+DV+BS	<i>Lethrinus miniatus</i>
rough9	4.881403245	1.34611474	Mandu	BT+DV+BS	<i>Lethrinus miniatus</i>
NS3	3.296705001	1.328317118	Mandu	BT+DV+BS	<i>Lethrinus miniatus</i>
meanc21	5.686992604	1.312976755	Mandu	BT+DV+BS	<i>Lethrinus miniatus</i>
meanc15	4.01589963	1.227354021	Mandu	BT+DV+BS	<i>Lethrinus miniatus</i>

Variable	Mean Decrease Accuracy	Mean Decrease Gini	Location	Scenario	Species
meanc9	3.088055902	1.20589943	Mandu	BT+DV+BS	<i>Lethrinus miniatus</i>
SD3	3.865879363	1.19227094	Mandu	BT+DV+BS	<i>Lethrinus miniatus</i>
SD21	6.111006205	1.190430651	Mandu	BT+DV+BS	<i>Lethrinus miniatus</i>
TRI15	5.649799702	1.112882047	Mandu	BT+DV+BS	<i>Lethrinus miniatus</i>
SD9	4.626354696	1.079658855	Mandu	BT+DV+BS	<i>Lethrinus miniatus</i>
TRI9	4.252356839	1.056088249	Mandu	BT+DV+BS	<i>Lethrinus miniatus</i>
slope15	4.124552718	1.053157935	Mandu	BT+DV+BS	<i>Lethrinus miniatus</i>
TRI21	4.11491743	1.037697049	Mandu	BT+DV+BS	<i>Lethrinus miniatus</i>
profc9	2.46664653	1.029921382	Mandu	BT+DV+BS	<i>Lethrinus miniatus</i>
profc3	1.941929795	1.029854547	Mandu	BT+DV+BS	<i>Lethrinus miniatus</i>
BPI15	3.932168982	0.938031668	Mandu	BT+DV+BS	<i>Lethrinus miniatus</i>
fractal15	4.67970612	0.90487513	Mandu	BT+DV+BS	<i>Lethrinus miniatus</i>
meanc3	1.764428146	0.894968851	Mandu	BT+DV+BS	<i>Lethrinus miniatus</i>
planc15	2.78538007	0.865477208	Mandu	BT+DV+BS	<i>Lethrinus miniatus</i>
BPI9	3.653639695	0.852522687	Mandu	BT+DV+BS	<i>Lethrinus miniatus</i>
ARA_Phi	1.912997614	0.850575668	Mandu	BT+DV+BS	<i>Lethrinus miniatus</i>
slope9	2.984367836	0.841267093	Mandu	BT+DV+BS	<i>Lethrinus miniatus</i>
slope21	4.01694263	0.827554239	Mandu	BT+DV+BS	<i>Lethrinus miniatus</i>
BPI21	3.206696038	0.808070685	Mandu	BT+DV+BS	<i>Lethrinus miniatus</i>
TRI3	1.989819977	0.789115372	Mandu	BT+DV+BS	<i>Lethrinus miniatus</i>
BPI3	2.284233821	0.778280482	Mandu	BT+DV+BS	<i>Lethrinus miniatus</i>
fractal9	4.512954922	0.742037726	Mandu	BT+DV+BS	<i>Lethrinus miniatus</i>
WE21	2.478436909	0.729463015	Mandu	BT+DV+BS	<i>Lethrinus miniatus</i>
NS15	2.374557573	0.65356724	Mandu	BT+DV+BS	<i>Lethrinus miniatus</i>
Depth	35.44687907	4.362783458	PtCloates	BT+DV	<i>Lethrinus miniatus</i>
SD9	29.66654149	4.222392148	PtCloates	BT+DV	<i>Lethrinus miniatus</i>
rough9	22.84190411	3.329881231	PtCloates	BT+DV	<i>Lethrinus miniatus</i>
TRI21	20.08949482	3.211330973	PtCloates	BT+DV	<i>Lethrinus miniatus</i>
TRI9	19.53134758	3.207684862	PtCloates	BT+DV	<i>Lethrinus miniatus</i>
SD15	20.43167723	2.710040108	PtCloates	BT+DV	<i>Lethrinus miniatus</i>
TRI15	19.0989269	2.594583024	PtCloates	BT+DV	<i>Lethrinus miniatus</i>
SD21	17.2223664	2.592999369	PtCloates	BT+DV	<i>Lethrinus miniatus</i>
meanc21	11.90855257	2.392518649	PtCloates	BT+DV	<i>Lethrinus miniatus</i>
fractal21	11.51692643	2.219470192	PtCloates	BT+DV	<i>Lethrinus miniatus</i>
fractal15	12.72761493	2.14824949	PtCloates	BT+DV	<i>Lethrinus miniatus</i>
profc21	9.247219308	2.013468312	PtCloates	BT+DV	<i>Lethrinus miniatus</i>
rough15	11.67381626	1.896878022	PtCloates	BT+DV	<i>Lethrinus miniatus</i>
rough3	12.42738228	1.862958164	PtCloates	BT+DV	<i>Lethrinus miniatus</i>
slope9	14.29357533	1.849704574	PtCloates	BT+DV	<i>Lethrinus miniatus</i>
SD3	10.60093933	1.843289119	PtCloates	BT+DV	<i>Lethrinus miniatus</i>
slope3	12.6104518	1.774527931	PtCloates	BT+DV	<i>Lethrinus miniatus</i>
slope15	13.6355657	1.709986529	PtCloates	BT+DV	<i>Lethrinus miniatus</i>
slope21	12.02341784	1.467229129	PtCloates	BT+DV	<i>Lethrinus miniatus</i>
profc15	7.460505483	1.303242762	PtCloates	BT+DV	<i>Lethrinus miniatus</i>
meanc9	10.2207855	1.16028502	PtCloates	BT+DV	<i>Lethrinus miniatus</i>

Variable	Mean Decrease Accuracy	Mean Decrease Gini	Location	Scenario	Species
ARA_Phi	12.97753385	5.751144875	PtCloates	BT+DV+BS	<i>Lethrinus miniatus</i>
SD9	9.870279753	4.379546789	PtCloates	BT+DV+BS	<i>Lethrinus miniatus</i>
Depth	9.817219211	3.59304461	PtCloates	BT+DV+BS	<i>Lethrinus miniatus</i>
rough9	7.201819602	3.529760166	PtCloates	BT+DV+BS	<i>Lethrinus miniatus</i>
SD15	7.481014199	3.083839203	PtCloates	BT+DV+BS	<i>Lethrinus miniatus</i>
TRI9	5.656368997	2.996787385	PtCloates	BT+DV+BS	<i>Lethrinus miniatus</i>
TRI21	5.577581447	2.620855554	PtCloates	BT+DV+BS	<i>Lethrinus miniatus</i>
TRI15	5.528301818	2.427629741	PtCloates	BT+DV+BS	<i>Lethrinus miniatus</i>
SD21	6.053168812	2.117186871	PtCloates	BT+DV+BS	<i>Lethrinus miniatus</i>
meanc21	4.776333252	2.08923436	PtCloates	BT+DV+BS	<i>Lethrinus miniatus</i>
fractal15	4.649325579	1.988449099	PtCloates	BT+DV+BS	<i>Lethrinus miniatus</i>
profc21	4.936413148	1.95993082	PtCloates	BT+DV+BS	<i>Lethrinus miniatus</i>
fractal21	3.013338155	1.905077288	PtCloates	BT+DV+BS	<i>Lethrinus miniatus</i>
BS	4.408391474	1.722748521	PtCloates	BT+DV+BS	<i>Lethrinus miniatus</i>
rough15	5.118409244	1.701178028	PtCloates	BT+DV+BS	<i>Lethrinus miniatus</i>
SD3	4.196691059	1.678724034	PtCloates	BT+DV+BS	<i>Lethrinus miniatus</i>
slope9	4.386769238	1.658539482	PtCloates	BT+DV+BS	<i>Lethrinus miniatus</i>
rough3	4.244741565	1.580637395	PtCloates	BT+DV+BS	<i>Lethrinus miniatus</i>
slope21	4.633335241	1.47797688	PtCloates	BT+DV+BS	<i>Lethrinus miniatus</i>
TRI3	3.730232309	1.382854776	PtCloates	BT+DV+BS	<i>Lethrinus miniatus</i>
slope15	3.637256914	1.363173457	PtCloates	BT+DV+BS	<i>Lethrinus miniatus</i>
slope3	2.789852727	1.352650306	PtCloates	BT+DV+BS	<i>Lethrinus miniatus</i>
profc9	3.817520696	1.303393327	PtCloates	BT+DV+BS	<i>Lethrinus miniatus</i>
meanc9	2.603456657	1.028343117	PtCloates	BT+DV+BS	<i>Lethrinus miniatus</i>
Depth	57.29127338	7.264568996	Gnaraloo	BT+DV	<i>Lethrinus miniatus</i>
TRI9	13.95639425	1.464776642	Gnaraloo	BT+DV	<i>Lethrinus miniatus</i>
Depth	17.33289711	6.344534437	Gnaraloo	BT+DV+BS	<i>Lethrinus miniatus</i>
BS	7.543162487	2.885705041	Gnaraloo	BT+DV+BS	<i>Lethrinus miniatus</i>
ARA_Phi	3.914670416	1.723022504	Gnaraloo	BT+DV+BS	<i>Lethrinus miniatus</i>
TRI9	3.874472267	1.299048351	Gnaraloo	BT+DV+BS	<i>Lethrinus miniatus</i>
profc15	4.028558673	1.094171294	Gnaraloo	BT+DV+BS	<i>Lethrinus miniatus</i>

Variable	Mean Decrease Accuracy	Mean Decrease Gini	Location	Scenario	Species
Depth	11.94216657	3.168653912	Mandu	BT+DV	<i>Loxodon macrorhinus</i>
NS3	6.536278445	2.092641735	Mandu	BT+DV	<i>Loxodon macrorhinus</i>
rough3	16.02859152	2.032771267	Mandu	BT+DV	<i>Loxodon macrorhinus</i>
TRI3	14.38323405	1.920184455	Mandu	BT+DV	<i>Loxodon macrorhinus</i>
planc9	6.015008699	1.882870721	Mandu	BT+DV	<i>Loxodon macrorhinus</i>
slope3	10.66085366	1.854212998	Mandu	BT+DV	<i>Loxodon macrorhinus</i>
fractal15	12.73923668	1.852846529	Mandu	BT+DV	<i>Loxodon macrorhinus</i>
fractal9	11.95372597	1.811747562	Mandu	BT+DV	<i>Loxodon macrorhinus</i>
SD3	12.49244014	1.808666151	Mandu	BT+DV	<i>Loxodon macrorhinus</i>
NS9	7.565317365	1.676780299	Mandu	BT+DV	<i>Loxodon macrorhinus</i>
fractal21	10.55089987	1.585200145	Mandu	BT+DV	<i>Loxodon macrorhinus</i>
NS15	4.050732305	1.477103253	Mandu	BT+DV	<i>Loxodon macrorhinus</i>
meanc9	4.100598063	1.456789977	Mandu	BT+DV	<i>Loxodon macrorhinus</i>
WE3	6.573327648	1.424110379	Mandu	BT+DV	<i>Loxodon macrorhinus</i>
profc21	9.357075655	1.411652885	Mandu	BT+DV	<i>Loxodon macrorhinus</i>
NS21	7.330300367	1.376327558	Mandu	BT+DV	<i>Loxodon macrorhinus</i>
BPI21	3.715835785	1.301740187	Mandu	BT+DV	<i>Loxodon macrorhinus</i>
meanc15	4.54013541	1.23121186	Mandu	BT+DV	<i>Loxodon macrorhinus</i>
WE21	4.407118323	1.204427516	Mandu	BT+DV	<i>Loxodon macrorhinus</i>
WE15	4.127552948	1.163563495	Mandu	BT+DV	<i>Loxodon macrorhinus</i>
rough9	12.38048908	1.14380708	Mandu	BT+DV	<i>Loxodon macrorhinus</i>
TRI9	13.09292611	1.128531885	Mandu	BT+DV	<i>Loxodon macrorhinus</i>
profc15	5.026743341	1.093265363	Mandu	BT+DV	<i>Loxodon macrorhinus</i>
slope9	10.91359008	1.06225447	Mandu	BT+DV	<i>Loxodon macrorhinus</i>
meanc21	5.365747256	1.045030215	Mandu	BT+DV	<i>Loxodon macrorhinus</i>
TRI21	11.8973857	0.987035007	Mandu	BT+DV	<i>Loxodon macrorhinus</i>
SD9	11.66492949	0.983109025	Mandu	BT+DV	<i>Loxodon macrorhinus</i>
TRI15	10.77027104	0.943883687	Mandu	BT+DV	<i>Loxodon macrorhinus</i>
rough15	8.534596505	0.935140994	Mandu	BT+DV	<i>Loxodon macrorhinus</i>
slope21	9.648495849	0.934311241	Mandu	BT+DV	<i>Loxodon macrorhinus</i>
SD21	9.301303597	0.895544756	Mandu	BT+DV	<i>Loxodon macrorhinus</i>
rough21	4.947083673	0.892881979	Mandu	BT+DV	<i>Loxodon macrorhinus</i>
slope15	9.966113088	0.866908517	Mandu	BT+DV	<i>Loxodon macrorhinus</i>
SD15	8.032590466	0.795968067	Mandu	BT+DV	<i>Loxodon macrorhinus</i>
Depth	5.616267293	2.817264122	Mandu	BT+DV+BS	<i>Loxodon macrorhinus</i>
TRI3	5.56658528	1.909316798	Mandu	BT+DV+BS	<i>Loxodon macrorhinus</i>
BS	2.656636911	1.897941183	Mandu	BT+DV+BS	<i>Loxodon macrorhinus</i>
rough3	4.105507799	1.853460343	Mandu	BT+DV+BS	<i>Loxodon macrorhinus</i>
planc9	2.456636513	1.682725083	Mandu	BT+DV+BS	<i>Loxodon macrorhinus</i>
slope3	3.188090715	1.682549624	Mandu	BT+DV+BS	<i>Loxodon macrorhinus</i>
SD3	4.93004554	1.606826229	Mandu	BT+DV+BS	<i>Loxodon macrorhinus</i>
fractal9	2.814119945	1.555834436	Mandu	BT+DV+BS	<i>Loxodon macrorhinus</i>
fractal15	3.098169141	1.522542613	Mandu	BT+DV+BS	<i>Loxodon macrorhinus</i>
fractal21	4.336293461	1.504123011	Mandu	BT+DV+BS	<i>Loxodon macrorhinus</i>
NS21	2.349248527	1.478051911	Mandu	BT+DV+BS	<i>Loxodon macrorhinus</i>
BPI21	3.146747711	1.277245004	Mandu	BT+DV+BS	<i>Loxodon macrorhinus</i>
meanc15	1.742673579	1.218842512	Mandu	BT+DV+BS	<i>Loxodon macrorhinus</i>
WE3	1.16419366	1.187951097	Mandu	BT+DV+BS	<i>Loxodon macrorhinus</i>
meanc3	1.918984321	1.183181231	Mandu	BT+DV+BS	<i>Loxodon macrorhinus</i>
meanc9	1.788152828	1.16634556	Mandu	BT+DV+BS	<i>Loxodon macrorhinus</i>
profc21	2.947460623	1.105446645	Mandu	BT+DV+BS	<i>Loxodon macrorhinus</i>
slope9	3.736121772	1.06962217	Mandu	BT+DV+BS	<i>Loxodon macrorhinus</i>
profc15	1.884212793	1.047819329	Mandu	BT+DV+BS	<i>Loxodon macrorhinus</i>

Variable	Mean Decrease Accuracy	Mean Decrease Gini	Location	Scenario	Species
TRI9	3.091603688	1.018807826	Mandu	BT+DV+BS	<i>Loxodon macrorhinus</i>
meanc21	1.788283884	0.999249292	Mandu	BT+DV+BS	<i>Loxodon macrorhinus</i>
rough9	2.991506194	0.994106963	Mandu	BT+DV+BS	<i>Loxodon macrorhinus</i>
WE15	1.321954211	0.967935588	Mandu	BT+DV+BS	<i>Loxodon macrorhinus</i>
TRI15	4.29764675	0.945394934	Mandu	BT+DV+BS	<i>Loxodon macrorhinus</i>
TRI21	3.705801658	0.916559255	Mandu	BT+DV+BS	<i>Loxodon macrorhinus</i>
SD15	3.215209958	0.856978729	Mandu	BT+DV+BS	<i>Loxodon macrorhinus</i>
SD9	3.197261998	0.854405583	Mandu	BT+DV+BS	<i>Loxodon macrorhinus</i>
rough15	2.683564834	0.854250229	Mandu	BT+DV+BS	<i>Loxodon macrorhinus</i>
slope15	2.192181391	0.818045277	Mandu	BT+DV+BS	<i>Loxodon macrorhinus</i>
slope21	2.726451032	0.791613549	Mandu	BT+DV+BS	<i>Loxodon macrorhinus</i>
SD21	2.973470286	0.710162635	Mandu	BT+DV+BS	<i>Loxodon macrorhinus</i>
TRI21	27.81787302	3.109111567	PtCloates	BT+DV	<i>Loxodon macrorhinus</i>
TRI15	29.90340757	2.891886417	PtCloates	BT+DV	<i>Loxodon macrorhinus</i>
TRI9	26.0195349	2.651162115	PtCloates	BT+DV	<i>Loxodon macrorhinus</i>
SD9	24.84789847	2.308386885	PtCloates	BT+DV	<i>Loxodon macrorhinus</i>
SD21	18.01439278	1.785678961	PtCloates	BT+DV	<i>Loxodon macrorhinus</i>
SD15	19.0391548	1.703630838	PtCloates	BT+DV	<i>Loxodon macrorhinus</i>
slope9	14.80868138	1.666532045	PtCloates	BT+DV	<i>Loxodon macrorhinus</i>
rough9	20.25818923	1.639012699	PtCloates	BT+DV	<i>Loxodon macrorhinus</i>
fractal9	14.50629155	1.585931282	PtCloates	BT+DV	<i>Loxodon macrorhinus</i>
planc9	11.41859246	1.579971851	PtCloates	BT+DV	<i>Loxodon macrorhinus</i>
slope15	11.70934131	1.423301045	PtCloates	BT+DV	<i>Loxodon macrorhinus</i>
planc3	8.672289362	1.307700079	PtCloates	BT+DV	<i>Loxodon macrorhinus</i>
TRI3	18.25387226	1.290367184	PtCloates	BT+DV	<i>Loxodon macrorhinus</i>
NS9	8.788535087	1.144867442	PtCloates	BT+DV	<i>Loxodon macrorhinus</i>
SD3	15.18116057	1.05745702	PtCloates	BT+DV	<i>Loxodon macrorhinus</i>
rough15	14.7406743	1.038550016	PtCloates	BT+DV	<i>Loxodon macrorhinus</i>
slope3	11.33326316	0.991571747	PtCloates	BT+DV	<i>Loxodon macrorhinus</i>
profc3	7.248182883	0.967910457	PtCloates	BT+DV	<i>Loxodon macrorhinus</i>
rough21	11.17341939	0.937056443	PtCloates	BT+DV	<i>Loxodon macrorhinus</i>
rough3	12.99818766	0.843371449	PtCloates	BT+DV	<i>Loxodon macrorhinus</i>
meanc9	6.415051512	0.816809733	PtCloates	BT+DV	<i>Loxodon macrorhinus</i>
TRI21	7.821436663	3.076597305	PtCloates	BT+DV+BS	<i>Loxodon macrorhinus</i>
TRI15	8.590538498	2.928773847	PtCloates	BT+DV+BS	<i>Loxodon macrorhinus</i>
SD9	8.140858528	2.231382036	PtCloates	BT+DV+BS	<i>Loxodon macrorhinus</i>
TRI9	7.839086922	2.195609889	PtCloates	BT+DV+BS	<i>Loxodon macrorhinus</i>
slope9	4.634792624	1.962544825	PtCloates	BT+DV+BS	<i>Loxodon macrorhinus</i>
SD15	6.180962978	1.705340222	PtCloates	BT+DV+BS	<i>Loxodon macrorhinus</i>
SD21	5.619094591	1.578300953	PtCloates	BT+DV+BS	<i>Loxodon macrorhinus</i>
rough9	6.410101622	1.539971093	PtCloates	BT+DV+BS	<i>Loxodon macrorhinus</i>
slope15	3.941519943	1.516346449	PtCloates	BT+DV+BS	<i>Loxodon macrorhinus</i>
planc3	2.852382929	1.49164319	PtCloates	BT+DV+BS	<i>Loxodon macrorhinus</i>
fractal9	3.686420679	1.359126592	PtCloates	BT+DV+BS	<i>Loxodon macrorhinus</i>
TRI3	5.605240345	1.29780936	PtCloates	BT+DV+BS	<i>Loxodon macrorhinus</i>
planc9	3.537514102	1.245095408	PtCloates	BT+DV+BS	<i>Loxodon macrorhinus</i>
SD3	6.842665075	1.145425282	PtCloates	BT+DV+BS	<i>Loxodon macrorhinus</i>
rough15	4.469895659	1.058633158	PtCloates	BT+DV+BS	<i>Loxodon macrorhinus</i>
NS9	2.528691796	1.014118554	PtCloates	BT+DV+BS	<i>Loxodon macrorhinus</i>
slope3	5.026951784	1.002292829	PtCloates	BT+DV+BS	<i>Loxodon macrorhinus</i>
fractal15	1.767547174	0.98314182	PtCloates	BT+DV+BS	<i>Loxodon macrorhinus</i>
profc3	2.271817556	0.967278209	PtCloates	BT+DV+BS	<i>Loxodon macrorhinus</i>
WE21	1.730898292	0.933867332	PtCloates	BT+DV+BS	<i>Loxodon macrorhinus</i>

Variable	Mean Decrease Accuracy	Mean Decrease Gini	Location	Scenario	Species
rough21	3.067827667	0.924099403	PtCloates	BT+DV+BS	<i>Loxodon macrorhinus</i>
rough3	5.780780025	0.907501288	PtCloates	BT+DV+BS	<i>Loxodon macrorhinus</i>
meanc9	2.695509831	0.879598986	PtCloates	BT+DV+BS	<i>Loxodon macrorhinus</i>
Depth	3.042973015	0.656566433	PtCloates	BT+DV+BS	<i>Loxodon macrorhinus</i>
BS	2.567156216	0.579748945	PtCloates	BT+DV+BS	<i>Loxodon macrorhinus</i>
BPI21	2.347168174	0.57909993	PtCloates	BT+DV+BS	<i>Loxodon macrorhinus</i>
NS3	14.12202968	2.268169929	Gnaraloo	BT+DV	<i>Loxodon macrorhinus</i>
WE15	13.96943624	1.705266833	Gnaraloo	BT+DV	<i>Loxodon macrorhinus</i>
WE21	6.634350736	1.479829081	Gnaraloo	BT+DV	<i>Loxodon macrorhinus</i>
SD3	12.91216833	1.47865553	Gnaraloo	BT+DV	<i>Loxodon macrorhinus</i>
rough3	8.975894622	1.322040406	Gnaraloo	BT+DV	<i>Loxodon macrorhinus</i>
WE3	5.287735678	1.220757749	Gnaraloo	BT+DV	<i>Loxodon macrorhinus</i>
WE9	5.479165329	1.110191279	Gnaraloo	BT+DV	<i>Loxodon macrorhinus</i>
slope3	8.077410752	1.065020188	Gnaraloo	BT+DV	<i>Loxodon macrorhinus</i>
fractal21	5.01504891	0.947388893	Gnaraloo	BT+DV	<i>Loxodon macrorhinus</i>
rough15	6.925856566	0.938583001	Gnaraloo	BT+DV	<i>Loxodon macrorhinus</i>
fractal15	3.349154735	0.915325958	Gnaraloo	BT+DV	<i>Loxodon macrorhinus</i>
meanc9	6.584473208	0.878492488	Gnaraloo	BT+DV	<i>Loxodon macrorhinus</i>
slope9	11.45302322	0.840273857	Gnaraloo	BT+DV	<i>Loxodon macrorhinus</i>
planc3	4.977720872	0.839870754	Gnaraloo	BT+DV	<i>Loxodon macrorhinus</i>
NS15	3.047515225	0.838384411	Gnaraloo	BT+DV	<i>Loxodon macrorhinus</i>
planc15	3.284253275	0.817839368	Gnaraloo	BT+DV	<i>Loxodon macrorhinus</i>
BPI9	4.646888689	0.804278231	Gnaraloo	BT+DV	<i>Loxodon macrorhinus</i>
SD9	10.54229303	0.787777074	Gnaraloo	BT+DV	<i>Loxodon macrorhinus</i>
BPI21	6.871666762	0.778706078	Gnaraloo	BT+DV	<i>Loxodon macrorhinus</i>
TRI9	8.966035318	0.719858041	Gnaraloo	BT+DV	<i>Loxodon macrorhinus</i>
BPI15	5.643972473	0.715189102	Gnaraloo	BT+DV	<i>Loxodon macrorhinus</i>
TRI15	10.66118211	0.706741707	Gnaraloo	BT+DV	<i>Loxodon macrorhinus</i>
TRI21	8.220078958	0.697614723	Gnaraloo	BT+DV	<i>Loxodon macrorhinus</i>
slope21	6.292058537	0.692431309	Gnaraloo	BT+DV	<i>Loxodon macrorhinus</i>
SD15	7.758088739	0.677511875	Gnaraloo	BT+DV	<i>Loxodon macrorhinus</i>
slope15	4.488666025	0.652601597	Gnaraloo	BT+DV	<i>Loxodon macrorhinus</i>
rough9	6.299148925	0.622704006	Gnaraloo	BT+DV	<i>Loxodon macrorhinus</i>
SD21	4.2260587	0.615792564	Gnaraloo	BT+DV	<i>Loxodon macrorhinus</i>
NS3	3.156319191	2.16951018	Gnaraloo	BT+DV+BS	<i>Loxodon macrorhinus</i>
WE15	3.485904187	1.687449635	Gnaraloo	BT+DV+BS	<i>Loxodon macrorhinus</i>
BS	4.21838262	1.511115586	Gnaraloo	BT+DV+BS	<i>Loxodon macrorhinus</i>
Depth	1.507497362	1.415673572	Gnaraloo	BT+DV+BS	<i>Loxodon macrorhinus</i>
SD3	5.013637627	1.404979159	Gnaraloo	BT+DV+BS	<i>Loxodon macrorhinus</i>
ARA_Phi	1.134274038	1.381085074	Gnaraloo	BT+DV+BS	<i>Loxodon macrorhinus</i>
WE21	1.177170785	1.35732789	Gnaraloo	BT+DV+BS	<i>Loxodon macrorhinus</i>
rough3	3.544015103	1.355207346	Gnaraloo	BT+DV+BS	<i>Loxodon macrorhinus</i>
WE3	1.66190386	1.194667571	Gnaraloo	BT+DV+BS	<i>Loxodon macrorhinus</i>
WE9	2.639525259	1.125487124	Gnaraloo	BT+DV+BS	<i>Loxodon macrorhinus</i>
slope3	1.9523693	1.058463943	Gnaraloo	BT+DV+BS	<i>Loxodon macrorhinus</i>
planc3	1.473347142	0.866766647	Gnaraloo	BT+DV+BS	<i>Loxodon macrorhinus</i>
fractal9	1.344564667	0.822690008	Gnaraloo	BT+DV+BS	<i>Loxodon macrorhinus</i>
meanc9	2.752797216	0.821100271	Gnaraloo	BT+DV+BS	<i>Loxodon macrorhinus</i>
BPI21	2.334581426	0.79266897	Gnaraloo	BT+DV+BS	<i>Loxodon macrorhinus</i>
rough15	2.243670594	0.759099052	Gnaraloo	BT+DV+BS	<i>Loxodon macrorhinus</i>
BPI9	3.089523236	0.735290473	Gnaraloo	BT+DV+BS	<i>Loxodon macrorhinus</i>
profc15	1.495573534	0.710519889	Gnaraloo	BT+DV+BS	<i>Loxodon macrorhinus</i>
TRI21	1.873009458	0.69726926	Gnaraloo	BT+DV+BS	<i>Loxodon macrorhinus</i>

Variable	Mean Decrease Accuracy	Mean Decrease Gini	Location	Scenario	Species
SD9	1.305004889	0.690448298	Gnaraloo	BT+DV+BS	<i>Loxodon macrorhinus</i>
NS15	1.325210534	0.667752044	Gnaraloo	BT+DV+BS	<i>Loxodon macrorhinus</i>
TRI15	1.134068715	0.653778017	Gnaraloo	BT+DV+BS	<i>Loxodon macrorhinus</i>
SD15	1.865466897	0.595111102	Gnaraloo	BT+DV+BS	<i>Loxodon macrorhinus</i>
slope9	2.653627771	0.593429274	Gnaraloo	BT+DV+BS	<i>Loxodon macrorhinus</i>
SD21	1.798595849	0.577495494	Gnaraloo	BT+DV+BS	<i>Loxodon macrorhinus</i>
slope21	1.107139779	0.564649117	Gnaraloo	BT+DV+BS	<i>Loxodon macrorhinus</i>

Variable	Mean Decrease Accuracy	Mean Decrease Gini	Location	Scenario	Species
fractal15	12.21504168	1.012707434	Mandu	BT+DV	<i>Lutjanus sebae</i>
fractal9	13.16195068	0.94459306	Mandu	BT+DV	<i>Lutjanus sebae</i>
meanc15	12.0233472	1.603399137	Mandu	BT+DV	<i>Lutjanus sebae</i>
meanc21	11.67401998	1.591723693	Mandu	BT+DV	<i>Lutjanus sebae</i>
meanc3	12.85809257	1.044694659	Mandu	BT+DV	<i>Lutjanus sebae</i>
meanc9	12.74355213	1.115663938	Mandu	BT+DV	<i>Lutjanus sebae</i>
profc15	18.66832944	1.753434309	Mandu	BT+DV	<i>Lutjanus sebae</i>
profc21	17.77679806	2.15792748	Mandu	BT+DV	<i>Lutjanus sebae</i>
profc3	13.02162725	1.224135021	Mandu	BT+DV	<i>Lutjanus sebae</i>
profc9	6.281678692	1.050286641	Mandu	BT+DV	<i>Lutjanus sebae</i>
slope15	11.68601944	0.779443054	Mandu	BT+DV	<i>Lutjanus sebae</i>
slope21	11.45328712	0.713060024	Mandu	BT+DV	<i>Lutjanus sebae</i>
slope3	19.97430482	1.371105497	Mandu	BT+DV	<i>Lutjanus sebae</i>
slope9	10.00320842	0.725128012	Mandu	BT+DV	<i>Lutjanus sebae</i>
BPI15	16.39576797	1.099142905	Mandu	BT+DV	<i>Lutjanus sebae</i>
BPI21	11.70526809	1.139193978	Mandu	BT+DV	<i>Lutjanus sebae</i>
BPI3	9.441270329	0.972384257	Mandu	BT+DV	<i>Lutjanus sebae</i>
BPI9	13.06262136	0.98384194	Mandu	BT+DV	<i>Lutjanus sebae</i>
Depth	28.48499945	3.8620408	Mandu	BT+DV	<i>Lutjanus sebae</i>
NS15	5.77375421	0.788523036	Mandu	BT+DV	<i>Lutjanus sebae</i>
NS21	6.732649108	0.828853429	Mandu	BT+DV	<i>Lutjanus sebae</i>
NS9	6.617278931	0.728206622	Mandu	BT+DV	<i>Lutjanus sebae</i>
rough15	21.13357053	1.263658224	Mandu	BT+DV	<i>Lutjanus sebae</i>
rough21	11.85374888	1.088292631	Mandu	BT+DV	<i>Lutjanus sebae</i>
rough3	18.8365614	1.663974801	Mandu	BT+DV	<i>Lutjanus sebae</i>
rough9	20.20076571	1.422941449	Mandu	BT+DV	<i>Lutjanus sebae</i>
SD15	11.69692596	0.770492532	Mandu	BT+DV	<i>Lutjanus sebae</i>
SD21	10.47786213	0.708936775	Mandu	BT+DV	<i>Lutjanus sebae</i>
SD3	16.40786148	1.37580903	Mandu	BT+DV	<i>Lutjanus sebae</i>
SD9	11.2611923	0.799202017	Mandu	BT+DV	<i>Lutjanus sebae</i>
TRI15	13.96981279	0.897604067	Mandu	BT+DV	<i>Lutjanus sebae</i>
TRI21	12.78384952	0.878326345	Mandu	BT+DV	<i>Lutjanus sebae</i>
TRI3	11.09843969	1.016263566	Mandu	BT+DV	<i>Lutjanus sebae</i>
TRI9	10.95612272	1.092200104	Mandu	BT+DV	<i>Lutjanus sebae</i>
WE9	7.159325934	0.846664903	Mandu	BT+DV	<i>Lutjanus sebae</i>
fractal15	4.254362243	0.983886379	Mandu	BT+DV+BS	<i>Lutjanus sebae</i>
fractal21	2.068282794	0.667705901	Mandu	BT+DV+BS	<i>Lutjanus sebae</i>
fractal9	2.673111917	0.929992026	Mandu	BT+DV+BS	<i>Lutjanus sebae</i>
meanc15	5.2982599	1.652102431	Mandu	BT+DV+BS	<i>Lutjanus sebae</i>
meanc21	2.186068936	1.480745579	Mandu	BT+DV+BS	<i>Lutjanus sebae</i>
meanc3	2.298244227	0.989571989	Mandu	BT+DV+BS	<i>Lutjanus sebae</i>
meanc9	4.681008253	1.069498105	Mandu	BT+DV+BS	<i>Lutjanus sebae</i>
planc21	1.860155814	0.866825961	Mandu	BT+DV+BS	<i>Lutjanus sebae</i>
profc15	6.658013953	1.595559517	Mandu	BT+DV+BS	<i>Lutjanus sebae</i>
profc21	5.742818876	1.791862769	Mandu	BT+DV+BS	<i>Lutjanus sebae</i>
profc3	3.794977206	1.060677992	Mandu	BT+DV+BS	<i>Lutjanus sebae</i>
profc9	1.897688996	1.038966642	Mandu	BT+DV+BS	<i>Lutjanus sebae</i>
slope15	4.845455818	0.751163015	Mandu	BT+DV+BS	<i>Lutjanus sebae</i>
slope21	3.354473607	0.614839839	Mandu	BT+DV+BS	<i>Lutjanus sebae</i>
slope3	7.563292796	1.497000487	Mandu	BT+DV+BS	<i>Lutjanus sebae</i>
slope9	4.5535924	0.649208138	Mandu	BT+DV+BS	<i>Lutjanus sebae</i>
BPI15	4.439529937	0.910246255	Mandu	BT+DV+BS	<i>Lutjanus sebae</i>
BPI21	4.998119816	1.157687283	Mandu	BT+DV+BS	<i>Lutjanus sebae</i>
BPI3	4.795097577	0.851804438	Mandu	BT+DV+BS	<i>Lutjanus sebae</i>

Variable	Mean Decrease Accuracy	Mean Decrease Gini	Location	Scenario	Species
BPI9	4.194957868	1.058852087	Mandu	BT+DV+BS	<i>Lutjanus sebae</i>
Depth	8.450897088	3.571008138	Mandu	BT+DV+BS	<i>Lutjanus sebae</i>
NS15	2.689476382	0.784001032	Mandu	BT+DV+BS	<i>Lutjanus sebae</i>
rough15	5.99462278	1.383802098	Mandu	BT+DV+BS	<i>Lutjanus sebae</i>
rough21	3.534163207	1.030743397	Mandu	BT+DV+BS	<i>Lutjanus sebae</i>
rough3	6.054969618	1.86623859	Mandu	BT+DV+BS	<i>Lutjanus sebae</i>
rough9	6.089293177	1.535200329	Mandu	BT+DV+BS	<i>Lutjanus sebae</i>
SD15	3.389203424	0.808990639	Mandu	BT+DV+BS	<i>Lutjanus sebae</i>
SD21	3.035185144	0.726419589	Mandu	BT+DV+BS	<i>Lutjanus sebae</i>
SD3	4.597990551	1.332874183	Mandu	BT+DV+BS	<i>Lutjanus sebae</i>
SD9	4.609786695	0.790149129	Mandu	BT+DV+BS	<i>Lutjanus sebae</i>
TRI15	3.264265075	0.847391259	Mandu	BT+DV+BS	<i>Lutjanus sebae</i>
TRI21	3.882798266	0.820256136	Mandu	BT+DV+BS	<i>Lutjanus sebae</i>
TRI3	3.805458306	1.013536402	Mandu	BT+DV+BS	<i>Lutjanus sebae</i>
TRI9	3.404548783	1.149059543	Mandu	BT+DV+BS	<i>Lutjanus sebae</i>
WE9	2.041940391	0.800934738	Mandu	BT+DV+BS	<i>Lutjanus sebae</i>
fractal15	6.088551445	0.861087138	PtCloates	BT+DV	<i>Lutjanus sebae</i>
fractal21	8.386639152	1.121082647	PtCloates	BT+DV	<i>Lutjanus sebae</i>
fractal9	7.79042401	0.711950536	PtCloates	BT+DV	<i>Lutjanus sebae</i>
meanc15	12.98063542	0.960289642	PtCloates	BT+DV	<i>Lutjanus sebae</i>
meanc21	10.63843473	0.925934521	PtCloates	BT+DV	<i>Lutjanus sebae</i>
meanc3	11.50942723	1.358155181	PtCloates	BT+DV	<i>Lutjanus sebae</i>
meanc9	7.353586872	0.568522401	PtCloates	BT+DV	<i>Lutjanus sebae</i>
planc21	6.289986953	0.867177285	PtCloates	BT+DV	<i>Lutjanus sebae</i>
planc9	6.2396591	0.956162827	PtCloates	BT+DV	<i>Lutjanus sebae</i>
profc15	9.377932334	0.864455385	PtCloates	BT+DV	<i>Lutjanus sebae</i>
profc21	7.219302349	0.871649633	PtCloates	BT+DV	<i>Lutjanus sebae</i>
profc9	6.21262904	0.602787364	PtCloates	BT+DV	<i>Lutjanus sebae</i>
slope15	10.61982965	0.778089692	PtCloates	BT+DV	<i>Lutjanus sebae</i>
slope21	10.23722407	0.892950161	PtCloates	BT+DV	<i>Lutjanus sebae</i>
slope3	9.559580448	0.660211143	PtCloates	BT+DV	<i>Lutjanus sebae</i>
slope9	7.619170034	0.602939696	PtCloates	BT+DV	<i>Lutjanus sebae</i>
BPI15	8.888062826	0.617076657	PtCloates	BT+DV	<i>Lutjanus sebae</i>
BPI21	11.6303594	0.775171166	PtCloates	BT+DV	<i>Lutjanus sebae</i>
BPI9	7.948998335	0.776282696	PtCloates	BT+DV	<i>Lutjanus sebae</i>
Depth	28.08490091	4.040962113	PtCloates	BT+DV	<i>Lutjanus sebae</i>
NS15	10.84359975	1.469542368	PtCloates	BT+DV	<i>Lutjanus sebae</i>
NS21	9.667369157	1.234159685	PtCloates	BT+DV	<i>Lutjanus sebae</i>
NS9	7.848647351	0.951080898	PtCloates	BT+DV	<i>Lutjanus sebae</i>
rough15	11.87979455	0.941857491	PtCloates	BT+DV	<i>Lutjanus sebae</i>
rough21	15.87510137	1.119622134	PtCloates	BT+DV	<i>Lutjanus sebae</i>
rough3	6.722532422	0.63729793	PtCloates	BT+DV	<i>Lutjanus sebae</i>
rough9	10.07794978	0.673053975	PtCloates	BT+DV	<i>Lutjanus sebae</i>
SD15	13.76417571	0.855543559	PtCloates	BT+DV	<i>Lutjanus sebae</i>
SD21	14.84811039	0.857863017	PtCloates	BT+DV	<i>Lutjanus sebae</i>
SD3	10.34370947	0.639794191	PtCloates	BT+DV	<i>Lutjanus sebae</i>
SD9	12.56250645	0.669035541	PtCloates	BT+DV	<i>Lutjanus sebae</i>
TRI15	10.46108638	0.570677213	PtCloates	BT+DV	<i>Lutjanus sebae</i>
TRI21	11.86214192	0.590094083	PtCloates	BT+DV	<i>Lutjanus sebae</i>
TRI3	8.766214591	0.798553465	PtCloates	BT+DV	<i>Lutjanus sebae</i>
TRI9	8.68664136	0.559222828	PtCloates	BT+DV	<i>Lutjanus sebae</i>
WE21	10.28192806	1.516378761	PtCloates	BT+DV	<i>Lutjanus sebae</i>
fractal15	2.651927634	0.78266446	PtCloates	BT+DV+BS	<i>Lutjanus sebae</i>
fractal21	2.546870289	0.876229981	PtCloates	BT+DV+BS	<i>Lutjanus sebae</i>

Variable	Mean Decrease Accuracy	Mean Decrease Gini	Location	Scenario	Species
fractal9	3.295970738	0.698424873	PtCloates	BT+DV+BS	<i>Lutjanus sebae</i>
meanc15	5.41499111	1.029864117	PtCloates	BT+DV+BS	<i>Lutjanus sebae</i>
meanc21	3.390771872	0.818759275	PtCloates	BT+DV+BS	<i>Lutjanus sebae</i>
meanc3	3.972422746	1.155907811	PtCloates	BT+DV+BS	<i>Lutjanus sebae</i>
meanc9	2.074637837	0.368547615	PtCloates	BT+DV+BS	<i>Lutjanus sebae</i>
profc15	2.396741194	0.67331848	PtCloates	BT+DV+BS	<i>Lutjanus sebae</i>
slope15	2.766346493	0.771431354	PtCloates	BT+DV+BS	<i>Lutjanus sebae</i>
slope21	2.644268494	0.677212713	PtCloates	BT+DV+BS	<i>Lutjanus sebae</i>
slope9	3.6124239	0.601190211	PtCloates	BT+DV+BS	<i>Lutjanus sebae</i>
ARA_Phi	5.59315477	2.432823723	PtCloates	BT+DV+BS	<i>Lutjanus sebae</i>
BPI15	2.506202058	0.663590401	PtCloates	BT+DV+BS	<i>Lutjanus sebae</i>
BPI21	3.066229724	0.610664996	PtCloates	BT+DV+BS	<i>Lutjanus sebae</i>
BS	7.312891464	1.875473147	PtCloates	BT+DV+BS	<i>Lutjanus sebae</i>
Depth	9.000246092	3.164257843	PtCloates	BT+DV+BS	<i>Lutjanus sebae</i>
NS15	3.432027274	1.560310452	PtCloates	BT+DV+BS	<i>Lutjanus sebae</i>
NS21	2.228624294	1.188100535	PtCloates	BT+DV+BS	<i>Lutjanus sebae</i>
rough15	3.132601904	0.938422721	PtCloates	BT+DV+BS	<i>Lutjanus sebae</i>
rough21	4.590653613	1.051985533	PtCloates	BT+DV+BS	<i>Lutjanus sebae</i>
rough3	1.913476806	0.514598411	PtCloates	BT+DV+BS	<i>Lutjanus sebae</i>
rough9	1.966208039	0.565675516	PtCloates	BT+DV+BS	<i>Lutjanus sebae</i>
SD15	4.095980385	0.729805522	PtCloates	BT+DV+BS	<i>Lutjanus sebae</i>
SD21	4.793688913	0.737935874	PtCloates	BT+DV+BS	<i>Lutjanus sebae</i>
SD3	2.997550876	0.496211231	PtCloates	BT+DV+BS	<i>Lutjanus sebae</i>
SD9	4.326195903	0.553196207	PtCloates	BT+DV+BS	<i>Lutjanus sebae</i>
TRI15	3.006445948	0.493146387	PtCloates	BT+DV+BS	<i>Lutjanus sebae</i>
TRI21	2.689719997	0.528377524	PtCloates	BT+DV+BS	<i>Lutjanus sebae</i>
TRI3	4.359611938	0.719440343	PtCloates	BT+DV+BS	<i>Lutjanus sebae</i>
TRI9	2.407745374	0.4771056	PtCloates	BT+DV+BS	<i>Lutjanus sebae</i>
WE15	2.781713097	0.813310227	PtCloates	BT+DV+BS	<i>Lutjanus sebae</i>
fractal15	4.871901125	0.87181638	Gnaraloo	BT+DV	<i>Lutjanus sebae</i>
fractal21	12.86710833	1.757155982	Gnaraloo	BT+DV	<i>Lutjanus sebae</i>
meanc15	4.672463108	0.775054605	Gnaraloo	BT+DV	<i>Lutjanus sebae</i>
meanc9	7.103756678	1.236080755	Gnaraloo	BT+DV	<i>Lutjanus sebae</i>
planc15	8.646067948	0.907251356	Gnaraloo	BT+DV	<i>Lutjanus sebae</i>
planc9	10.58285711	1.494947852	Gnaraloo	BT+DV	<i>Lutjanus sebae</i>
profc21	5.372192629	0.823966688	Gnaraloo	BT+DV	<i>Lutjanus sebae</i>
profc9	15.75473583	1.83505429	Gnaraloo	BT+DV	<i>Lutjanus sebae</i>
slope15	9.962557464	1.141939896	Gnaraloo	BT+DV	<i>Lutjanus sebae</i>
slope21	5.020931479	1.001270704	Gnaraloo	BT+DV	<i>Lutjanus sebae</i>
slope9	22.24782196	2.525190937	Gnaraloo	BT+DV	<i>Lutjanus sebae</i>
BPI15	7.358704616	1.059479937	Gnaraloo	BT+DV	<i>Lutjanus sebae</i>
BPI21	8.631070927	1.105052635	Gnaraloo	BT+DV	<i>Lutjanus sebae</i>
BPI9	11.39047118	1.573409727	Gnaraloo	BT+DV	<i>Lutjanus sebae</i>
Depth	10.63895234	2.41575269	Gnaraloo	BT+DV	<i>Lutjanus sebae</i>
rough15	10.53104512	1.034684518	Gnaraloo	BT+DV	<i>Lutjanus sebae</i>
rough21	20.66891289	1.840649081	Gnaraloo	BT+DV	<i>Lutjanus sebae</i>
rough9	10.40692851	1.086612425	Gnaraloo	BT+DV	<i>Lutjanus sebae</i>
SD15	10.25043905	0.807719582	Gnaraloo	BT+DV	<i>Lutjanus sebae</i>
SD21	10.84375573	1.054891734	Gnaraloo	BT+DV	<i>Lutjanus sebae</i>
SD9	7.357782541	0.785952653	Gnaraloo	BT+DV	<i>Lutjanus sebae</i>
TRI15	8.053222973	0.688718234	Gnaraloo	BT+DV	<i>Lutjanus sebae</i>
TRI21	8.921552501	0.693782399	Gnaraloo	BT+DV	<i>Lutjanus sebae</i>
TRI9	9.242801297	0.923032477	Gnaraloo	BT+DV	<i>Lutjanus sebae</i>
WE15	9.759264954	1.321021938	Gnaraloo	BT+DV	<i>Lutjanus sebae</i>

Variable	Mean Decrease Accuracy	Mean Decrease Gini	Location	Scenario	Species
WE3	6.29281655	0.949400347	Gnaraloo	BT+DV	<i>Lutjanus sebae</i>
fractal21	3.003106387	1.676384704	Gnaraloo	BT+DV+BS	<i>Lutjanus sebae</i>
meanc15	1.61286145	0.877901304	Gnaraloo	BT+DV+BS	<i>Lutjanus sebae</i>
planc15	3.571525193	0.835337528	Gnaraloo	BT+DV+BS	<i>Lutjanus sebae</i>
planc21	2.687811518	1.010320182	Gnaraloo	BT+DV+BS	<i>Lutjanus sebae</i>
planc9	2.077011447	1.364707284	Gnaraloo	BT+DV+BS	<i>Lutjanus sebae</i>
profc9	4.371731094	1.787503713	Gnaraloo	BT+DV+BS	<i>Lutjanus sebae</i>
slope15	1.738408418	0.933013119	Gnaraloo	BT+DV+BS	<i>Lutjanus sebae</i>
slope21	2.418394355	0.857950898	Gnaraloo	BT+DV+BS	<i>Lutjanus sebae</i>
slope9	7.047326078	2.335257573	Gnaraloo	BT+DV+BS	<i>Lutjanus sebae</i>
BPI15	2.030474441	0.830575161	Gnaraloo	BT+DV+BS	<i>Lutjanus sebae</i>
BPI21	3.508222121	1.20640954	Gnaraloo	BT+DV+BS	<i>Lutjanus sebae</i>
BPI9	3.608242811	1.333546204	Gnaraloo	BT+DV+BS	<i>Lutjanus sebae</i>
Depth	5.635301371	2.338246399	Gnaraloo	BT+DV+BS	<i>Lutjanus sebae</i>
rough15	4.429080188	1.089534076	Gnaraloo	BT+DV+BS	<i>Lutjanus sebae</i>
rough21	6.66481005	1.888410756	Gnaraloo	BT+DV+BS	<i>Lutjanus sebae</i>
rough9	2.64192328	1.093230431	Gnaraloo	BT+DV+BS	<i>Lutjanus sebae</i>
SD15	3.250694217	0.799080062	Gnaraloo	BT+DV+BS	<i>Lutjanus sebae</i>
SD21	2.394059374	1.105812005	Gnaraloo	BT+DV+BS	<i>Lutjanus sebae</i>
SD9	2.060020227	0.722418175	Gnaraloo	BT+DV+BS	<i>Lutjanus sebae</i>
TRI15	2.521889676	0.652251845	Gnaraloo	BT+DV+BS	<i>Lutjanus sebae</i>
TRI21	3.03568141	0.607134154	Gnaraloo	BT+DV+BS	<i>Lutjanus sebae</i>
TRI9	2.838509714	0.836983354	Gnaraloo	BT+DV+BS	<i>Lutjanus sebae</i>
WE15	1.472630055	1.166968214	Gnaraloo	BT+DV+BS	<i>Lutjanus sebae</i>
WE3	2.023080402	0.756553068	Gnaraloo	BT+DV+BS	<i>Lutjanus sebae</i>

Variable	Mean Decrease Accuracy	Mean Decrease Gini	Location	Scenario	Species
fractal15	21.53894248	2.031319682	Mandu	BT+DV	<i>Pristipomoides multidentis</i>
profc3	22.58892269	3.46092	Mandu	BT+DV	<i>Pristipomoides multidentis</i>
Depth	89.82604637	20.59653564	Mandu	BT+DV	<i>Pristipomoides multidentis</i>
fractal15	7.066962703	2.307497152	Mandu	BT+DV+BS	<i>Pristipomoides multidentis</i>
profc3	7.554208864	3.472080793	Mandu	BT+DV+BS	<i>Pristipomoides multidentis</i>
Depth	26.42859392	18.34552326	Mandu	BT+DV+BS	<i>Pristipomoides multidentis</i>
slope15	10.22236062	0.303985358	PtCloates	BT+DV	<i>Pristipomoides multidentis</i>
slope9	13.1536005	0.47720209	PtCloates	BT+DV	<i>Pristipomoides multidentis</i>
Depth	50.89535317	6.753849339	PtCloates	BT+DV	<i>Pristipomoides multidentis</i>
NS15	13.45334773	0.86622732	PtCloates	BT+DV	<i>Pristipomoides multidentis</i>
NS9	11.34396331	0.834335214	PtCloates	BT+DV	<i>Pristipomoides multidentis</i>
rough15	12.81480378	0.407174221	PtCloates	BT+DV	<i>Pristipomoides multidentis</i>
rough21	10.29571306	0.288438721	PtCloates	BT+DV	<i>Pristipomoides multidentis</i>
SD15	10.98936427	0.292586588	PtCloates	BT+DV	<i>Pristipomoides multidentis</i>
SD21	10.74819185	0.278098662	PtCloates	BT+DV	<i>Pristipomoides multidentis</i>
SD9	10.65612197	0.357464287	PtCloates	BT+DV	<i>Pristipomoides multidentis</i>
WE21	16.64158479	1.179279041	PtCloates	BT+DV	<i>Pristipomoides multidentis</i>
slope15	3.312666552	0.314838241	PtCloates	BT+DV+BS	<i>Pristipomoides multidentis</i>
slope9	4.566533394	0.41609149	PtCloates	BT+DV+BS	<i>Pristipomoides multidentis</i>
ARA_Phi	9.936263481	3.025666146	PtCloates	BT+DV+BS	<i>Pristipomoides multidentis</i>
BPI15	3.078948923	0.13719238	PtCloates	BT+DV+BS	<i>Pristipomoides multidentis</i>
BS	5.26116684	1.176999715	PtCloates	BT+DV+BS	<i>Pristipomoides multidentis</i>
Depth	13.82693806	5.560833959	PtCloates	BT+DV+BS	<i>Pristipomoides multidentis</i>
NS15	4.720604679	0.658611235	PtCloates	BT+DV+BS	<i>Pristipomoides multidentis</i>
NS21	2.863563779	0.457064218	PtCloates	BT+DV+BS	<i>Pristipomoides multidentis</i>
NS9	3.158818886	0.666187843	PtCloates	BT+DV+BS	<i>Pristipomoides multidentis</i>
SD21	4.031195967	0.360993258	PtCloates	BT+DV+BS	<i>Pristipomoides multidentis</i>
SD9	4.093655857	0.305159776	PtCloates	BT+DV+BS	<i>Pristipomoides multidentis</i>
TRI21	2.913886718	0.1739254	PtCloates	BT+DV+BS	<i>Pristipomoides multidentis</i>
WE21	4.137520061	0.760575529	PtCloates	BT+DV+BS	<i>Pristipomoides multidentis</i>
WE9	2.918873487	0.342578945	PtCloates	BT+DV+BS	<i>Pristipomoides multidentis</i>
slope15	19.2980654	2.271668832	Gnaraloo	BT+DV	<i>Pristipomoides multidentis</i>
Depth	76.8027483	14.90696952	Gnaraloo	BT+DV	<i>Pristipomoides multidentis</i>
fractal15	4.870153777	1.643016491	Gnaraloo	BT+DV+BS	<i>Pristipomoides multidentis</i>
slope15	6.903574434	2.015998188	Gnaraloo	BT+DV+BS	<i>Pristipomoides multidentis</i>
ARA_Phi	12.71375999	5.747694745	Gnaraloo	BT+DV+BS	<i>Pristipomoides multidentis</i>
BS	8.346534005	3.409356947	Gnaraloo	BT+DV+BS	<i>Pristipomoides multidentis</i>
Depth	23.52270035	13.43514927	Gnaraloo	BT+DV+BS	<i>Pristipomoides multidentis</i>

Variable	Mean Decrease Accuracy	Mean Decrease Gini	Location	Scenario	Species
Depth	90.74691116	21.0854806	Mandu	BT+DV	<i>Pristipomoides typus</i>
Depth	27.52057949	19.83924407	Mandu	BT+DV+BS	<i>Pristipomoides typus</i>
slope15	14.23014612	0.664737549	PtCloates	BT+DV	<i>Pristipomoides typus</i>
Depth	69.60455647	11.91126441	PtCloates	BT+DV	<i>Pristipomoides typus</i>
rough15	22.55313478	1.1550287	PtCloates	BT+DV	<i>Pristipomoides typus</i>
rough21	24.39168937	1.239679152	PtCloates	BT+DV	<i>Pristipomoides typus</i>
rough9	14.2393079	0.852252092	PtCloates	BT+DV	<i>Pristipomoides typus</i>
SD15	19.07157116	0.911346306	PtCloates	BT+DV	<i>Pristipomoides typus</i>
SD21	20.26985298	1.018448768	PtCloates	BT+DV	<i>Pristipomoides typus</i>
SD9	19.46358907	1.003311964	PtCloates	BT+DV	<i>Pristipomoides typus</i>
TRI15	16.85755461	0.703893359	PtCloates	BT+DV	<i>Pristipomoides typus</i>
TRI21	19.69217629	0.84924883	PtCloates	BT+DV	<i>Pristipomoides typus</i>
fractal15	3.802629164	0.489569271	PtCloates	BT+DV+BS	<i>Pristipomoides typus</i>
fractal21	3.631783028	0.433932126	PtCloates	BT+DV+BS	<i>Pristipomoides typus</i>
profc15	4.391731539	0.326190382	PtCloates	BT+DV+BS	<i>Pristipomoides typus</i>
slope15	4.602407634	0.463872679	PtCloates	BT+DV+BS	<i>Pristipomoides typus</i>
ARA_Phi	14.20199106	6.874501415	PtCloates	BT+DV+BS	<i>Pristipomoides typus</i>
BS	7.278166564	2.163787598	PtCloates	BT+DV+BS	<i>Pristipomoides typus</i>
Depth	17.90324923	8.957247052	PtCloates	BT+DV+BS	<i>Pristipomoides typus</i>
NS9	4.055158943	0.697344032	PtCloates	BT+DV+BS	<i>Pristipomoides typus</i>
rough15	6.195572176	0.797990904	PtCloates	BT+DV+BS	<i>Pristipomoides typus</i>
rough21	6.433043479	0.916241048	PtCloates	BT+DV+BS	<i>Pristipomoides typus</i>
SD15	5.97188065	0.893931314	PtCloates	BT+DV+BS	<i>Pristipomoides typus</i>
SD21	6.043573274	0.951466014	PtCloates	BT+DV+BS	<i>Pristipomoides typus</i>
SD9	4.758294872	0.670801999	PtCloates	BT+DV+BS	<i>Pristipomoides typus</i>
TRI15	5.601636756	0.600936084	PtCloates	BT+DV+BS	<i>Pristipomoides typus</i>
TRI21	5.104563989	0.666666898	PtCloates	BT+DV+BS	<i>Pristipomoides typus</i>
profc9	7.90760746	0.619493889	Gnaraloo	BT+DV	<i>Pristipomoides typus</i>
Depth	36.10122079	3.781761425	Gnaraloo	BT+DV	<i>Pristipomoides typus</i>
NS21	11.26334099	0.735929798	Gnaraloo	BT+DV	<i>Pristipomoides typus</i>
rough15	8.596443347	0.496273724	Gnaraloo	BT+DV	<i>Pristipomoides typus</i>
SD15	8.104858012	0.402355204	Gnaraloo	BT+DV	<i>Pristipomoides typus</i>
TRI15	11.4144733	0.424099919	Gnaraloo	BT+DV	<i>Pristipomoides typus</i>
TRI21	8.187343996	0.425926009	Gnaraloo	BT+DV	<i>Pristipomoides typus</i>
TRI9	8.673271251	0.548740587	Gnaraloo	BT+DV	<i>Pristipomoides typus</i>
ARA_Phi	5.162269019	1.373856992	Gnaraloo	BT+DV+BS	<i>Pristipomoides typus</i>
BPI21	2.523128211	0.319860842	Gnaraloo	BT+DV+BS	<i>Pristipomoides typus</i>
BS	3.764920938	1.204948747	Gnaraloo	BT+DV+BS	<i>Pristipomoides typus</i>
Depth	10.45712574	3.567092425	Gnaraloo	BT+DV+BS	<i>Pristipomoides typus</i>
NS21	3.899684965	0.650453495	Gnaraloo	BT+DV+BS	<i>Pristipomoides typus</i>
rough15	2.564481453	0.414094212	Gnaraloo	BT+DV+BS	<i>Pristipomoides typus</i>
rough21	2.211675109	0.381652389	Gnaraloo	BT+DV+BS	<i>Pristipomoides typus</i>
rough9	2.299394052	0.336296062	Gnaraloo	BT+DV+BS	<i>Pristipomoides typus</i>
SD21	3.197082912	0.325944781	Gnaraloo	BT+DV+BS	<i>Pristipomoides typus</i>

Variable	Mean Decrease Accuracy	Mean Decrease Gini	Location	Scenario	Species
fractal15	21.58226866	1.831905589	Mandu	BT+DV	<i>Scomberomorus queenslandicus</i>
fractal21	26.90396209	2.682681234	Mandu	BT+DV	<i>Scomberomorus queenslandicus</i>
fractal9	23.9014804	1.640659169	Mandu	BT+DV	<i>Scomberomorus queenslandicus</i>
slope15	17.97973646	0.844798536	Mandu	BT+DV	<i>Scomberomorus queenslandicus</i>
slope21	17.23637228	0.918981391	Mandu	BT+DV	<i>Scomberomorus queenslandicus</i>
slope3	10.65093577	0.738048052	Mandu	BT+DV	<i>Scomberomorus queenslandicus</i>
slope9	14.42361961	0.82811341	Mandu	BT+DV	<i>Scomberomorus queenslandicus</i>
BPI15	6.546208542	0.842112148	Mandu	BT+DV	<i>Scomberomorus queenslandicus</i>
BPI21	7.259298663	0.879087523	Mandu	BT+DV	<i>Scomberomorus queenslandicus</i>
BPI3	6.13445288	1.022090677	Mandu	BT+DV	<i>Scomberomorus queenslandicus</i>
BPI9	9.134986059	0.900782793	Mandu	BT+DV	<i>Scomberomorus queenslandicus</i>
BT	20.58620086	3.2165856	Mandu	BT+DV	<i>Scomberomorus queenslandicus</i>
rough15	12.62360508	0.995363341	Mandu	BT+DV	<i>Scomberomorus queenslandicus</i>
rough21	7.190946596	0.73024108	Mandu	BT+DV	<i>Scomberomorus queenslandicus</i>
rough3	11.84684803	1.196786801	Mandu	BT+DV	<i>Scomberomorus queenslandicus</i>
rough9	14.04093084	1.098237567	Mandu	BT+DV	<i>Scomberomorus queenslandicus</i>
SD15	14.7331805	0.907317505	Mandu	BT+DV	<i>Scomberomorus queenslandicus</i>
SD21	14.623122	0.72670349	Mandu	BT+DV	<i>Scomberomorus queenslandicus</i>
SD3	7.006166024	0.909281711	Mandu	BT+DV	<i>Scomberomorus queenslandicus</i>
SD9	12.92638832	1.119370459	Mandu	BT+DV	<i>Scomberomorus queenslandicus</i>
TRI15	15.60805855	0.86803845	Mandu	BT+DV	<i>Scomberomorus queenslandicus</i>
TRI21	15.02469054	0.77162074	Mandu	BT+DV	<i>Scomberomorus queenslandicus</i>
TRI3	11.08520476	1.006867315	Mandu	BT+DV	<i>Scomberomorus queenslandicus</i>
TRI9	12.68466776	0.869338464	Mandu	BT+DV	<i>Scomberomorus queenslandicus</i>
WE15	6.662797644	1.221315887	Mandu	BT+DV	<i>Scomberomorus queenslandicus</i>
fractal15	7.21262449	1.676984288	Mandu	BT+DV+BS	<i>Scomberomorus queenslandicus</i>
fractal21	7.998381957	2.407737387	Mandu	BT+DV+BS	<i>Scomberomorus queenslandicus</i>
fractal9	7.705787973	1.520899337	Mandu	BT+DV+BS	<i>Scomberomorus queenslandicus</i>
slope15	5.627371803	0.862829686	Mandu	BT+DV+BS	<i>Scomberomorus queenslandicus</i>
slope21	6.601195469	0.807412385	Mandu	BT+DV+BS	<i>Scomberomorus queenslandicus</i>
slope3	3.736672086	0.729777734	Mandu	BT+DV+BS	<i>Scomberomorus queenslandicus</i>
slope9	4.099444589	0.76787703	Mandu	BT+DV+BS	<i>Scomberomorus queenslandicus</i>
BPI15	1.613336512	0.797826093	Mandu	BT+DV+BS	<i>Scomberomorus queenslandicus</i>
BPI21	3.463578872	0.84560303	Mandu	BT+DV+BS	<i>Scomberomorus queenslandicus</i>
BPI3	2.085109667	0.882293268	Mandu	BT+DV+BS	<i>Scomberomorus queenslandicus</i>
BPI9	1.865092784	0.995438366	Mandu	BT+DV+BS	<i>Scomberomorus queenslandicus</i>
BT	6.179105986	2.989801957	Mandu	BT+DV+BS	<i>Scomberomorus queenslandicus</i>
NS21	1.882016476	0.786506773	Mandu	BT+DV+BS	<i>Scomberomorus queenslandicus</i>
NS9	1.632823797	0.615747735	Mandu	BT+DV+BS	<i>Scomberomorus queenslandicus</i>
rough15	2.433051915	0.845110067	Mandu	BT+DV+BS	<i>Scomberomorus queenslandicus</i>
rough21	4.166307831	0.913383145	Mandu	BT+DV+BS	<i>Scomberomorus queenslandicus</i>
rough3	3.460546146	0.985777888	Mandu	BT+DV+BS	<i>Scomberomorus queenslandicus</i>
rough9	3.73795308	1.062831296	Mandu	BT+DV+BS	<i>Scomberomorus queenslandicus</i>
SD15	4.563116867	1.029010646	Mandu	BT+DV+BS	<i>Scomberomorus queenslandicus</i>
SD21	5.022382385	0.67597223	Mandu	BT+DV+BS	<i>Scomberomorus queenslandicus</i>

Variable	Mean Decrease Accuracy	Mean Decrease Gini	Location	Scenario	Species
SD3	2.846393524	0.873058885	Mandu	BT+DV+BS	<i>Scomberomorus queenslandicus</i>
SD9	4.436392191	1.069694044	Mandu	BT+DV+BS	<i>Scomberomorus queenslandicus</i>
TRI15	5.808861731	0.935366853	Mandu	BT+DV+BS	<i>Scomberomorus queenslandicus</i>
TRI21	5.393514959	0.845283655	Mandu	BT+DV+BS	<i>Scomberomorus queenslandicus</i>
TRI3	3.433082176	1.027542274	Mandu	BT+DV+BS	<i>Scomberomorus queenslandicus</i>
TRI9	4.043848978	0.779798178	Mandu	BT+DV+BS	<i>Scomberomorus queenslandicus</i>
WE15	2.022760892	1.284121639	Mandu	BT+DV+BS	<i>Scomberomorus queenslandicus</i>
fractal15	14.85173103	1.26544007	PtCloates	BT+DV	<i>Scomberomorus queenslandicus</i>
fractal21	14.30598934	1.213318333	PtCloates	BT+DV	<i>Scomberomorus queenslandicus</i>
fractal9	9.526401906	0.940788089	PtCloates	BT+DV	<i>Scomberomorus queenslandicus</i>
meanc15	15.39848101	1.282825421	PtCloates	BT+DV	<i>Scomberomorus queenslandicus</i>
meanc21	16.28819065	1.478429524	PtCloates	BT+DV	<i>Scomberomorus queenslandicus</i>
meanc3	4.402329777	0.846569254	PtCloates	BT+DV	<i>Scomberomorus queenslandicus</i>
meanc9	14.77209283	1.22838024	PtCloates	BT+DV	<i>Scomberomorus queenslandicus</i>
planc15	19.59106866	2.286705942	PtCloates	BT+DV	<i>Scomberomorus queenslandicus</i>
planc21	7.973259371	1.068113817	PtCloates	BT+DV	<i>Scomberomorus queenslandicus</i>
planc3	7.61841865	1.08061577	PtCloates	BT+DV	<i>Scomberomorus queenslandicus</i>
planc9	7.116133984	1.750163872	PtCloates	BT+DV	<i>Scomberomorus queenslandicus</i>
profc15	15.64795617	1.436456008	PtCloates	BT+DV	<i>Scomberomorus queenslandicus</i>
profc21	14.30261399	1.585487696	PtCloates	BT+DV	<i>Scomberomorus queenslandicus</i>
profc9	10.48971446	1.12629122	PtCloates	BT+DV	<i>Scomberomorus queenslandicus</i>
slope15	10.78314201	0.752462779	PtCloates	BT+DV	<i>Scomberomorus queenslandicus</i>
slope21	9.218341445	0.945705381	PtCloates	BT+DV	<i>Scomberomorus queenslandicus</i>
slope3	12.15832388	0.943794412	PtCloates	BT+DV	<i>Scomberomorus queenslandicus</i>
slope9	12.58179191	0.882946075	PtCloates	BT+DV	<i>Scomberomorus queenslandicus</i>
BPI15	11.24427877	0.929457977	PtCloates	BT+DV	<i>Scomberomorus queenslandicus</i>
BPI21	14.86177561	1.154087286	PtCloates	BT+DV	<i>Scomberomorus queenslandicus</i>
BPI3	9.549193723	1.152491741	PtCloates	BT+DV	<i>Scomberomorus queenslandicus</i>
BPI9	19.10927085	1.416896925	PtCloates	BT+DV	<i>Scomberomorus queenslandicus</i>
BT	9.881014906	1.095787488	PtCloates	BT+DV	<i>Scomberomorus queenslandicus</i>
NS15	7.260399271	1.192816679	PtCloates	BT+DV	<i>Scomberomorus queenslandicus</i>
NS21	7.839787664	1.251982647	PtCloates	BT+DV	<i>Scomberomorus queenslandicus</i>
NS9	12.11253024	1.345043289	PtCloates	BT+DV	<i>Scomberomorus queenslandicus</i>
rough15	7.655491654	0.723021974	PtCloates	BT+DV	<i>Scomberomorus queenslandicus</i>
rough21	10.32462245	0.857009239	PtCloates	BT+DV	<i>Scomberomorus queenslandicus</i>
rough3	13.75496381	1.222029629	PtCloates	BT+DV	<i>Scomberomorus queenslandicus</i>
rough9	10.86077904	0.876997668	PtCloates	BT+DV	<i>Scomberomorus queenslandicus</i>
SD15	9.473806546	0.712477436	PtCloates	BT+DV	<i>Scomberomorus queenslandicus</i>
SD21	8.563585367	0.699296528	PtCloates	BT+DV	<i>Scomberomorus queenslandicus</i>
SD3	13.06383226	1.197853139	PtCloates	BT+DV	<i>Scomberomorus queenslandicus</i>
SD9	10.9598396	0.793367645	PtCloates	BT+DV	<i>Scomberomorus queenslandicus</i>
TRI15	12.16039155	0.793109459	PtCloates	BT+DV	<i>Scomberomorus queenslandicus</i>
TRI21	13.79169205	0.854809464	PtCloates	BT+DV	<i>Scomberomorus queenslandicus</i>
TRI3	11.57756444	1.173887675	PtCloates	BT+DV	<i>Scomberomorus queenslandicus</i>
TRI9	12.48449073	0.794078073	PtCloates	BT+DV	<i>Scomberomorus queenslandicus</i>

Variable	Mean Decrease Accuracy	Mean Decrease Gini	Location	Scenario	Species
WE9	5.653676791	1.384345599	PtCloates	BT+DV	<i>Scomberomorus queenslandicus</i>
fractal15	4.080814847	1.307158387	PtCloates	BT+DV+BS	<i>Scomberomorus queenslandicus</i>
fractal21	3.888324795	1.183668047	PtCloates	BT+DV+BS	<i>Scomberomorus queenslandicus</i>
fractal9	3.248692735	0.923925359	PtCloates	BT+DV+BS	<i>Scomberomorus queenslandicus</i>
meanc15	5.459217552	1.145804095	PtCloates	BT+DV+BS	<i>Scomberomorus queenslandicus</i>
meanc21	4.635528194	1.246536317	PtCloates	BT+DV+BS	<i>Scomberomorus queenslandicus</i>
meanc3	1.788746963	0.710850882	PtCloates	BT+DV+BS	<i>Scomberomorus queenslandicus</i>
meanc9	4.19814397	1.159805034	PtCloates	BT+DV+BS	<i>Scomberomorus queenslandicus</i>
planc15	5.335628254	1.872410453	PtCloates	BT+DV+BS	<i>Scomberomorus queenslandicus</i>
planc21	1.952140746	0.861251046	PtCloates	BT+DV+BS	<i>Scomberomorus queenslandicus</i>
planc3	1.711418234	0.872185439	PtCloates	BT+DV+BS	<i>Scomberomorus queenslandicus</i>
profc15	3.696088087	1.175540318	PtCloates	BT+DV+BS	<i>Scomberomorus queenslandicus</i>
profc21	4.952741203	1.598968912	PtCloates	BT+DV+BS	<i>Scomberomorus queenslandicus</i>
profc9	1.892060608	0.912300281	PtCloates	BT+DV+BS	<i>Scomberomorus queenslandicus</i>
slope15	4.383668899	0.922369726	PtCloates	BT+DV+BS	<i>Scomberomorus queenslandicus</i>
slope21	3.17498583	0.814407136	PtCloates	BT+DV+BS	<i>Scomberomorus queenslandicus</i>
slope3	2.947916807	0.729130639	PtCloates	BT+DV+BS	<i>Scomberomorus queenslandicus</i>
slope9	3.729987121	0.92200745	PtCloates	BT+DV+BS	<i>Scomberomorus queenslandicus</i>
ARA_Phi	5.907602282	2.242131294	PtCloates	BT+DV+BS	<i>Scomberomorus queenslandicus</i>
BPI15	4.131920206	0.849059392	PtCloates	BT+DV+BS	<i>Scomberomorus queenslandicus</i>
BPI21	4.44148968	0.933931033	PtCloates	BT+DV+BS	<i>Scomberomorus queenslandicus</i>
BPI3	2.807359695	1.126526742	PtCloates	BT+DV+BS	<i>Scomberomorus queenslandicus</i>
BPI9	6.436886832	1.326897867	PtCloates	BT+DV+BS	<i>Scomberomorus queenslandicus</i>
BS	3.935951756	1.879042013	PtCloates	BT+DV+BS	<i>Scomberomorus queenslandicus</i>
BT	2.256614061	0.797475131	PtCloates	BT+DV+BS	<i>Scomberomorus queenslandicus</i>
NS15	2.788500183	1.124924784	PtCloates	BT+DV+BS	<i>Scomberomorus queenslandicus</i>
NS21	3.128378524	1.240251661	PtCloates	BT+DV+BS	<i>Scomberomorus queenslandicus</i>
NS9	4.44252699	1.217367641	PtCloates	BT+DV+BS	<i>Scomberomorus queenslandicus</i>
rough15	4.015311793	0.659672727	PtCloates	BT+DV+BS	<i>Scomberomorus queenslandicus</i>
rough21	3.189242623	0.807706072	PtCloates	BT+DV+BS	<i>Scomberomorus queenslandicus</i>
rough3	3.871809499	1.224855614	PtCloates	BT+DV+BS	<i>Scomberomorus queenslandicus</i>
rough9	3.15829546	0.853382293	PtCloates	BT+DV+BS	<i>Scomberomorus queenslandicus</i>
SD15	3.137320123	0.600214229	PtCloates	BT+DV+BS	<i>Scomberomorus queenslandicus</i>
SD21	3.17187585	0.645945389	PtCloates	BT+DV+BS	<i>Scomberomorus queenslandicus</i>
SD3	3.945591604	1.104357884	PtCloates	BT+DV+BS	<i>Scomberomorus queenslandicus</i>
SD9	3.443281291	0.729010188	PtCloates	BT+DV+BS	<i>Scomberomorus queenslandicus</i>
TRI15	4.486797073	0.729785788	PtCloates	BT+DV+BS	<i>Scomberomorus queenslandicus</i>
TRI21	5.164376033	0.991324399	PtCloates	BT+DV+BS	<i>Scomberomorus queenslandicus</i>
TRI3	4.071662779	1.00016576	PtCloates	BT+DV+BS	<i>Scomberomorus queenslandicus</i>
TRI9	4.641261114	0.75015377	PtCloates	BT+DV+BS	<i>Scomberomorus queenslandicus</i>
WE3	1.489883636	1.572937405	PtCloates	BT+DV+BS	<i>Scomberomorus queenslandicus</i>
fractal21	16.20911029	1.784413954	Gnaraloo	BT+DV	<i>Scomberomorus queenslandicus</i>
BT	63.0204896	10.32157749	Gnaraloo	BT+DV	<i>Scomberomorus queenslandicus</i>
NS15	14.95726886	2.095271498	Gnaraloo	BT+DV	<i>Scomberomorus queenslandicus</i>
NS21	23.38146792	3.143805826	Gnaraloo	BT+DV	<i>Scomberomorus queenslandicus</i>

Variable	Mean Decrease Accuracy	Mean Decrease Gini	Location	Scenario	Species
WE15	19.15577732	2.476752009	Gnaraloo	BT+DV	<i>Scomberomorus queenslandicus</i>
WE21	29.66553499	3.759459301	Gnaraloo	BT+DV	<i>Scomberomorus queenslandicus</i>
WE9	18.29055556	2.51601681	Gnaraloo	BT+DV	<i>Scomberomorus queenslandicus</i>
fractal21	3.625752094	1.543078793	Gnaraloo	BT+DV+BS	<i>Scomberomorus queenslandicus</i>
ARA_Phi	12.80440794	6.298371845	Gnaraloo	BT+DV+BS	<i>Scomberomorus queenslandicus</i>
BS	6.780324257	3.570283435	Gnaraloo	BT+DV+BS	<i>Scomberomorus queenslandicus</i>
BT	15.99377986	8.311024073	Gnaraloo	BT+DV+BS	<i>Scomberomorus queenslandicus</i>
NS15	4.17438652	1.580200944	Gnaraloo	BT+DV+BS	<i>Scomberomorus queenslandicus</i>
NS21	5.334185415	2.330830453	Gnaraloo	BT+DV+BS	<i>Scomberomorus queenslandicus</i>
rough15	3.94857398	1.046901668	Gnaraloo	BT+DV+BS	<i>Scomberomorus queenslandicus</i>
SD15	4.804162452	0.82981009	Gnaraloo	BT+DV+BS	<i>Scomberomorus queenslandicus</i>
WE15	4.703817513	2.076598071	Gnaraloo	BT+DV+BS	<i>Scomberomorus queenslandicus</i>
WE21	9.010263813	3.138009317	Gnaraloo	BT+DV+BS	<i>Scomberomorus queenslandicus</i>
WE9	5.503697194	2.098016218	Gnaraloo	BT+DV+BS	<i>Scomberomorus queenslandicus</i>

Variable	Inc MSE	Inc Node Purity	Location	Scenario	Variable
meanc21	0.684171762	239.0756089	Mandu	BT+DV	Richness
slope15	1.970500922	206.9369522	Mandu	BT+DV	Richness
slope21	0.705064833	118.2103774	Mandu	BT+DV	Richness
slope9	1.171376614	169.1627795	Mandu	BT+DV	Richness
Depth	3.194470457	632.3415041	Mandu	BT+DV	Richness
rough15	1.351522596	154.2773862	Mandu	BT+DV	Richness
rough21	1.073392232	153.5371061	Mandu	BT+DV	Richness
rough9	1.109809196	95.60168275	Mandu	BT+DV	Richness
SD15	1.321585934	151.396141	Mandu	BT+DV	Richness
SD21	0.854590167	145.8312573	Mandu	BT+DV	Richness
SD9	1.067914732	100.6490904	Mandu	BT+DV	Richness
TRI15	0.961796211	148.9456046	Mandu	BT+DV	Richness
TRI21	0.865002373	135.9573822	Mandu	BT+DV	Richness
meanc21	0.641462082	245.303232	Mandu	BT+DV+BS	Richness
slope15	1.865696182	208.7529388	Mandu	BT+DV+BS	Richness
slope21	0.81840436	121.1484873	Mandu	BT+DV+BS	Richness
slope9	1.169915281	171.9628225	Mandu	BT+DV+BS	Richness
Depth	2.883813468	643.3723491	Mandu	BT+DV+BS	Richness
rough15	1.211875227	146.6713104	Mandu	BT+DV+BS	Richness
rough21	1.080289337	153.3006568	Mandu	BT+DV+BS	Richness
rough9	0.886523143	93.70011401	Mandu	BT+DV+BS	Richness
SD15	0.947095066	138.4958493	Mandu	BT+DV+BS	Richness
SD21	0.870790281	124.9318525	Mandu	BT+DV+BS	Richness
SD9	0.883422485	96.35844633	Mandu	BT+DV+BS	Richness
TRI15	1.015199777	147.4734433	Mandu	BT+DV+BS	Richness
TRI21	0.675994565	140.5189722	Mandu	BT+DV+BS	Richness
profc21	7.238184337	1055.638811	PtCloates	BT+DV	Richness
BPI15	2.9963735	525.2536321	PtCloates	BT+DV	Richness
SD15	10.0825605	774.5912959	PtCloates	BT+DV	Richness
SD21	3.237357344	297.362718	PtCloates	BT+DV	Richness
SD9	4.821650246	580.5415326	PtCloates	BT+DV	Richness
TRI15	14.25002759	1355.657	PtCloates	BT+DV	Richness
TRI21	5.793321049	657.5686764	PtCloates	BT+DV	Richness
TRI9	7.800502304	847.709105	PtCloates	BT+DV	Richness
profc21	7.244775232	1020.656111	PtCloates	BT+DV+BS	Richness
ARA_Phi	3.767640316	529.7296318	PtCloates	BT+DV+BS	Richness
SD15	9.832571247	767.1961157	PtCloates	BT+DV+BS	Richness
SD21	3.150636277	289.4000616	PtCloates	BT+DV+BS	Richness
SD9	4.734120683	573.7450976	PtCloates	BT+DV+BS	Richness
TRI15	14.8739821	1385.372304	PtCloates	BT+DV+BS	Richness
TRI21	5.275486377	620.0643442	PtCloates	BT+DV+BS	Richness
TRI9	7.807231453	861.1451356	PtCloates	BT+DV+BS	Richness
profc9	0.645166477	243.8803779	Gnaraloo	BT+DV	Richness
slope9	0.693675745	189.9988875	Gnaraloo	BT+DV	Richness
BPI21	0.29683352	113.4118748	Gnaraloo	BT+DV	Richness
Depth	0.99081213	239.6834681	Gnaraloo	BT+DV	Richness

Variable	Inc MSE	Inc Node Purity	Location	Scenario	Variable
TRI3	0.274681427	62.98532549	Gnaraloo	BT+DV	Richness
TRI9	0.23266465	61.96251105	Gnaraloo	BT+DV	Richness
WE9	0.303554545	151.0179043	Gnaraloo	BT+DV	Richness
ARA_Phi	1.979540908	151.3312181	Gnaraloo	BT+DV+BS	Richness
BS	2.7616397	235.7935866	Gnaraloo	BT+DV+BS	Richness
Depth	4.219343591	248.2354905	Gnaraloo	BT+DV+BS	Richness

Appendix B

List of species identified with the stereo-BRUVS in Cockburn Sound.

Apogonidae

Ostorhinchus victoriae

Carangidae

Pseudocaranx spp

Seriola hippos

Trachurus novaezelandiae

Dasyatidae

Dasyatis brevicaudata

Heterodontidae

Heterodontus portusjacksoni

Kyphosidae

Girella tephraeops

Labridae

Austrolabrus maculatus

Choerodon rubescens

Coris auricularis

Notolabrus parilus

Monacanthidae

Acanthaluteres vittiger

Meuschenia freycineti

Nelusetta ayraud

Scobinichthys granulatus

Myliobatidae

Myliobatis tenuicaudatus

Nemipteridae

Pentapodus vitta

Neosebastidae

Neosebastes pandus

Ostraciidae

Anoplocapros amygdaloides

Pempheridae

Pempheris klunzingeri

Rhinobatidae

Trygonorrhina dumerilii

Scorpididae

Microcanthus strigatus

Neatypus obliquus

Sillaginidae

Sillaginodes punctata

Sparidae

Chrysophrys auratus

Rhabdosargus sarba

Tetraodontidae

Lagocephalus sceleratus

Torquigener pleurogramma

Appendix C

List of species identified with the stereo-BRUVS in Ningaloo Marine Park.

Acanthuridae

Naso annulatus

Naso fageni

Apogonidae

Pristiapogon fraenatus

Balistidae

Abalistes stellatus

Sufflamen chrysopterum

Sufflamen fraenatum

Blenniidae

Aspidontus dussumieri

Carangidae

Alectis ciliaris

Carangoides chrysophrys

Carangoides ferdau

Carangoides fulvoguttatus

Carangoides gymnostethus

Caranx ignobilis

Decapterus spp

Elagatis bipinnulata

Gnathanodon speciosus

Pseudocaranx georgianus

Seriola dumerili

Seriola rivoliana

Seriolina nigrofasciata

Ulua mentalis

Carcharhinidae

Carcharhinus falciformis
Carcharhinus plumbeus
Carcharhinus sorrah
Carcharhinus sp
Carcharhinus sp1
Carcharhinus spp
Galeocerdo cuvier
Triaenodon obesus

Chaetodontidae

Chaetodon assarius

Cirrhitidae

Cirrhitichthys aprinus

Dasyatidae

Bathytoshia lata
Pastinachus ater

Echeneidae

Echeneis naucrates

Fistulariidae

Fistularia commersonii
Fistularia petimba

Gobiidae

Amblyeleotris wheeleri
Valenciennesa puellaris

Haemulidae

Diagramma pictum
Diagramma spp
Plectorhinchus albivittatus

Hydrophiidae

spp

Labridae

Bodianus perditio
Choerodon jordani
Coris auricularis
Coris caudimacula
Diproctacanthus xanthurus
Iniistius pavo
Labroides dimidiatus
Thalassoma lunare

Lethrinidae

Gymnocranius elongatus
Gymnocranius grandoculis
Lethrinus genivittatus
Lethrinus laticaudis
Lethrinus nebulosus
Lethrinus ravus
Lethrinus rubrioperculatus
Lethrinus semicinctus
Lethrinus variegatus

Lutjanidae

Lutjanus bohar
Lutjanus sebae
Pristipomoides multidens

Malacanthidae

Malacanthus brevisrostris

Monacanthidae

Cantherhines dumerilii
Cantherhines fronticinctus

Mullidae

sp1

Parupeneus barberinoides

Parupeneus heptacanthus

Parupeneus spilurus

Muraenidae

Gymnothorax javanicus

Nemipteridae

Nemipterus furcosus

Nemipterus spp

Pentapodus nagasakiensis

Oneirodidae

Oneirodes spp

Pinguipedidae

Parapercis diplospilus

Pomacanthidae

Chaetodontoplus personifer

Pomacanthus sexstriatus

Pomacentridae

Chromis fumea

Neopomacentrus cyanomos

Rachycentridae

Rachycentron canadum

Rhinidae

Rhynchobatus australiae

Scaridae

Chlorurus strongylocephalus

Scarus chameleon

Scarus dimidiatus

Scarus niger

Scombridae

Cybiosarda elegans

Sarda orientalis

Scomberomorus munroi

Serranidae

Epinephelus chlorostigma

Epinephelus coioides

Epinephelus malabaricus

Epinephelus multinotatus

Epinephelus rivulatus

Pseudanthias bicolor

Pseudanthias cooperi

Siganidae

Siganus fuscescens

Sparidae

Argyrops spinifer

Sphyraenidae

Sphyraena obtusata

Tetraodontidae

Arothron spp

Canthigaster rivulata

Lagocephalus sceleratus